ANALYSIS AND DESIGN OF ISOLATED BIDIRECTIONAL DC-DC CONVERTER WITH NOVEL TRIPLE PHASE-SHIFT CONTROL

by

KUIYUAN WU

B. A. Sc., Southwest Jiao Tong University, 1990
M. A. Sc., Chinese Academy of Sciences, 1997
M. A. Sc., The University of British Columbia, 2008

A THESIS SUBMITTED IN PARTIAL FULFILLMENT OF

THE REQUIREMENTS FOR THE DEGREE OF

DOCTOR OF PHILOSOPHY

in

THE FACULTY OF GRADUATE STUDIES

(Electrical and Computer Engineering)

THE UNIVERSITY OF BRITISH COLUMBIA

(Vancouver)

July 2012

Abstract

The bidirectional DC-DC converter is widely used in automobiles, energy storage systems, uninterruptible power supplies and aviation power systems. At present, there are three main problems in this area. The first problem concerns stability of the bidirectional converter when parameters change; the second is maintaining high efficiency of the bidirectional converter over wide load range; the third concerns the sensitivity of the efficiency of the bidirectional converter to parameter changes.

This thesis presents a new method to determine the stability of the bidirectional converter using the Lyapunov function method under arbitrary parameter changes. As another new contribution, the stability analysis with eigenvalue method is presented when only the input voltage changes. Although these two methods are used in this thesis to determine the stability of bidirectional dual full bridge DC-DC converter with triple phase-shift control, they can be used to determine the stability of other power converters composed of various power switches and controlled with different control methods.

A novel triple phase-shift control method is developed in this thesis to make the bidirectional converter operate at high efficiency and make it robust to parameters changes and output power variations. Simulation results illustrate that the novel control method is better than several other commonly used control methods for the bidirectional converter when component parameters and output power change. The working theory of the bidirectional converter with novel triple phase-shift control method is comprehensively described in the thesis. As another new contribution, the maximum output power of the bidirectional converter is analyzed in detail in the thesis. Simulation studies of this project have provided satisfactory results. Conclusions are made on the presented work and possible future directions in continuing the work are indicated.

Preface

Dr. William G. Dunford and Dr. Clarence W. de Silva suggested me to do the analysis and design of isolated bidirectional DC-DC converter during my PhD study. This is a MITACS project collaborated with Alpha Technologies Ltd. Ethics approval is not required for the research of this PhD project.

According to the suggestions of Dr. Dunford, Dr. de Silva and Dr. Cosmin Pondiche, I read many papers relevant to bidirectional DC-DC converters and selected three different power circuits for this project. Dr. Dunford suggested the dual full bridge converter to be the first choice for this project. During this process, I developed a novel triple phase-shift control method for the dual full bridge power circuit and analyzed the working theory of the isolated bidirectional DC-DC converter with novel triple phase-shift control method. Dr. Dunford suggested me to analyze the maximum output power of the bidirectional converter. I corrected several errors about the maximum output power in this area. Dr. de Silva suggested me to analyze the stability of this bidirectional DC-DC converter with Lyapunov function method. I separated this nonlinear converter into several stages in one period to analyze the stability of the bidirectional converter in every stage with the Lyapunov function method and the stability of the bidirectional converter at the interface of two neighbouring stages under parameter variation. Based on this new idea, I analyzed the stability of the bidirectional converter with the eigenvalue method when the input voltage changes.

Under the careful supervision of Dr. Dunford and Dr. de Silva, I began to prepare relevant journal manuscripts and this PhD dissertation after I completed the performance of various parts of the research and the analysis of the research data. Eight journal papers related to this thesis have been submitted to international journals. The published or

accepted journal papers are listed below:

[1] Kuiyuan Wu, Clarence W. de Silva and William G. Dunford, "Stability Analysis of Isolated Bidirectional Dual Active Full Bridge DC-DC Converter with Triple Phase-shift Control," *IEEE Transactions on Power Electronics*, Vol. 27, No. 4, pp. 2007-2017, April 2012 (Chapter 3).

[2] Kuiyuan Wu, Clarence W. de Silva and William G. Dunford, "Theoretical Stability Analysis of Isolated Bidirectional Dual Full Bridge DC-DC Converter," accepted by *Asian Power Electronics Journal* in 2011 (Chapter 4).

[3] Kuiyuan Wu, William G. Dunford and Clarence W. de Silva, "Maximum Output Power Analysis of Isolated Bidirectional Dual Full Bridge DC-DC Converter with Phase-shift Control Methods," accepted by *Asian Power Electronics Journal* in 2012 (Chapter 6).

Table of Contents

List of Tables

List of Figures

Acknowledgements

First, I must express my great thanks to my research supervisors, Dr. William G. Dunford and Dr. Clarence W. de Silva for their support and valuable guidance throughout the whole process of my graduate studies and project research at UBC. I appreciate the effort of committee members, Dr. Nicolas Jaeger, Dr. Shahriar Mirabbasi, Dr. Juri Jatskevich, Dr. L. Linares, Dr. Daan Maijer and Dr. Siegfried F. Stiemer. I expect to acknowledge Dr. John Madden's advice about simulation circuits and the relevance of the specifications. In particular, I would also like to express my thanks to Dr. Cosmin Pondiche, who led me to this research direction.

Numerous interactions with my colleagues, Mr. Brian Cheng, Dr. Weidong Xiao and Dr. Liwei Wang，have as well inspired me throughout my graduate studies at UBC.

Many thanks are due to both Alpha Technologies Ltd. and Mathematics of Information Technology and Complex Systems (MITACS) for providing the necessary funding for my PhD project.

Finally, I must express my sincere gratitude to my parents, my wife and my brothers for their inspiration and support during all my studies.

Chapter 1 Introduction

1.1 Power Circuits and Control Techniques for Bidirectional DC-DC Converters

In recent years, the development of high power and wide load range isolated bidirectional DC-DC converters has become an important topic because of the requirements of electric automobiles, uninterruptible power supplies and aviation power systems. A 1kW/250W isolated bidirectional DC-DC converter is a typical application and forms the focus for this thesis.

The block diagram for this converter is given in Figure 1.1.

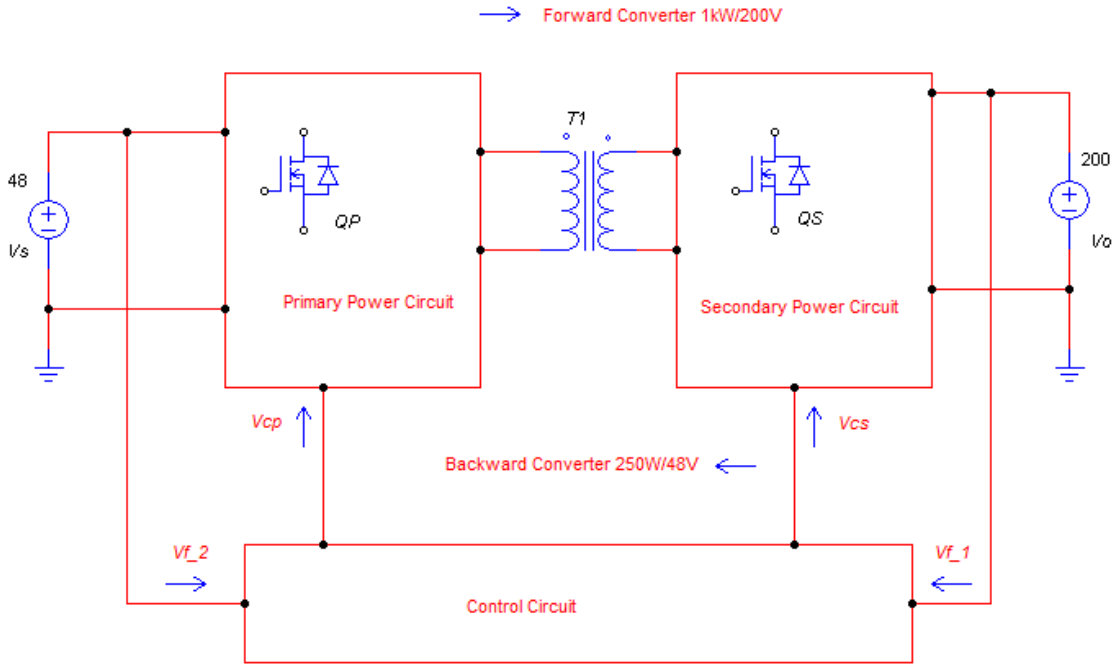

Fig. 1.1 Block Diagram of Bidirectional DC-DC Converter

This converter can be controlled to transfer energy both forwards and backwards. The

most commonly used control technique for the bidirectional converter is the Lead-Lag PI compensator [7], [15], [17]. For different power circuits, there exist different control methods. According to the specific controller terminology used in bidirectional converter area, they are:

1. Phase-shift Control [1], [3]: When the half duty cycle control signals for the power switches in the primary power circuit lead to the corresponding half duty cycle control signals for the power switches in the secondary power circuit, the power is transferred to the secondary side from the primary side. Otherwise, the power is transferred to the primary side from the secondary side.

2. Phase-shift Control plus Pulse-Width Modulation [4], [5], [12]: At present, this control method is used in this manner: The power is transferred by phase-shift control and PWM (Pulse Width Modulator) is mainly used to balance the primary voltage and the secondary voltage of the transformer. This reduces the *rms* current of the transformer, and the duty cycle can vary from zero to one. The second control variable is not fully used.

3. Dual-phase-shift Control [6]: This method uses the first phase-shift between the half duty cycle control signals for the primary and secondary power switches as the main controller to transfer power; it uses the second phase-shift between the half duty cycle control signals for diagonal power switches in the same side of the transformer as the auxiliary controller to transfer power and adjust the reactive power. These two phase-shift-controls are independent. At present, it is only used in dual active full bridge converters and the efficiency is not very satisfactory. It is still in the experimental research stage. Essentially, it can be viewed as a combination of two lead-lag compensators.

4. Intelligent Fuzzy Logic Control [10]: It uses the fuzzy logic control to realize PWM control for a bidirectional converter. Although it has good dynamic performance, the efficiency of the converter is not satisfactory. At present, this method is in the

experimental research stage.

5. Intelligent Artificial Neural Network Controller: It uses the artificial neural network control methodology to realize PWM control for a bidirectional converter. It has good dynamic characteristics, but the efficiency of the converter is not satisfactory. This method is also still in the experimental research stage.

At present, the most commonly used control method for the isolated bidirectional converter is phase-shift control. Certainly, different control methods should be used for different power circuits in realizing the required specifications of the project. Common combination modes of power circuits with concrete control techniques are as follows:

1: Dual Active Bidirectional Full Bridge Power Circuit with Phase-shift Control [1], [11]: This paper introduces a dual full active bridge isolated bidirectional converter with rated power of 10kW for an energy storage system. The phase-shift control method is used for this converter. It analyzes the switching loss for hard switching operation, ZVS operation and incomplete ZVS operation, and other losses. It gives the condition for hard switching operation. In the end, it suggests that the power loss and peak current through the transformer impose limits on the power transfer and output voltage.

2: Dual Active Bidirectional Full-half Bridge Power Circuit with Phase-shift Control plus Pulse-Width Modulation [2]: This paper introduces a bidirectional full-half bridge DC-DC converter for an extended run time DC UPS system. It explains its stable operation mode with phase-shift control and its dynamic operation mode with phase-shift plus duty cycle control. In the end, this paper introduces the control design and gives experimental results. Its maximum efficiency is 91% for 1kW and 70% for 320W. Its duty cycle is defined as:

$$D = V_o/(4 * N * V_i) \quad (1\text{-}1)$$

Here, V_o is the output voltage and is assumed constant; V_i is the input voltage; N is the turns ratio of the transformer. This converter will transfer from phase-shift control to phase-shift plus duty ratio control only when the input voltage is lower than the nominal

voltage. This means that the converter will still use phase-shift control when the output power is low and input voltage is equal to the nominal voltage. This will make the circuit operate in hard switching mode. Switching loss will increase rapidly and the efficiency will be very low for low output power operation.

3: A Novel Bidirectional Converter with Phase-shift Control [3]: This paper introduces a novel bidirectional DC-DC converter composed of two symmetrical active-clamped circuits, one on each side of an isolation transformer. It briefly explains the working process, and gives the computing equation for some variables. In the end, it gives the converter experimental results with efficiency of 90% for output power of 30W. Input voltage and output voltage are all equal to 12V. It uses phase-shift control. It is very difficult to apply advanced control to improve efficiency and performance of this converter. Besides this, this converter is particularly suitable for low power DC UPS systems.

4: Dual Active Bidirectional Full Bridge Power Circuit with Dual Phase-shift Control [6]: This paper presents a dual-phase-control method in detail. It compares the dual-phase-shift control with the PI-based phase-shift control and gives the relevant formulae to calculate the active power, reactive power and the transformer current. It uses the experimental waveforms to suggest that this control method can reduce reactive power, decrease the peak inrush current, improve system efficiency and increase its ZVS range. The dead band effect is also easier to compensate in dual-phase-shift control systems than in phase-shift control systems. Its efficiency is still lower than 90% for 5kW output power. This suggests that this new method should be revised in order to improve its efficiency.

5: Current-voltage-fed Zero-Voltage-Switching Bidirectional DC-DC Converter with Phase-shift plus PWM Control Method [4]: This paper describes a current-voltage-fed ZVS bidirectional DC-DC converter with phase-shift plus PWM control method. It explains the converter’s working process in a simple manner. Its duty ratio is defined as:

$$D = 1 - 2 * N_2 * V_1/(N_1 * V_2) \quad (1\text{-}2)$$

Here, V_1 is the input voltage of the converter; V_2 is the output voltage of the converter; and N_2/N_1 is the turns ratio of the transformer. Its duty cycle control is used only to match the transformer primary side voltage and secondary side voltage, not to directly control the output power and the output voltage. In the end, this paper presents experimental results. Its forward efficiency for 1kW is about 95%; its backward efficiency for 250W is about 92%.

6: Dual Half Bridge Bidirectional DC-DC Converter with Atypical Duty Ratio and Phase-shift Control [8]: This paper describes a two-phase, triple-voltage (14V/42V/High Voltage) dual half bridge isolated bidirectional DC-DC converter for hybrid electric vehicles. It realizes triple-voltage output by using atypical duty ratio (1/3) and phase-shift control with one bidirectional converter. Then, it analyzes its working process and gives simulation and experimental results to verify that the power can transfer among these three different voltage-level ports. In the end, the paper presents the efficiency curve (93%~95.8%) over the tested range.

The disadvantage of the method is that it uses two-phase bidirectional converters; more specifically, two dual-half-bridge converters to realize its specification. Its behavior and efficiency will degrade if it uses only one bidirectional dual-half bridge converter. Its duty ratio is constant (1/3) only for the triple voltage outputs. The power transfer relies only on phase-shift control.

7: Half Bridge plus Push-pull Bidirectional Converter with the Adaptive Fuzzy Logic Controller [10]: This paper introduces a half bridge plus push-pull bidirectional converter with the adaptive fuzzy logic controller. The general control method is PWM. It describes the design step of the fuzzy logic controller and gives the simulation and experimental waveforms. This paper does not provide efficiency results for this converter. Its dynamic performance is acceptable.

1.2 Problem Identification

From the relevant papers as summarized above, it can be seen that the main problems in this field are as follows:

(1) It is not known whether these bidirectional converters can remain stable when the parameters change. If the bidirectional converter is not stable when the parameters change, it is not useful. This question is very difficult to answer because the bidirectional converter is a very complicated nonlinear system. This stability problem can be solved using the Lyapunov function method for the general case or with the eigenvalue method for special linear time-invariant system.

(2) The efficiency of the bidirectional converter is not high over a wide range of operating conditions. It changes dramatically with load changes. This is mainly because the efficiency is not robust to parameter and output power changes. This can be solved through a novel control method that will make the efficiency of the converter more robust to parameter and output power changes.

(3) An effective method to reduce the switching loss is to make the power switches operate in the zero-voltage-switching (ZVS) mode. Because the ferrite core of the transformer has very low hysteresis B-H loop and very high resistivity, the transformer core loss and eddy current loss are very low. Because the on-resistance of the power switches is very low, the conduction loss of the power converter is also very low. Switching loss is the major loss of a high frequency power converter. Therefore, we should find appropriate methods to enlarge the ZVS scope and reduce the switching loss [13], [14], [16]. This should be solved through the combination of power circuit and control circuit designs. ZVS is realized by charging and discharging snubber capacitors in parallel with the power switches, with the energy stored in transformer leakage inductor or the combination of another serial small inductor and the leakage inductor.

(4) In order to reduce the conduction loss, measures should be taken to reduce the *rms* values of the primary and secondary currents with the same output power. During some working stages, the current will circulate in the primary and secondary loops without power transfer. This will produce current spikes and increase the *rms* value of the current. Certainly, the conduction loss and the reactive power will also increase. This problem can be solved by designing a suitable power circuit and a good controller.

(5) The stability of the output voltage of the bidirectional converter has to satisfy the design requirements. In order to ensure that the product works well and to widen its application range, the output voltage should be able to satisfy the required specification when some component parameters change.

At present, the output filter capacitor is often pre-charged or uses soft start technology to reduce the inrush current during the start of the converter. During large load change transients, it is expected that the current changes smoothly, and not too dramatically. This belongs to the dynamic property of the bidirectional converter. We should try to make it more satisfactory by applying new control techniques.

The methods proposed by other experts cannot satisfy the specifications for this project. We need to find a proper method to study the stability of the bidirectional converter in the general case and should develop a novel control method and an appropriate power circuit to satisfy the project requirements. The main reason for the failure of the other methods to satisfy the project requirements is that an isolated bidirectional converter is a complex essentially nonlinear system with several unknown parameters. Therefore, it is very difficult to develop an accurate model for the isolated bidirectional power circuit. We can determine the stability of the bidirectional converter using the Lyapunov function method by separating the converter into several stages in one period. Generally, PSIM, simulation software for power electronics and motor drive systems, is used to design controller and directly simulate the entire system. When the control method is designed to solve some of

the problems, it may not adequately resolve all problems.

1.3 Motivation and Objectives of the Thesis

The main objectives of the proposed research are to analyze the stability of the bidirectional DC-DC converter and to develop a novel control method to satisfy the project specifications. In particularly, the research is will carry out the following:

1. Develop an appropriate isolated bidirectional DC-DC power circuit for this project to make this bidirectional converter realize ZVS over a wide load range.

2. Analyze the stability of this isolated bidirectional DC-DC converter using the Lyapunov function method so as to ensure it is bounded-input bounded-output stable for arbitrary parameter changes. If a suitable Lyapunov function cannot be found for a complex bidirectional converter, analyze stability using the eigenvalue method only for input voltage changes.

3. Develop a novel control method to make the bidirectional converter realize high efficiency and make it robust (insensitive) to parameter and output power variations.

4. Demonstrate the performance of this bidirectional isolated DC-DC converter using computer simulations.

1.4 Thesis Organization

This thesis is organized into seven chapters. Chapter 1 gives a brief introduction of the commonly used power circuits and control methods of isolated bidirectional DC-DC converter, and the main problems that exist in this area. It outlines the objectives of the thesis. In Chapter 2, dual full bridge power circuit topology and three corresponding control methods of the bidirectional converter are described; an appropriate isolated bidirectional dual full bridge DC-DC converter power circuit topology and a novel triple phase-shift control method for this project are determined by comparing efficiency,

output voltage stability and robustness to parameter and output power changes. Chapter 3 is focused on the theoretical stability analysis of the isolated bidirectional dual full bridge DC-DC converter using the Lyapunov method for arbitrary parameter changes when a novel triple phase-shift control method is used. Chapter 4 is focused on theoretical stability analysis of the isolated bidirectional dual full bridge DC-DC converter using the eigenvalue method under input voltage changes only when a novel triple phase-shift control method is used. Chapter 5 analyzes the working theory of the isolated bidirectional dual full bridge DC-DC converter with the novel triple phase-shift control method. Maximum output power of the isolated bidirectional dual full bridge DC-DC converter with phase-shift control methods is analyzed theoretically in Chapter 6. The last chapter gives the conclusions of this thesis and suggests some meaningful directions for future work.

1.5 Project Specifications

According to the requirements of the isolated bidirectional dual full bridge DC-DC converter, the specifications for the project are as follows:

(1) Forward converter: P_{out} =1000W; V_o=200V; η≥93%

(2) Backward converter: P_{out} =250W; V_o =48V; η≥95%

(3) Output voltage stability of the bidirectional converter: S≤1‰

$$S = \frac{(V_{omax} - V_{omin})}{(V_{omax} + V_{omin})} * 100\% \quad (1\text{-}3)$$

S: Output Voltage Stability

V_{omax}: Maximum Output Voltage

V_{omin}: Minimum Output Voltage

From the efficiency specifications, it can be derived that a suitable ZVS or ZCS power circuit must be selected for this project to eliminate the switching loss of the power converter. Otherwise, it will be very difficult to satisfy the efficiency specifications because the switching loss will be dominant in high frequency power converters when

compared with the conduction loss and the transformer core loss. Besides, this bidirectional converter must be able to realize ZVS or ZCS from 250W to 1kW load scope because the power circuit is the same for the forward converter and the backward converter. Otherwise, the efficiency of the backward converter with 250W output power will be much smaller than 95%. If the bidirectional converter can realize ZVS or ZCS in the desired load range, the efficiency for 250W output power will be slightly higher than the efficiency for 1kW output power because the conduction loss will increase with the increase of the output power.

Additionally, the efficiency of the bidirectional converter must be robust to output power variation and parameter changes. This means that the efficiency of the forward converter must be greater than or equal to 95% with 250W output power and the efficiency of the backward converter must be greater than or equal to 93% with 1kW output power. This is because all components in the power circuit are entirely the same for the forward converter and the backward converter. Theoretically, the current through every component is the same for the same output power with fixed input voltage and output voltage.

From the specification for the output voltage stability as listed above, it can be derived that the output voltage of this bidirectional converter must be robust to output power variation and parameter changes. Besides, it can be derived that this bidirectional converter has many uses. It can be connected between two different DC power sources; it can also be connected between a DC power source and a DC load; e.g., a DC motor to realize regenerative braking.

In order to satisfy these strict project specifications, a combination of an appropriate ZVS or ZCS power circuit and a suitable control circuit must be selected for the bidirectional converter. These concepts will be explained in detail in the following chapters.

Chapter 2 Topologies of Isolated Bidirectional DC-DC Converter

2.1 Objectives and Rationale

The first step for a project design is to choose an appropriate topology for this project. The objective of this chapter is to develop a novel topology for this project, including a suitable power circuit topology and a novel control method to make the bidirectional DC-DC converter work with high efficiency when parameters change.

It is well known that it is very important to establish a good topology for a successful project design. Only when a suitable topology is determined for a bidirectional converter, can it satisfy the project requirement; otherwise, the bidirectional converter cannot work satisfactorily because the efficiency and voltage stability of the bidirectional converter are determined by the combination of power circuit, control method and their elements parameters. This can be seen clearly in the following simulation results of different topologies for this project. After comparison of different topologies for this project, an isolated bidirectional dual full bridge DC-DC converter with novel triple phase-shift control topology is determined for this project. The bidirectional converter with this novel topology can work with high efficiency over wide load scope. Its efficiency is robust (insensitive) to parameter change.

2.2 Power Circuit Topology

It is very important to choose an appropriate power circuit topology in project design; otherwise, it is impossible to make the bidirectional converter perform satisfactorily. Theoretically, many kinds of bidirectional DC-DC converter, such as bidirectional dual full bridge converter, bidirectional full-half bridge converter and other simple

bidirectional converters can be used as the power circuit of a bidirectional DC-DC converter, but the bidirectional dual full bridge converter is widely used because of its special advantages [11], [16]. Finally, the isolated dual full bridge converter is chosen to be the power circuit of this bidirectional DC-DC converter project. This power circuit is shown in Fig.2.1. The corresponding simulation circuits are attached in appendix A for triple phase-shift control, appendix B for dual phase-shift control and appendix C for single phase-shift control.

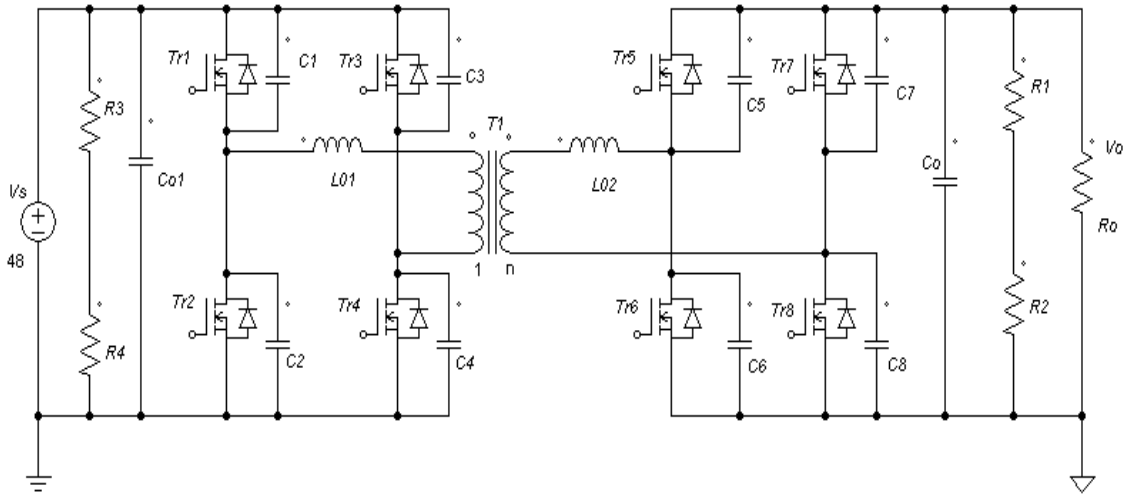

Fig. 2.1 Bidirectional Dual Full Bridge Converter

The isolated bidirectional dual full bridge ZVS DC-DC converter is symmetrical on both sides of the transformer. It is suitable to transfer energy back and forth. The important advantage of this topology is that several more control methods can be used for this power circuit. In particular, using the novel triple phase-shift control method will make the efficiency and output voltage of the bidirectional converter much more robust (insensitive) to parameters change. Certainly, it will also make the bidirectional converter have high efficiency over wide load scope as well.

2.3 Control Methods of the Bidirectional Dual Full Bridge Converter

Generally, there are three commonly used control methods for bidirectional converter. They are single phase-shift control method [1], [3], single phase-shift plus PWM control

method [4], [5], [12] and dual phase-shift control [6]. Among these three methods, the single phase-shift control method is often used because it is simple. However, the efficiency and output voltage of the bidirectional converter with these existing control methods are sensitive to parameter change. The parameters of the bidirectional converter may change during the practical application of the bidirectional converter, for example, the on resistance of the power switches, leakage inductance of the transformer, magnetizing inductance of transformer, input voltage and equivalent load resistance. Additionally, the rule of the parameter change is unknown. Therefore, a novel triple phase-shift control method needs to be developed for this project.

2.3.1 Introduction of Single Phase-shift Control

For the bidirectional dual full bridge converter, single phase-shift control means there is only one phase-shift between primary control signal and corresponding secondary control signal [1], [8]. If the primary control signals lead the corresponding secondary control signals, the energy will transfer from the primary side to the secondary side. If the secondary control signals lead the corresponding primary control signals, the energy will transfer from the secondary side to the primary side with the same power circuit. The control signal waveforms for single phase-shift control are shown in Fig.2.2.

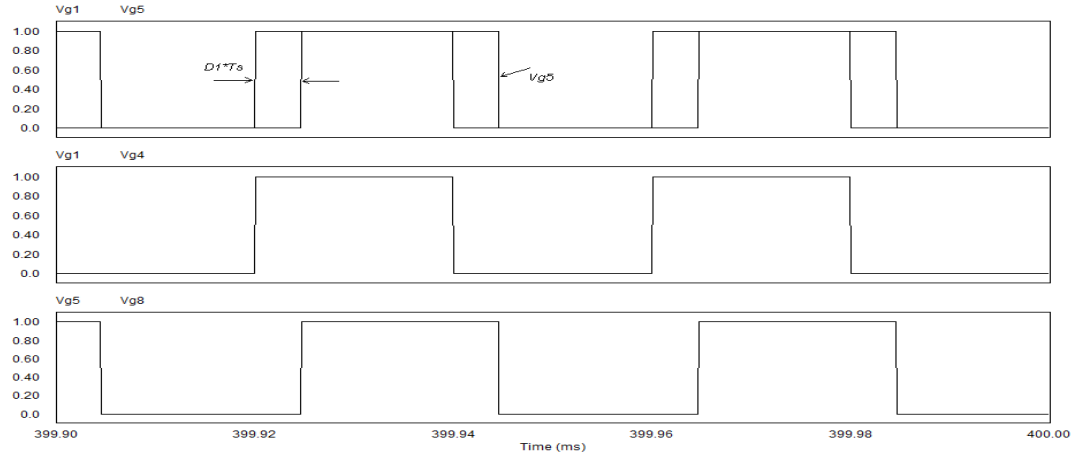

Fig. 2.2 Forward Control Signal Waveforms of Single Phase-shift Control

V_{g1}: Control Signal for Power Switch Tr1

V_{g4}: Control Signal for Power Switch Tr4

V_{g5}: Control Signal for Power Switch Tr5

V_{g8}: Control Signal for Power Switch Tr8

D_1: Phase-shift Ratio between V_{g1} and V_{g5}

T_s: Period of Control Signals

In Fig.2.2, it can be seen there is only one phase-shift between V_{g1} and V_{g5}. V_{g1} leads to V_{g5}, therefore, the energy is transferred from primary side to the secondary side. The power transfer formula of the bidirectional dual full bridge converter with single phase-shift control is as following [1]:

$$Po = \frac{Vs*Vo}{\omega L} * \left(\delta - \frac{\delta^2}{\pi}\right) \quad (2\text{-}1)$$

From this output power formula, it can be found there is only one control variable (δ =2π*D_1) to adjust the output power. Therefore, there is only one control variable to adjust its efficiency when parameters change or output power varies. The robustness of the efficiency of bidirectional converter with single phase-shift control is not satisfactory.

2.3.2 Introduction of Dual Phase-shift Control Method

For the bidirectional dual full bridge converter, dual phase-shift control includes the first phase-shift between primary control signal and corresponding secondary control signal and the second phase-shift between the diagonal control signals [6]. If the primary control signals lead the corresponding secondary control signals, the energy will transfer from the primary side to the secondary side. If the secondary control signals lead the corresponding primary control signals, the energy will transfer from the secondary side to the primary side with the same power circuit. The control signal waveforms for dual phase-shift control are shown in Fig.2.3.

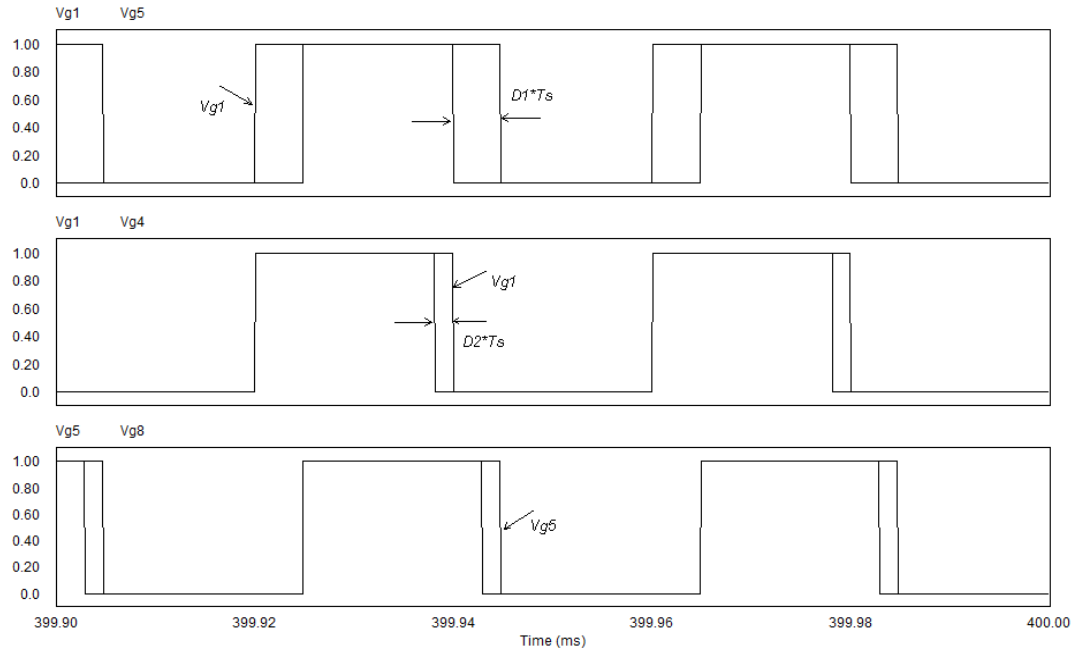

Fig. 2.3 Forward Control Signal Waveforms of Dual Phase-shift Control

V_{g1}: Control Signal for Power Switch Tr1

V_{g4}: Control Signal for Power Switch Tr4

V_{g5}: Control Signal for Power Switch Tr5

V_{g8}: Control Signal for Power Switch Tr8

D_1: Phase-shift Ratio between V_{g1} and V_{g5}

D_2: Phase-shift Ratio between V_{g1} and V_{g4}

T_s: Period of Control Signals

In Fig.2.3, it can be seen there are two phase-shifts. The first is phase-shift between V_{g1} and V_{g5}; the second is phase-shift between V_{g1} and V_{g4} (V_{g5} and V_{g8}). V_{g1} leads to V_{g5}, therefore, the energy is transferred from primary side to the secondary side. The power transfer formula of the bidirectional dual full bridge converter with dual phase-shift control is as following [6]:

When $D_1 \leq 1/2$, the expression of the output power is:

$$P_{out} = \frac{n*Vs*Vo}{2*fs*L} * \begin{cases} D_2 * (2 - 2 * D_1 - D_2) & 0 \le D_2 \le D_1 \\ D_2 * (1 - D_1 - D_2) + D_1 - D_1^2 & D_1 \le D_2 \le 1\text{-}D_1 \\ (1 - D_1) * (1 - D_2) & 1\text{-}D_1 \le D_2 \le 1 \end{cases} \quad (2\text{-}2)$$

When D_1>1/2, the expression of the output power is:

$$P_{out} = \frac{n*Vs*Vo}{2*fs*L} * \begin{cases} D_2 * (2 - 2 * D_1 - D_2) & 0 \le D_2 \le 1\text{-}D_1 \\ (1 - D_1)^2 & 1\text{-}D_1 \le D_2 \le D_1 \\ (1 - D_1) * (1 - D_2) & D_1 \le D_2 \le 1 \end{cases} \quad (2\text{-}3)$$

From this output power formula, it can be found there are two control variables to adjust the output power. Therefore, there are two control variables to adjust its efficiency when parameters change or output power varies. The robustness of the efficiency of bidirectional converter with dual phase-shift control is better than that with single phase-shift control, but it is still not satisfactory for the project specifications.

2.3.3 Introduction of Novel Triple Phase-shift Control Method

For the bidirectional dual full bridge converter, triple phase-shift control includes the first phase-shift between primary control signal and corresponding secondary control signal, the second phase-shift between the diagonal control signals in the primary power circuit and the third phase-shift between the diagonal control signals in the secondary power circuit. If the primary control signals lead the corresponding secondary control signals, the energy will transfer from the primary side to the secondary side. If the secondary control signals lead the corresponding primary control signals, the energy will transfer from the secondary side to the primary side with the same power circuit. Because there are three control variables in novel triple phase-shift control, this will make the

energy transfer more flexibly and more effectively. The control signal waveforms for novel triple phase-shift control are shown in Fig.2.4.

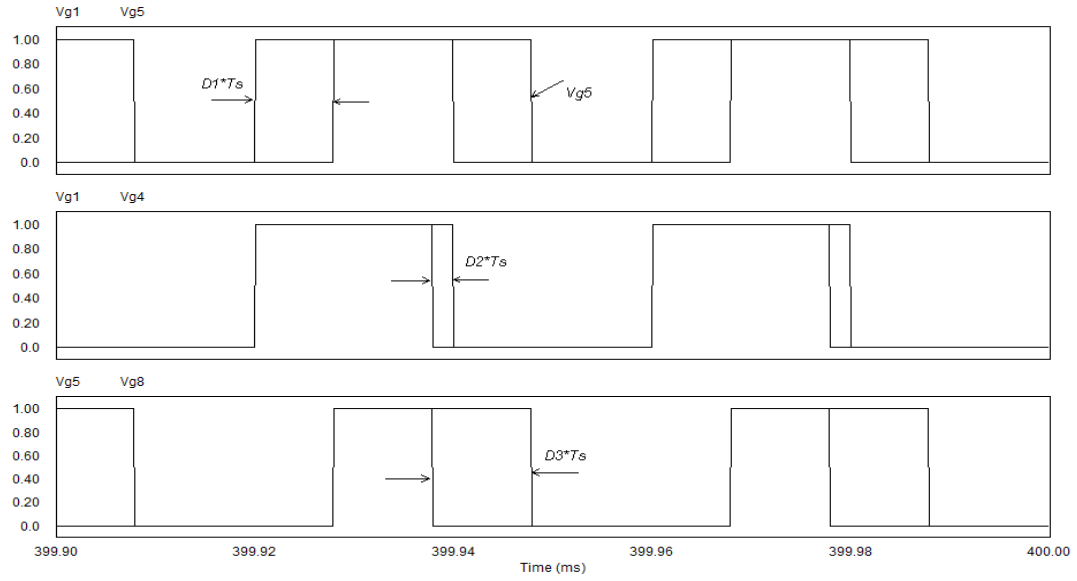

Fig. 2.4 Forward Control Signal Waveforms of Novel Triple Phase-shift Control

V_{g1}: Control Signal for Power Switch Tr1

V_{g4}: Control Signal for Power Switch Tr4

V_{g5}: Control Signal for Power Switch Tr5

V_{g8}: Control Signal for Power Switch Tr8

D_1: Phase-shift Ratio between V_{g1} and V_{g5}

D_2: Phase-shift Ratio between V_{g1} and V_{g4}

D_3: Phase-shift Ratio between V_{g5} and V_{g8}

T_s: Period of Control Signals

In Fig.2.4, it can be seen there are three phase-shifts. The first is phase-shift between V_{g1} and V_{g5}; the second is phase-shift between V_{g1} and V_{g4}; the third is phase-shift betweenV_{g5} and V_{g8}. V_{g1} leads to V_{g5}, therefore, the energy is transferred from primary side to the secondary side. The power transfer formula of the bidirectional dual full bridge converter with novel triple phase-shift control is as following:

$$P_{out} = \frac{2*Vs^2*(1+2*D1-2*D3)}{Ts*(1+2*D2-2*D3)} * \left[\frac{(D2-D1)*(1-2*D2)*Ts}{(1+2*D2-2*D3)*Req2} - \frac{2*D1*(D2-D1)*Ts}{(1+2*D2-2*D3)*Req2}\right]$$

$$+\frac{2*Vs^2*(1+2*D1-2*D3)}{Ts*(1+2*D2-2*D3)}$$

$$*\left[-\frac{Leq}{Req1*Req2}*\left(1-e^{\frac{-Req1*D1*Ts}{Leq}}\right)*e^{\frac{-Req2*(0.5-D2)*Ts}{Leq}}+\frac{Leq}{Req1*Req2}\right.$$

$$*\left(1-e^{\frac{-Req1*D1*Ts}{Leq}}\right)*e^{\frac{-Req2*D1*Ts}{Leq}}+\frac{2*(D2-D1)*Leq}{(1+2*D2-2*D3)*Req2^2}$$

$$*e^{\frac{-Req2*(0.5-D2)*Ts}{Leq}}-\frac{2*(D2-D1)*Leq}{(1+2*D2-2*D3)*Req2^2}*e^{\frac{-Req2*D1*Ts}{Leq}}$$

$$-\frac{(1+2*D1-2*D3)*Ts}{2*(1+2*D2-2*D3)*Req3}+\frac{(1+2*D1-2*D3)*(0.5-D2)*Ts}{(1+2*D2-2*D3)*Req3}$$

$$-\frac{2*(D2-D1)*Leq}{Req2*Req3*(1+2*D2-2*D3)}*e^{\frac{-Req3*Ts}{2*Leq}}$$

$$+\frac{2*(D2-D1)*Leq}{Req2*Req3*(1+2*D2-2*D3)}*e^{\frac{-Req3*(0.5-D2)Ts}{Leq}}-\frac{Leq}{Req1*Req3}$$

$$*e^{\frac{-Req2*(0.5-D2)*Ts-0.5*Req3*Ts}{Leq}}+\frac{Leq}{Req1*Req3}$$

$$*e^{\frac{-Req1*D1*Ts-Req2*(0.5-D2)*Ts-0.5*Req3*Ts}{Leq}}+\frac{2*(D2-D1)*Leq}{Req2*Req3*(1+2*D2-2D3)}$$

$$*e^{\frac{-Req2*(0.5-D2)*Ts-0.5*Req3*Ts}{Leq}}+\frac{Leq}{Req1*Req3}*e^{\frac{-Req2*(0.5-D2)*Ts-Req3*(0.5-D2)*Ts}{Leq}}$$

$$-\frac{Leq}{Req1*Req3}*e^{\frac{-Req1*D1*Ts-Req2*(0.5-D2)*Ts-Req3*(0.5-D2)*Ts}{Leq}}$$

$$-\frac{2*(D2-D1)*Leq}{Req2*Req3*(1+2*D2-2D3)}*e^{\frac{-Req2*(0.5-D2)*Ts-Req3*(0.5-D2)*Ts}{Leq}}$$

$$-\frac{Leq*(1+2*D1-2*D3)}{Req3^2*(1+2*D2-2*D3)}*e^{\frac{Req3*Ts}{2*Leq}}+\frac{Leq*(1+2*D1-2*D3)}{Req3^2*(1+2*D2-2*D3)}$$

$$\left.*e^{\frac{Req3*(0.5-D2)*Ts}{Leq}}\right] \tag{2-4}$$

From this output power formula, it can be found that there are three control variables to adjust the output power. Therefore, there are three control variables in the efficiency formula to adjust its efficiency when parameters change. The robustness of the efficiency of bidirectional converter with triple phase-shift control is much better than that with dual phase-shift control or single phase-shift control. If its efficiency is satisfactory in normal operating modes, it will remain nearly unchanged when parameters change.

2.3.4 Comparison of Three Control Methods

In this section, single phase-shift control, dual phase-shift control and novel triple phase-shift control are compared with each other for the same bidirectional dual full bridge converter when magnetizing inductance is uncertain. In this situation, the magnetizing inductance will change during the whole simulation process.

1: Bidirectional Dual Full Bridge Converter with Novel Triple Phase-shift Control

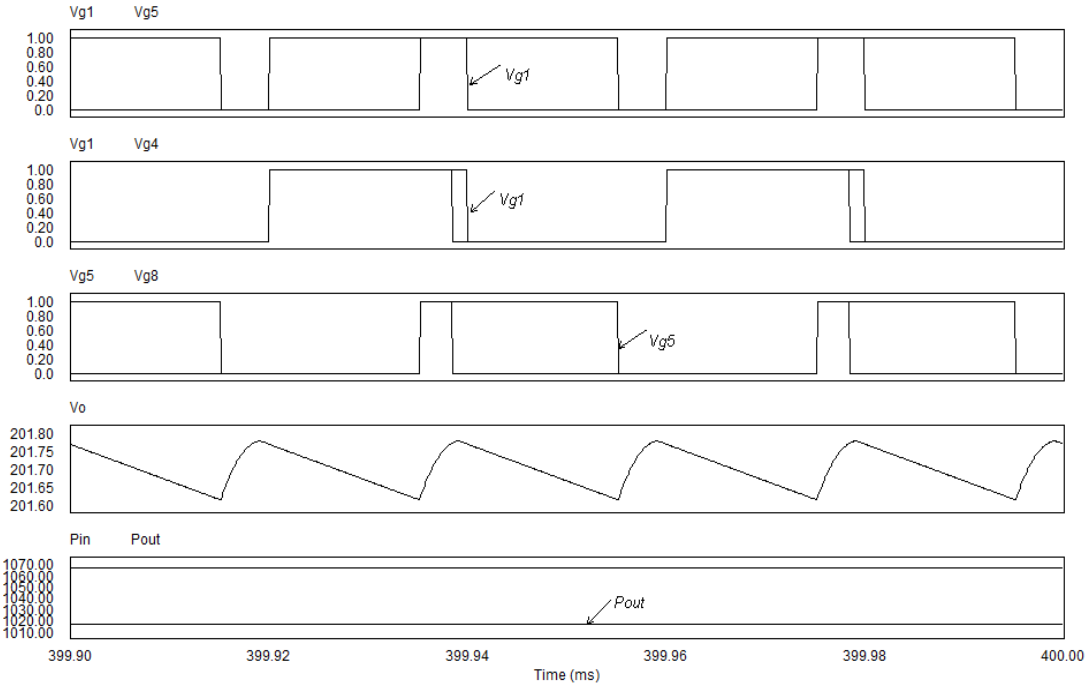

Fig. 2.5 Forward Simulation Results with Triple Phase-shift Control for Vref1=8V under Uncertain Lm

V_{g1}: Control Signal for Power Switch Tr1

V_{g4}: Control Signal for Power Switch Tr4

V_{g5}: Control Signal for Power Switch Tr5

V_{g8}: Control Signal for Power Switch Tr8

V_o: Output Voltage of Forward Converter (Volts)

P_{in}: Average Input Power of Forward Converter (Watts)

P_{out}: Average Output Power of Forward Converter (Watts)

The simulation circuit and elements parameters of this converter are attached in Appendix A. In Fig.2.5, the average input power and average output power can be observed. The efficiency of the forward converter under full load situation can be calculated.

P_{in}=1067.1W

P_{out}=1017.1W

$$\eta = \frac{P_{out}}{P_{in}} = \frac{1017.1}{1067.1} = 95.3\% \qquad (2\text{-}5)$$

V_o=201.70±0.075V

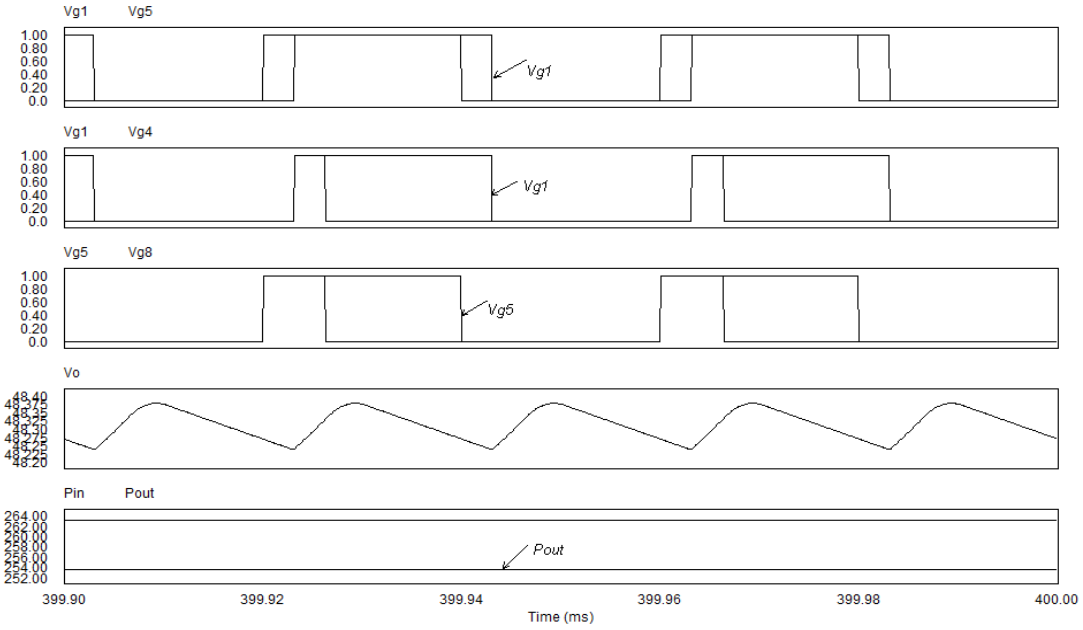

Fig. 2.6 Backward Simulation Results with Triple Phase-shift Control for Vref1=8V under Uncertain Lm

V_{g1}: Control Signal for Power Switch Tr1

V_{g4}: Control Signal for Power Switch Tr4

V_{g5}: Control Signal for Power Switch Tr5

V_{g8}: Control Signal for Power Switch Tr8

V_o: Output Voltage of Backward Converter (Volts)

P_{in}: Average Input Power of Backward Converter (Watts)

P_{out}: Average Output Power of Backward Converter (Watts)

In Fig.2.6, the average input power and average output power can be observed. The efficiency of the backward converter under full load situation can be calculated.

P_{in}=263.22W

P_{out}=253.73W

$$\eta = \frac{P_{out}}{P_{in}} = \frac{253.73}{263.22} = 96.4\% \quad (2\text{-}6)$$

V_o=48.31±0.06V

2: Bidirectional Dual Full Bridge Converter with Dual Phase-shift Control

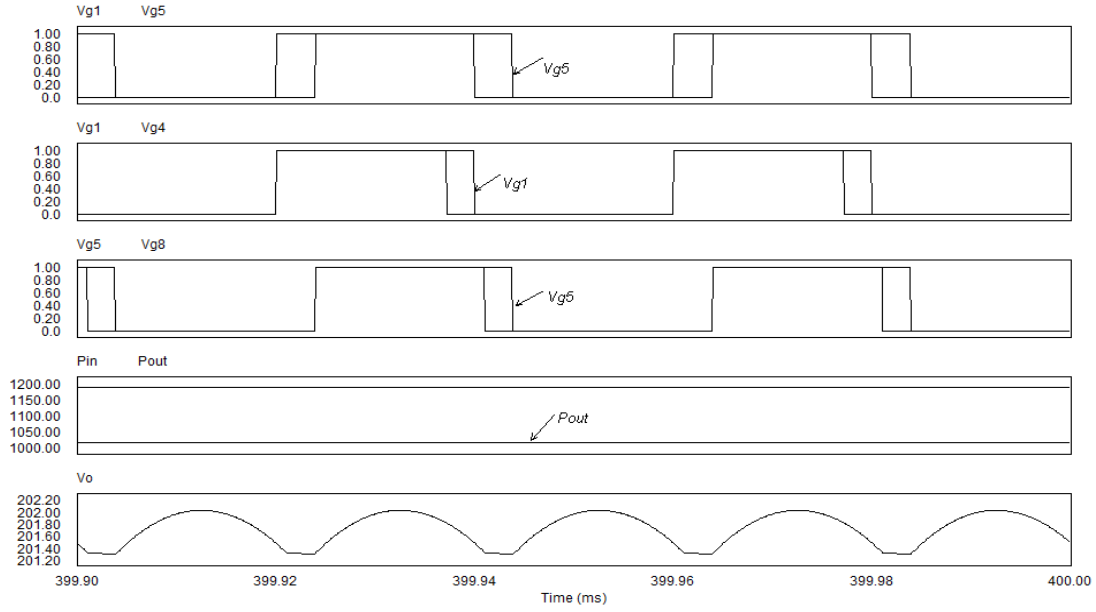

Fig. 2.7 Forward Simulation Results with Dual Phase-shift Control for Vref1=5V under Uncertain Lm

V_{g1}: Control Signal for Power Switch Tr1

V_{g4}: Control Signal for Power Switch Tr4

V_{g5}: Control Signal for Power Switch Tr5

V_{g8}: Control Signal for Power Switch Tr8

V_o: Output Voltage of Forward Converter (Volts)

P_{in}: Average Input Power of Forward Converter (Watts)

P_{out}: Average Output Power of Forward Converter (Watts)

The simulation circuit and elements parameters of this converter are attached in Appendix B. In Fig.2.7, the average input power and average output power can be observed. The efficiency of the forward converter under full load situation can be calculated.

P_{in}=1189.75W

P_{out}=1017.31W

$$\eta = \frac{P_{out}}{P_{in}} = \frac{1017.31}{1189.75} = 85.5\% \qquad (2\text{-}7)$$

V_o=201.7±0.3V

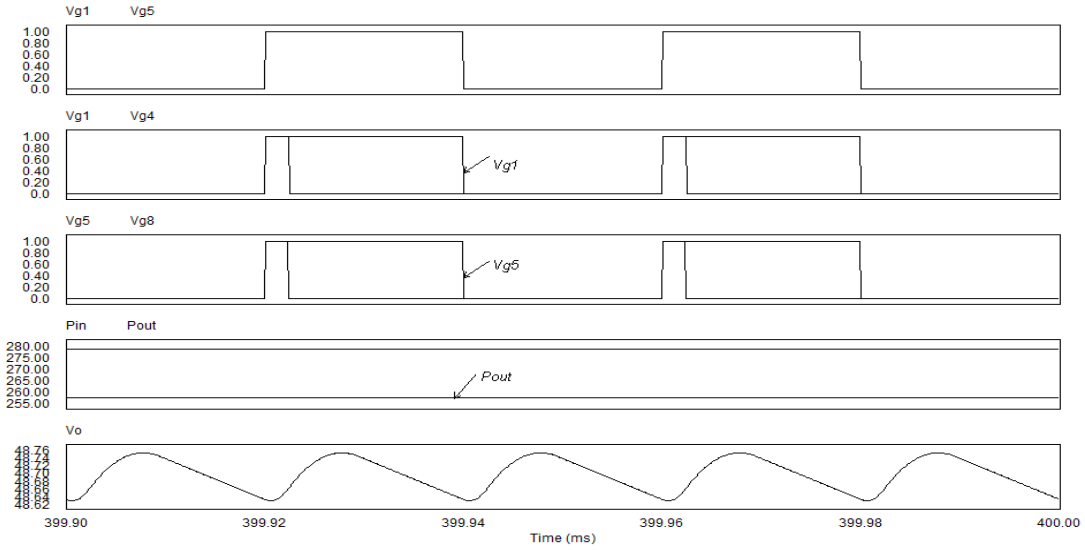

Fig. 2.8 Backward Simulation Results with Dual Phase-shift Control for Vref1=5V under Uncertain Lm

V_{g1}: Control Signal for Power Switch Tr1

V_{g4}: Control Signal for Power Switch Tr4

V_{g5}: Control Signal for Power Switch Tr5

V_{g8}: Control Signal for Power Switch Tr8

V_o: Output Voltage of Backward Converter (Volts)

P_{in}: Average Input Power of Backward Converter (Watts)

P_{out}: Average Output Power of Backward Converter (Watts)

In Fig.2.8, the average input power and average output power can be observed. The efficiency of the backward converter under full load situation can be calculated.

P_{in}=278.48W

P_{out}=257.75W

$$\eta = \frac{P_{out}}{P_{in}} = \frac{257.75}{278.48} = 92.5\% \qquad (2\text{-}8)$$

V_o=48.7±0.05V

3: Bidirectional Dual Full Bridge Converter with Single Phase-shift Control

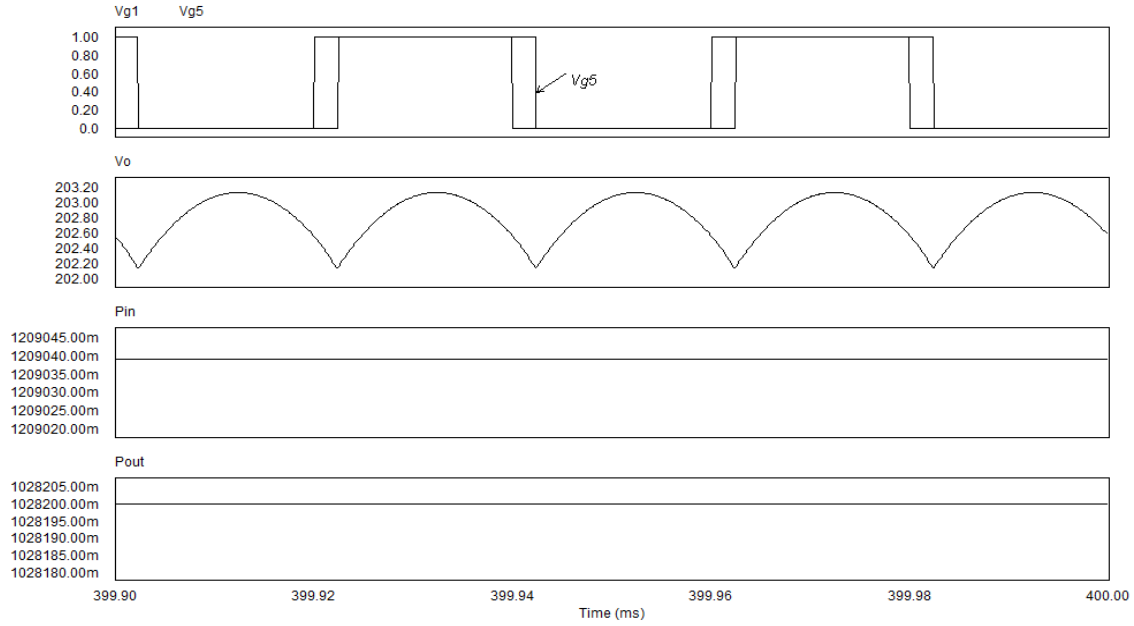

Fig. 2.9 Forward Simulation Results with Single Phase-shift Control for Vref1=5V under Uncertain Lm

V_{g1}: Control Signal for Power Switch Tr1

V_{g5}: Control Signal for Power Switch Tr5

V_o: Output Voltage of Forward Converter (Volts)

P_{in}: Average Input Power of Forward Converter (Watts)

P_{out}: Average Output Power of Forward Converter (Watts)

The simulation circuit and elements parameters of this converter are attached in

Appendix C. In Fig.2.9, the average input power and average output power can be observed. The efficiency of the forward converter under full load situation can be calculated.

P_{in}=1209.04W

P_{out}=1028.2W

$$\eta = \frac{P_{out}}{P_{in}} = \frac{1028.2}{1209.04} = 85\% \qquad (2\text{-}9)$$

V_o=202.8±0.33V

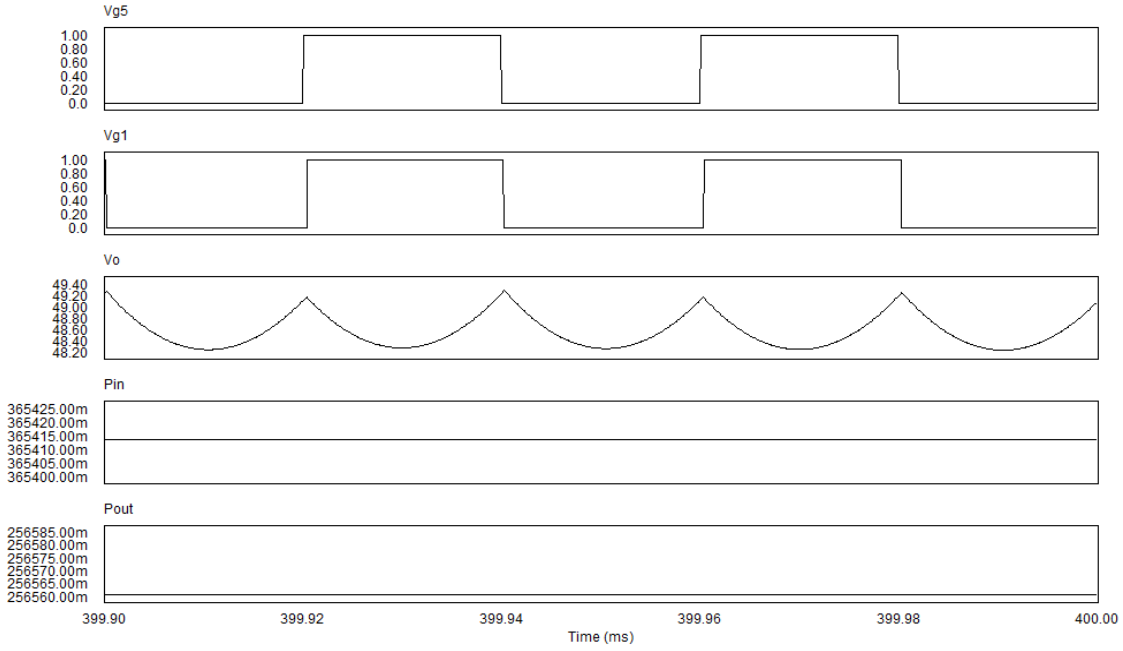

Fig. 2.10 Backward Simulation Results with Single Phase-shift Control for Vref1=5V under Uncertain Lm

V_{g1}: Control Signal for Power Switch Tr1

V_{g5}: Control Signal for Power Switch Tr5

V_o: Output Voltage of Backward Converter (Volts)

P_{in}: Average Input Power of Backward Converter (Watts)

P_{out}: Average Output Power of Backward Converter (Watts)

In Fig.2.10, the average input power and average output power can be observed. The

efficiency of the backward converter under full load situation can be calculated.

P_{in}=365.41W

P_{out}=256.56W

$$\eta = \frac{P_{out}}{P_{in}} = \frac{256.56}{365.41} = 70.2\% \quad (2\text{-}10)$$

V_o=48.58±0.71V

4: Efficiency Comparison of Bidirectional Converter with Three Control Methods

Table 2.1 Comparison of Three Control Methods under Uncertain *Lm*

	Triple Phase-shift Control	Dual Phase-shift Control	Single Phase-shift Control
Forward Efficiency (*Pout*=1kW)	95.3%	85.5%	85%
Backward Efficiency (*Pout*=250W)	96.4%	92.5%	70.2%

From the simulation results of these three control topologies, it can be found that the efficiency of dual full bridge converter controlled with the novel triple-phase control method will be much more robust to parameter change. This is because there are more control variable combinations available for this method than for others. This novel controller can still make the bidirectional converter realize ZVS for this situation with an effective control variable combination. Therefore, the dual full bridge bidirectional DC-DC converter with novel triple phase-shift control method is chosen for this project.

2.4 Determination of Components Parameters

Because the working process of the bidirectional dual full bridge ZVS DC-DC converter with triple phase-shift control is very complicated, the steady state working

process of this bidirectional converter will be explained in detail in chapter 5. The main components' values of this bidirectional converter are obtained by theoretical calculation and simulation adjustments. They are listed in the following.

2.4.1 Main Components Parameters

L_{01}=7.3μH; L_{02}=6.9μH;

Csnubber=1nF; Co=500μF;

Forward load resistance: Ro=40Ω;

Forward voltage feedback resistance: 100kΩ/1.85kΩ;

Backward load resistance: Ro=9.2Ω;

Backward voltage feedback resistance: 100kΩ/13.8kΩ

The parameters of the main transformer are as following:

Primary leakage inductance: Lp=0.6μH;

Secondary leakage inductance: Ls=1μH;

Magnetizing inductance: Lm=0.5H;

Primary winding resistance: Rp=7mΩ;

Secondary winding resistance: Rs=10mΩ;

Turns ratio: n=2/7

The parameters of the 8 power switches are as following:

Tr1~Tr4: On resistance: 5mΩ; Diode Voltage drop: 1V

Tr5~Tr8: On resistance: 23mΩ; Diode Voltage drop: 0.6V

Here, the parameters of 8 power switches are selected by checking the data sheet of power MOSFET according to the data listed above. The parameters of transformer are selected according to the commonly used high frequency transformer data. The method to determine a suitable inductance value for the bidirectional converter will be introduced in chapter 6. The method to determine other components values is simple and not explained in detail here.

2.4.2 Determination of Output Capacitance in Power Circuit

The factors involved in deciding the output capacitance include the switching frequency current ripple, the DC output voltage, the output voltage ripple and the hold-up time. The total current through the output capacitor is the RMS value of the switching frequency ripple current. Large electrolytic capacitors which are normally chosen for the output capacitor have an equivalent series resistance (ESR) which changes with frequency and is generally high at low frequencies. The amount of current which the capacitor can handle is generally determined by the temperature rise. It is usually not necessary to calculate an exact value for the temperature rise. It is usually adequate to calculate the temperature rise due to the high frequency ripple current and the low frequency ripple current and add them together. The capacitor data sheet will provide the necessary ESR and temperature rise information. The hold-up time of the output voltage often dominates any other consideration in output capacitor selection. Hold-up time is the length of time that the output voltage remains within a specified range after input power has been turned off. Hold-up time of 15 to 50 milliseconds is typical. If hold-up time is not required, the capacitance will be much smaller, generally 0.2μF per Watt, and then ripple current and ripple voltage are the major concern [18]. For this 1kW/250W bidirectional converter project, the output capacitance is selected as 500 μF.

2.4.3 Switching Frequency and Main Power Switch

Here, the choice of the switching frequency and main power switch will be explained separately because they are important for the converter to have satisfactory performance.

1: The Choice of the Switching Frequency

It is well known that the switching frequency correlates to the performance of the power converter. When the frequency is lower than 20kHz, the performance of the power converter will not be satisfactory; the ripple will be large; the response will be slow; the weight and volume of the equipment will increase greatly and it will produce the

tiresome ac noise [13], [14], [16]. When the switching frequency is higher than 150 kHz, it will be favorable to improve the function of the power converter, such as to lower the ripple, to shorten the response time and to reduce the volume and weight. However, it will also bring about some defects, such as to increase radio-frequency interference (RFI), to make more strict requirements on the high frequency properties of the main power switches, high frequency inductors and capacitors. Most importantly, the switching loss will increase and the efficiency will be decreased obviously for large power application [13], [14], [16]. All of these factors will increase the difficulty and the cost to build this bidirectional DC-DC converter. Considering all of these factors, it is appropriate to choose a frequency from 20 kHz to 150 kHz for this power converter. In this range, there is no tiring ac noise and the bidirectional converter achieves high power density, low ripple, fast response time and the low cost. Therefore, it can satisfy the requirement of many products [18]. In the end, the value of 25 kHz is chosen as the switching frequency of the main converter; and the validity of this is shown in the final simulation results.

2：The Choice of the Main Power Switch

The power MOSFET is chosen as the main power switch for the bidirectional converter. The advantages of power MOSFET include its high operation speed and bidirectional conduction. Besides these aspects, the driving power for the MOSFET is very low. These are suitable for the bidirectional converter. The equivalent circuit of power MOSFET is an on-resistance in parallel with a diode, as shown in Fig. 2.11.

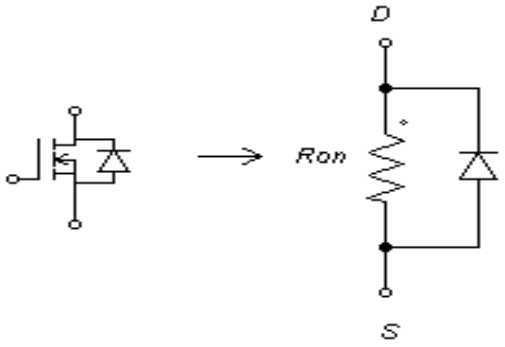

Fig. 2.11 Equivalent Circuit of Power MOSFET

2.5 Simulation Studies and Discussion

1: Simulation of Bidirectional Dual Full Bridge Converter with Novel Triple Phase-shift Control

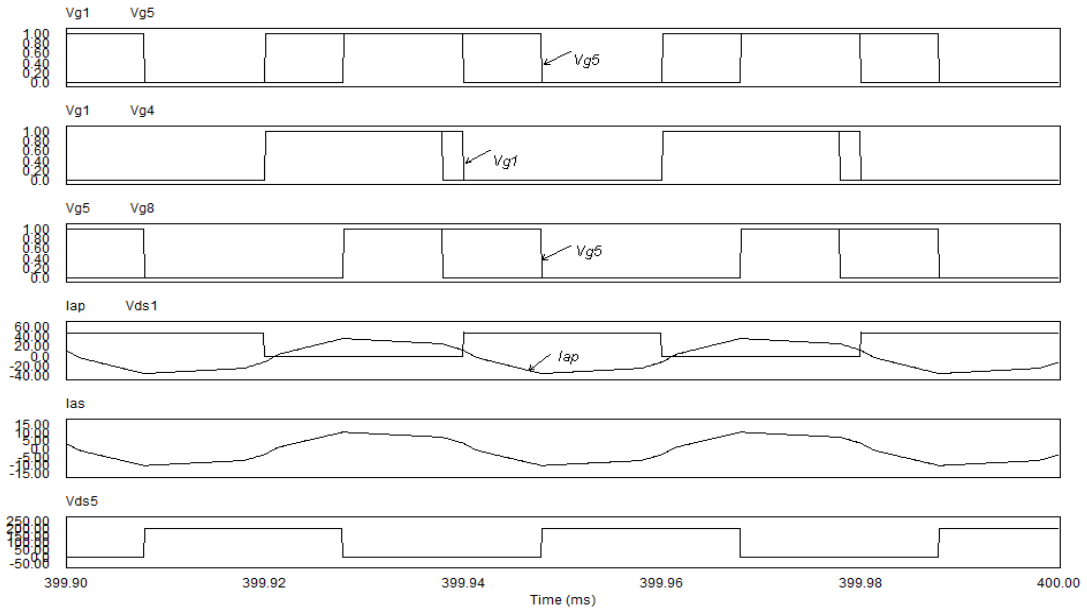

Fig. 2.12 Forward Simulation Results of Iap, Ias, Vds1, Vds5 for Po=1kW with Vref1=6V

V_{g1}: Control Signal for Power Switch Tr1

V_{g4}: Control Signal for Power Switch Tr4

V_{g5}: Control Signal for Power Switch Tr5

V_{g8}: Control Signal for Power Switch Tr8

V_{ds1}: Voltage across Power Switch Tr1 (Volts)

V_{ds5}: Voltage across Power Switch Tr5 (Volts)

I_{ap}: Primary Current of the Bidirectional Converter (Amperes)

I_{as}: Secondary Current of the Bidirectional Converter (Amperes)

The simulation circuit and elements parameters are attached in Appendix A. In Fig.2.12, it can be seen clearly that the primary current value is negative at the rising edge of the control signals V_{g1} and V_{g4}; the secondary current value is positive at the

rising edge of the control signals V_{g5} and V_{g8}. Therefore, this bidirectional converter can realize zero-voltage-switching (ZVS) very well.

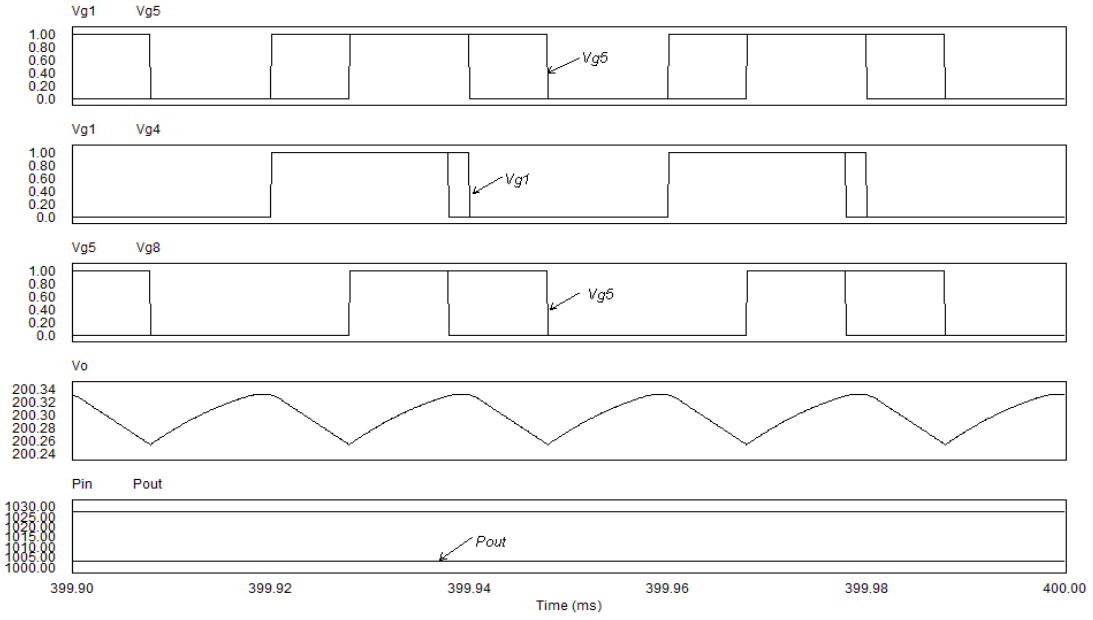

Fig. 2.13 Forward Simulation Results of Vo, Pin, Pout for Po=1kW with Vref1=6V

V_{g1}: Control Signal for Power Switch Tr1

V_{g4}: Control Signal for Power Switch Tr4

V_{g5}: Control Signal for Power Switch Tr5

V_{g8}: Control Signal for Power Switch Tr8

V_o: Output Voltage of Forward Converter (Volts)

P_{in}: Average Input Power of Forward Converter (Watts)

P_{out}: Average Output Power of Forward Converter (Watts)

In Fig.2.13, the average input power and average output power can be observed. The efficiency of the forward converter under full load condition can be calculated as follows.

P_{in}=1027.28W

P_{out}=1003W

$$\eta = \frac{P_{out}}{P_{in}} = \frac{1003}{1027.28} = 97.6\% \qquad (2\text{-}11)$$

V_o=200.3±0.03V

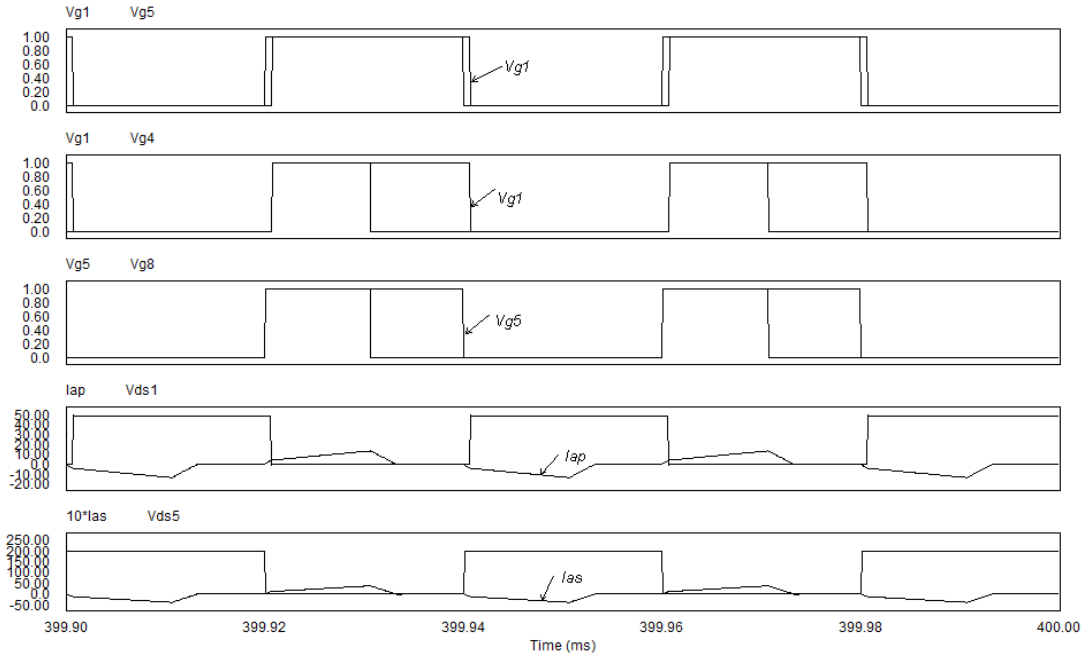

Fig. 2.14 Backward Simulation Results of Iap, Ias, Vds1, Vds5 for Po=250W with Vref1=6V

V_{g1}: Control Signal for Power Switch Tr1

V_{g4}: Control Signal for Power Switch Tr4

V_{g5}: Control Signal for Power Switch Tr5

V_{g8}: Control Signal for Power Switch Tr8

V_{ds1}: Voltage across Power Switch Tr1 (Volts)

V_{ds5}: Voltage across Power Switch Tr5 (Volts)

I_{ap}: Primary Current of the Bidirectional Converter (Amperes)

I_{as}: Secondary Current of the Bidirectional Converter (Amperes)

In Fig.2.14, it can be seen clearly that the primary current value is positive at the rising edge of the control signals V_{g1} and V_{g4}; and the secondary current value is zero before the rising edge of the control signals V_{g5} and V_{g8}. Therefore, the primary power circuit can realize ZVS and the secondary power circuit can realize zero-current-switching (ZCS) very well.

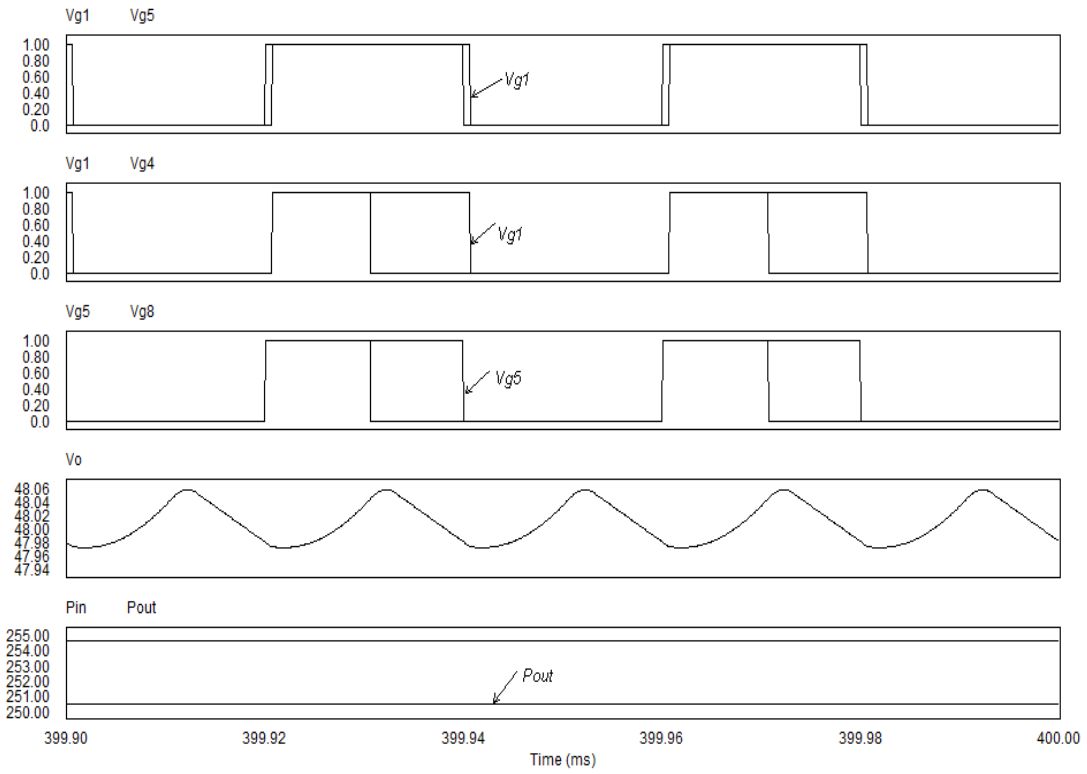

Fig. 2.15 Backward Simulation Results of Vo, Pin, Pout for Po=250W with Vref1=6V

V_{g1}: Control Signal for Power Switch Tr1

V_{g4}: Control Signal for Power Switch Tr4

V_{g5}: Control Signal for Power Switch Tr5

V_{g8}: Control Signal for Power Switch Tr8

V_o: Output Voltage of Backward Converter (Volts)

P_{in}: Average Input Power of Backward Converter (Watts)

P_{out}: Average Output Power of Backward Converter (Watts)

In Fig.2.15, the average input power and average output power can be observed. The efficiency of the backward converter under full load condition can be calculated as follows.

P_{in}=254.7W

P_{out}=250.53W

$$\eta = \frac{P_{out}}{P_{in}} = \frac{250.53}{254.7} = 98.4\% \quad (2\text{-}12)$$

V_o=48.01±0.05V

It can be found that the efficiency and voltage stability of bidirectional dual full bridge converter with novel triple phase-shift control method are satisfactory.

2: Efficiency of Bidirectional Dual Full Bridge Converter with Novel Triple Phase-shift Control in Large Load Scope

Table 2.2 Forward Output Power, Voltage and Efficiency

Pout (W)	1003	754.75	502.50	252.53
Vo (V)	200.3±0.01%	200.57±0.01%	200.54±0.01%	201±0.006%
Efficiency	97.6%	97.6%	98.4%	98.5%

Table 2.3 Backward Output Power, Voltage and Efficiency

Pout(W)	1008.32	751.88	499.84	250.53
Vo (V)	48.2±0.25%	48.04±0.19%	47.95±0.15%	48.01±0.1%
Efficiency	96.9%	97.3%	98.1%	98.4%

It can be found the efficiency of this bidirectional dual full bridge converter with novel triple phase-shift control is high in large load scope. Therefore, it is a good topology for this bidirectional DC-DC converter project.

3: Simulation of Bidirectional Full-half Converter with Dual Phase-shift Control

The power circuit of bidirectional full-half converter is shown in Fig.2.16 [2]. Compared with isolated bidirectional dual full bridge DC-DC power circuit, the isolated bidirectional full-half bridge power circuit uses 6 power switches. However, this topology will not allow the use of certain control methods. Its simulation circuit and parameters are attached in Appendix D. When magnetizing inductance is uncertain, the simulation results of bidirectional full-half bridge converter with dual phase-shift control method are listed in the following.

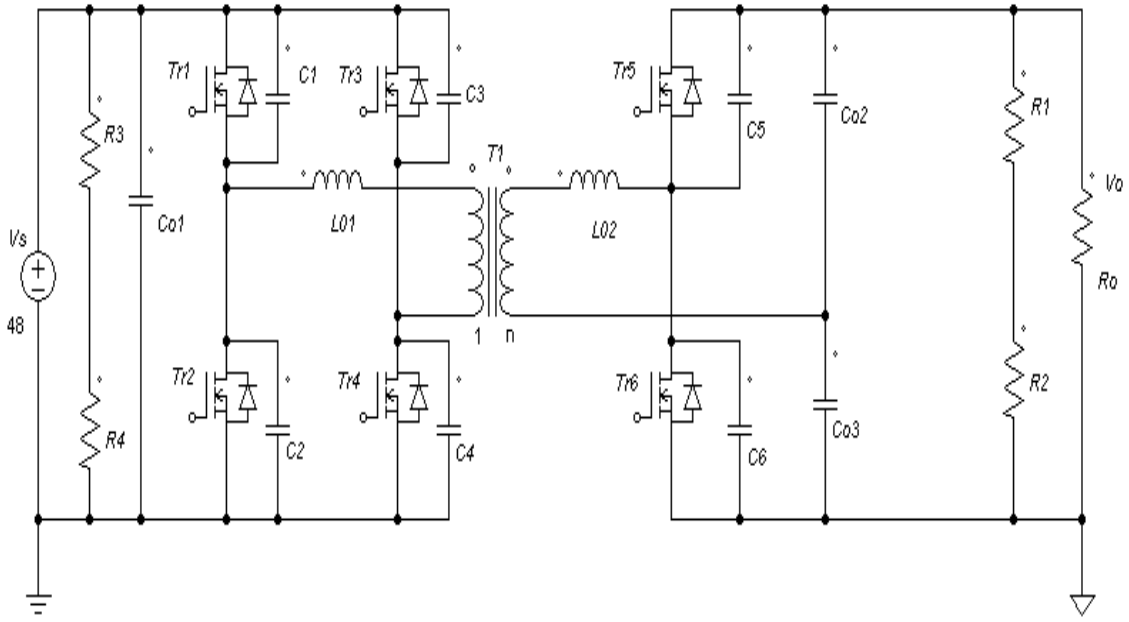

Fig. 2.16 Bidirectional Full-half Bridge Converter

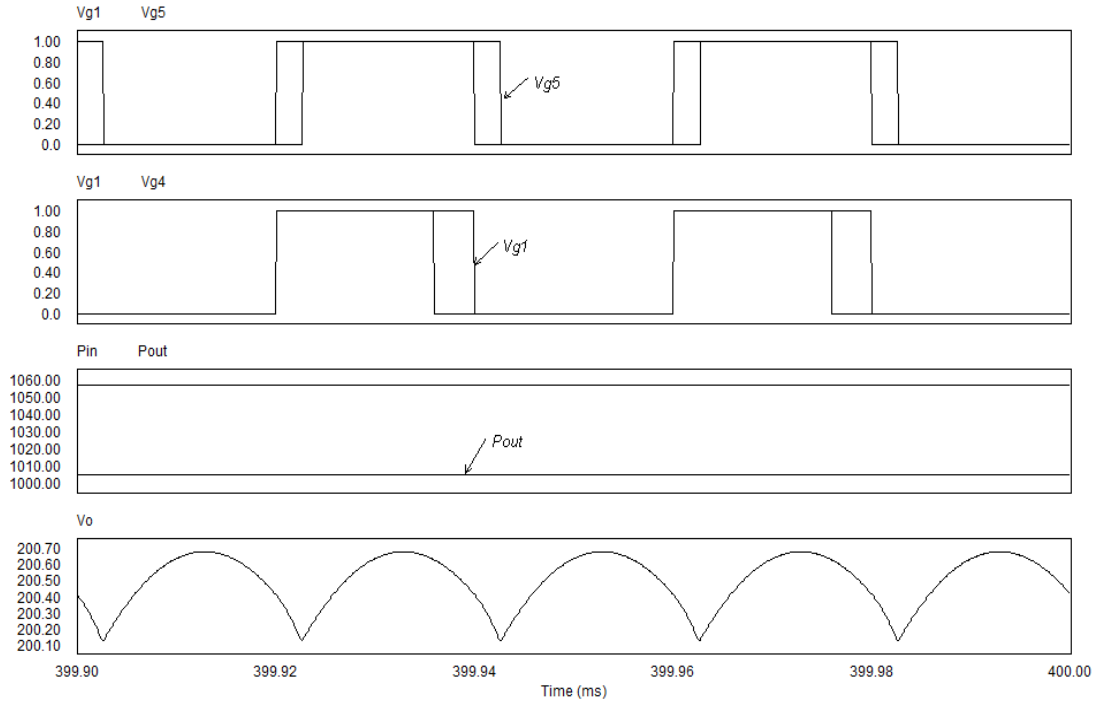

Fig. 2.17 Forward Simulation Results of Bidirectional Full-half Bridge Converter with Dual Phase-shift Control for Vref1=5V under Uncertain Lm

V_{g1}: Control Signal for Power Switch Tr1

V_{g4}: Control Signal for Power Switch Tr4

V_{g5}: Control Signal for Power Switch Tr5

V_o: Output Voltage of Forward Converter (Volts)

P_{in}: Average Input Power of Forward Converter (Watts)

P_{out}: Average Output Power of Forward Converter (Watts)

In Fig.2.17, the average input power and average output power can be observed. The efficiency of the forward converter under full load condition can be calculated as follows.

P_{in}=1056.97W

P_{out}=1005.03W

$$\eta = \frac{P_{out}}{P_{in}} = \frac{1005.03}{1056.97} = 95.1\% \quad (2\text{-}13)$$

V_o=200.5±0.2V

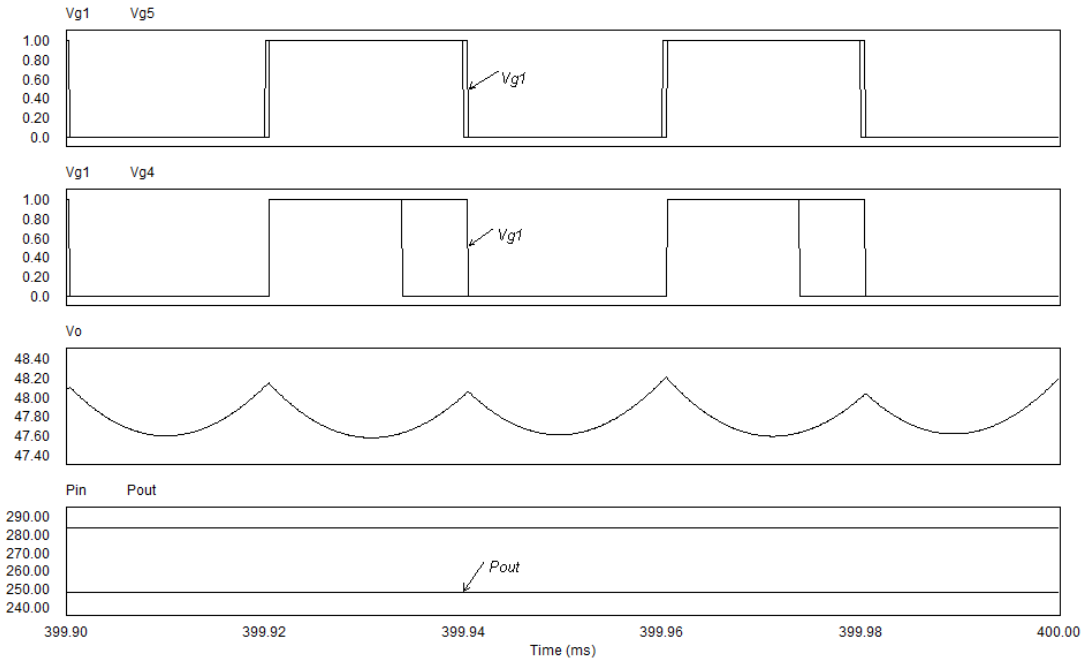

Fig. 2.18 Backward Simulation Results of Bidirectional Full-half Bridge Converter with Dual Phase-shift Control for Vref1=5V under Uncertain Lm

V_{g1}: Control Signal for Power Switch Tr1

V_{g4}: Control Signal for Power Switch Tr4

V_{g5}: Control Signal for Power Switch Tr5

V_o: Output Voltage of Backward Converter (Volts)

P_{in}: Average Input Power of Backward Converter (Watts)

P_{out}: Average Output Power of Backward Converter (Watts)

In Fig.2.18, the average input power and average output power can be observed. The efficiency of the backward converter under full load condition can be calculated as follows.

P_{in}=284.1W

P_{out}=248.3W

$$\eta = \frac{P_{out}}{P_{in}} = \frac{248.3}{284.1} = 87.4\% \qquad (2\text{-}14)$$

V_o=47.8±0.4V

4: Simulation of Bidirectional Voltage Clamped Converter with Single Phase-shift Control

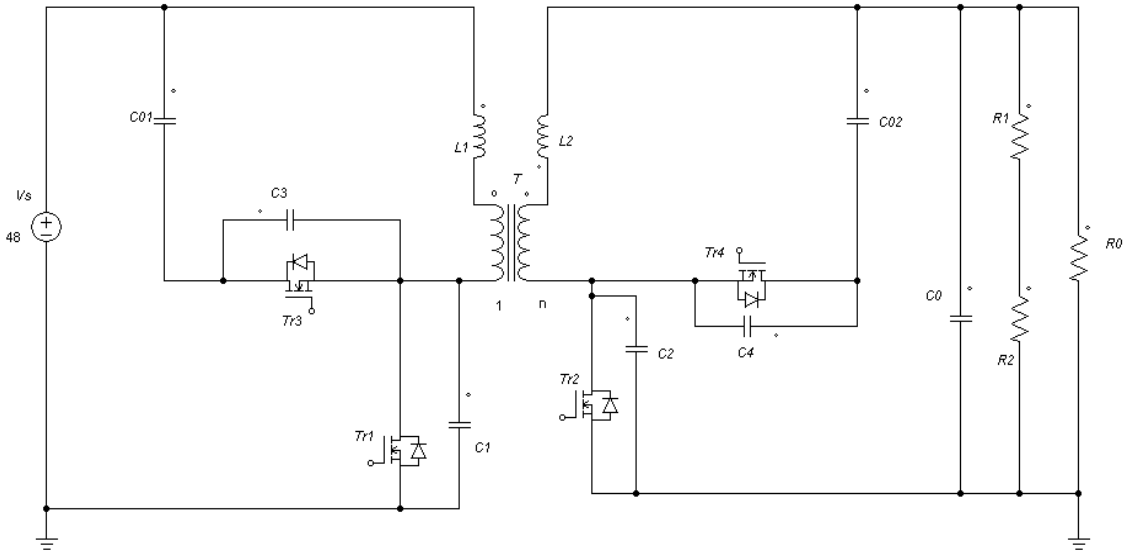

Fig. 2.19 Bidirectional Voltage Clamped Converter

The bidirectional voltage clamped converter is shown in Fig.2.19 [3]. The advantage of this simple bidirectional converter topology is that it contains only 4 power switches.

However, the number of available control methods will be less when compared with the bidirectional dual full bridge converter and bidirectional full-half bridge converter described above. Its simulation circuit is attached in Appendix E. The simulation results of bidirectional voltage clamped converter with single phase-shift control method are shown in Fig.2.20.

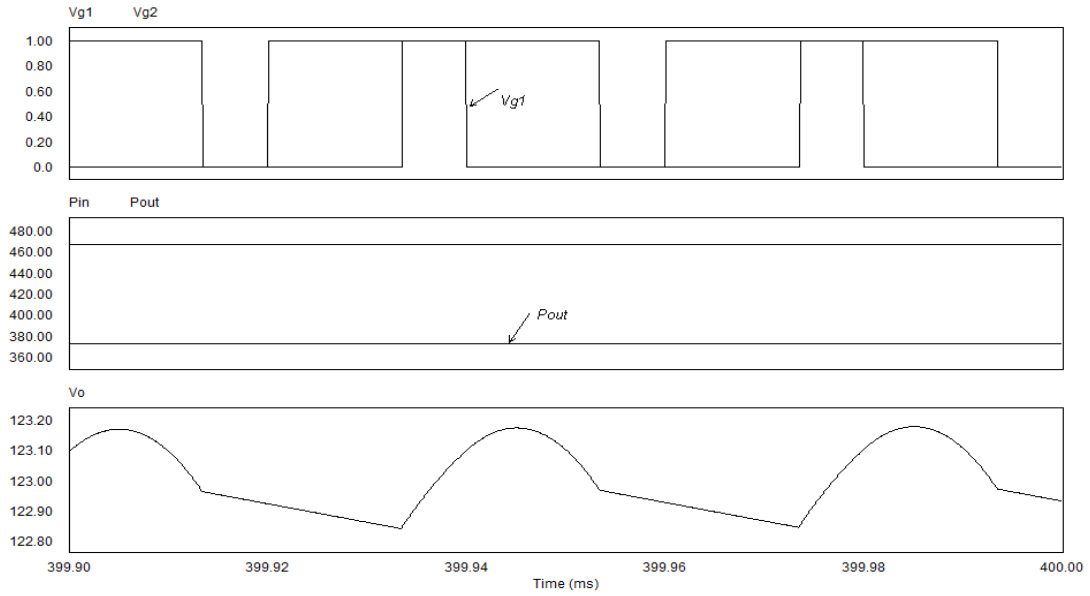

Fig. 2.20 Forward Simulation Results of Bidirectional Voltage Clamped Converter with Single Phase-shift Control for Vref1=5V under Uncertain Lm

V_{g1}: Control Signal for Power Switch Tr1

V_{g2}: Control Signal for Power Switch Tr2

V_o: Output Voltage of Forward Converter (Volts)

P_{in}: Average Input Power of Forward Converter (Watts)

P_{out}: Average Output Power of Forward Converter (Watts)

In Fig.2.20, it can be seen clearly that the bidirectional voltage clamped converter cannot transfer 1kW of output power when the value of the magnetizing inductance is uncertain no matter how to adjust the control circuit or feedback resistance. The output power always remains approximately 380W; the output voltage always remains approximately 123V. The efficiency is only equal to 76.3%. Certainly, this efficiency is

meaningless since the converter cannot transfer rated power (1kW).

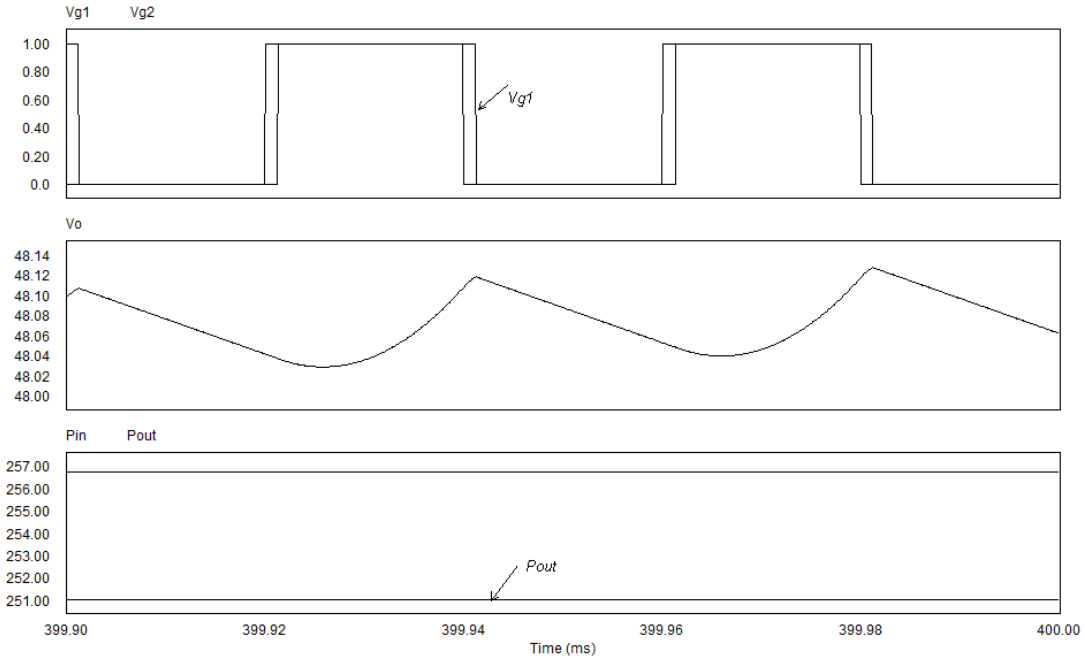

Fig. 2.21 Backward Simulation Results of Bidirectional Voltage Clamped Converter with Single Phase-shift Control for Vref1=5V under Uncertain Lm

V_{g1}: Control Signal for Power Switch Tr1

V_{g2}: Control Signal for Power Switch Tr2

V_o: Output Voltage of Backward Converter (Volts)

P_{in}: Average Input Power of Backward Converter (Watts)

P_{out}: Average Output Power of Backward Converter (Watts)

In Fig.2.21, the average input power and average output power can be observed. The efficiency of the backward converter under full load condition can be calculated as follows.

P_{in}=256.8W

P_{out}=251W

$$\eta = \frac{P_{out}}{P_{in}} = \frac{251}{256.8} = 97.7\% \qquad (2\text{-}15)$$

V_o=48±0.12V

5: Comparison of Three Different Bidirectional Converter Topologies when Parameter Changes

Table 2.4 Comparison of Three Bidirectional Converter Topologies under Uncertain *Lm*

	Bidirectional Dual Full Bridge Converter with Triple Phase-shift Control	Bidirectional Full Half Bridge Converter with Dual Phase-shift Control	Bidirectional Voltage Clamped Converter with Single Phase-shift Control
Forward Efficiency (*Pout*=1kW)	95.3%	95.1%	Cannot transfer 1kW output power 76.3%
Backward Efficiency (*Pout*=250W)	96.4%	87.4%	97.7%

By comparison of these three bidirectional converter topologies shown in Table 2.4, it can be found that bidirectional dual full bridge converter with triple phase-shift control is much better than the other two topologies. Therefore, the choice of bidirectional dual full bridge converter with triple phase-shift control as the topology for this project is correct.

2.6 Main Contribution

The main contribution of this chapter is to develop a novel triple phase-shift control method for the bidirectional dual full bridge DC-DC power circuit. Based on this novel triple phase-shift control method, a suitable topology has been determined for this project. The bidirectional dual full bridge DC-DC converter with novel triple phase-shift control method can work with high efficiency and output voltage stability in large load scope. Its efficiency is robust (insensitive) to parameter change. There have been no relevant papers

published on the topic of a triple phase-shift control algorithm for the bidirectional dual full bridge DC-DC power circuit until now.

2.7 Summary

In this chapter, three bidirectional power converters, namely, the bidirectional dual full bridge converter, the bidirectional full-half bridge converter and the bidirectional voltage clamped converter have been evaluated. After comparison, the bidirectional dual full bridge ZVS DC-DC power circuit was determined to be the most suitable for this project.

Single phase-shift control, dual phase-shift control and novel triple phase-shift control methods have been compared with each other with the same bidirectional dual full bridge power circuit when parameter changes. After comparison, the bidirectional dual full bridge converter with novel triple phase-shift control is used for this project because the efficiency is high in wide load scope. It was found that the efficiency and output voltage of the bidirectional converter with triple phase-shift control are robust (insensitive) to parameter change.

Chapter 3 Stability Analysis of Isolated Bidirectional Dual Active Full Bridge DC-DC Converter with Triple Phase-shift Control

[1]Based on the theory discussed in chapter 2, an isolated bidirectional dual full bridge DC-DC converter with novel triple phase-shift control is chosen for this project. In this chapter, detailed analysis will be given on how to study the stability of this bidirectional converter theoretically with Lyapunov function method.

3.1 Introduction

An identical dual active full bridge converter with zero voltage switching can be used on both sides of the isolation transformer as shown in Fig. 3.1 [1], [21]. A novel triple phase-shift control method can be used with this power circuit. Because this novel control method can make the system operate with high efficiency in large load scope and improve the adaptability of the system to parameters change, the isolated dual full bridge converter with triple phase-shift control method is used for this project. The circuit for this project is shown in Figure 3.1.

It is well known that the system must be stable if it is used to finish a task; if it is not stable, the system cannot be used [7], [15], [17]. From published papers about stability analysis of power converters with Lyapunov function method, they all use one Lyapunov function expressed as a convex combination of the energy functions of all possible

[1] A version of this chapter has been published. K. Wu, C. de Silva, W. Dunford, "Stability Analysis of Isolated Bidirectional Dual Active Full Bridge DC-DC Converter with Triple Phase-shift control," *IEEE Transactions on Power Electronics*, Vol. 27, No. 4, pp. 2007-2017, April 2012

switching stages in one period or a convex combination of multiple positive definite functions of all possible switching stages in one period to determine the stability of the power converter in the whole switching period [46-47]. As the number of power switches used in the power converter increases or soft switching technology is used, there will be many switching stages or sub-stages in one working period of the power converter. It will be very difficult to select many suitable coefficients to construct one suitable Lyapunov function to determine the stability of the power converter in one period with those published methods.

This chapter introduces a new method with Lypunov function to determine the stability of a nonlinear bidirectional DC-DC converter theoretically when parameters change randomly. In this new method, a suitable Lyapunov function is selected to determine the stability of the power converter in one switching stage or sub-stage, not to determine the stability of the power converter in one period. This is the basic difference between the published methods and this new method. Compared with published methods, the advantage of this new method is that it will be much more convenient to select several suitable Lyapunov functions to determine the stability of the power converter in one period. The similarity between the published methods and this new method is that they all use suitable Lyapunov function to determine the stability of the power converter.

In this new method, the power converter is separated into several stages in one period according to its normal simulation results. According to the working theory of the power converter in every stage, the equivalent circuit is built in the corresponding stage and state space model is built according to the equivalent circuit in every stage. The total energy of the equivalent inductors and capacitors in one stage is selected as a Lyapunov function to determine the stability of the power converter in that stage. If the derivative of this Lyapunov function is negative definite, the power converter will be stable in this stage. The stability of the power converter in every stage can be determined in this way. If the power converter is determined to be stable in every stage, the stability of the power

converter at the interface of two neighboring stages or sub-stages must be analyzed. If there are no abrupt state changes at the interface of two neighboring stages or sub-stages, it can be derived this power converter will be stable in the whole period.

It is very important to verify the bidirectional converter operates normally because some parameters may change during the working process of the bidirectional converter. This approach to stability analysis does not appear to have been published until now. Besides this, this method can be used to detect the stability of other similar nonlinear time-varying systems.

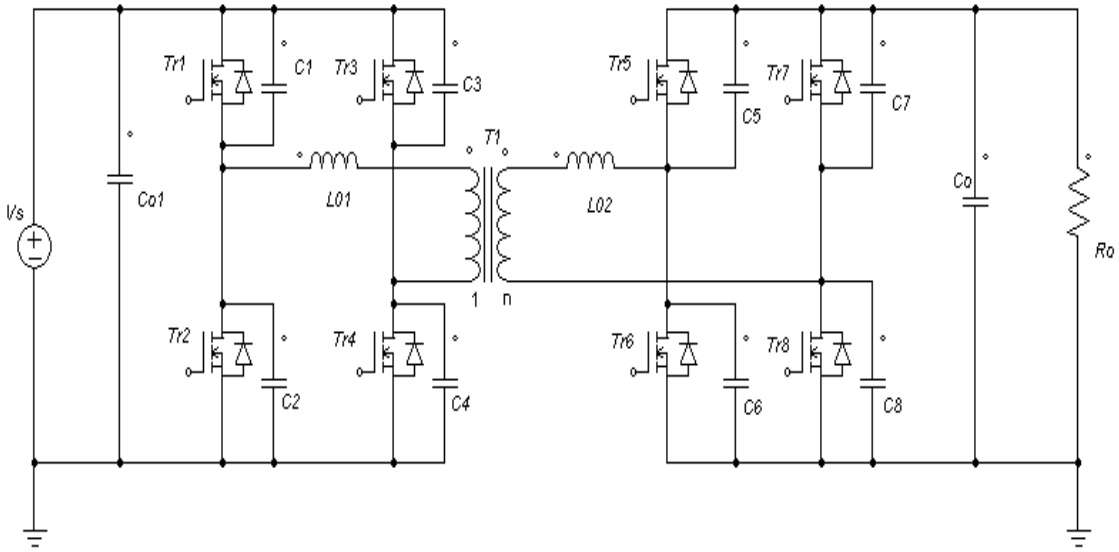

Fig. 3.1 Power Circuit of the Bidirectional Converter

3.2 Problem Description

1、*Statement of the Problem*

In power electronics, stability is usually determined by observing simulation results because the power converter is nonlinear and theoretical stability analysis is very difficult. This is especially true for high power zero voltage switching (ZVS) converters [11], [16]. However, the simulation method is not always correct because simulation results only provide information for separate working states. When parameters change due to

possibly unknown reasons, the converter will work in different states. Its stability is unknown if the corresponding simulation is not made for this new state. It is impossible to simulate the infinite number of possible working conditions. Only when the stability is analyzed theoretically, will the answer to the stability problem be definite [27].

The problem is to find an effective method to determine the stability of a bidirectional DC-DC converter with triple phase-shift control and possible parameters change. In order to solve this problem theoretically, an available mathematical model should be built for this bidirectional converter with triple phase-shift control. The bidirectional converter with triple phase-shift control is a nonlinear system. Besides this, the parameter-change must be taken into account when determine its stability. An even more complicated problem is that the rule of parameter-change is unknown.

Although this problem is very difficult and complex, it can be found this bidirectional converter works periodically according to its working theory. This bidirectional converter can be separated into several stages in one period according to its normal simulation results. According to its working theory, an equivalent circuit can be built for every stage or sub-stage by replacing the nonlinear power switches and diodes with its approximate linear models, e.g. replacing the power MOSFET with its on-resistance when it conducts and replacing the diodes with voltage sources which are equal to their conduction voltage values. In this way, an approximately linear time-varying equivalent circuit model can be built for each stage or sub-stage. According to the equivalent circuit, the approximately time-varying state equation can be built for each stage or sub-stage. This makes it possible to determine theoretically the stability of the bidirectional converter in every stage and in the whole period.

2: Components in Power Circuit

L_{01}, L_{02} ---- Two series inductors

$C_1=C_2=C_3=C_4=C_5=C_6=C_7=C_8$ --- Eight snubber capacitors

C_o, C_{o1} ---Two large filter capacitors

Ro --- Forward load resistor

The parameters of the main transformer are as follows:

Lp ---Primary leakage inductance

Ls --- Secondary leakage inductance

Rp --- Primary winding resistance

Rs--- Secondary winding resistance

Turns ratio: 1: n

The parameters of the eight power MOSFETs are as follows:

R_1, R_2, R_3, R_4, R_5, R_6, R_7, R_8 ---- On resistance

D_1, D_2, D_3, D_4, D_5, D_6, D_7, D_8 --- Anti-parallel diodes with power MOSFETs.

3: Variables Used in the Chapter

iap, ias ---Power circuit primary current and secondary current of the transformer

Vc1, Vc2, Vc3, Vc4, Vc5, Vc6, Vc7, Vc8 ---Voltages across corresponding parallel capacitors.

Vs ---Input voltage

Vo ---Output voltage

V_{D1}, V_{D2}, V_{D3}, V_{D4}, V_{D5}, V_{D6}, V_{D7}, V_{D8} ----Forward conduction voltages of anti-parallel diodes.

3.3 Objectives and Rationale

The objective of this chapter is to analyze the stability of a bidirectional DC-DC converter with Lyapunov function method theoretically for any parameter change. After a novel topology is determined, the stability of this topology should be analyzed. If it is not stable, this topology cannot be used.

Although the isolated bidirectional dual full bridge power circuit is often used by others, the novel triple phase-shift control method is developed the first time in the world. It is well known the stability of a control system is determined by the combination of its

main circuit and control circuit. Its stability is unknown. Therefore, the stability of this novel topology should be analyzed. The bidirectional dual full bridge converter with triple phase-shift control is a nonlinear system. The parameters of the power circuit elements and input voltage will always change during real application. Therefore, the bidirectional dual full bridge converter with novel triple phase-shift control is a nonlinear time varying system. The first choice of its stability analysis is to use Lyapunov method.

3.4 Equivalent Circuits of this Bidirectional Converter Topology

The forward simulation wave-forms of the bidirectional converter with normal steady state operation are as follows:

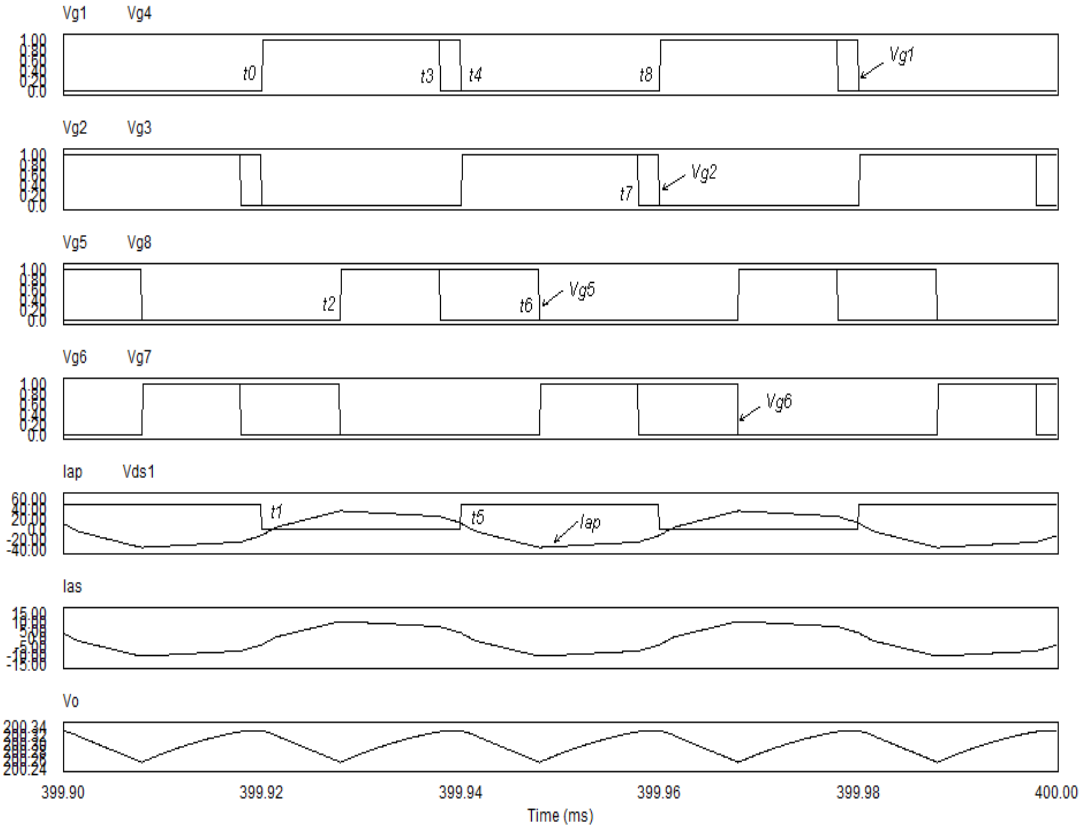

Fig. 3.2 Simulation Wave-Forms of the Forward Bidirectional Converter with Triple Phase-shift Control

As shown in Fig.3.2, this novel triple phase-shift control method includes three

phase-shifts. The first is the phase-shift between the primary control signal and the corresponding secondary control signal, for example, between V_{g1} and V_{g5}; the second is the phase-shift between the diagonal control signals in the primary power circuit, for example, between V_{g1} and V_{g4}; the third is the phase-shift between the diagonal control signals in the secondary power circuit, for example, between V_{g5} and V_{g8}. The forward bidirectional dual full bridge converter is separated into eight stages in one period. Its operation and equivalent circuit for each stage are described below.

1: Stage 1 (t_0~t_1): Power switches *Tr1* and *Tr4* will turn on at "$t=t_0$". Because the primary current is still negative during this period, the inductor energy flows back to the power source. The primary current will flow through *Tr4*/*Tr1*. This is because the voltage drop across the on-resistance of the power MOSFET during conduction is lower than the required conduction voltage drop of the anti-parallel diode. Therefore, the diode will not conduct. This is normally the case.

Because V_{g5}/V_{g8}/V_{g7} are equal to zero, *Tr5*/*Tr8*/*Tr7* all in "Off" state; V_{g6}=1, *Tr6* is "On". Because *ias*<0, secondary current flows through *Tr6*/D_7. The inductor L_{02} and output capacitor provide energy to the load. The output voltage reduces during this stage. The equivalent circuit in this stage is as follows:

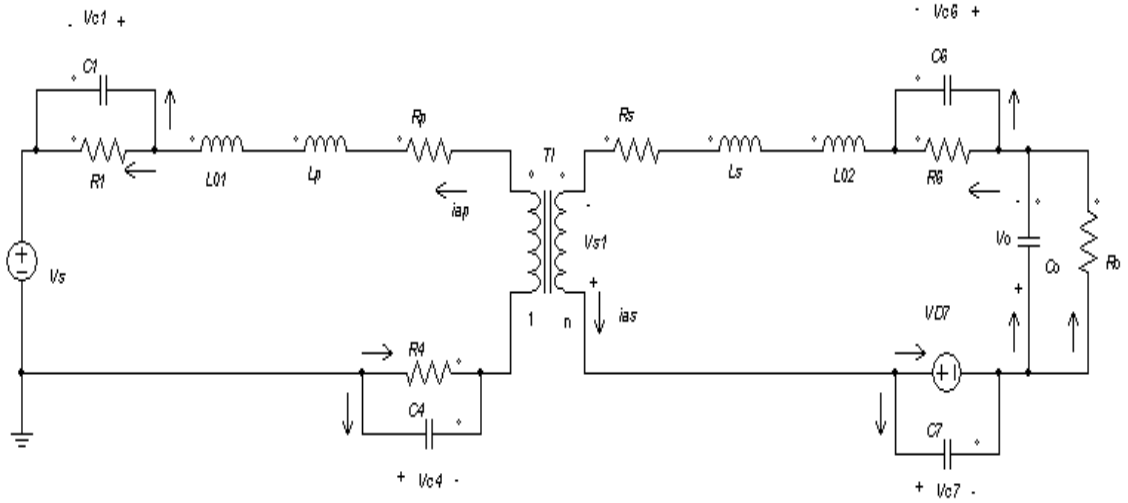

Fig. 3.3 Equivalent Circuit in Stage 1

2: Stage 2 (t_1~t_2): Because V_{g1}/ V_{g4} =1, power switches *Tr1* and *Tr4* are in "On" state in

this stage. Because the primary current is positive during this stage, the primary current will flow through *Tr1*/*Tr4* and the inductor L_{01} and transformer leakage inductance. The energy will transfer from the primary side to the secondary side.

Because V_{g5}/V_{g8}/V_{g7} are equal to zero, *Tr5*/*Tr8*/*Tr7* are in "Off" state; V_{g6}=1, *Tr6* is "On". Because *ias*>0, secondary current will charge capacitor C_7 and discharge capacitor C_8 till its voltage reduces to the forward conduction voltage of diode D_8. The equivalent circuit in this sub-stage is as follows:

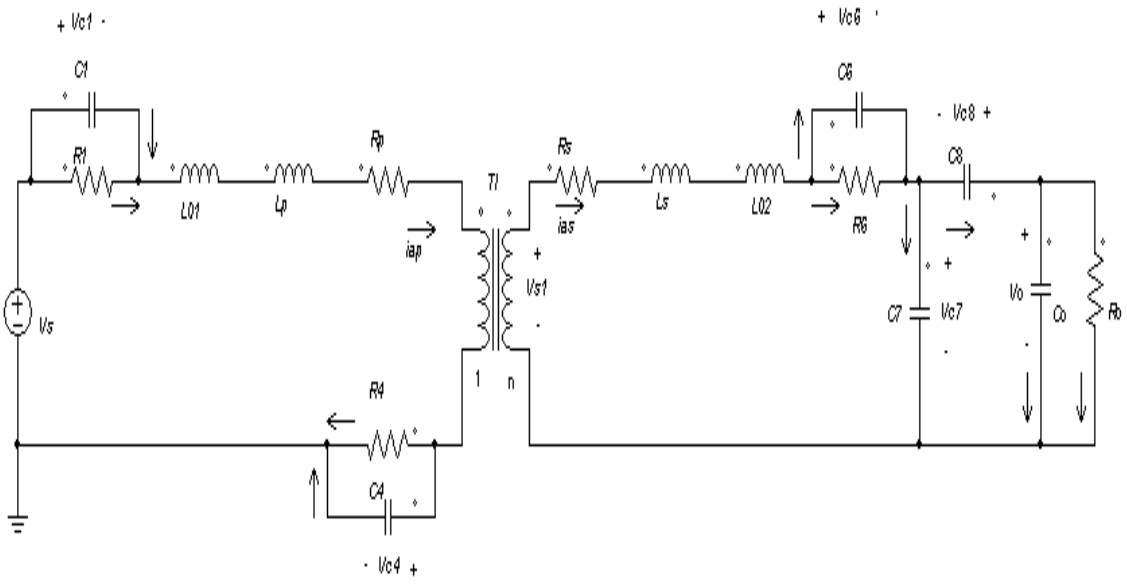

Fig. 3.4 C_8 Discharging Equivalent Circuit in Stage 2

Then the current flows through *Tr6*/D_8. The energy is stored in the secondary inductor L_{02} and leakage inductor because this is a free-wheeling sub-stage with no power transferred to the load theoretically. Output capacitor provides energy to the load. The output voltage continues to reduce in this sub-stage. The equivalent circuit in this sub-stage is as follows:

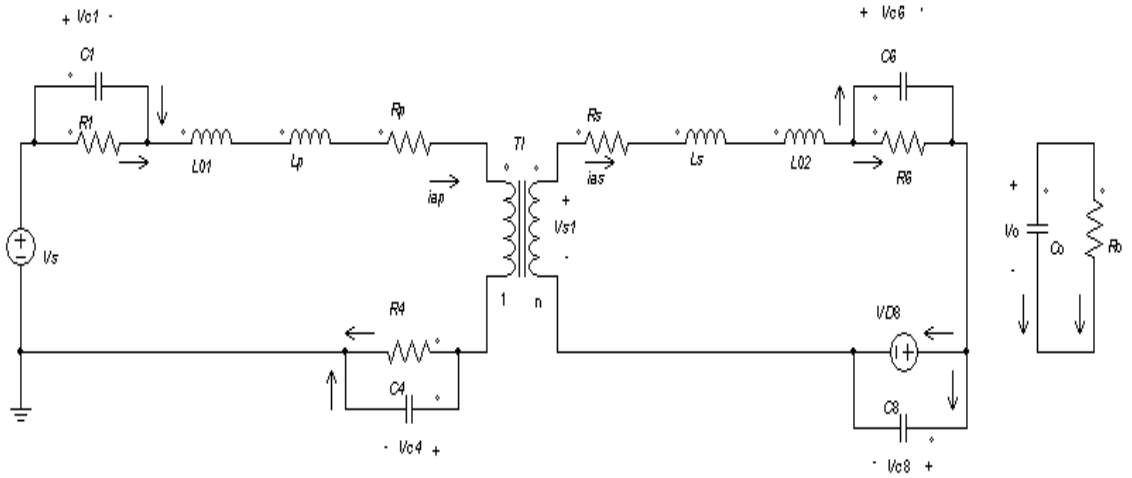

Fig. 3.5 Free Wheeling Equivalent Circuit in Stage 2

Tr6 turns off a little before t_2. The secondary current will charge snubber capacitor C_6 and discharge snubber capacitor C_5. During this very short transitional time, the secondary current flows through D_8 to charge and discharge the snubber capacitors. When C_5 is totally discharged ($Vds5$=0), the secondary current will flow through D_5/D_8 and the energy will be transferred to the load. The corresponding equivalent circuits are as follows:

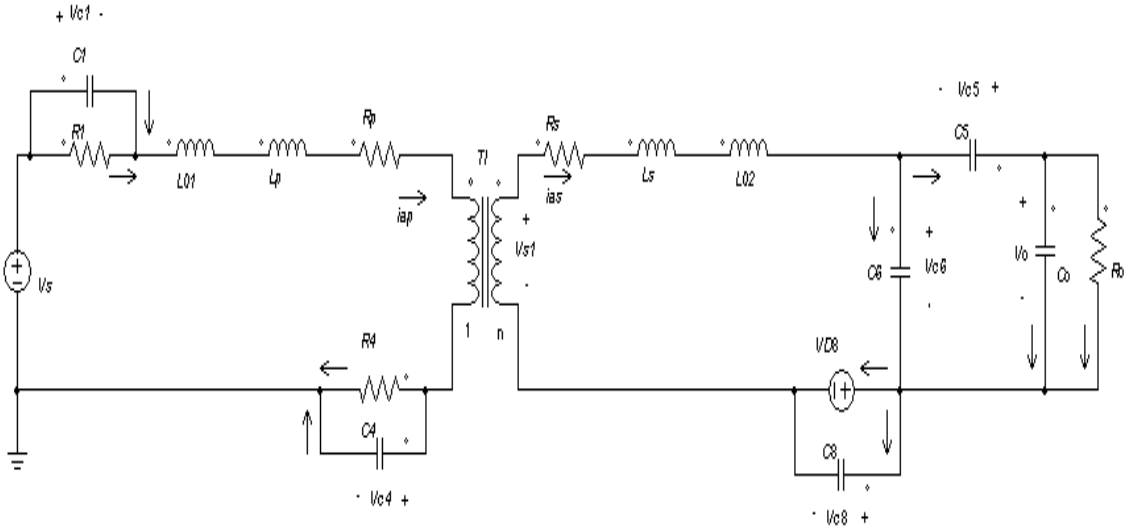

Fig. 3.6 Charge-Discharge Equivalent Circuit in Stage 2

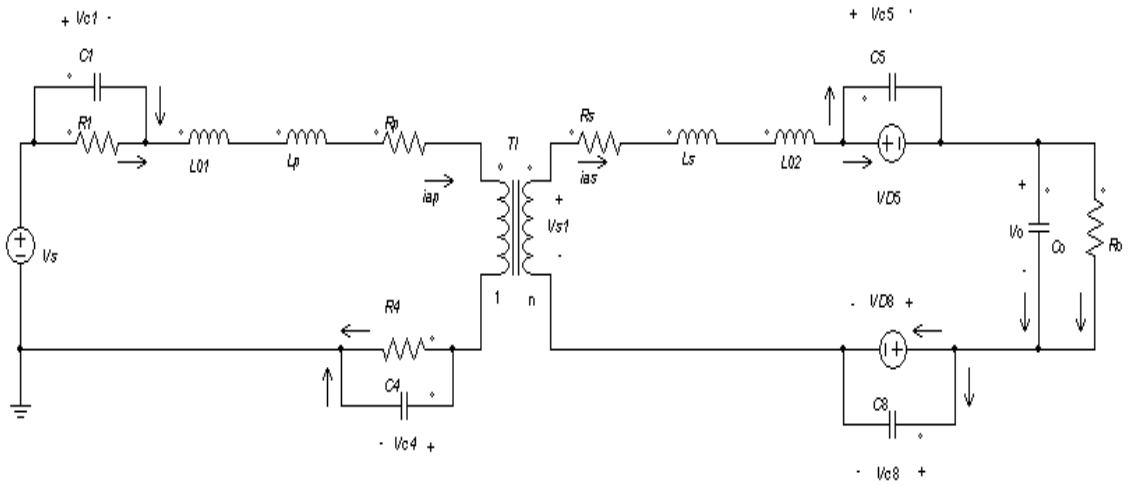

Fig. 3.7 Diode Conduct Equivalent Circuit in Stage 2

3: Stage 3 (t_2~t_3): The control signal V_{g5}/V_{g8}=1, power switches *Tr5*/*Tr8* will turn on at t_2. Because *ias*>0 during this stage, the secondary side current will flow through *Tr5*/*Tr8* and transfer energy to the load in this stage. The output voltage will increase in this stage. The equivalent circuit in this stage is as follows:

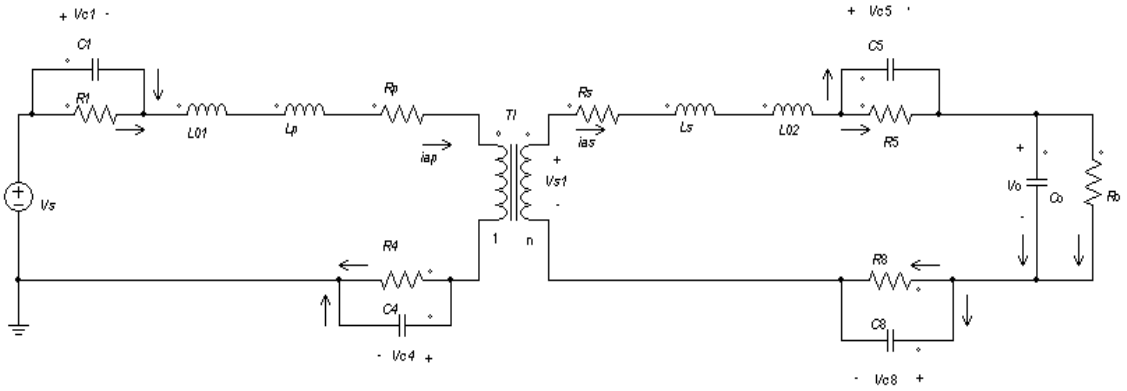

Fig. 3.8 Energy Transfer Equivalent Circuit in Stage 3

4: Stage 4 (t_3~t_4): V_{g4}/V_{g8}=0, so, *Tr4*/*Tr8* will turn off at t_3. For the primary side, *Tr4* turns off at t_3. The primary current will charge snubber capacitor C_4 and discharge snubber capacitor C_3. When C_3 is totally discharged (*Vds3*=0), the primary current will flow through *Tr1*/D_3 and form a free-wheeling sub-stage. No power is transferred to the secondary side theoretically.

For the secondary side, the current *ias*>0, this indicates *Tr5*/D_8 will continue to conduct in this period of time. The additional inductor L_{02} and secondary leakage inductance will provide energy to transfer to the load. The output voltage will continue to increase in this stage. The equivalent circuits are shown in Fig. 3.9 and Fig. 3.10.

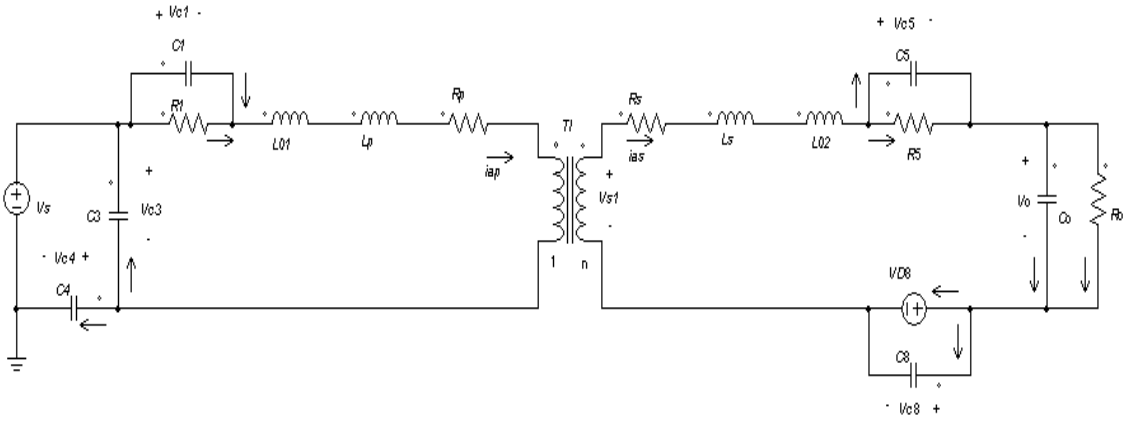

Fig. 3.9 C_3 Discharge Equivalent Circuit in Stage 4

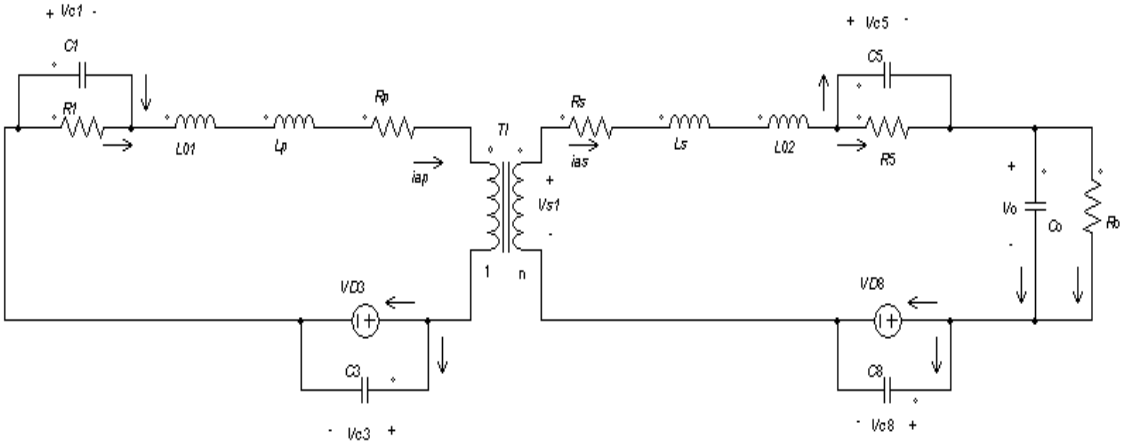

Fig. 3.10 Free Wheeling Equivalent Circuit in Stage 4

Tr1 turns off a little before t_4. The primary current will discharge snubber capacitor C_2 and charge snubber capacitor C_1. During this very short transitional time, the current will flow through D_3 to charge and discharge capacitors. When C_2 is totally discharged (*Vds2*=0), D_2 will conduct and form an energy feedback to power source. This will make it feasible for *Tr2*/*Tr3* to turn on under ZVS. The equivalent circuits are shown in Fig. 3.11 and Fig. 3.12.

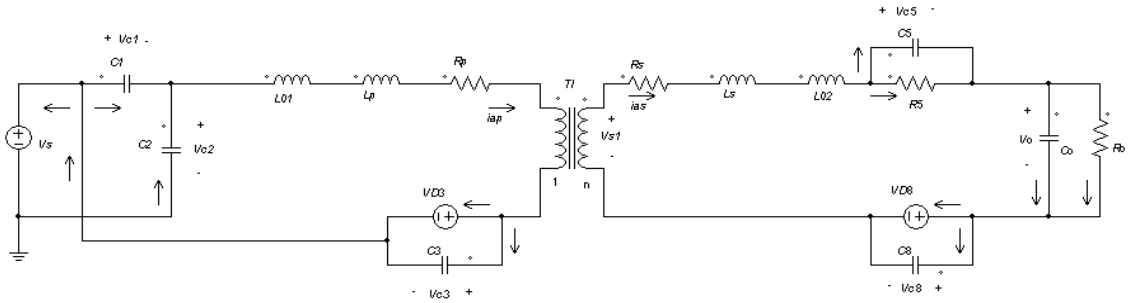

Fig. 3.11 C_2 Discharge Equivalent Circuit in Stage 4

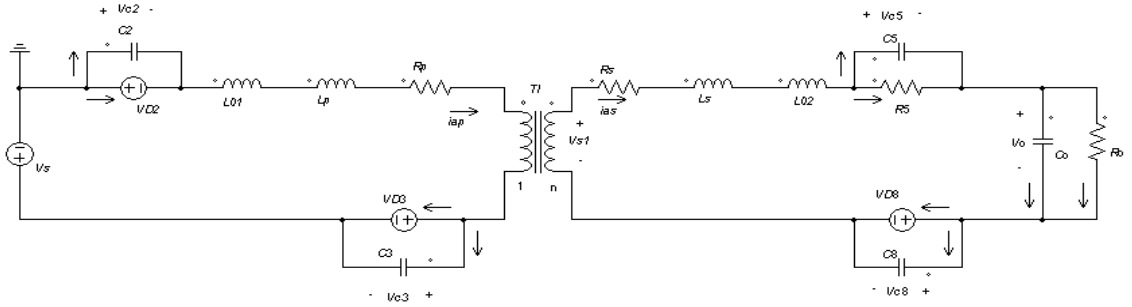

Fig. 3.12 Energy Feedback Equivalent Circuit in Stage 4

5: Stage 5 (t_4~t_5): Because V_{g2}/V_{g3}=1, *Tr2*/*Tr3* will turn on at t_4 under ZVS. Because the primary current *iap*>0, the energy will feedback to the primary source in this stage.

For the secondary side, V_{g5}=1, so, *Tr5* is "On" in this stage. $V_{g6}/V_{g7}/V_{g8}$=0, so, *Tr6*/*Tr7*/*Tr8* will be in off state during this period of time. Because the secondary current *ias*>0, *Tr5*/D_8 will conduct in this period of time. The inductor L_{02}, the secondary leakage inductor and output capacitor will provide energy to the load together in this stage. The output voltage begins to reduce in this stage. According to this analysis, the equivalent circuits in this stage can be obtained.

6: Stage 6 (t_5~t_6): Because V_{g2}/V_{g3}=1, *Tr2*/*Tr3* will be on in this stage. Because the primary current *iap*<0, the energy will transfer to the secondary side again.

For the secondary side, V_{g5}=1, so, *Tr5* is on in this stage. $V_{g6}/V_{g7}/V_{g8}$=0, so, *Tr6*/*Tr7*/*Tr8* will be in the off state. Because the secondary current *ias*<0, the secondary current will charge capacitor C_8 and discharge capacitor C_7 till its voltage reduces to the

forward conduction voltage of diode D_7. Then the current flows through $Tr5/D_7$ and forms a free-wheeling sub-stage with no energy transferred to the load theoretically in this stage. The energy from primary source is stored in L_{02} and the leakage inductor. The output capacitor provides energy to the load and the output voltage will continue to reduce in this stage. The equivalent circuit can be obtained.

7: Stage 7 (t_6~t_7): Because V_{g6}/V_{g7}=1, *Tr6*/*Tr7* will turn on at t_6. V_{g5}=0, so *Tr5* turns off a little before t_6. The secondary current will charge C_5 and discharge C_6. During this very short transitional time, the secondary current flows through D_7 to charge and discharge snubber capacitors. When C_6 is totally discharged (*Vds6*=0), D_6 will turn on and D_6/D_7 will conduct to form ZVS and transfer energy to the load. Because the secondary side current *ias*<0, *Tr6*/*Tr7* will conduct in this period of time and transfer energy to the load in this stage. The output voltage will increase in this stage. The equivalent circuits in this stage can be obtained.

8: Stage 8 (t_7~t_8)*:* Because V_{g3}/V_{g7}=0 at t_7, *Tr3*/*Tr7* will turn off at t_7. For the primary side, *Tr3* turns off. The primary current will charge C_3 and discharge C_4. During this very short transitional time, the primary current flows through *Tr2* to charge and discharge snubber capacitors C_3 and C_4. When C_4 is totally discharged (*Vds4*=0), D_4 will turn on.$Tr2/D_4$ conduct, this forms a free-wheeling sub-stage with no energy transferred to the secondary side.

Tr2 turns off a little before t_8. The energy stored in additional inductor L_{01} and transformer leakage inductance will charge the snubber capacitor C_2 and discharge snubber capacitor C_1. During this very short transitional time, the primary current flows through D_4 to charge and discharge snubber capacitors. When C_1 is totally discharged (*Vds1*=0), then the primary current will flow through D_4/D_1 and the inductor energy flows back to the power source.

For the secondary side, $Tr6/D_7$ will continue conduct during this period of time and transfer energy to the load. This is because the secondary side current *ias*<0. The energy

mainly comes from the stored energy of additional inductor L_{02} and the leakage inductance. The output voltage will continue to increase in this stage. The corresponding equivalent circuits can be obtained.

3.5 Stability Analysis

The stability of the bidirectional dual full bridge DC-DC converter can be determined theoretically with Lyapunov method for any parameter change. This method will be explained in the following discussion.

1、Brief Statement of this Method

The bidirectional DC-DC converter is an essentially nonlinear system in the whole working period due to the operation of nonlinear elements. However, it can be separated into several stages according to the simulation wave-forms at a normal working situation. Each stage is basically linear. Its equivalent circuit and corresponding state equation in every stage can be built. Therefore, its stability can be analyzed theoretically in every stage. If the converter is stable in every stage and there is no abrupt state change at the interface of two stages, this converter will be stable during the whole working period.

Here, abrupt state change means instantaneous change in state variables at the interface of different stages. In the present system, the state variables are capacitor voltages and inductor currents. It is known that state variables cannot change instantaneously under bounded input conditions [17]. This can be seen clearly from the operation of the converter as presented in Section 3.4. The capacitor voltage or inductor current cannot change instantaneously at the interface of any two stages unless an infinite current input or noise is applied to the capacitor or an infinite voltage input or noise is applied to the inductor at that instant [17]. Infinite inputs or infinite noise are not realizable in a converter.

2、Stability Analysis of Power Converters under Parameter Changes

A linear homogeneous time-invariant system has the origin as an equilibrium point. Its

stability is characterized by the locations of the eigenvalues of the stability matrix **A**. The equilibrium point is asymptotically stable if the real parts of eigenvalues of **A** are negative. Asymptotic stability of the origin can also be investigated by using the Lyapunov method.

The parameters of the bidirectional converter may change during operation. For example, the input voltage and output load may vary; resistance of power MOSFET may change with the temperature change; the leakage inductance of the transformer and other parameters are subjected to variations and aging; and so on. In general, how parameters change during the operation of the converter is unknown. The converter in every stage is approximately a linear time-varying system. The Hurwitz matrix A is variable and it is not possible to determine the eigenvalues of matrix A to decide the stability of the bidirectional converter for this general case. Therefore, the Lyapunov method is used to determine the stability of the bidirectional converter when parameters change.

If a positive definite Lyapunov function can be found for the bidirectional converter in a stage and its derivative is negative definite in this stage, the equilibrium point of the bidirectional converter is internally asymptotically stable in this stage. The complete bidirectional converter with input signal will be bounded-input-bounded-output (BIBO) stable in this stage [7].

There is no need to find a common Lyapunov function for all stages. If every stage can be proved BIBO stable using the Lyapunov method, the entire converter will be BIBO stable if the state variables do not change instantaneously at the interface of different stages.

3. Stability Determination of a Bidirectional Converter with Triple Phase-shift Control

Based on the equivalent circuits in each stage, the corresponding state equation can be built for this bidirectional DC-DC converter in each stage. The equivalent circuits are got by the analysis of the combination act of the input signal, output signal and control signal of this closed-loop converter. According to model identification [23], [26], the equivalent circuits in

each stage are closed-loop models for this nonlinear converter. The corresponding state equation will be a closed-loop state space model of this bidirectional converter in each linear stage. It can be used to determine the stability of this bidirectional converter in every linear stage directly.

Although there is a small signal model for the bidirectional dual full bridge converter for the controller design [24], it cannot be used for the stability analysis when parameters change. This is because the small signal model is got by assuming the parameters are fixed. Some parameters are always changing in practical application. Small signal model is only an approximate model of the bidirectional converter.

(1)： Stability Analysis in Stage t_0~t_1

From the equivalent circuit of the converter as shown in Fig.3.3, the state equation of the converter can be built in this stage. In order to be convenient, write：

$$Leq = L_{01} + Lp + \frac{1}{n^2} * L_{02} + \frac{1}{n^2} * Ls \ ; \ Req = Rp + \frac{1}{n^2} * Rs;$$

$$\begin{cases} Leq * \frac{diap}{dt} = -Req * iap \ - Vc1 - Vc4 - \frac{1}{n} * Vc6 - \frac{1}{n} * Vo - \frac{1}{n} * V_{D7} - Vs \\ C_1 * \frac{dVc1}{dt} = iap - \frac{Vc1}{R_1} \\ C_4 * \frac{dVc4}{dt} = iap - \frac{Vc4}{R_4} \\ C_6 * \frac{dVc6}{dt} = \frac{1}{n} * iap - \frac{Vc6}{R_6} \\ Co * \frac{dVo}{dt} = \frac{1}{n} * iap - \frac{Vo}{Ro} \\ Vo = Vo \end{cases} \tag{3-1}$$

Therefore, the closed-loop state space model of this converter during this stage can be expressed as follows:

$$\begin{cases} \dot{\boldsymbol{x}} = \boldsymbol{A}(\boldsymbol{t})\boldsymbol{x} + \boldsymbol{B}(\boldsymbol{t})\boldsymbol{u} \\ y = \boldsymbol{C}\boldsymbol{x} \end{cases} \tag{3-2}$$

$\boldsymbol{x} = [iap\ Vc1\ Vc4\ Vc6\ Vo]^T$

$\boldsymbol{u} = [V_{D7}\ Vs]^T$

$y = Vo$

The internal stability of this system can be decided by its corresponding homogeneous system with the Lyapunov method [7], [15]. Its homogeneous system is:

$$\dot{\boldsymbol{x}} = \boldsymbol{A}(\boldsymbol{t})\boldsymbol{x} \tag{3-3}$$

The Lyapunov function is chosen as:

$$V(x) = \frac{1}{2} * Leq * iap^2 + \frac{1}{2} * C_1 * Vc1^2 + \frac{1}{2} * C_4 * Vc4^2 + \frac{1}{2} * C_6 * Vc6^2 + \frac{1}{2} * Co * Vo^2 \tag{3-4}$$

Obviously, this Lyapunov function is positive definite. The derivative of this Lyapunov function is as follows:

$$\dot{V}(x) = -Req * iap^2 - \frac{Vc1^2}{R_1} - \frac{Vc4^2}{R_4} - \frac{Vc6^2}{R_6} - \frac{Vo^2}{Ro} \tag{3-5}$$

The derivative of this Lyapunov function is negative definite. Therefore, the homogeneous system in this stage is asymptotically internal stable and the bidirectional converter with input and output is BIBO stable in this stage.

(2)： Stability Analysis in Stage t_1~t_2

From the previous analysis of the converter working process, it can be found there are four sub-stages and four corresponding equivalent circuits in this stage. The stability of the converter can be analyzed in these four sub-stages with their equivalent circuits, state equations and Lyapunov method one by one.

(A) Sub-stage of Charge-discharge of C_7 and C_8

According to the equivalent circuit of the converter shown in Fig.3.4, the corresponding state equation for this converter can be built. In order to be convenient, write:

$$Ceq = \frac{C_7 * C_8 + Co * C_7 + Co * C_8}{Co + C_8}$$

$$\begin{cases} Leq\frac{diap}{dt} = -Req * iap - Vc1 - Vc4 - \frac{1}{n} * Vc6 - \frac{1}{n} * V_{C7} + Vs \\ C_1 * \frac{dVc1}{dt} = iap - \frac{Vc1}{R_1} \\ C_4 * \frac{dVc4}{dt} = iap - \frac{Vc4}{R_4} \\ C_6 * \frac{dVc6}{dt} = \frac{1}{n} * iap - \frac{Vc6}{R_6} \\ Ceq * \frac{dV_{C7}}{dt} = \frac{1}{n} * iap - \frac{C_8}{Ro*(C_8*Co)} * (Vc7 + Vc8) \\ Co * \frac{dVo}{dt} = -\frac{Vo}{Ro} \\ Vo = Vc7 + Vc8 \\ Vo = Vo \end{cases}$$

(3-6)

Therefore, the closed-loop state space model of this converter during this sub-stage can be expressed as follows:

$$\begin{cases} \dot{\boldsymbol{x}} = \boldsymbol{A}(\boldsymbol{t})\boldsymbol{x} + \boldsymbol{B}(\boldsymbol{t})u \\ y = \boldsymbol{C}\boldsymbol{x} \end{cases}$$

(3-7)

$\boldsymbol{x}$ =$[iap\ Vc1\ Vc4\ Vc6\ Vc7\ Vo]^T$

u =Vs

y = Vo

The Lyapunov function for the bidirectional converter in this sub-stage can be chosen as follows:

$$V(x) = \frac{1}{2} * Leq * iap^2 + \frac{1}{2} * C_1 * Vc1^2 + \frac{1}{2} * C_4 * Vc4^2 + \frac{1}{2} * C_6 * Vc6^2 + \frac{1}{2} * Ceq * Vc7^2 + \frac{1}{2} * Co * Vo^2 \quad (3\text{-}8)$$

Obviously, this Lyapunov function is positive definite. Its derivative in this sub-stage is as follows:

$$\dot{V}(x) = -Req * iap^2 - \frac{Vc1^2}{R_1} - \frac{Vc4^2}{R_4} - \frac{Vc6^2}{R_6} - \frac{C_8 * Vc7 * Vo}{Ro*(Co+C_8)} - \frac{Vo^2}{Ro} \quad (3\text{-}9)$$

In this sub-stage, capacitor C_7 is charged. Therefore, *Vc7* increases from zero to *Vo* gradually. If *Vo* is not equal to zero, this means the sign of *Vc7* and *Vo* is the same. Therefore, the product of *Vc7* and *Vo* is positive. Besides this, the capacitance of *Co* is far greater than that of C_8; there is the following relation:

$$\frac{C_8 * Vc7 * Vo}{Ro*(Co+C_8)} \ll \frac{Vo^2}{Ro} \quad (3\text{-}10)$$

Therefore, the derivative of the Lyapunov function in this sub-stage is negative definite. The homogeneous system is asymptotically internal stable and the bidirectional converter with input is BIBO stable in this sub-stage. If *Vo* is equal to zero, the duration time of this sub-stage will be equal to zero and this sub-stage will disappear.

(B) Sub-stage of Free Wheeling in Stage 2

According to the equivalent circuit of the converter in free-wheeling stage shown in Fig.3.5, the corresponding state equation for this converter during this sub-stage can be built as following:

$$\begin{cases} Leq\frac{diap}{dt} = -Req * iap - Vc1 - Vc4 - \frac{1}{n} * Vc6 - \frac{1}{n} * V_{D8} + Vs \\ C_1 * \frac{dVc1}{dt} = iap - \frac{Vc1}{R_1} \\ C_4 * \frac{dVc4}{dt} = iap - \frac{Vc4}{R_4} \\ C_6 * \frac{dVc6}{dt} = \frac{1}{n} * iap - \frac{Vc6}{R_6} \\ Co * \frac{dVo}{dt} = -\frac{Vo}{Ro} \\ Vo = Vo \end{cases} \quad (3\text{-}11)$$

Therefore, the closed-loop state space model of this converter during this sub-stage can be expressed as follows:

$$\begin{cases} \dot{\boldsymbol{x}} = \boldsymbol{A}(\boldsymbol{t})\boldsymbol{x} + \boldsymbol{B}(\boldsymbol{t})\boldsymbol{u} \\ y = \boldsymbol{C}\boldsymbol{x} \end{cases} \tag{3-12}$$

$\boldsymbol{x} = [iap\ Vc1\ Vc4\ Vc6\ Vo]^T$

$\boldsymbol{u} = [V_{D8}\ Vs]^T$

$y = Vo$

The Lyapunov function is chosen as:

$$V(x) = \frac{1}{2} * Leq * iap^2 + \frac{1}{2} * C_1 * Vc1^2 + \frac{1}{2} * C_4 * Vc4^2 + \frac{1}{2} * C_6 * Vc6^2 + \frac{1}{2} * Co * Vo^2 \tag{3-13}$$

Obviously, this Lyapunov function is positive definite. Its derivative in this sub-stage is as follows:

$$\dot{V}(x) = -Req * iap^2 - \frac{Vc1^2}{R_1} - \frac{Vc4^2}{R_4} - \frac{Vc6^2}{R_6} - \frac{Vo^2}{Ro} \tag{3-14}$$

The derivative of this Lyapunov function in this sub-stage is negative definite. Therefore, the homogeneous system in this stage is asymptotically internal stable and the bidirectional converter with input and output is BIBO stable in this sub-stage. There is no state value abrupt change between these two sub-stages. There is no infinite noise to the converter.

The stability of the converter in other stages can be analyzed similarly in this way. It can be found that the bidirectional converter is BIBO stable in every stage. From the detailed analysis of the operation of the bidirectional converter with triple-phase-shift control described in Section 3.4, it can be found there is no capacitor voltage abrupt change or inductor current abrupt change in the whole period. Therefore, there are no abrupt state variable value changes at the interface of different stages or sub-stages. This means there is no infinite noise into the converter. Therefore, this converter is BIBO

stable during the whole period. The stability of the backward bidirectional dual full bridge converter with triple phase-shift control method can be analyzed similarly.

3.6 Simulation Studies and Discussion

From the stability analysis described in Section 3.5, it can be found it is an effective method to detect the stability of bidirectional converter with novel triple phase-shift control when parameter changes. Because three phase-shifts change due to parameters change will only make the time duration of some working stages change, the general equivalent circuit and state equation in every stage are still the same. If the converter is proved stable theoretically in these stages, it will remain stable when the time durations of those stages change. This can be validated by simulation results.

Fig.3.13 is obtained by simulating the same bidirectional converter with triple phase-shift control when on resistances of four power MOSFETs (*Tr1*, *Tr2*, *Tr3*, *Tr4*) vary from 5mΩ to 15mΩ and load resistance changes from 40Ω to 50Ω. Obviously, there are 6 stages in one period at present. If Fig.3.13 is compared with Fig.3.2, it can be found that two stages disappear and the duration time of other stages becomes different when parameter changes, but the output voltage still remains very close to 200V with small error and the bidirectional converter is still BIBO stable. This suggests the method proposed in this chapter is correct to detect stability of bidirectional converter with triple phase-shift control when parameter changes. Therefore, only after its stability is analyzed theoretically, can the converter be decided stable or not under different operating conditions. If it is unstable, a different topology should be considered for this project [22], [25], [28].

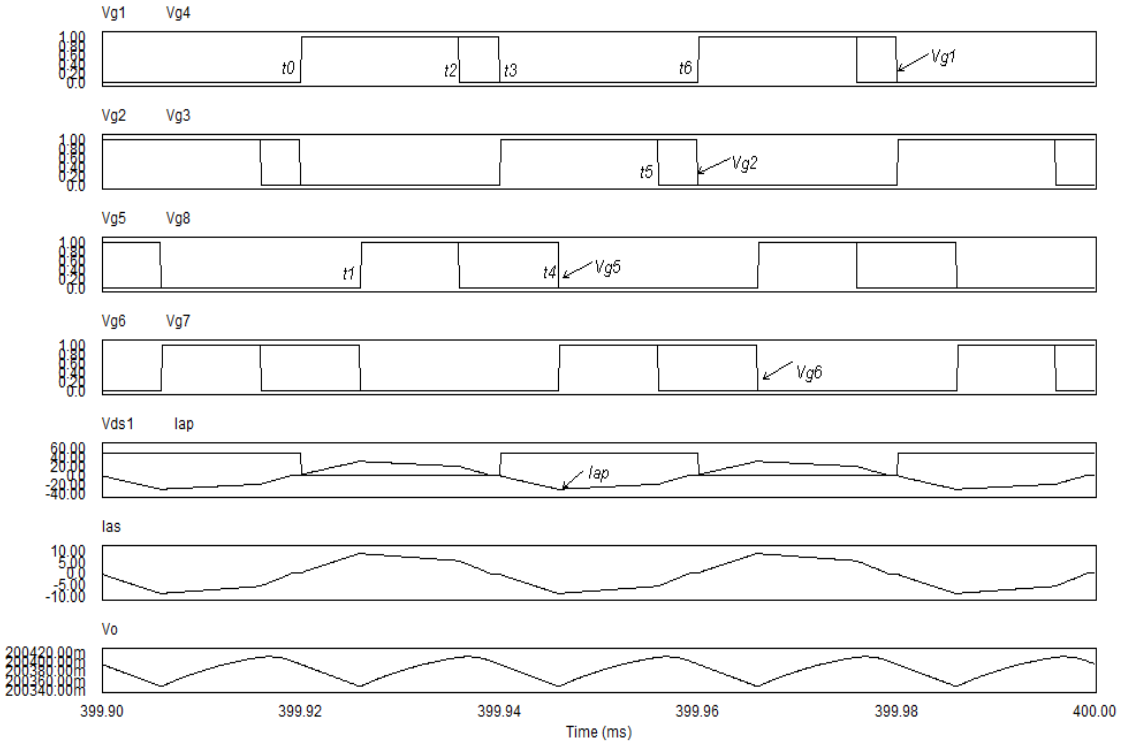

Fig. 3.13 Simulation Results of Forward Bidirectional Converter with Triple Phase-shift Control when Parameter Changes

As an illustrative example, the method developed in this chapter is used to check the stability of a bidirectional DC-DC converter with triple phase-shift control under parameter changes. In fact, the present method of stability analysis may be used in a variety of problems in the field of power electronics, including various power converters composed of different power switches and controlled with different control methods. For this purpose, a Lyapunov function has to be found for every stage or sub-stage and it should be justified that abrupt state changes or infinite noise do not exist at the interface of different stages or sub-stages.

Certainly, there is a limit to the application of the present stability analysis method because the Lyapunov function method is a sufficient condition for stability analysis. If the structure of the system is too complex for an expert to find either a suitable Lyapunov function for one stage or sub-stage, the expert cannot use this new method to determine the stability of the control system.

3.7 Main Contribution

The main contribution of this chapter is to illustrate that the Lyapunov function method can be effectively used for theoretical stability analysis for the whole power electronics area if a suitable Lyapunov function can be selected for every stage of the power converter. By separating the power converter into several stages or sub-stages in one period, determining the stability of the bidirectional converter in every stage with Lyapunov function method and analyzing the stability at the interface of two neighboring stages, the stability of the bidirectional converter in one period can be determined. If suitable Lyapunov functions can be found for every stage, the stability of other power converters with other control methods can be analyzed theoretically with this new method in the future. There is no relevant paper published about this new stability analysis method until now. As an example, the stability of the bidirectional dual full bridge DC-DC converter with novel triple phase-shift control is analyzed successfully with this new method in this chapter.

3.8 Summary

This chapter introduces a new method to determine the stability theoretically of an essentially nonlinear bidirectional dual full bridge DC-DC converter with novel triple phase-shift control when parameter changes. It separates the nonlinear converter into several linear time-varying stages in one period; derives their equivalent circuits and builds corresponding state equations for each stage. It proves that this converter is stable in every stage with Lyapunov method and shows that there are no abrupt state changes at the interface of different stages or sub-stages. This means the converter will still remain stable at the interface of different stages or sub-stages because the state variables, input signals and output signals all remain bounded during this transition. This suggests the converter is stable for the entire period. This method can be used to determine the

stability theoretically of other power converters if suitable Lyapunov functions can be found.

Chapter 4 Theoretical Stability Analysis of Isolated Bidirectional Dual Full Bridge DC-DC Converter

[2]The stability analysis of the bidirectional converter with Lyapunov method is described in last chapter. Based on the similar new idea, the stability analysis of the bidirectional converter with eigenvalues method will be introduced in this chapter.

4.1 Introduction

An identical dual active full bridge converter with zero voltage switching can be used on both sides of the isolation transformer as shown in Fig. 4.1 [1], [21], [24]. A novel triple phase-shift control method can be used in this power circuit. Because this novel control method can make the system with high efficiency in large load scope and improve the adaptability of the system to parameters change, the isolated dual full bridge converter with triple phase-shift control method is used for this project. The circuit for this project is shown in Figure 4.1.

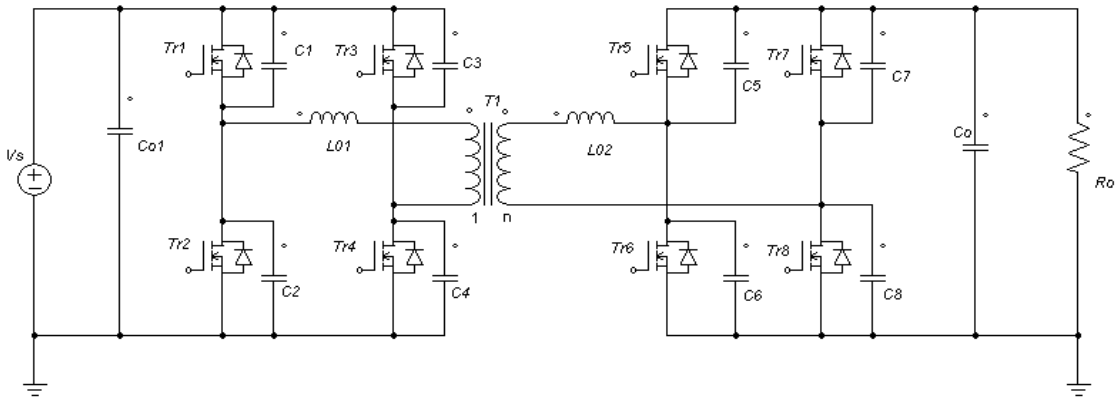

Fig. 4.1 Power Circuit of the Bidirectional Converter

[2] A version of this chapter has been accepted for publication. K. Wu, C.W. de Silva and W.G. Dunford, "Theoretical Stability Analysis of Isolated Bidirectional Dual Full Bridge DC-DC Converter," accepted by *Asian Power Electronics Journal* in 2011.

It is well known that the system must be stable if it is used to finish a task; if it is not stable, the system cannot be used [7], [15], [17]. This chapter introduces an effective method with eigenvalues of the system matrix to determine the stability of a nonlinear bidirectional DC-DC converter theoretically when input voltage changes randomly. It is very important to ensure the bidirectional converter operate normally because input voltage maybe changes during the working process of the bidirectional converter. This new method does not appear to have been published in this area. Besides this, this method can also be used to detect the stability of other similar nonlinear control systems.

4.2 Problem Description

1、*Statement of the Problem*

In recent years, the development of high power and wide power range isolated bidirectional DC-DC converters has become an important topic because of the requirements of electric automobiles, uninterruptible power supplies and aviation power systems [6], [12], [19], [20]. In power electronics, stability is usually determined by observing simulation results because the power converter is nonlinear and theoretical stability analysis is very difficult. This is especially true for high power zero voltage switching (ZVS) converters [11], [16]. However, the simulation method is not always correct because simulation results only provide information for separate working states. When input voltage varies, the converter will work in different states. Its stability is unknown if the corresponding simulation has not been made for these new states. It is impossible to simulate the infinite number of possible working conditions. Only when the stability is analyzed theoretically for this converter, will the answer to this problem be definite [27].

The problem is to find an effective method to determine the stability of a bidirectional DC-DC converter with triple phase-shift control that is subjected to input voltage variation. In order to solve this problem theoretically, an available mathematical model

should be built for this bidirectional converter with triple phase-shift control. This is not a simple problem since the bidirectional converter with triple phase-shift control is a nonlinear system. Additionally, the input voltage change must be taken into account when determine its stability. The more difficult is the rule of input voltage change is unknown.

Although this problem is very difficult and complex, it can be found this bidirectional converter operates periodically according to its working theory. This bidirectional converter can be separated into several stages in one period according to its normal simulation results. According to its working theory, an equivalent circuit can be built for every stage or sub-stage by replacing the nonlinear power switches and diodes with its approximate linear models, e.g. replacing the power MOSFET with its on-resistance when it conducts and replacing the diodes with voltage sources which are equal to their conduction voltage values. In this way, an approximately linear time-varying equivalent circuit model can be built for each stage or sub-stage. According to the equivalent circuit, the approximately state equation can be built for each stage or sub-stage. This makes it possible to determine theoretically the stability of the bidirectional converter in every stage and for the entire period.

2: Components in Power Circuit

L_{01}, L_{02} ---- Two series inductors

C_1=C_2=C_3=C_4=C_5=C_6=C_7=C_8 --- Eight snubber capacitors

Co, *Co1* ---Two large filter capacitors

Ro --- Forward load resistor

The parameters of the main transformer are as follows:

Lp ---Primary leakage inductance

Ls --- Secondary leakage inductance

Rp --- Primary winding resistance

Rs--- Secondary winding resistance

Turns ratio: 1: n

The parameters of the eight power MOSFETs are as follows:

R_1, R_2, R_3, R_4, R_5, R_6, R_7, R_8 ---- On resistance

D_1, D_2, D_3, D_4, D_5, D_6, D_7, D_8 --- Anti-parallel diodes with power MOSFETs.

3: Variables Used in the Chapter

iap, ias ---Power circuit primary current and secondary current of the transformer

Vc1, Vc2, Vc3, Vc4, Vc5, Vc6, Vc7, Vc8 ---Voltages across corresponding parallel capacitors.

Vs ---Input voltage

Vo ---Output voltage

V_{D1}, V_{D2}, V_{D3}, V_{D4}, V_{D5}, V_{D6}, V_{D7}, V_{D8} ----Forward conduction voltages of anti-parallel diodes.

4.3 Objectives and Rationale

The objective of this chapter is to analyze the stability of a bidirectional DC-DC converter with eigenvalues method theoretically for any input change. After a novel topology is determined, the stability of this topology should be analyzed. If it is not stable, this topology cannot be used.

Because Lyapunov method is a sufficient condition to determine the stability of a control system, the stability of a control system cannot be analyzed with this method if a suitable Lyapunov function cannot be found for this system. An alternative eigenvalues method can be used to determine the stability of the complex system approximately. Although the parameters of the power circuit elements and input voltage will always change during real application, eigenvalues method can be used to determine the stability of the bidirectional converter for only input voltage change. If other parameters change is considered, this method cannot be used because the eigenvalues of the bidirectional converter cannot be calculated. Therefore, it is an approximate theoretical stability

analysis method. Certainly, it is still more precise than stability analysis with simulation method.

4.4 Equivalent Circuits of this Bidirectional Converter Topology

The forward simulation wave-forms of the bidirectional converter with normal steady state operation are as follows:

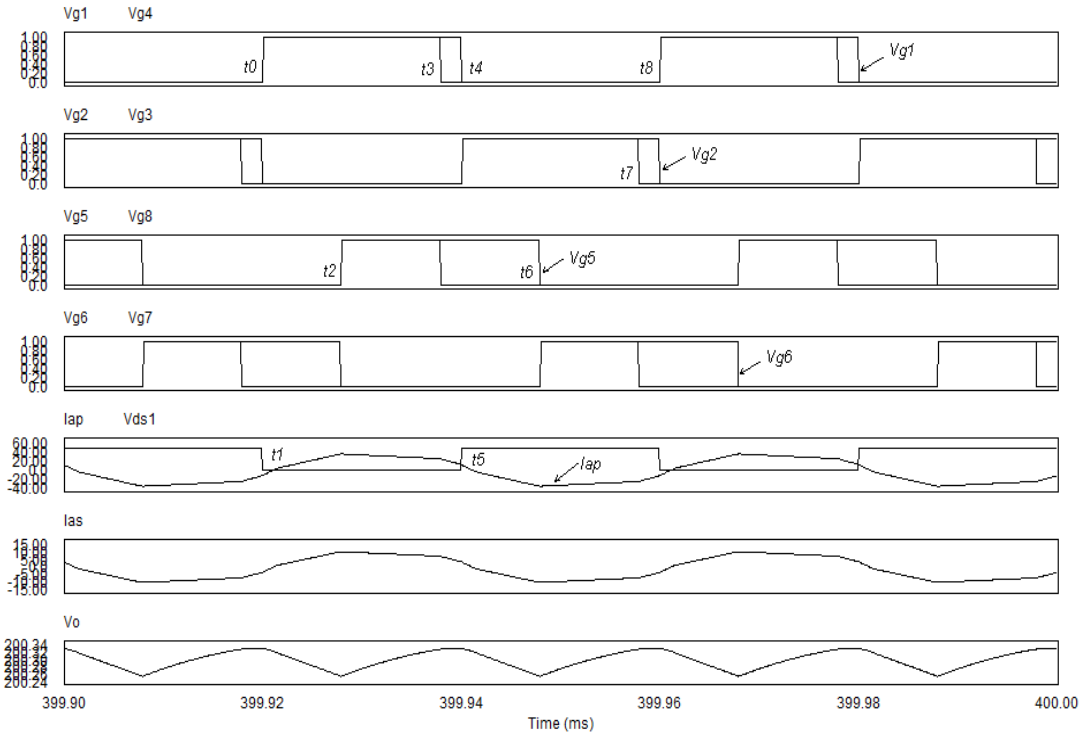

Fig. 4.2 Simulation Wave-Forms of the Forward Bidirectional Converter with Triple Phase-shift Control

As shown in Fig.4.2, this novel triple phase-shift control method includes three phase-shifts. The first is the phase-shift between the primary control signal and the corresponding secondary control signal, for example, between V_{g1} and V_{g5}; the second is the phase-shift between the diagonal control signals in the primary power circuit, for example, between V_{g1} and V_{g4}; the third is the phase-shift between the diagonal control signals in the secondary power circuit, for example, between V_{g5} and V_{g8}. The forward bidirectional dual full bridge converter is separated into eight stages in one period. Its

operation and equivalent circuit for every stage are described below.

1: Stage 1 (t_0~t_1): Power switches *Tr1* and *Tr4* will turn on at "t=t_0". Because the primary current is still negative during this period, the inductor energy flows back to the power source. The primary current will flow through *Tr4*/*Tr1*. This is because the voltage drop across on resistance of the power MOSFET when it conducts is lower than the required conduction voltage drop of anti-parallel diode. The diode will not conduct. This is normally the case.

Because V_{g5}/V_{g8}/V_{g7} are equal to zero, *Tr5*/*Tr8*/*Tr7* all in "Off" state; V_{g6}=1, *Tr6* is "On". Because *ias*<0, secondary current flows through *Tr6*/D_7. The inductor L_{02} and output capacitor provide energy to the load. The output voltage reduces during this stage. The equivalent circuit in this stage is as follows:

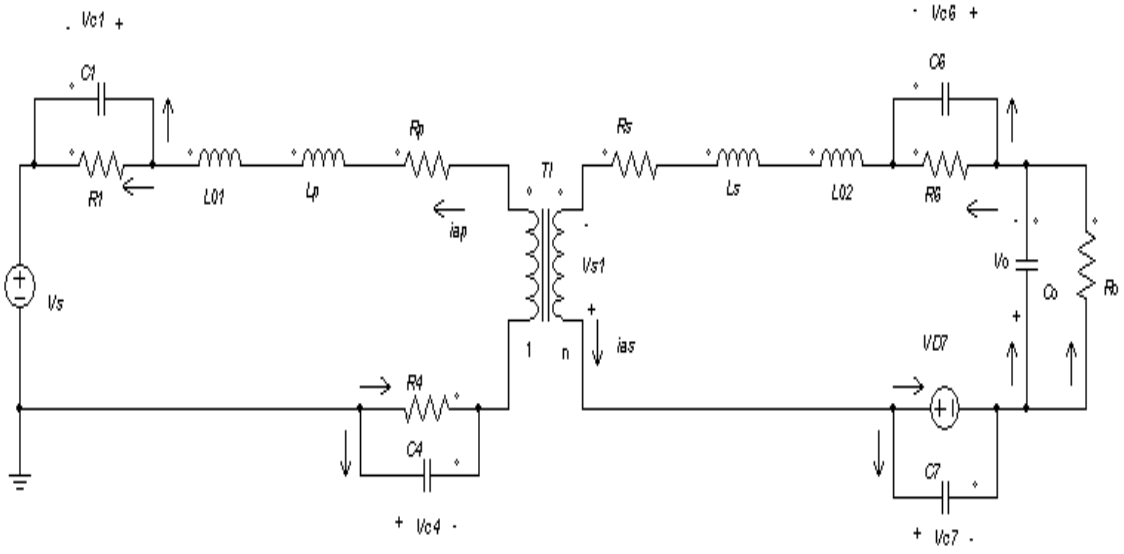

Fig. 4.3 Equivalent Circuit in Stage 1

2: Stage 2 (t_1~t_2): Because V_{g1}/ V_{g4} =1, power switches *Tr1* and *Tr4* are in "On" state in this stage. Because the primary current is positive during this stage, the primary current will flow through *Tr1*/*Tr4* and the inductor L_{01} and transformer leakage inductance. The energy will transfer from the primary side to the secondary side.

Because V_{g5}/V_{g8}/V_{g7} are equal to zero, *Tr5*/*Tr8*/*Tr7* are in "Off" state; V_{g6}=1, *Tr6* is "On". Because *ias*>0, secondary current will charge capacitor C_7 and discharge capacitor

C_8 till its voltage reduces to the forward conduction voltage of diode D_8. The equivalent circuit in this sub-stage is as follows:

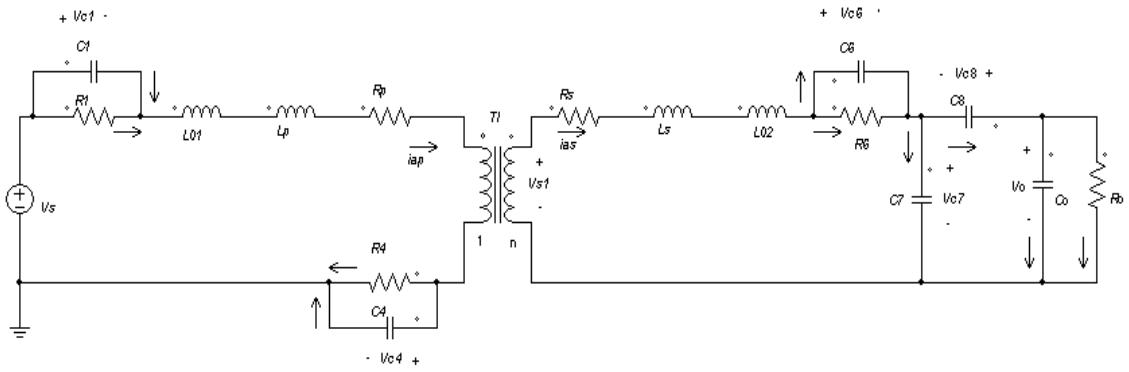

Fig. 4.4 C_8 Discharging Equivalent Circuit in Stage 2

Then the current flows through *Tr6*/D_8. The energy is stored in the secondary inductor L_{02} and leakage inductor because this is a free-wheeling sub-stage with no power transferred to the load theoretically. Output capacitor provides energy to the load. The output voltage continues to reduce in this sub-stage. The equivalent circuit in this sub-stage is as follows:

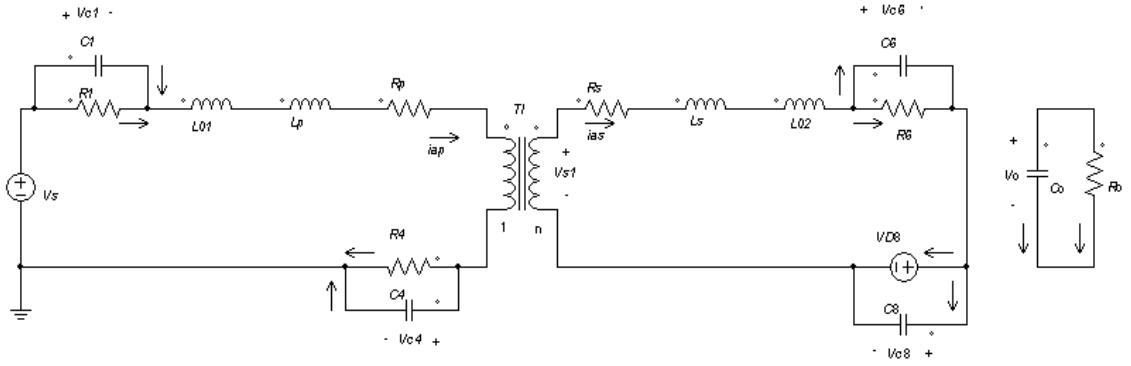

Fig. 4.5 Free Wheeling Equivalent Circuit in Stage 2

Tr6 turns off a little before t_2. The secondary current will charge snubber capacitor C_6 and discharge snubber capacitor C_5. During this very short transitional time, the secondary current flows through D_8 to charge and discharge the snubber capacitors. When C_5 is totally discharged (*Vds5*=0), the secondary current will flow through D_5/D_8

and the energy will be transferred to the load. The corresponding equivalent circuits are as follows:

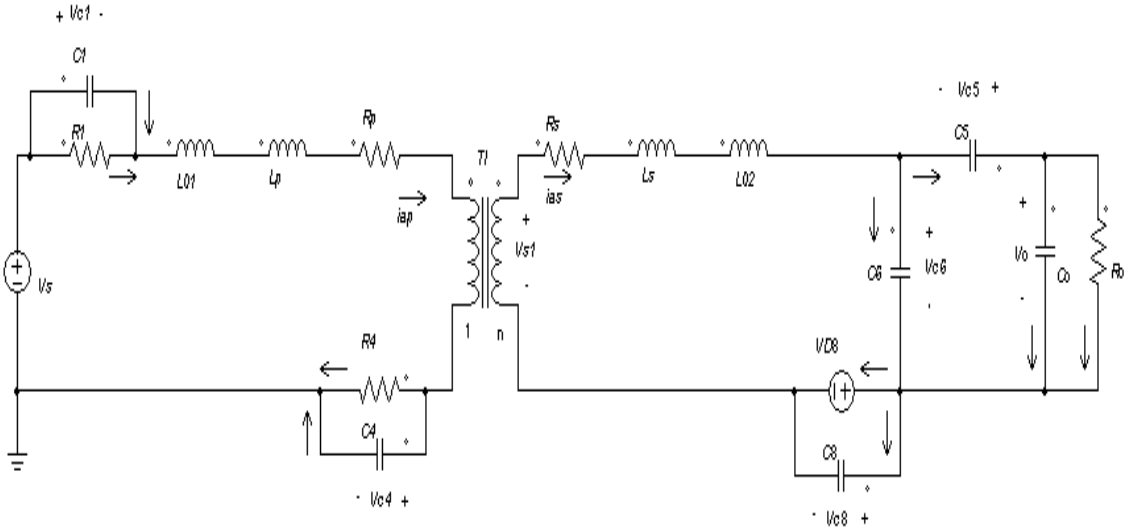

Fig. 4.6 Charge-Discharge Equivalent Circuit in Stage 2

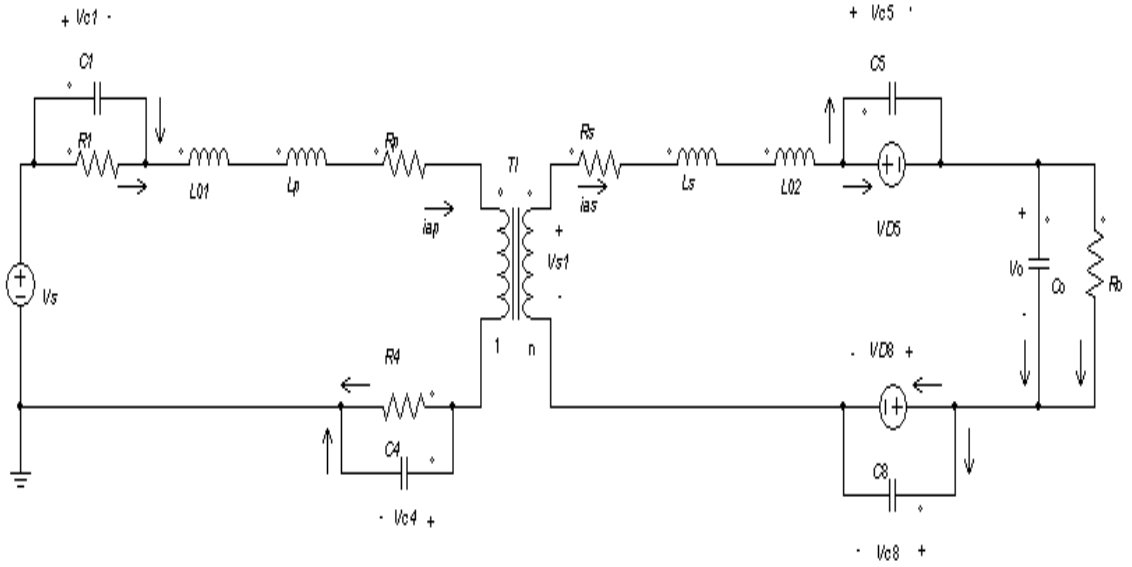

Fig. 4.7 Diode Conduct Equivalent Circuit in Stage 2

3: Stage 3 (t_2~t_3): The control signal V_{g5}/V_{g8}=1, power switches *Tr5*/*Tr8* will turn on at t_2. Because *ias*>0 during this stage, the secondary side current will flow through *Tr5*/*Tr8* and transfer energy to the load in this stage. The output voltage will increase in this stage.

The equivalent circuit in this stage is as follows:

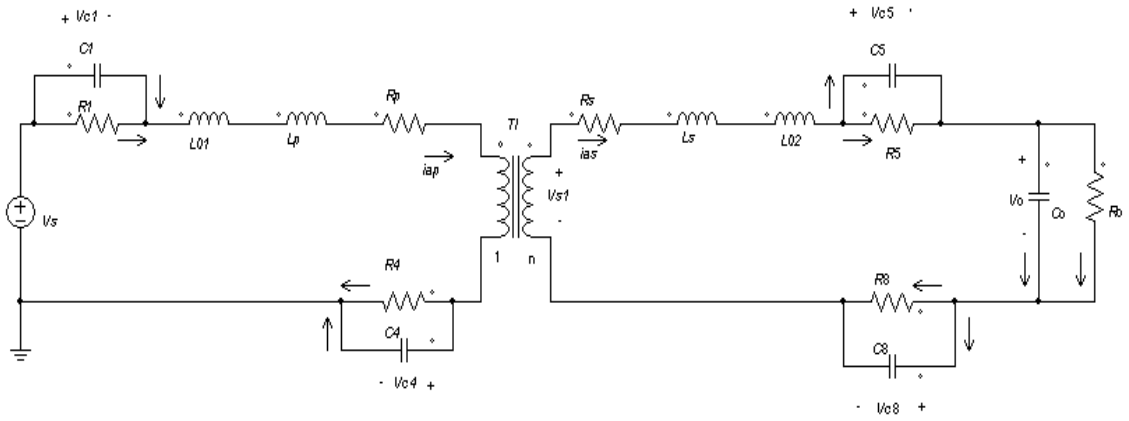

Fig. 4.8 Energy Transfer Equivalent Circuit in Stage 3

4: Stage 4 (t_3~t_4): V_{g4}/V_{g8}=0, so, *Tr4*/*Tr8* will turn off at t_3. For the primary side, *Tr4* turns off at t_3. The primary current will charge snubber capacitor C_4 and discharge snubber capacitor C_3. When C_3 is totally discharged (*Vds3*=0), the primary current will flow through *Tr1*/D_3 and form a free-wheeling sub-stage. No power is transferred to the secondary side theoretically.

For the secondary side, the current *ias*>0, this indicates *Tr5*/D_8 will continue to conduct in this period of time. The additional inductor L_{02} and secondary leakage inductance will provide energy to transfer to the load. The output voltage will continue to increase in this stage. The equivalent circuits are shown in Fig. 4.9 and Fig. 4.10.

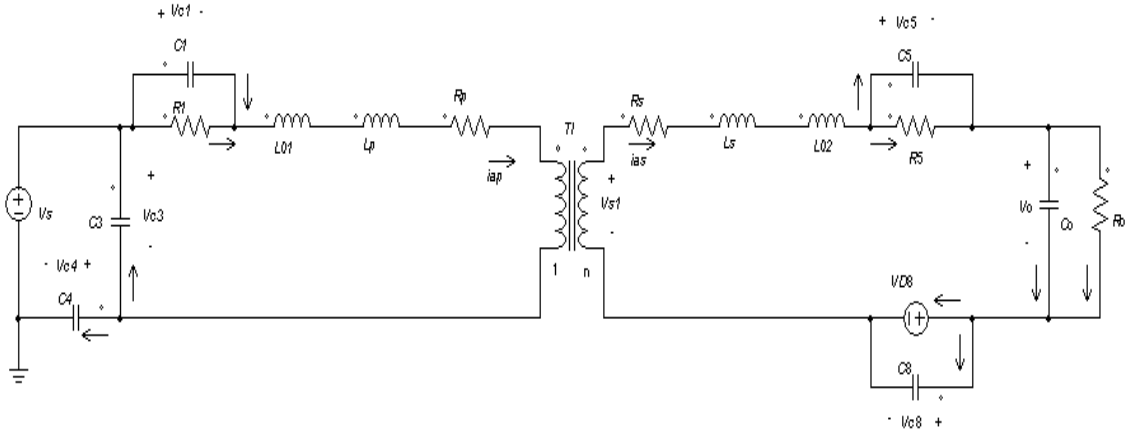

Fig. 4.9 C_3 Discharge Equivalent Circuit in Stage 4

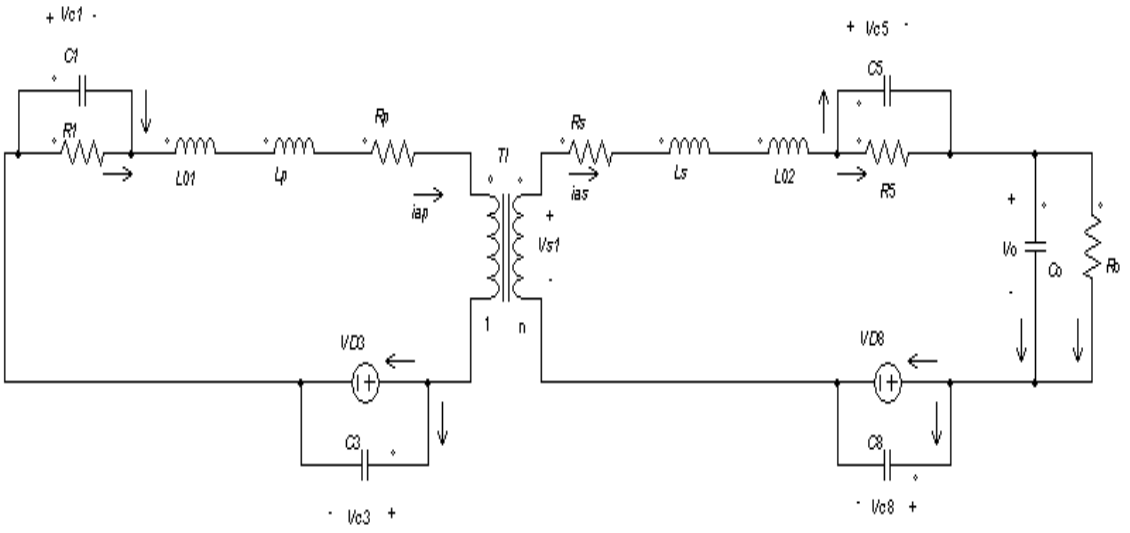

Fig. 4.10 Free Wheeling Equivalent Circuit in Stage 4

Tr1 turns off a little before t_4. The primary current will discharge snubber capacitor C_2 and charge snubber capacitor C_1. During this very short transitional time, the current will flow through D_3 to charge and discharge capacitors. When C_2 is totally discharged (*Vds2*=0), D_2 will conduct and form an energy feedback to power source. This will make it feasible for *Tr2*/*Tr3* to turn on under ZVS. The equivalent circuits are shown in Fig. 4.11 and Fig. 4.12.

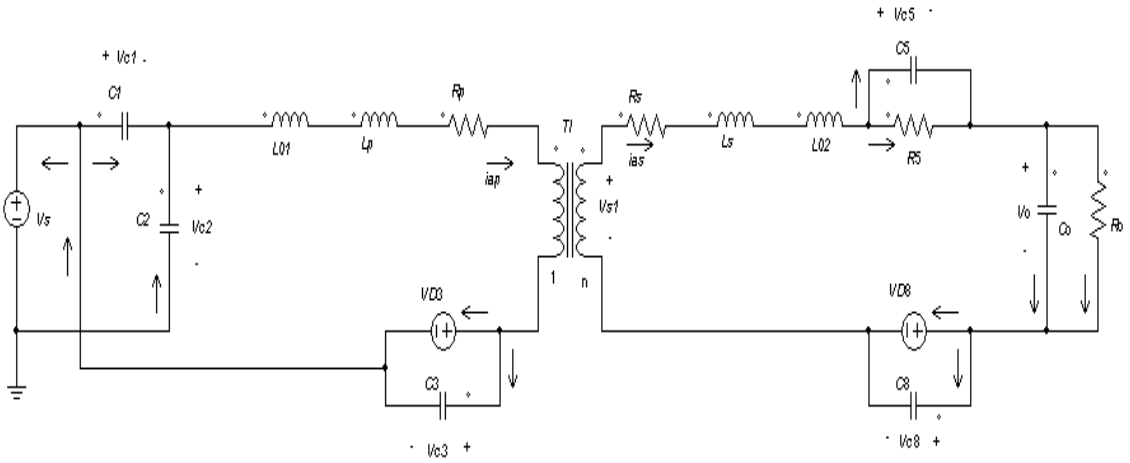

Fig. 4.11 C_2 Discharge Equivalent Circuit in Stage 4

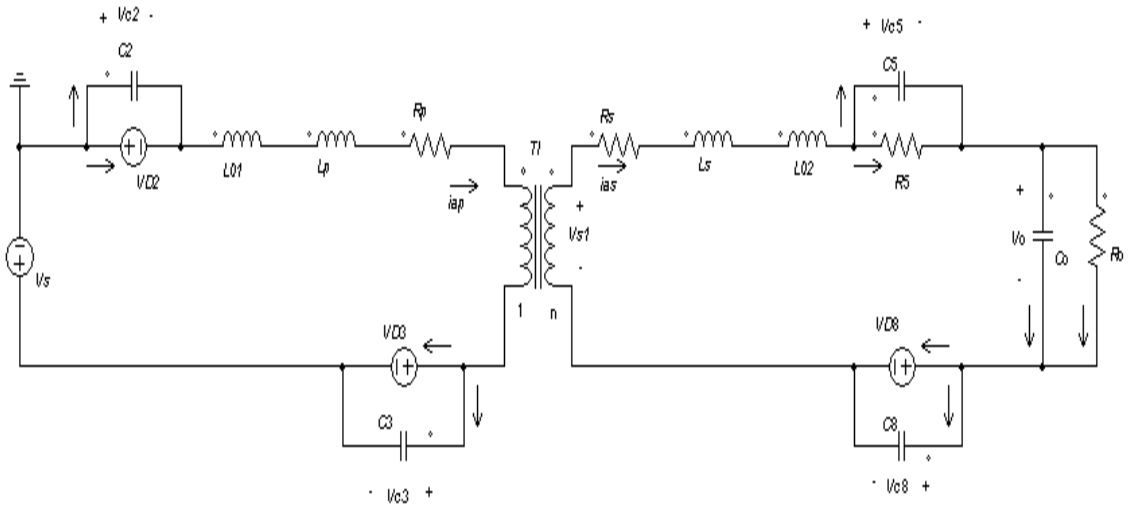

Fig. 4.12 Energy Feedback Equivalent Circuit in Stage 4

5: Stage 5 (t_4~t_5): Because V_{g2}/V_{g3}=1, *Tr2*/*Tr3* will turn on at t_4 under ZVS. Because the primary current *iap*>0, the energy will feedback to the primary source in this stage.

For the secondary side, V_{g5}=1, so, *Tr5* is "On" in this stage. $V_{g6}/V_{g7}/V_{g8}$=0, so, *Tr6*/*Tr7*/*Tr8* will be in off state during this period of time. Because the secondary current *ias*>0, *Tr5*/D_8 will conduct in this period of time. The inductor L_{02}, the secondary leakage inductor and output capacitor will provide energy to the load together in this stage. The output voltage begins to reduce in this stage. According to this analysis, the equivalent circuits in this stage can be obtained.

6: Stage 6 (t_5~t_6): Because V_{g2}/V_{g3}=1, *Tr2*/*Tr3* will be on in this stage. Because the primary current *iap*<0, the energy will transfer to the secondary side again.

For the secondary side, V_{g5}=1, so, *Tr5* is on in this stage. $V_{g6}/V_{g7}/V_{g8}$=0, so, *Tr6*/*Tr7*/*Tr8* will be in the off state. Because the secondary current *ias*<0, the secondary current will charge capacitor C_8 and discharge capacitor C_7 till its voltage reduces to the forward conduction voltage of diode D_7. Then the current flows through *Tr5*/D_7 and forms a free-wheeling sub-stage with no energy transferred to the load theoretically in this stage. The energy from primary source is stored in L_{02} and the leakage inductor. The output capacitor provides energy to the load and the output voltage will continue to

reduce in this stage. The equivalent circuit can be obtained.

7: Stage 7 (t_6~t_7): Because V_{g6}/V_{g7}=1, *Tr6*/*Tr7* will turn on at t_6. V_{g5}=0, so *Tr5* turns off a little before t_6. The secondary current will charge C_5 and discharge C_6. During this very short transitional time, the secondary current flows through D_7 to charge and discharge snubber capacitors. When C_6 is totally discharged (*Vds6*=0), D_6 will turn on and D_6/D_7 will conduct to form ZVS and transfer energy to the load. Because the secondary side current *ias*<0, *Tr6*/*Tr7* will conduct in this period of time and transfer energy to the load in this stage. The output voltage will increase in this stage. The equivalent circuits in this stage can be obtained.

8: Stage 8 (t_7~t_8)*:* Because V_{g3}/V_{g7}=0 at t_7, *Tr3*/*Tr7* will turn off at t_7. For the primary side, *Tr3* turns off. The primary current will charge C_3 and discharge C_4. During this very short transitional time, the primary current flows through *Tr2* to charge and discharge snubber capacitors C_3 and C_4. When C_4 is totally discharged (*Vds4*=0), D_4 will turn on.*Tr2*/D_4 conduct, this forms a free-wheeling sub-stage with no energy transferred to the secondary side.

Tr2 turns off a little before t_8. The energy stored in additional inductor L_{01} and transformer leakage inductance will charge the snubber capacitor C_2 and discharge snubber capacitor C_1. During this very short transitional time, the primary current flows through D_4 to charge and discharge snubber capacitors. When C_1 is totally discharged (*Vds1*=0), then the primary current will flow through D_4/D_1 and the inductor energy flows back to the power source.

For the secondary side, *Tr6*/D_7 will continue conduct during this period of time and transfer energy to the load. This is because the secondary side current *ias*<0. The energy mainly comes from the stored energy of additional inductor L_{02} and the leakage inductance. The output voltage will continue to increase in this stage. The corresponding equivalent circuits can be obtained.

4.5 Stability Analysis with Eigenvalues Method

If the structure of the system is too complex for an expert to find either a single Lyapunov function for the system or several Lyapunov functions for corresponding stages or sub-stages, the Lyapunov method cannot be used. As another stability analysis method, eigenvalues method can be used to determine the stability of the bidirectional converter for only input voltage change.

1、Description of Eigenvalues Method

The bidirectional DC-DC converter is essentially nonlinear system during the whole working period. However, it can be separated into several stages according to the simulation wave forms at a concrete operating point. Each stage is essentially linear. Its equivalent circuit and corresponding state equation in every stage can be built. Therefore, its stability can be analyzed theoretically in every stage. If the converter is stable in every stage and there is no abrupt state change during the transition of two stages, then this converter will be stable during the whole working period.

Based on this idea, the forward bidirectional dual full bridge converter is separated into eight big stages to analyze its stability theoretically. There are no abrupt state changes during the transition between two stages because the two stages are connected with each other by the capacitor voltages and inductor currents. It is well known they cannot change abruptly. Therefore, the forward bidirectional dual full bridge converter with triple phase-shift control method will be stable if it is stable in each stage. The working theory of the bidirectional converter in every stage has been described carefully; the corresponding equivalent circuit in every stage is given in Section 4.4. If only input voltage change is considered and other parameters of the bidirectional converter are assumed constant, the stability of the bidirectional converter in every stage can be determined with eigenvalues method. If the real parts of the eigenvalues are negative in one stage or sub-stage, the bidirectional converter will be BIBO stable in that stage or sub-stage. The stability of the backward bidirectional dual full bridge converter with

triple phase-shift control method can be analyzed similarly.

2: Components Parameters in Power Circuit

Two serial inductors:

L_{01}=7.3μH; L_{02}=6.9μH;

Eight snubbber capacitors paralleled with power switches:

C_1=C_2=C_3=C_4=C_5=C_6=C_7=C_8=1nF;

Output-filter capacitance:

Co=Co1=500μF;

Forward load resistance: Ro=40Ω;

The parameters of the main transformer are as following:

Primary leakage inductance: Lp=0.6μH;

Secondary leakage inductance: Ls=1μH;

Primary winding resistance: Rp=7mΩ;

Secondary winding resistance: Rs=10mΩ;

Turns ratio: n=7/2

The parameters of the 8 power switches are as following:

Tr1~Tr4: On resistance: 5mΩ; Diode Voltage drop: 1V

Tr5~Tr8: On resistance: 23mΩ; Diode Voltage drop: 0.6V

3. Stability Determination of a Bidirectional Converter with Triple Phase-shift Control

Based on the equivalent circuits in each stage, the corresponding state equation can be built for this bidirectional DC-DC converter in each stage. The equivalent circuits are obtained by the analysis of the combination act of the input signal, output signal and control signal of this closed-loop converter. According to model identification [23], [26], the equivalent circuits in each stage are closed-loop models for this nonlinear converter. The corresponding state equation will be a closed-loop state space model of this bidirectional converter in each linear stage. It can be used to determine the stability of this bidirectional converter in every linear stage directly.

(1)： Stability Analysis in Stage t_0~t_1

From the equivalent circuit of the converter shown in Fig.4.3, the state equation of the converter can be built in this stage. In order to be convenient, write：

$$Leq = L_{01} + Lp + \frac{1}{n^2} * L_{02} + \frac{1}{n^2} * Ls \ ;$$

$$Req = Rp + \frac{1}{n^2} * Rs;$$

$$\begin{cases} Leq * \frac{diap}{dt} = -Req * iap \ - Vc1 - Vc4 - \frac{1}{n} * Vc6 - \frac{1}{n} * Vo - \frac{1}{n} * V_{D7} - Vs \\ C_1 * \frac{dVc1}{dt} = iap - \frac{Vc1}{R_1} \\ C_4 * \frac{dVc4}{dt} = iap - \frac{Vc4}{R_4} \\ C_6 * \frac{dVc6}{dt} = \frac{1}{n} * iap - \frac{Vc6}{R_6} \\ Co * \frac{dVo}{dt} = \frac{1}{n} * iap - \frac{Vo}{Ro} \\ Vo = Vo \end{cases}$$

(4-1)

Substitute the corresponding values into this general state equation, the concrete state equation can be obtained as following:

$$\begin{cases} \frac{diap}{dt} = 915.26 * iap - 117096 * Vc1 - 117096 * Vc4 - 33456 * Vc6 - 33456 * \\ Vo - \ 33456 * V_{D7} - 117096 * Vs \\ \frac{dVc1}{dt} = 10^9 * iap - 2 * 10^{11} * Vc1 \\ \frac{dVc4}{dt} = 10^9 * iap - 2 * 10^{11} * Vc4 \\ \frac{dVc6}{dt} = 2.86 * 10^8 * iap - 4.35 * 10^{10} * Vc6 \\ \frac{dVo}{dt} = 571 * iap - 50 * Vo \end{cases}$$

(4-2)

Therefore, the closed-loop state space model of this converter during this stage can be

expressed as following:

$$\begin{cases} \dot{\boldsymbol{x}} = \boldsymbol{Ax} + \boldsymbol{Bu} \\ y = \boldsymbol{Cx} \end{cases} \tag{4-3}$$

$\boldsymbol{x} = [iap\ Vc1\ Vc4\ Vc6\ Vo]^T$

$\boldsymbol{u} = [V_{D7}\ Vs]^T$

$y = Vo$

The eigenvalues of the system matrix *A* for this converter in this stage are:

$$\begin{cases} s_1 = -43499999780 \\ s_2 = -1178.092 + 4222.65 * i \\ s_3 = -1178.092 - 4222.65 * i \\ s_4 = -1.999 * 10^{11} \\ s_5 = -2.0 * 10^{11} \end{cases} \tag{4-4}$$

Therefore, the converter is state asymptotically stable in this stage. Its stability is independent to the input signal Vs and forward diode voltage V_{D7}because they only influence system input matrix and do not influence the system matrix.

2：Stability Analysis in Stage t_1~t_2

From the previous analysis of the converter working process, it can be found there are four sub-stages and corresponding four equivalent circuits in this stage. The stability of the converter can be analyzed in these four sub-stages with their equivalent circuits one by one.

(1) Sub-stage of Charge-discharge of C_7 and C_8

According to the equivalent circuit of the converter shown in Fig.4.4, the corresponding state equation for this converter can be built. In order to be convenient,

write:

$$Ceq = \frac{C_7 * C_8 + Co * C_7 + Co * C_8}{Co + C_8}$$

$$\begin{cases} Leq * \frac{diap}{dt} = -Req * iap - Vc1 - Vc4 - \frac{1}{n} * Vc6 - \frac{1}{n} * V_{C7} + Vs \\ C_1 * \frac{dVc1}{dt} = iap - \frac{Vc1}{R_1} \\ C_4 * \frac{dVc4}{dt} = iap - \frac{Vc4}{R_4} \\ C_6 * \frac{dVc6}{dt} = \frac{1}{n} * iap - \frac{Vc6}{R_6} \\ Ceq * \frac{dV_{C7}}{dt} = \frac{1}{n} * iap - \frac{C_8}{Ro * (C_8 * Co)} * (Vc7 + Vc8) \\ Co * \frac{dVo}{dt} = -\frac{Vo}{Ro} \\ Vo = Vc7 + Vc8 \\ Vo = Vo \end{cases}$$

(4-5)

Substitute the corresponding components values into this general state equation, the concrete state equation for this converter in this sub-stage can be gotten as following:

$$\begin{cases} \frac{diap}{dt} = -915.26 * iap - 117096 * Vc1 - 117096 * Vc4 - 33456 * Vc6 - \\ 33456 * V_{C7} + 117096 * Vs \\ \frac{dVc1}{dt} = 10^9 * iap - 2 * 10^{11} * Vc1 \\ \frac{dVc4}{dt} = 10^9 * iap - 2 * 10^{11} * Vc4 \\ \frac{dVc6}{dt} = 2.86 * 10^8 * iap - 4.35 * 10^{10} * Vc6 \\ \frac{dV_{C7}}{dt} = 1.43 * 10^8 * iap - 25 * V_{C7} - 25 * V_{C8} \\ \frac{dV_{C8}}{dt} = -1.43 * 10^8 * iap - 25 * V_{C7} - 25 * V_{C8} \\ Vo = V_{C7} + V_{C8} \end{cases}$$

(4-6)

Therefore, the closed-loop state space model of this converter during this sub-stage can be expressed as follows:

$$\begin{cases} \dot{\boldsymbol{x}} = \boldsymbol{A}\boldsymbol{x} + \boldsymbol{B}u \\ y = \boldsymbol{C}\boldsymbol{x} \end{cases} \tag{4-7}$$

$\boldsymbol{x} = [iap\ Vc1\ Vc4\ Vc6\ Vc7\ Vo]^T$

$u = Vs$

$y = Vo$

The eigenvalues of the system matrix in this sub-stage are equal to:

$$\begin{cases} s_1 = -1153.09 + 2187282.95 * i \\ s_2 = -1153.09 - 2187282.95 * i \\ s_3 = -43499999780 \\ s_4 = -1.999 * 10^{11} \\ s_5 = -2.0 * 10^{11} \\ s_6 = -50 \end{cases} \tag{4-8}$$

Because all eigenvalues have negative real part, the converter in this sub-stage is state asymptotically stable. There is no state abrupt change from stage 1 to stage 2. There is no infinite noise to the converter.

(B) Sub-stage of Free Wheeling in Stage 2

According to the equivalent circuit of the converter in free-wheeling stage shown in Fig.4.5, the corresponding state equation for this converter during this sub-stage can be built as following:

$$\begin{cases} Leq * \frac{diap}{dt} = -Req * iap - Vc1 - Vc4 - \frac{1}{n} * Vc6 - \frac{1}{n} * V_{D8} + Vs \\ C_1 * \frac{dVc1}{dt} = iap - \frac{Vc1}{R_1} \\ C_4 * \frac{dVc4}{dt} = iap - \frac{Vc4}{R_4} \\ C_6 * \frac{dVc6}{dt} = \frac{1}{n} * iap - \frac{Vc6}{R_6} \\ Co * \frac{dVo}{dt} = -\frac{Vo}{Ro} \\ Vo = Vo \end{cases}$$

(4-9)

Substitute the corresponding components values into this general state equation, the concrete state equation for this converter in this sub-stage can be gotten as following:

$$\begin{cases} \frac{diap}{dt} = 915.26 * iap - 117096 * Vc1 - 117096 * Vc4 - 33456 * Vc6 - 33456 * V_{D8} + 117096 * Vs \\ \frac{dVc1}{dt} = 10^9 * iap - 2 * 10^{11} * Vc1 \\ \frac{dVc4}{dt} = 10^9 * iap - 2 * 10^{11} * Vc4 \\ \frac{dVc6}{dt} = 2.86 * 10^8 * iap - 4.35 * 10^{10} * Vc6 \\ \frac{dVo}{dt} = -50 * Vo \end{cases}$$

(4-10)

Therefore, the closed-loop state space model of this converter during this sub-stage can be expressed as follows:

$$\begin{cases} \dot{\boldsymbol{x}} = \boldsymbol{Ax} + \boldsymbol{Bu} \\ y = \boldsymbol{Cx} \end{cases}$$

(4-11)

$\boldsymbol{x} = [iap\ Vc1\ Vc4\ Vc6\ Vo]^T$

$\boldsymbol{u} = [V_{D8}\ Vs]^T$

$y = Vo$

The eigenvalues of the system matrix in this sub-stage are equal to:

$$\begin{cases} s_1 = -2306.18 \\ s_2 = -1.999 * 10^{11} \\ s_3 = -43499999780 \\ s_4 = -2.0 * 10^{11} \\ s_5 = -50 \end{cases} \quad (4\text{-}12)$$

Because all eigenvalues have negative real part, the converter in this sub-stage is state asymptotically stable. There is no state abrupt change between these two sub-stages. There is no infinite noise to the converter.

The stability of the converter in other stages can be analyzed similarly in this way. It can be found that the bidirectional converter is asymptotically stable in every stage. There are no state abrupt changes between stages or sub-stages. This means there is no infinite noise into the converter. Therefore, this converter is stable during the whole working period.

4.6 Simulation Studies and Discussion

From the stability analysis described in Section 4.5, it can be found it is an effective method to detect the stability of bidirectional converter with novel triple phase-shift control when input voltage changes. Three phase-shifts change due to input voltage change will only make the time duration of some working stages change. However, the general equivalent circuit and state equation in every stage are still the same. If the converter is proved to be stable theoretically in these stages, it will remain stable when the time durations of these stages change. This can be validated by simulation results.

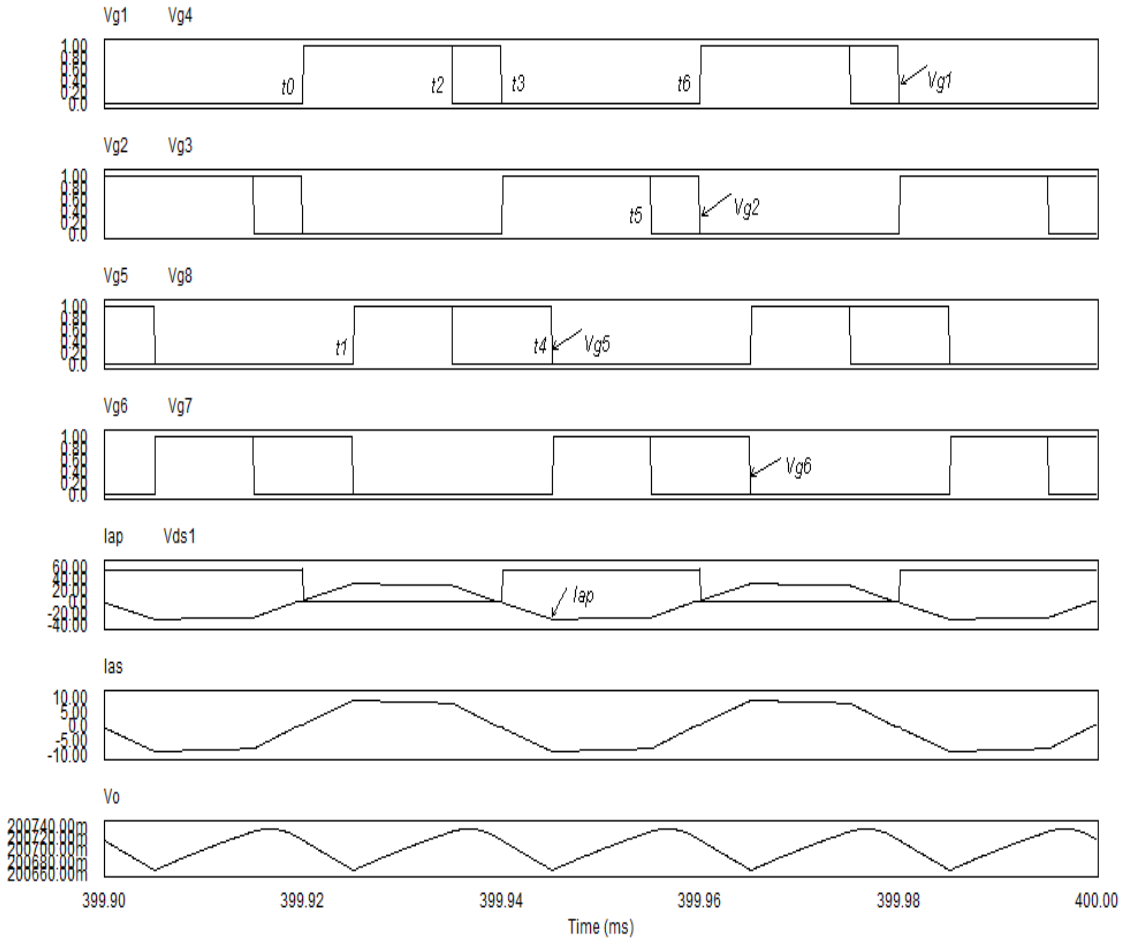

Fig. 4.13 Simulation Results of Forward Bidirectional Converter with Triple Phase-shift Control when Input Voltage Changes

Fig.4.13 is obtained by simulating the same bidirectional converter with triple phase-shift control when input voltage changes from 48V to 55V. Obviously, there are 6 stages in one period at present. If Fig.4.13 is compared with Fig.4.2, it can be found that two stages disappear and the duration time of other stages becomes different when input voltage changes, but the output voltage still remains very close to 200V with small error which can be adjusted by altering the feedback resistance values to 100kΩ/2.28kΩ and the bidirectional converter is still BIBO stable. This suggests the eigenvalues method proposed in this section is correct to detect stability of bidirectional converter with triple phase-shift control when only input voltage changes. If it is unstable, a different topology

should be considered for this project [22], [25], [28]. Fig.2 and Fig.13 are simulated with PSIM.

Certainly, there is a limit to the application of the present method of stability analysis. If other parameters change of the system is considered, the present method cannot be used. This is because the rule of the parameters change during the working process of the converter is unknown. Although the converter in every stage is approximately linear time varying system, the system matrix A is uncertain. It is impossible to use eigenvalues of system matrix A to decide stability of the bidirectional converter.

4.7 Main Contribution

The main contribution of this chapter is to provide another new theoretical stability analysis with eigenvalues method for the whole power electronics area. By separating the power converter into several stages or sub-stages in one period, determining the stability of the bidirectional converter in every stage with eigenvalues method and analyzing the stability at the interface of two neighboring stages, the stability of the bidirectional converter in one period can be determined. The stability of other power converters with other control methods that is undergoing input voltage variations can be analyzed theoretically with this new method if an expert cannot find a suitable Lyapunov function for one stage or sub-stage. There are no relevant papers published about this particular stability analysis method until now. As an example, the stability of the bidirectional dual full bridge DC-DC converter with novel triple phase-shift control is successfully analyzed with this method.

4.8 Summary

This chapter introduces a new method to determine the stability theoretically of an essentially nonlinear bidirectional dual full bridge DC-DC converter with novel triple phase-shift control undergoing input voltage variations. The method separates the

nonlinear converter into several linear stages in one period; derives their equivalent circuits and builds the corresponding state equations for each stage. It proves that this converter is stable in every stage with eigenvalues method and there are no abrupt state changes at the interface of different stages or sub-stages. This means the converter will still remain stable at the interface of different stages or sub-stages because the state variables, input signals and output signals all remain bounded during this transition. This suggests the converter is stable for the whole period. This method can be used to determine the stability theoretically of other power converters, too.

Chapter 5 Theoretical Analysis and Simulation of Isolated Bidirectional Dual Full Bridge ZVS DC-DC Converter with Novel Triple Phase-shift Control

[3]The schematic circuit and theoretical stability analysis for this project have been described in the last three chapters. The next step is to analyze the working theory of the bidirectional dual full bridge converter with novel triple phase-shift control method, to derive the relation between *Vo*/*Vs* and three phase-shifts, to derive the general expressions of average input power and average output power. On the basis of these results, the general expression of efficiency is derived.

5.1 Introduction

In recent years, the development of high power and wide power range isolated bidirectional DC-DC converters has become an important topic because of the requirements of electric automobiles, energy storage systems and aviation power systems [20], [30], [33].This project is to design a forward 1kW/200V ($\eta \geq 93\%$) and backward 250W/48V ($\eta \geq 95\%$) bidirectional converter. The dual active full bridge converter is symmetrical on both sides of the isolation transformer. It is suitable to be used as the power circuit to transfer energy back and forth, especially for high power case [32], [34], [37]. The power circuit for this bidirectional DC-DC converter is shown in Fig.5.1.

[3] A version of this chapter has been conditionally accepted for publication. K. Wu, W.G. Dunford and C.W. de Silva, "Theoretical Analysis and Simulation of Isolated Bidirectional Dual Full Bridge ZVS DC-DC Converter with Novel Triple Phase-shift Control," conditionally accepted by *IEEE Transactions on Industrial Electronics* in 2011.

The topology includes two series inductors--- L_{01} and L_{02} as shown in Fig. 5.1. These two inductors are mainly used to enlarge ZVS scope which helps to eliminate the switching loss and ensure the converter have high efficiency over wide load scope [11], [16], [29], [38]. Its simulation circuit and parameters are attached in Appendix A.

There are several existing control methods for this power circuit, such as single phase-shift control [1] and dual phase-shift control [6]. However, the novel triple-phase-shift control method will make the system with high efficiency (Higher than 97%) in large load scope, especially when parameters change. It is very important to make the efficiency of the bidirectional converter more robust to parameters change and different load conditions because this will make the converter more suitable for different applications.

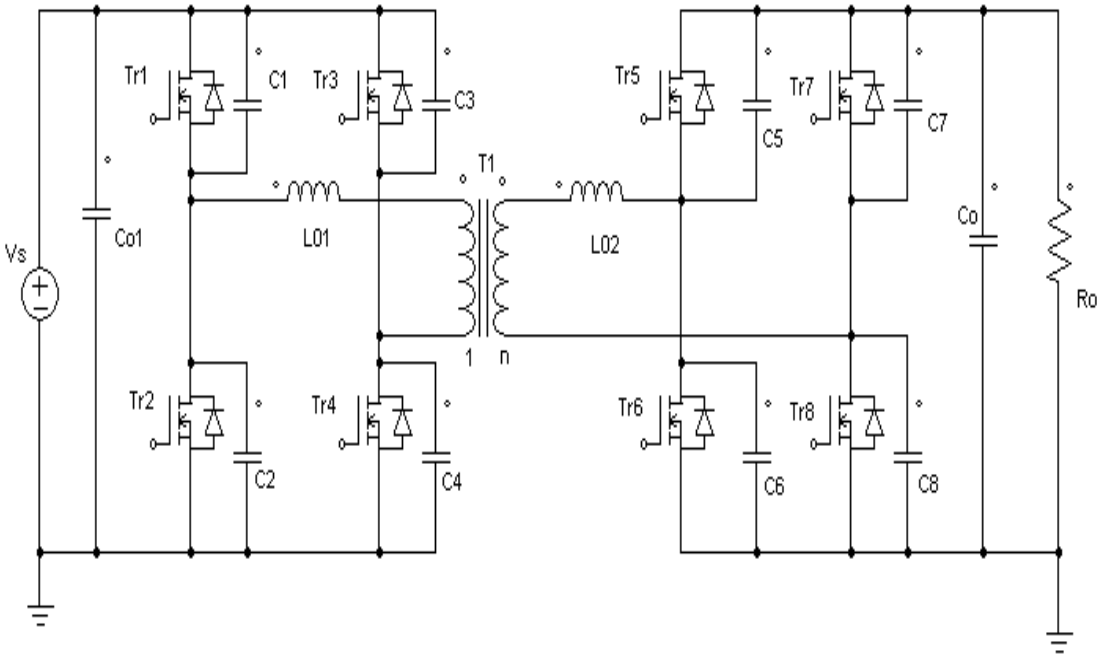

Fig. 5.1 Power Circuit of the Bidirectional Converter

In novel triple-phase-shift control method, three control variables cooperate together to adjust the efficiency of the bidirectional converter when parameters and output power change. Having three control variables available will make the efficiency of the

bidirectional converter more robust to parameter change and different output power. This project is simulated with PSIM software. Simulation results show that the efficiency of the bidirectional converter with novel triple-phase-shift control is higher than that of the same bidirectional converter with dual phase-shift control or with single phase-shift control when parameter and output power change. After careful theoretical analysis and simulation comparison, the novel triple-phase-shift control method is used for this project. This chapter will analyze the bidirectional dual full bridge ZVS DC-DC converter with the novel triple-phase-shift control method in detail.

5.2 Objectives and Rationale

The objective of this chapter is to analyze the working theory of the bidirectional dual full bridge ZVS DC-DC converter with novel triple phase-shift control quantitatively and to derive its general expressions of average input power, average output power and efficiency.

In order to thoroughly understand the working theory of novel triple phase-shift control method, both qualitative analysis and quantitative analysis are necessary. The working theory of the bidirectional dual full bridge converter with novel triple phase-shift control can be analyzed quantitatively by finding its equivalent circuits, inductor voltage equations and capacitor current equations in every stage and sub-stage. It is easy to understand why the efficiency of bidirectional dual full bridge converter with novel triple phase-shift control is robust (insensitive) to parameter change from its general expression. Meanwhile, the relationship between average output power and the three phase-shifts can be seen clearly with its general expression. Obviously, these expressions will also be very helpful for the satisfactory design of bidirectional dual full bridge converter with novel triple phase-shift control.

5.3 Novel Triple Phase-shift Control Method

1、Overview of Novel Triple Phase-Shift Control Method

The novel triple-phase-shift control method described in this chapter is neither the same as common phase-shift control methods in which all control signals are half duty cycle nor the same as common single phase-shift plus PWM control method in which the duty cycle of control signals can vary from zero to one [12]. In this method, four control signals (V_{g1},V_{g2},V_{g5},V_{g6}) operate with fixed half duty cycle; another two control signals (V_{g3},V_{g4}) with varying duty cycle between zero and 50%; and the last two control signals (V_{g7},V_{g8}) with another varying duty cycle between zero and 50%. This will make the controller easier to be realized with lead-lag compensator [7], [15], [17]. Because there are three distinct phase-shifts in this new control method, it is called novel triple-phase-shift control method in this chapter. This can be seen clearly in the following simulation results and operating theory analysis.

The novel triple-phase-shift controller for this bidirectional converter is mainly used to make the efficiency and output voltage more robust to parameter and output power changes. This control method also improves the overall efficiency of the bidirectional converter. The core idea of this control method is explained here. The controller combines the first phase-shift between the primary control signals and corresponding secondary control signals, the second phase-shift between the control signals for diagonal power switches in the primary power circuit and the third phase-shift between the diagonal control signals for power switches in the secondary power circuit. The combinations of these phase shifts are used to control power transfer between the primary and secondary side, as well as controlling the output voltage. In this method, control signals V_{g1}, V_{g2}, V_{g5} and V_{g6} have half duty cycle; control signals V_{g3} and V_{g4} have a varying duty cycle between zero and half; control signals V_{g7} and V_{g8} have another varying duty cycle between zero and half. The block diagram of this novel triple phase-shift controller is listed in the following.

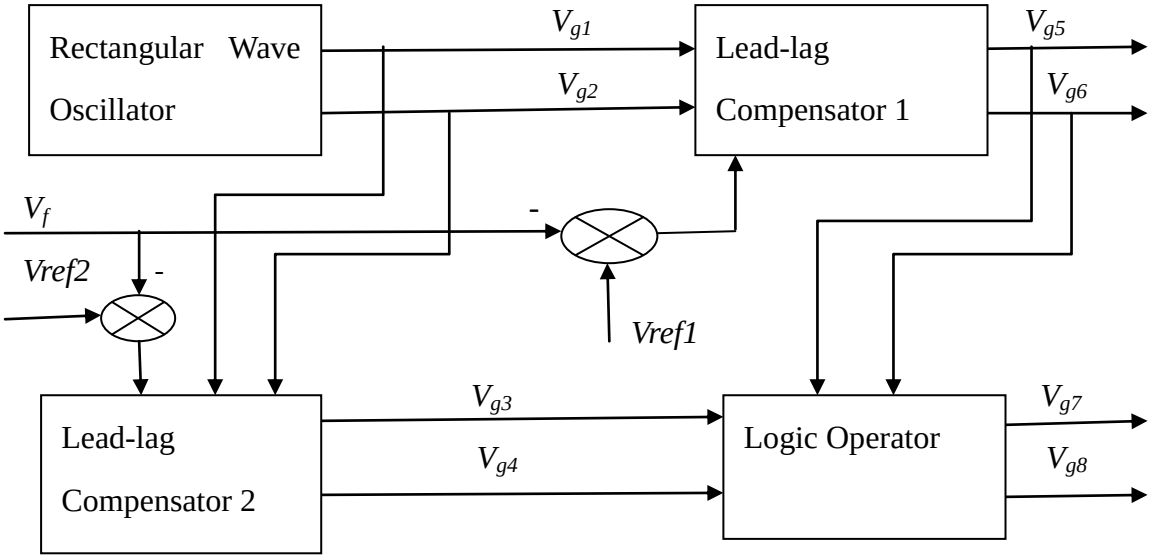

Fig. 5.2 Block Diagram of Novel Triple Phase-shift Controller

In this way, these three phase-shift control variables can cooperate very well to control the power transfer and the output voltage for different power levels. The system will be much more robust to parameter and output power change with triple phase-shift control method than with other control methods.

This novel triple-phase-shift controller combines effectively the first phase-shift between the half duty cycle control signals for primary and secondary power switches (V_{g1} and V_{g5}), the second phase-shift between the control signals for diagonal power switches in the primary side of the transformer (V_{g1} and V_{g4}) and the third phase-shift between the control signals for diagonal power switches in the secondary side of the transformer (V_{g5} and V_{g8}) to help transfer power and control the output voltage. The corresponding control wave-forms can be seen clearly in the following.

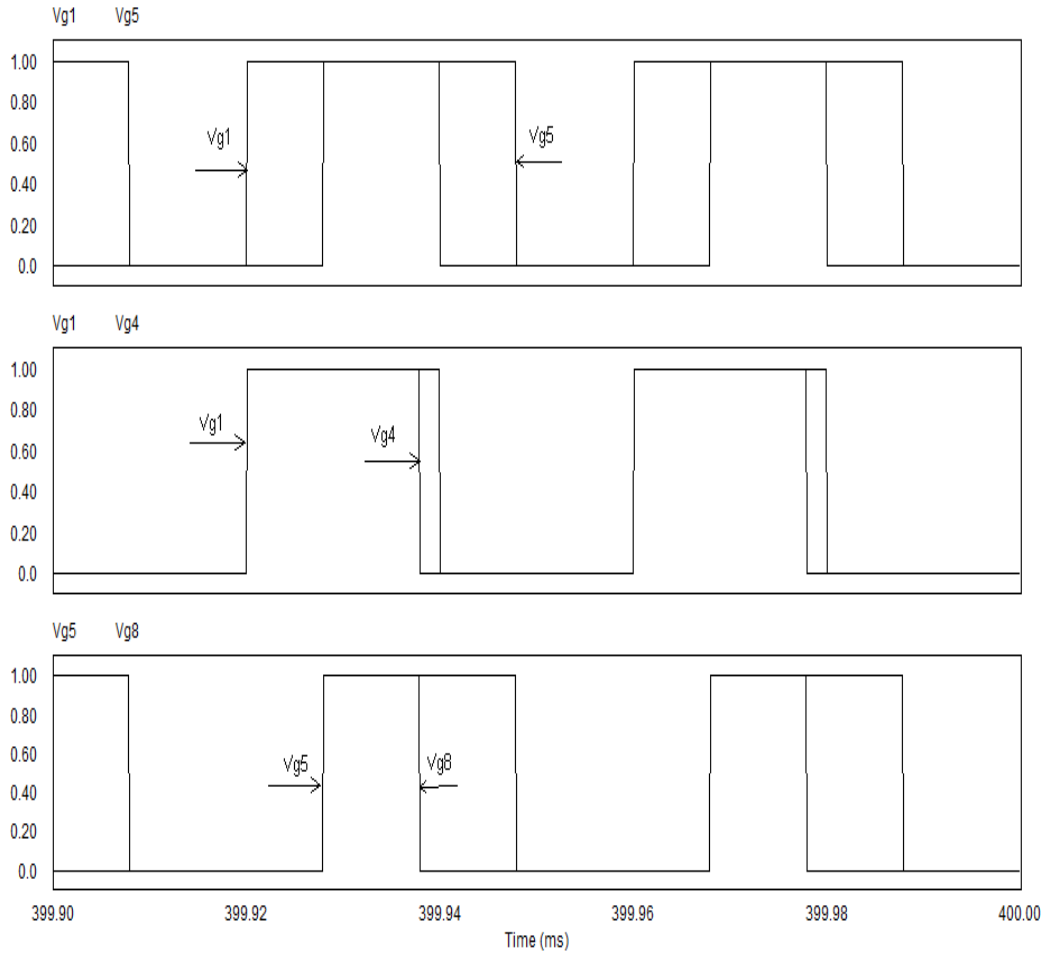

Fig. 5.3 Novel Triple Phase-shift Control Signal Waveforms

Based on the forward simulation results, the forward bidirectional converter can be separated into 8 stages. Corresponding equivalent circuits and necessary equations can be obtained in each stage. The backward converter can be analyzed similarly.

2：Simulation Results of Forward Bidirectional Dual Full Bridge Converter with Novel Triple-Phase-shift Control

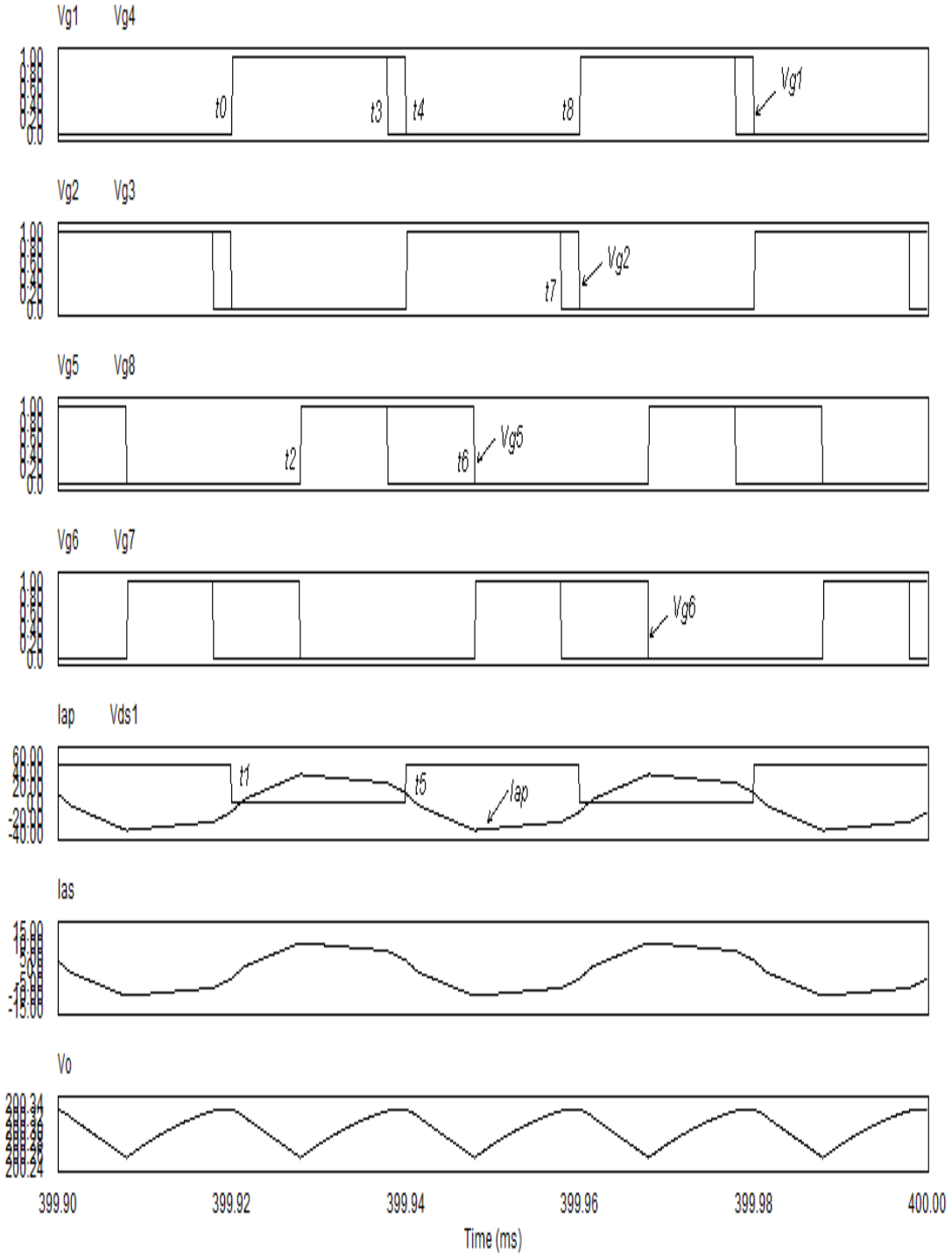

Fig. 5.4 Simulation Waveforms of Forward Bidirectional Converter with Novel Triple Phase-shift Control for *Vref1*=6V

3: Forward Simulation Results of Control Signals, Power Switch Voltages and Primary Current

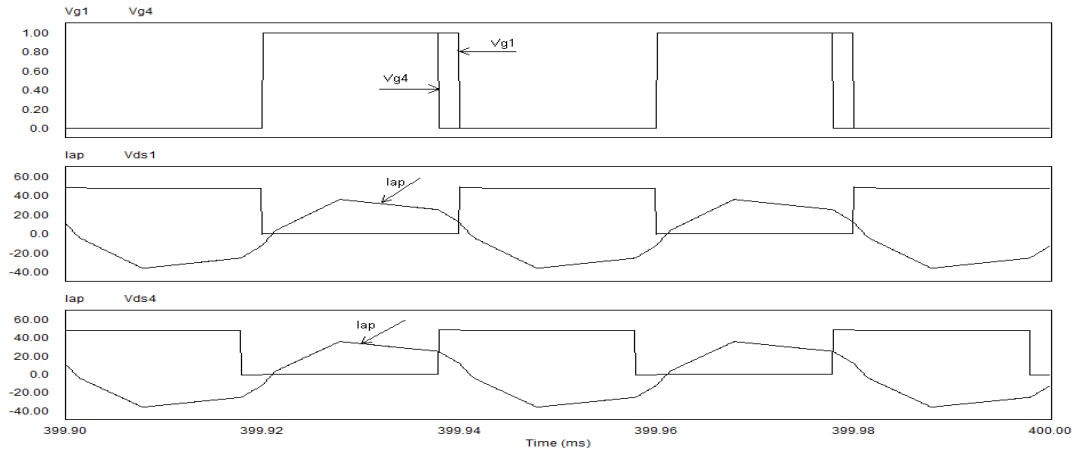

Fig. 5.5 Forward Control Signals, Power Switch Voltages and Primary Current with Novel Triple Phase-shift Control

From the simulation results, it can be found that the primary power circuit can realize ZVS very well because the primary current is negative when MOSFET1 and MOSFET4 turn on. This means the primary current passed through anti-parallel diodes D_1 and D_4 just before the power MOSFETs turn on; and therefore, ZVS can be realized very well.

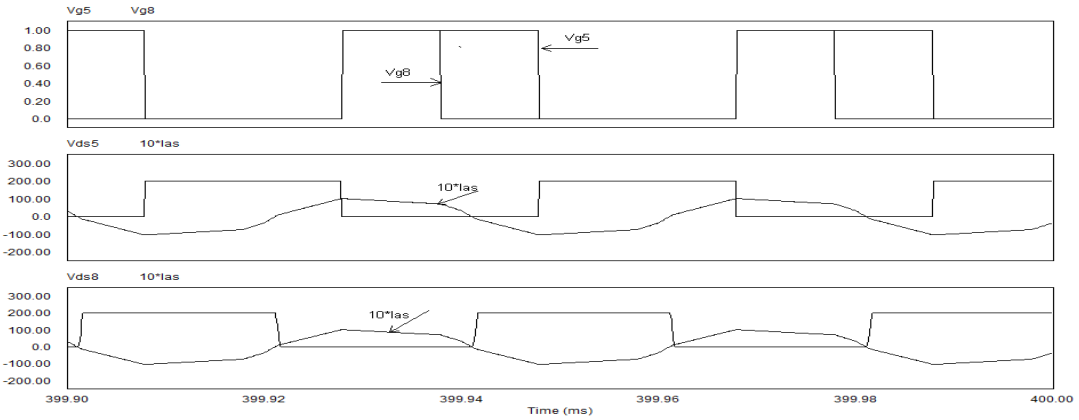

Fig. 5.6 Forward Control Signals, Power Switch Voltages and Secondary Current with Novel Triple Phase-shift Control

From the above simulation results, it can be found that the secondary power circuit can realize ZVS very well because the secondary current is positive when MOSFET5

and MOSFET8 turn on. From the positive direction of secondary current in Fig.5.1, it can be found that positive secondary current means it passed through anti-parallel diodes D_5 and D_8 just before the power MOSFETs turn on; ZVS can be realized very well, too. Therefore, the switching loss of this converter is eliminated [36]. For high frequency switching converters, switching loss is an important factor to influence efficiency [35].

5.4 Equivalent Circuits of this Bidirectional Converter Topology

The forward bidirectional dual full bridge converter is separated into eight stages in one period. Its operation and equivalent circuit for every stage are described below.

1: Stage 1 (t_0~t_1): Power switches *Tr1* and *Tr4* will turn on at "$t=t_0$". Because the primary current is still negative during this period, the inductor energy flows back to the power source. The primary current will flow through *Tr4*/*Tr1*. This is because the voltage drop across the on-resistance of the power MOSFET when it conducts is lower than the required conduction voltage drop of the anti-parallel diode. Thus, the diode will not conduct.

Because V_{g5}/V_{g8}/V_{g7} are all equal to zero, *Tr5*/*Tr8*/*Tr7* all in the "Off" state; V_{g6}=1, *Tr6* is "On". Because *ias*<0, the secondary current flows through *Tr6*/D_7. The inductor L_{02} and output capacitor provide energy to the load. The output voltage reduces during this stage. The equivalent circuit in this stage is as follows:

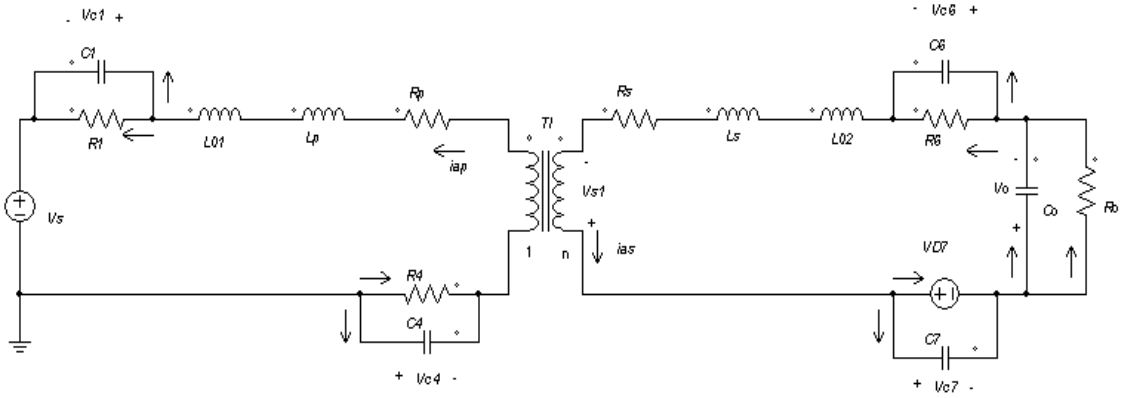

Fig. 5.7 Equivalent Circuit in Stage 1

2: Stage 2 (t_1~t_2): Because V_{g1}/ V_{g4} =1, power switches *Tr1* and *Tr4* are in the "On" state

in this stage. Because the primary current is positive during this stage, the primary current will flow through *Tr1*/*Tr4* and the inductor L_{01} and transformer leakage inductance. The energy will transfer from the primary side to the secondary side.

Because V_{g5}/V_{g8}/V_{g7} are all equal to zero, *Tr5*/*Tr8*/*Tr7* are in the "Off" state; V_{g6}=1, *Tr6* is "On". Because *ias*>0, the secondary current will charge capacitor C_7 and discharge capacitor C_8 till its voltage reduces to the forward conduction voltage of diode D_8. The equivalent circuit in this sub-stage is as follows:

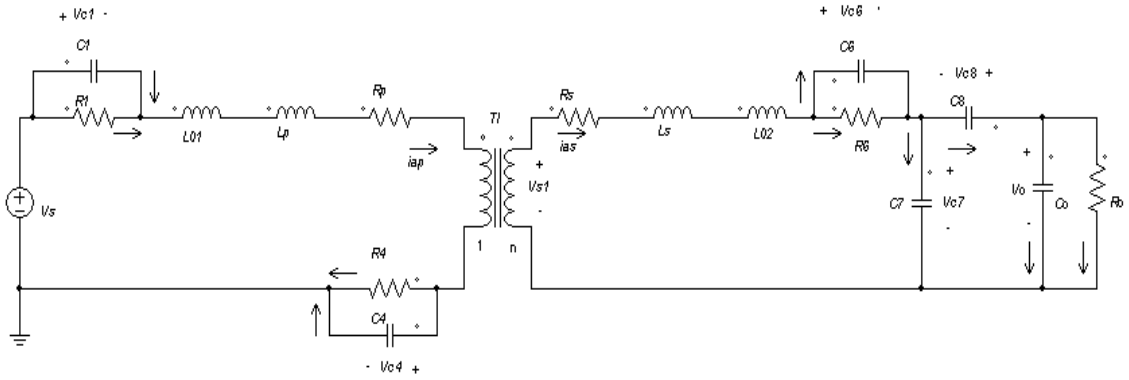

Fig. 5.8 C_8 Discharging Equivalent Circuit in Stage 2

Then the current flows through *Tr6*/D_8. The energy is stored in the secondary inductor L_{02} and leakage inductor because this is a free-wheeling sub-stage with no power transferred to the load theoretically. Output capacitor provides energy to the load. The output voltage continues to reduce in this sub-stage. The equivalent circuit in this sub-stage is as follows:

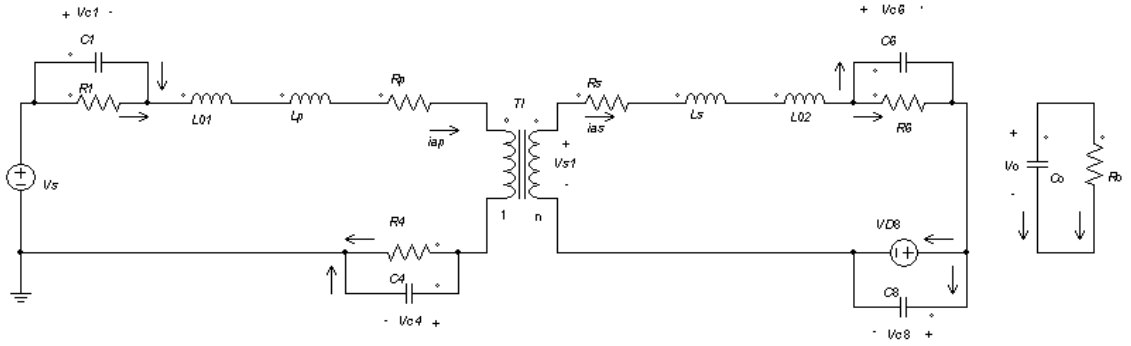

Fig. 5.9 Free Wheeling Equivalent Circuit in Stage 2

Tr6 turns off a little before t_2. The secondary current will charge snubber capacitor C_6

and discharge snubber capacitor C_5. During this very short transitional time, the secondary current flows through D_8 to charge and discharge the snubber capacitors. When C_5 is totally discharged ($Vds5$=0), the secondary current will flow through D_5/D_8 and the energy will be transferred to the load. The corresponding equivalent circuits are as follows:

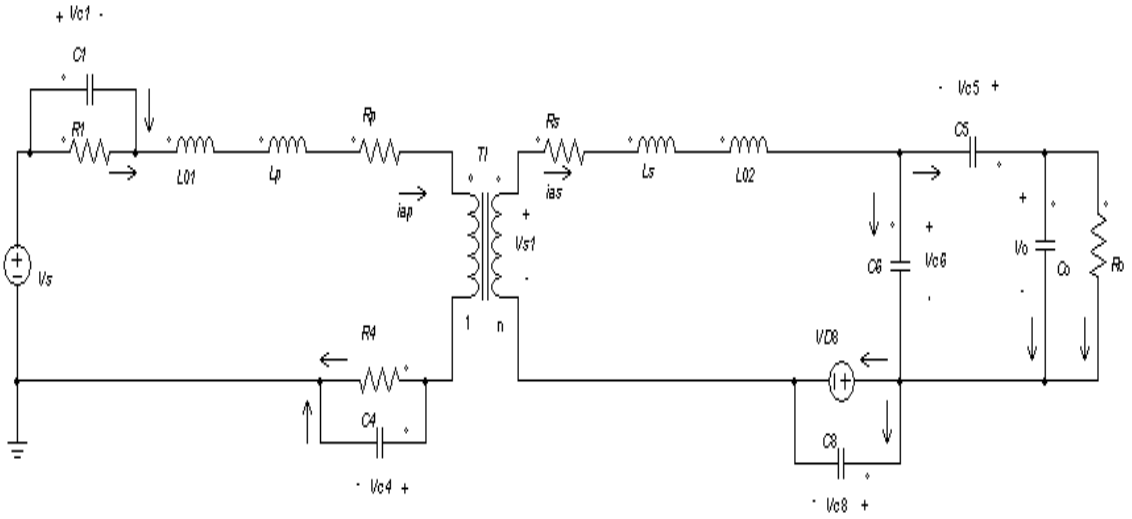

Fig. 5.10 Charge-Discharge Equivalent Circuit in Stage 2

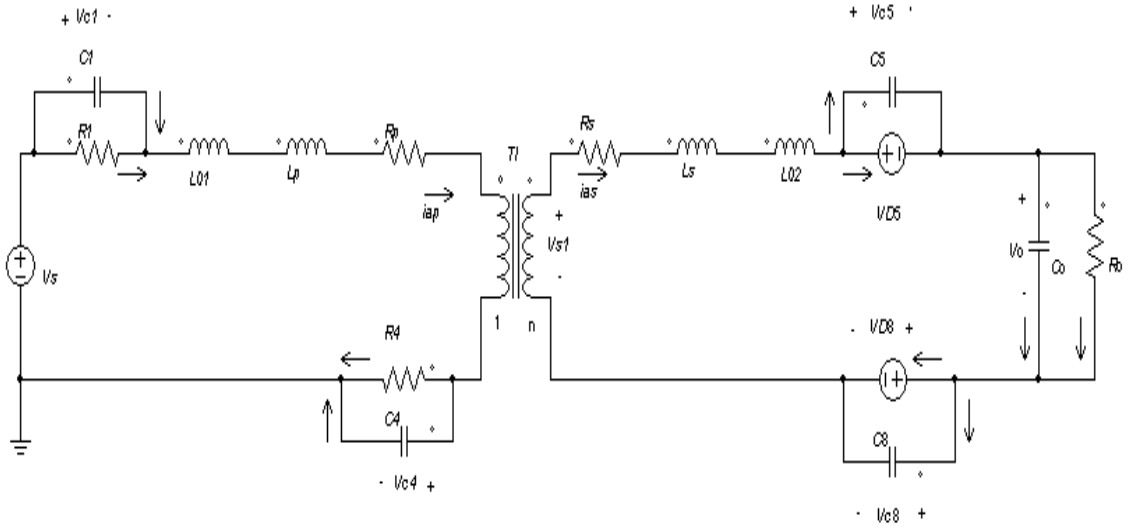

Fig. 5.11 Diode Conduct Equivalent Circuit in Stage 2

3: Stage 3 (t_2~t_3): The control signal V_{g5}/V_{g8}=1, and thus, the power switches *Tr5*/*Tr8* will

turn on at t_2. Because *ias*>0 during this stage, the secondary side current will flow through *Tr5*/*Tr8* and transfer energy to the load in this stage. The output voltage will increase in this stage. The equivalent circuit in this stage is as follows:

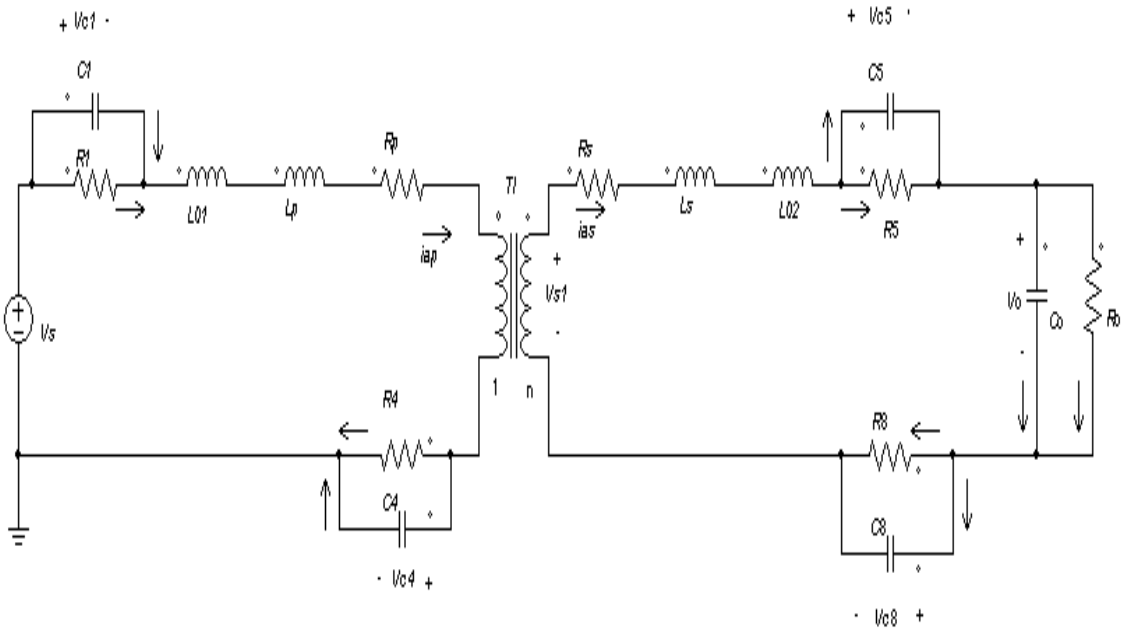

Fig. 5.12 Energy Transfer Equivalent Circuit in Stage 3

4: Stage 4 (t_3~t_4): V_{g4}/V_{g8}=0, so, *Tr4*/*Tr8* will turn off at t_3. For the primary side, *Tr4* turns off at t_3. The primary current will charge snubber capacitor C_4 and discharge snubber capacitor C_3. When C_3 is totally discharged (*Vds3*=0), the primary current will flow through *Tr1*/D_3 and form a free-wheeling sub-stage. No power is transferred to the secondary side theoretically.

For the secondary side, the current *ias*>0, this indicates that *Tr5*/D_8 will continue to conduct in this period of time. The additional inductor L_{02} and secondary leakage inductance will provide energy to transfer to the load. The output voltage will continue to increase in this stage. The equivalent circuits are shown in Fig.5.13 and Fig. 5.14.

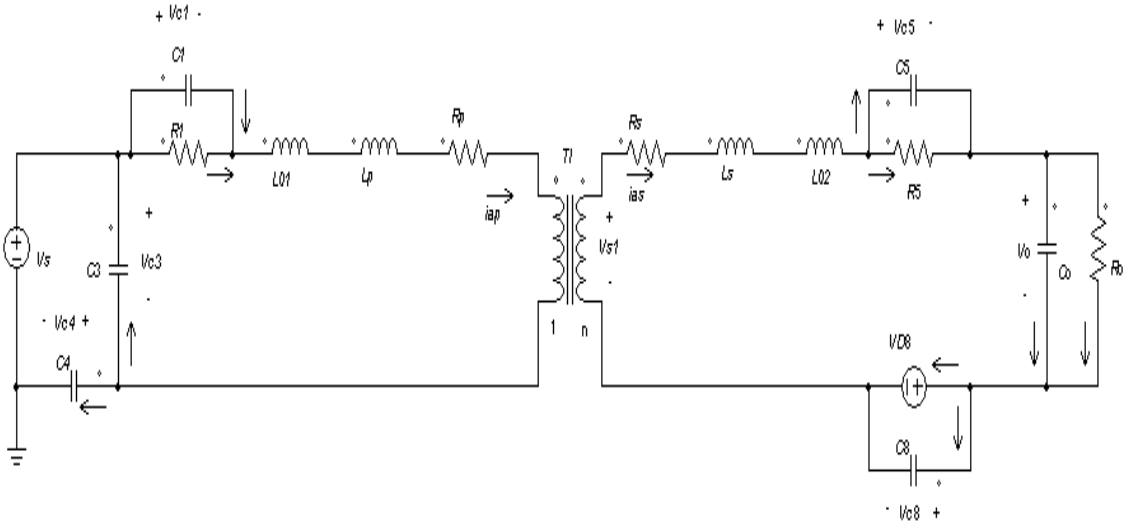

Fig. 5.13 C_3 Discharge Equivalent Circuit in Stage 4

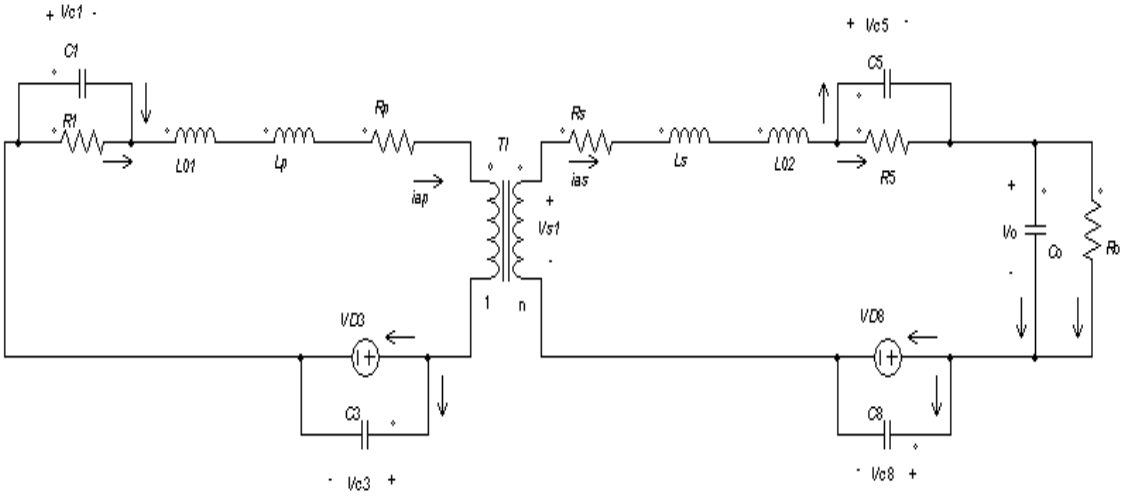

Fig. 5.14 Free Wheeling Equivalent Circuit in Stage 4

Tr1 turns off a little before t_4. The primary current will discharge snubber capacitor C_2 and charge snubber capacitor C_1. During this very short transitional time, the current will flow through D_3 to charge and discharge snubber capacitors. When C_2 is totally discharged (*Vds2*=0), D_2 will conduct. The energy will return to the power source. This will make it feasible for *Tr2*/*Tr3* to turn on under ZVS conditions. The equivalent circuits are shown in Fig. 5.15 and Fig. 5.16.

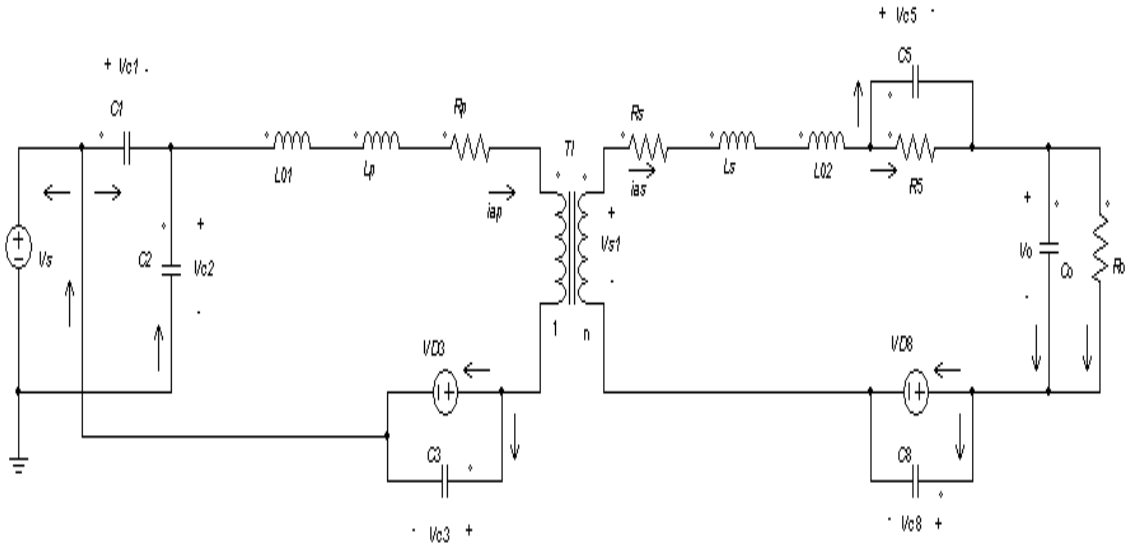

Fig. 5.15 C_2 Discharge Equivalent Circuit in Stage 4

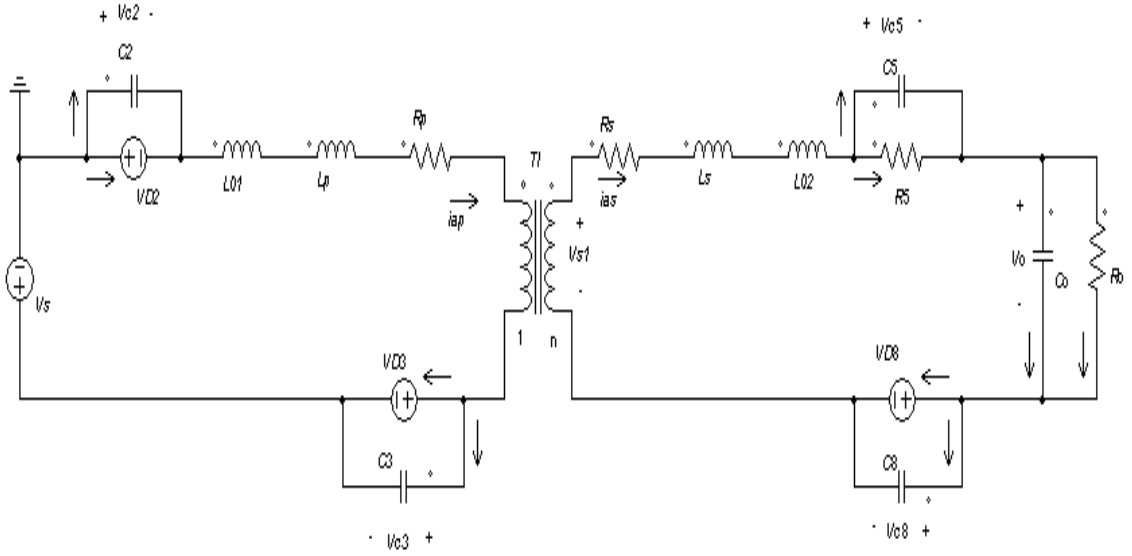

Fig. 5.16 Energy Feedback Equivalent Circuit in Stage 4

5: Stage 5 (t_4~t_5): Because V_{g2}/V_{g3}=1, *Tr2*/*Tr3* will turn on at t_4 under ZVS conditions. Because the primary current *iap*>0, the energy will feed back to the primary source in this stage.

For the secondary side, V_{g5}=1, so, *Tr5* is "On" in this stage. $V_{g6}/V_{g7}/V_{g8}$=0, so, *Tr6*/*Tr7*/*Tr8* will be in "Off" state during this period of time. Because the secondary

current *ias*>0, *Tr5*/D_8 will conduct in this period of time. The inductor L_{02}, the secondary leakage inductor and output capacitor will all provide energy to the load in this stage. The output voltage begins to reduce in this stage. According to this analysis, the equivalent circuits of this stage can be obtained.

6: Stage 6 (t_5~t_6): Because V_{g2}/V_{g3}=1, *Tr2*/*Tr3* will be turned on in this stage. Because the primary current *iap*<0, the energy will transfer to the secondary side again.

For the secondary side, V_{g5}=1, so, *Tr5* is turned on in this stage. V_{g6}/V_{g7}/V_{g8}=0, so, *Tr6*/*Tr7*/*Tr8* will be in the "Off" state. Because the secondary current *ias*<0, the secondary current will charge capacitor C_8 and discharge capacitor C_7 till its voltage reduces to the forward conduction voltage of diode D_7. Then the current flows through *Tr5*/D_7 and forms a free-wheeling sub-stage with no energy transferred to the load theoretically in this stage. The energy from primary source is stored in L_{02} and the leakage inductor. The output capacitor provides energy to the load and the output voltage will continue to reduce in this stage. The equivalent circuit can be obtained.

7: Stage 7 (t_6~t_7): Because V_{g6}/V_{g7}=1, *Tr6*/*Tr7* will turn on at t_6. V_{g5}=0, so *Tr5* turns off a little before t_6. The secondary current will charge snubber capacitor C_5 and discharge snubber capacitor C_6. During this very short transitional time, the secondary current flows through D_7 to charge and discharge the snubber capacitors. When C_6 is totally discharged (*Vds6*=0), D_6 will turn on and D_6/D_7 will conduct. This allows for ZVS conditions and energy will be transferred to the load. Because the secondary side current *ias*<0, *Tr6*/*Tr7* will conduct in this period of time and transfer energy to the load in this stage. The output voltage will increase in this stage. The equivalent circuits in this stage can be obtained.

8: Stage 8 (t_7~t_8)*:* Because V_{g3}/V_{g7}=0 at t_7, *Tr3*/*Tr7* will turn off at t_7. The primary current will charge snubber capacitor C_3 and discharge snubber capacitor C_4. During this very short transitional time, the primary current flows through *Tr2* to charge and discharge snubber capacitors C_3 and C_4. When C_4 is totally discharged (*Vds4*=0), D_4 will turn on.

Tr2/D_4 conduct; this forms a free-wheeling sub-stage with no energy transferred to the secondary side.

Tr2 turns off a little before t_8. The energy stored in additional inductor L_{01} and transformer leakage inductance will charge the snubber capacitor C_2 and discharge snubber capacitor C_1. During this very short transitional time, the primary current flows through D_4 to charge and discharge the snubber capacitors. When C_1 is totally discharged (*Vds1*=0), then the primary current will flow through D_4/D_1 and the inductor energy flows back to the power source.

On the secondary side, *Tr6*/D_7 will continue to conduct during this period of time and transfer energy to the load. This is because the secondary side current *ias*<0. The energy mainly comes from the stored energy of additional inductor L_{02} and the leakage inductance. The output voltage will continue to increase in this stage. The corresponding equivalent circuits can be obtained.

5.5 Necessary Equations of this Bidirectional Converter in Each Stage

Based on the equivalent circuits of each stage, the corresponding equivalent inductor voltage and output capacitor current equations can be built for this bidirectional DC-DC converter in each stage.

1：Necessary Equations for Stage t_0~t_1

The necessary equation of the converter can be built according to the equivalent circuit in this stage as follows:

$$\begin{cases} \left(L_{01}+Lp+\frac{1}{n^2}*L_{02}+\frac{1}{n^2}*Ls\right)*\frac{diap}{dt}=-\frac{1}{n}*Vo-Vs\ -\left(Rp+R_1+R_4+\frac{1}{n^2}*Rs+\frac{1}{n^2}*R_6\right)*iap \\ Co*\frac{dVo}{dt}=\frac{1}{n}*iap-\frac{Vo}{Ro} \end{cases} \tag{5-1}$$

2：Necessary Equations for Stage t_1~t_2

From the previous analysis of the converter working process, it can be found there are four sub-stages and corresponding four equivalent circuits in this stage.

(1) Sub-stage of Charge-discharge of C_7 and C_8

According to the equivalent circuit of the converter shown in Fig.5.8, the equation can be built as follows:

$$\begin{cases} \left(L_{01} + Lp + \frac{1}{n^2} * L_{02} + \frac{1}{n^2} * Ls\right) * \frac{diap}{dt} = -\left(Rp + R_1 + R_4 + \frac{1}{n^2} * Rs + \frac{1}{n^2} * R_6\right) * iap - \frac{1}{n} * Vc7 + Vs \\ Co * \frac{dVo}{dt} = -\frac{Vo}{Ro} \end{cases} \tag{5-2}$$

(2) Sub-stage of Free Wheeling in Stage 2

According to the equivalent circuit of the converter in the freewheeling stage shown in Fig.5.9, the corresponding equation can be built as follows:

$$\begin{cases} \left(L_{01} + Lp + \frac{1}{n^2} * L_{02} + \frac{1}{n^2} * Ls\right) * \frac{diap}{dt} = -\left(Rp + R_1 + R_4 + \frac{1}{n^2} * Rs + \frac{1}{n^2} * R_6\right) * iap + Vs \\ Co * \frac{dVo}{dt} = -\frac{Vo}{Ro} \end{cases} \tag{5-3}$$

(3) Sub-stage of C_5/C_6 Charge and Discharge in Stage 2

According to the equivalent circuit of the converter in this stage shown in Fig.5.10, the corresponding equation can be built as follows:

$$\begin{cases} \left(L_{01} + Lp + \frac{1}{n^2} * L_{02} + \frac{1}{n^2} * Ls\right) * \frac{diap}{dt} = -\left(Rp + R_1 + R_4 + \frac{1}{n^2} * Rs\right) * iap - \frac{1}{n} * Vc6 + Vs \\ Co * \frac{dVo}{dt} = -\frac{Vo}{Ro} \end{cases} \tag{5-4}$$

(4) Sub-stage of D_5/D_8Conduction in Stage 2

According to the equivalent circuit of the converter in this stage shown in Fig.5.11, the corresponding equation can be built as follows:

$$\begin{cases} \left(L_{01} + Lp + \frac{1}{n^2} * L_{02} + \frac{1}{n^2} * Ls\right) * \frac{diap}{dt} = -\left(Rp + R_1 + R_4 + \frac{1}{n^2} * Rs\right) * iap - \frac{1}{n} * Vo + Vs \\ Co * \frac{dVo}{dt} = \frac{1}{n} * i_{ap} - \frac{Vo}{Ro} \end{cases} \tag{5-5}$$

3：Necessary Equations for Stage t_2~t_3

The energy is transferred to the DC load in this stage. According to the equivalent circuit of the converter in this stage shown in Fig.5.12, the corresponding equation can be built as following:

$$\begin{cases} \left(L_{01}+Lp+\frac{1}{n^2}*L_{02}+\frac{1}{n^2}*Ls\right)*\frac{diap}{dt}=-\left(Rp+R_1+R_4+\frac{1}{n^2}*Rs+\frac{1}{n^2}*R_5+\frac{1}{n^2}*R_8\right)*iap-\frac{1}{n}*Vo+Vs \\ Co*\frac{dVo}{dt}=\frac{1}{n}*i_{ap}-\frac{Vo}{Ro} \end{cases} \tag{5-6}$$

4：Necessary Equations for Stage t_3~t_4

From the previous analysis of the converter working process, it can be found there are four sub-stages in this stage. The first two main sub-stages are analyzed here. The necessary equations can be built as follows:

(1) Sub-stage of C_3/C_4 Charge and Discharge in Stage 4

$$\begin{cases} \left(L_{01}+Lp+\frac{1}{n^2}*L_{02}+\frac{1}{n^2}*Ls\right)*\frac{diap}{dt}=-\left(Rp+R_1+\frac{1}{n^2}*Rs+\frac{1}{n^2}*R_5\right)*iap-Vc4-\frac{1}{n}*Vo+Vs \\ Co*\frac{dVo}{dt}=\frac{1}{n}*i_{ap}-\frac{Vo}{Ro} \end{cases} \tag{5-7}$$

(2) Sub-stage of Tr1/D_3Conduction in Stage 4

This is another free wheeling sub-stage in the primary power circuit. The necessary equations can be built as follows:

$$\begin{cases} \left(L_{01}+Lp+\frac{1}{n^2}*L_{02}+\frac{1}{n^2}*Ls\right)*\frac{diap}{dt}=-\left(Rp+R_1+\frac{1}{n^2}*Rs+\frac{1}{n^2}*R_5\right)*iap-\frac{1}{n}*Vo \\ Co*\frac{dVo}{dt}=\frac{1}{n}*i_{ap}-\frac{Vo}{Ro} \end{cases} \tag{5-8}$$

The necessary equations for other two very short sub-stages and the left four stages can be built similarly according to the working process analysis.

5.6 Voltage Ratio, Average Power and Efficiency of this Bidirectional Converter

It is well known that the converter losses mainly include conduction loss and switching loss [31], [35]. The switching loss of the converter is eliminated because this converter can realize ZVS very well over wide load scope. In the following power and efficiency expressions, only the conduction loss of power MOSFETs and the loss of the winding resistance of the transformer are considered.

1: The Expression of Voltage Ratio Vo/Vs

In order to see clearly the major role of triple phase-shift control method, the power MOSFETs and diodes are treated as ideal and the winding resistance of the transformer is neglected. From the working process analysis and the simulation waveforms shown in Fig.5.4, it can be found that the inductor current i_{ap} crosses zero at the half period of Ts. The first stage (t_0~t_1) and the fifth stage (t_4~t_5) are due to the dead band effect. They are neglected as well. In order to be convenient, write:

$$Leq = L_{01} + Lp + \frac{1}{n^2} * L_{02} + \frac{1}{n^2} * Ls$$

Because the time interval in which the snubber capacitors charge/discharge is very short compared with the stage time duration, it can be neglected, too. From Fig.5.4, it can be found the corresponding stages are equal to:

$$\begin{cases} t2 - t0 = D1*Ts \\ t3 - t2 = (0.5 - D3)*Ts \\ t4 - t3 = D2*Ts \end{cases} \quad (5\text{-}9)$$

Apply Volt-second balance and small ripple approximation to the combined equivalent inductor *Leq*, there is:

$$Vs * D1 + \left(-\frac{Vo}{n} + Vs\right) * (0.5 - D3) + \left(-\frac{Vo}{n}\right) * D2 = 0 \quad (5\text{-}10)$$

The relationship between the output voltage and source voltage can be obtained from Eq. 5-10 and written as:

$$\frac{Vo}{Vs} = \frac{n*(1+2*D1-2*D3)}{(1+2*D2-2*D3)} \quad (5\text{-}11)$$

This formula suggests that the output voltage depends on three control variables. This will make the output voltage more robust to parameter changes. With novel triple-phase-shift control, the output voltage behaves very well when the first reference voltage is equal to 5/6/7/8 Volts or other values in the control circuit. With dual or single phase-shift control, the average output voltage will be always equal to zero when the first reference voltage in the control circuit is equal to or higher than 6 Volts.

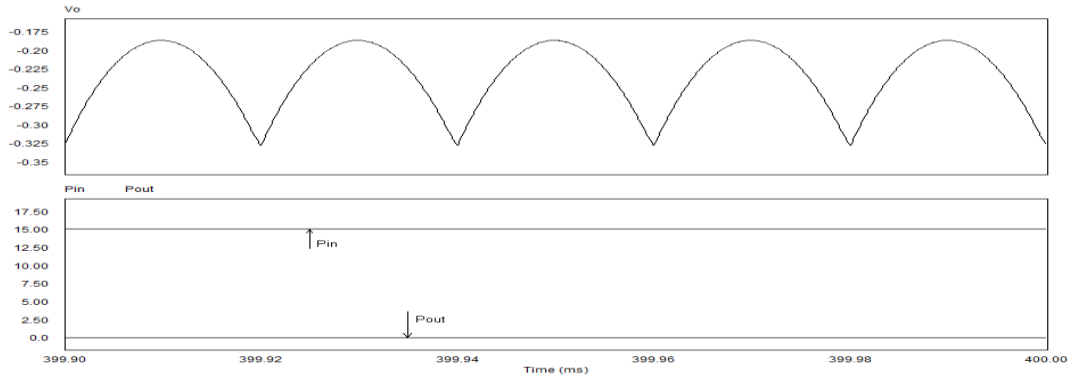

Fig. 5.17 Forward Simulation Results with Dual Phase-shift Control when *Vref1*>=6V

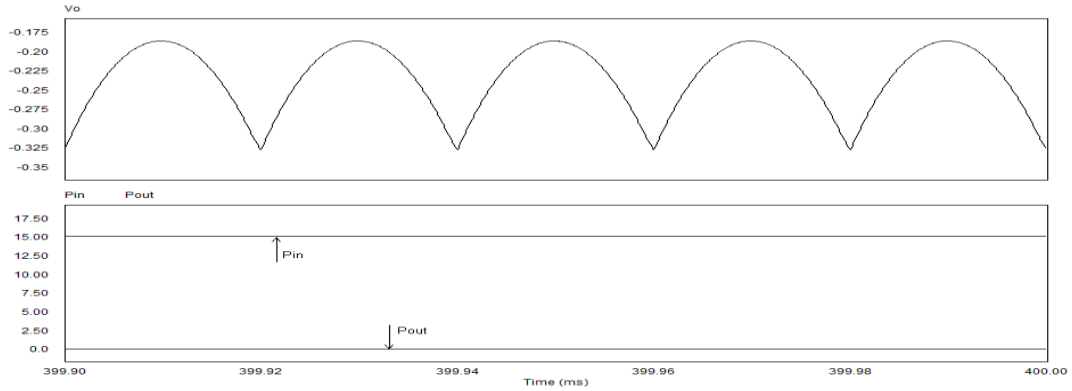

Fig. 5.18 Forward Simulation Results with Single Phase-shift Control when *Vref1*>=6V

2: The Expression of Primary Current in First Half Period

According to the primary current differential equation listed in section 5.5, there are three main current expressions in the first half period. The current expressions in ZVS sub-stages need not to be considered because the time for ZVS sub-stages are very short and there is no active power transfer in ZVS sub-stages theoretically.

(1) The Expression of Primary Current in Stage t_0~t_2

The equivalent resistance can be written as:

$$Req1 = Rp + R_1 + R_4 + \frac{1}{n^2} * Rs + \frac{1}{n^2} * R_6$$

Primary current in this stage can be found to be:

$$iap = \frac{Vs}{Req1} * \left(1 - e^{\frac{-Req1*t}{Leq}}\right) \quad (5\text{-}12)$$

(2) The Expression of Primary Current in Stage t_2~t_3

The equivalent resistance can be written as:

$$Req2 = Rp + R_1 + R_4 + \frac{1}{n^2} * Rs + \frac{1}{n^2} * R_5 + \frac{1}{n^2} * R_8$$

Primary current in this stage can be found to be:

$$\begin{cases} \text{iap(t2+) =iap(t2-) } = \frac{Vs}{Req1} * \left(1 - e^{\frac{-Req1*D1*Ts}{Leq}}\right) \\ iap = \frac{Vs - \frac{Vo}{n}}{Req2} + \left[iap(t2+) - \frac{Vs - \frac{Vo}{n}}{Req2}\right] * e^{\frac{-Req2*t}{Leq}} \end{cases} \quad (5\text{-}13)$$

(3) The Expression of Primary Current in Stage t_3~t_4

The equivalent resistance can be written as:

$$Req3 = Rp + R_1 + \frac{1}{n^2} * Rs + \frac{1}{n^2} * R_5$$

Primary current in this stage can be found to be:

$$\begin{cases} \text{iap(t3+) =iap(t3-) } = \frac{Vs - \frac{Vo}{n}}{Req2} + \left[iap(t2+) - \frac{Vs - \frac{Vo}{n}}{Req2}\right] * e^{\frac{-Req2*(0.5-D2)*Ts}{Leq}} \\ \text{iap} = \frac{-Vo}{n*Req3} + \left[iap(t3+) + \frac{Vo}{n*Req3}\right] * e^{\frac{-Req3*t}{Leq}} \end{cases} \quad (5\text{-}14)$$

The primary current expressions in the second half period are equal to the negative of

the corresponding expressions listed above.

3: The Expression of Average Input Power

Forward simulation waveforms of input current, primary current and power switch currents are listed in the following figure.

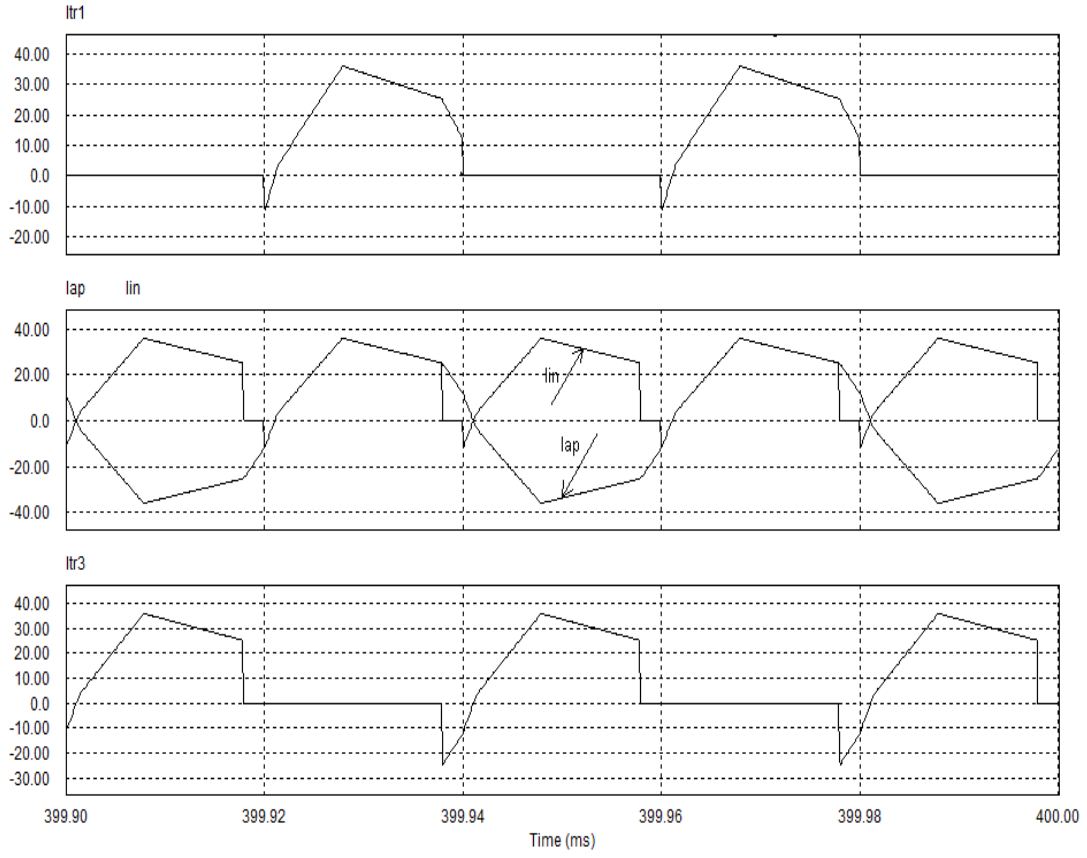

Fig. 5.19 Forward Simulation Waveforms of Input Current, Primary Current and Power Switch Currents

From the working process of the bidirectional converter and the above simulation results, it can be found the primary power circuit does not transfer power to the secondary side during the freewheeling stage (t_3~t_4) in the first half of the working period. A similar situation arises in the second half of the working period. Therefore, the average input active power is equal to:

$$P_{in} = \frac{2}{T_s} * \int_0^{\frac{T_s}{2}} Vs * i_{in}\, dt = \frac{2Vs}{T_s} * \int_0^{\frac{T_s}{2}} i_{ap}\, dt = \frac{2Vs}{T_s} * \left[\int_{t_0}^{t_2} i_{ap} dt + \int_{t_2}^{t_3} i_{ap} dt\right] \quad (5\text{-}15)$$

Substitute the corresponding expressions of i_{ap} into the above equation, the average active input power can be obtained.

$$P_{in} = \frac{2 * Vs^2}{Ts} * \left[\frac{D1 * Ts}{Req1} + \frac{Leq}{Req1^2} * e^{\frac{-Req1 * D1 * Ts}{Leq}} - \frac{Leq}{Req1^2} + \frac{Ts}{Req2} * \frac{(D2 - D1) * (1 - 2 * D2)}{(1 + 2 * D2 - 2 * D3)} \right.$$
$$- \frac{2 * D1 * (D2 - D1) * Ts}{(1 + 2 * D2 - 2 * D3) * Req2} - \frac{Leq}{Req1 * Req2} * \left(1 - e^{\frac{-Req1 * D1 * Ts}{Leq}}\right)$$
$$* e^{\frac{-Req2 * (0.5 - D2) * Ts}{Leq}} + \frac{Leq}{Req1 * Req2} * \left(1 - e^{\frac{-Req1 * D1 * Ts}{Leq}}\right) * e^{\frac{-Req2 * D1 * Ts}{Leq}}$$
$$\left. + \frac{2 * Leq * (D2 - D1)}{(1 + 2 * D2 - 2 * D3) * Req2^2} * e^{\frac{-Req2 * (0.5 - D2) * Ts}{Leq}} - \frac{2 * Leq * (D2 - D1)}{(1 + 2 * D2 - 2 * D3) * Req2^2} * e^{\frac{-Req2 * D1 * Ts}{Leq}} \right]$$

(5-16)

In order to be convenient, write:

$$Y_2 = \left[\frac{D1 * Ts}{Req1} + \frac{Leq}{Req1^2} * e^{\frac{-Req1 * D1 * Ts}{Leq}} - \frac{Leq}{Req1^2} + \frac{Ts}{Req2} * \frac{(D2 - D1) * (1 - 2 * D2)}{(1 + 2 * D2 - 2 * D3)} \right.$$
$$- \frac{2 * D1 * (D2 - D1) * Ts}{(1 + 2 * D2 - 2 * D3) * Req2} - \frac{Leq}{Req1 * Req2} * \left(1 - e^{\frac{-Req1 * D1 * Ts}{Leq}}\right)$$
$$* e^{\frac{-Req2 * (0.5 - D2) * Ts}{Leq}} + \frac{Leq}{Req1 * Req2} * \left(1 - e^{\frac{-Req1 * D1 * Ts}{Leq}}\right) * e^{\frac{-Req2 * D1 * Ts}{Leq}}$$
$$\left. + \frac{2 * Leq * (D2 - D1)}{(1 + 2 * D2 - 2 * D3) * Req2^2} * e^{\frac{-Req2 * (0.5 - D2) * Ts}{Leq}} - \frac{2 * Leq * (D2 - D1)}{(1 + 2 * D2 - 2 * D3) * Req2^2} * e^{\frac{-Req2 * D1 * Ts}{Leq}} \right]$$

(5-17)

It can be found the average input active power is decided by the three phase-shift ratios, the working period Ts, the power switch conduction loss, the equivalent inductance and the winding resistance of the transformer.

4: The Expression of Average Output Power

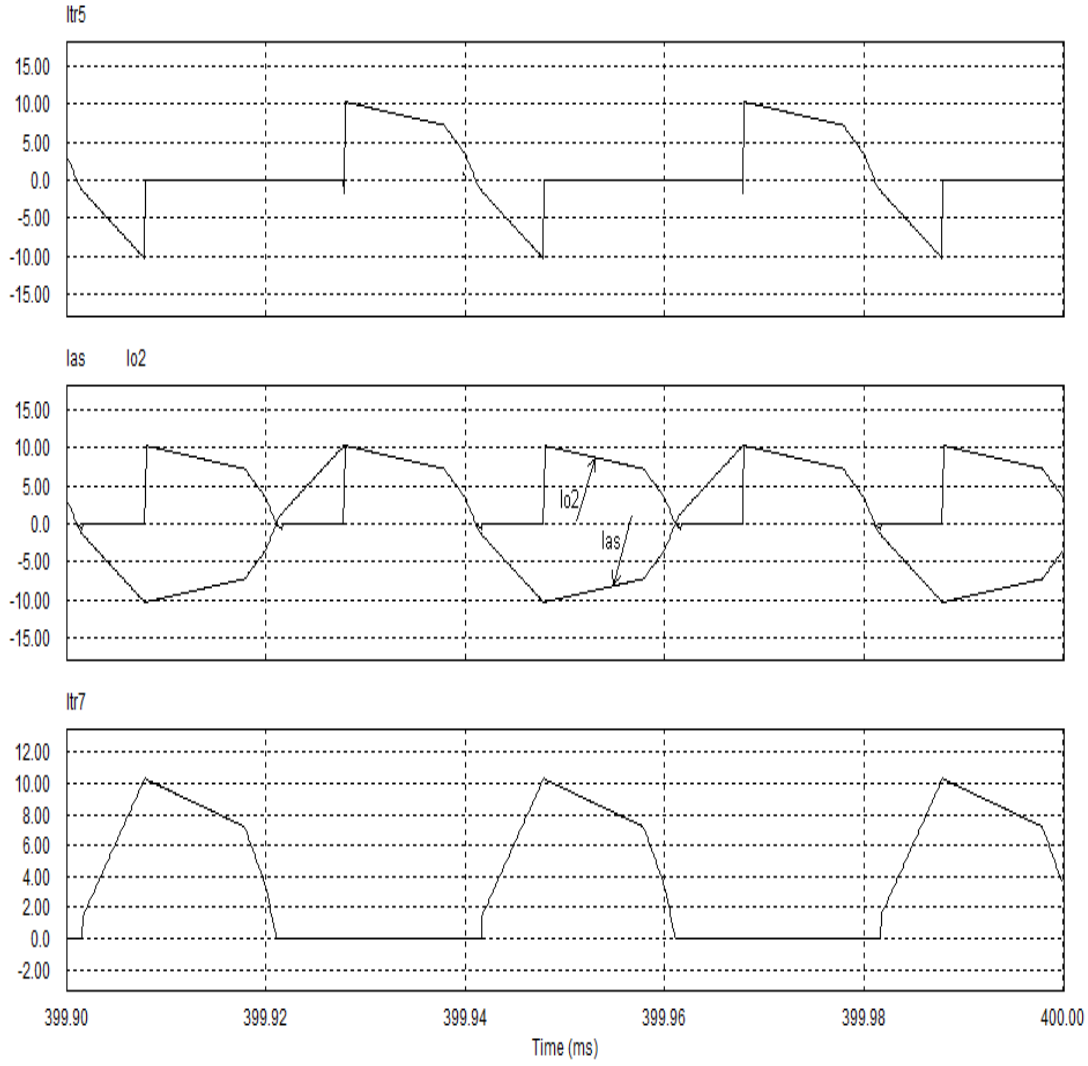

Fig. 5.20 Forward Simulation Waveforms of Output Current, Secondary Current and Power Switch Currents

From the working process of the bidirectional converter and the above simulation results, it can be found that the secondary power circuit does not transfer power to the load during the freewheeling stage (t_0~t_2) in the first half working period. A similar situation arises in the second half working period. Therefore, the average output active power is equal to:

$$P_{out} = \frac{2}{T_s} * \int_0^{\frac{T_s}{2}} Vo * i_o \, dt = \frac{2Vo}{nT_s} * \int_0^{\frac{T_s}{2}} i_{ap} \, dt = \frac{2Vo}{nT_s} * \left[\int_{t_2}^{t_3} i_{ap} dt + \int_{t_3}^{t_4} i_{ap} dt \right] \quad (5\text{-}18)$$

Substitute the corresponding expressions of i_{ap} into the above equation, the average active output power can be obtained.

$$P_{out} = \frac{2*Vs^2*(1+2*D1-2*D3)}{T_s*(1+2*D2-2*D3)} * \left[\frac{(D2-D1)*(1-2*D2)*Ts}{(1+2*D2-2*D3)*Req2} - \frac{2*D1*(D2-D1)*T_S}{(1+2*D2-2*D3)*Req2}\right]$$

$$+\frac{2*Vs^2*(1+2*D1-2*D3)}{Ts*(1+2*D2-2*D3)}$$

$$*\left[-\frac{Leq}{Req1*Req2}*\left(1-e^{\frac{-Req1*D1*Ts}{Leq}}\right)*e^{\frac{-Req2*(0.5-D2)*Ts}{Leq}}+\frac{Leq}{Req1*Req2}\right.$$

$$*\left(1-e^{\frac{-Req1*D1*Ts}{Leq}}\right)*e^{\frac{-Req2*D1*Ts}{Leq}}+\frac{2*(D2-D1)*Leq}{(1+2*D2-2*D3)*Req2^2}$$

$$*e^{\frac{-Req2*(0.5-D2)*Ts}{Leq}}-\frac{2*(D2-D1)*Leq}{(1+2*D2-2*D3)*Req2^2}*e^{\frac{-Req2*D1*Ts}{Leq}}$$

$$-\frac{(1+2*D1-2*D3)*Ts}{2*(1+2*D2-2*D3)*Req3}+\frac{(1+2*D1-2*D3)*(0.5-D2)*Ts}{(1+2*D2-2*D3)*Req3}$$

$$-\frac{2*(D2-D1)*Leq}{Req2*Req3*(1+2*D2-2*D3)}*e^{\frac{-Req3*Ts}{2*Leq}}$$

$$+\frac{2*(D2-D1)*Leq}{Req2*Req3*(1+2*D2-2*D3)}*e^{\frac{-Req3*(0.5-D2)Ts}{Leq}}-\frac{Leq}{Req1*Req3}$$

$$*e^{\frac{-Req2*(0.5-D2)*Ts-0.5*Req3*Ts}{Leq}}+\frac{Leq}{Req1*Req3}$$

$$*e^{\frac{-Req1*D1*Ts-Req2*(0.5-D2)*Ts-0.5*Req3*Ts}{Leq}}+\frac{2*(D2-D1)*Leq}{Req2*Req3*(1+2*D2-2D3)}$$

$$*e^{\frac{-Req2*(0.5-D2)*Ts-0.5*Req3*Ts}{Leq}}+\frac{Leq}{Req1*Req3}*e^{\frac{-Req2*(0.5-D2)*Ts-Req3*(0.5-D2)*Ts}{Leq}}$$

$$-\frac{Leq}{Req1*Req3}*e^{\frac{-Req1*D1*Ts-Req2*(0.5-D2)*Ts-Req3*(0.5-D2)*Ts}{Leq}}$$

$$-\frac{2*(D2-D1)*Leq}{Req2*Req3*(1+2*D2-2D3)}*e^{\frac{-Req2*(0.5-D2)*Ts-Req3*(0.5-D2)*Ts}{Leq}}$$

$$-\frac{Leq*(1+2*D1-2*D3)}{Req3^2*(1+2*D2-2*D3)}*e^{\frac{Req3*Ts}{2*Leq}}+\frac{Leq*(1+2*D1-2*D3)}{Req3^2*(1+2*D2-2*D3)}$$

$$\left.*e^{\frac{Req3*(0.5-D2)*Ts}{Leq}}\right] \tag{5-19}$$

In order to be convenient, write:

$$Y_1 = \left[\frac{(D2-D1)*(1-2*D2)*Ts}{(1+2*D2-2*D3)*Req2} - \frac{2*D1*(D2-D1)*T_S}{(1+2*D2-2*D3)*Req2}\right.$$

$$-\frac{Leq}{Req1*Req2}*\left(1-e^{\frac{-Req1*D1*Ts}{Leq}}\right)*e^{\frac{-Req2*(0.5-D2)*Ts}{Leq}}+\frac{Leq}{Req1*Req2}*\left(1-e^{\frac{-Req1*D1*Ts}{Leq}}\right)$$

$$*e^{\frac{-Req2*D1*Ts}{Leq}}+\frac{2*(D2-D1)*Leq}{(1+2*D2-2*D3)*Req2^2}*e^{\frac{-Req2*(0.5-D2)*Ts}{Leq}}$$

$$-\frac{2*(D2-D1)*Leq}{(1+2*D2-2*D3)*Req2^2}*e^{\frac{-Req2*D1*Ts}{Leq}}-\frac{(1+2*D1-2*D3)*Ts}{2*(1+2*D2-2*D3)*Req3}$$

$$+\frac{(1+2*D1-2*D3)*(0.5-D2)*Ts}{(1+2*D2-2*D3)*Req3}-\frac{2*(D2-D1)*Leq}{Req2*Req3*(1+2*D2-2*D3)}$$

$$*e^{\frac{-Req3*Ts}{2*Leq}}+\frac{2*(D2-D1)*Leq}{Req2*Req3*(1+2*D2-2*D3)}*e^{\frac{-Req3*(0.5-D2)Ts}{Leq}}-\frac{Leq}{Req1*Req3}$$

$$*e^{\frac{-Req2*(0.5-D2)*Ts-0.5*Req3*Ts}{Leq}}+\frac{Leq}{Req1*Req3}$$

$$*e^{\frac{-Req1*D1*Ts-Req2*(0.5-D2)*Ts-0.5*Req3*Ts}{Leq}}+\frac{2*(D2-D1)*Leq}{Req2*Req3*(1+2*D2-2D3)}$$

$$*e^{\frac{-Req2*(0.5-D2)*Ts-0.5*Req3*Ts}{Leq}}+\frac{Leq}{Req1*Req3}*e^{\frac{-Req2*(0.5-D2)*Ts-Req3*(0.5-D2)*Ts}{Leq}}$$

$$-\frac{Leq}{Req1*Req3}*e^{\frac{-Req1*D1*Ts-Req2*(0.5-D2)*Ts-Req3*(0.5-D2)*Ts}{Leq}}$$

$$-\frac{2*(D2-D1)*Leq}{Req2*Req3*(1+2*D2-2D3)}*e^{\frac{-Req2*(0.5-D2)*Ts-Req3*(0.5-D2)*Ts}{Leq}}$$

$$-\frac{Leq*(1+2*D1-2*D3)}{Req3^2*(1+2*D2-2*D3)}*e^{\frac{Req3*Ts}{2*Leq}}+\frac{Leq*(1+2*D1-2*D3)}{Req3^2*(1+2*D2-2*D3)}$$

$$\left.*e^{\frac{Req3*(0.5-D2)*Ts}{Leq}}\right] \tag{5-20}$$

It can be found that the average active output power is decided by the three phase-shift ratios, the working period Ts, the power switch conduction losses, the equivalent inductance and the winding resistance of the transformer.

5: The Efficiency of the Bidirectional Converter

The efficiency of a converter is given by Eq. 5-21.

$$\eta = \frac{P_{out}}{P_{in}} \tag{5-21}$$

Substitute the expressions of average input power and average output power into the above equation, the efficiency of this bidirectional converter with triple phase-shift control method can be calculated.

$$\eta = \frac{(1+2*D1-2*D3)*Y1}{(1+2*D2-2*D3)*Y2} \quad (5\text{-}22)$$

It is clear that the efficiency of the bidirectional converter with novel triple-phase-shift control mainly depends on three control variables. This will make it more robust to parameters change and output power variation.

The efficiency of the forward bidirectional converter using three different control methods is simulated and compared below. The robustness of each method is tested by varying some circuit parameters, as well as the output power.

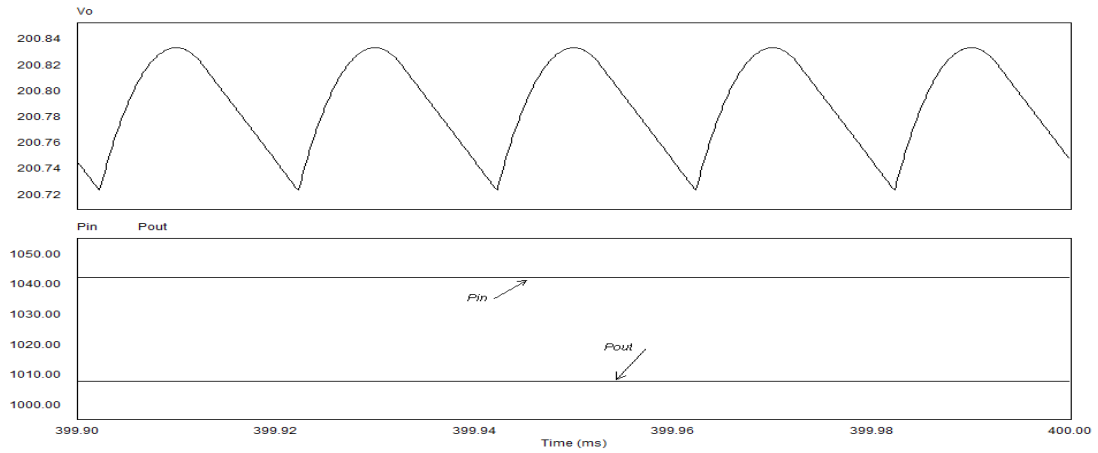

Fig. 5.21 Simulation Results of Forward Converter with Novel Triple Phase-shift Control (L_{01}=L_{02}=0, *Pout*=1kW)

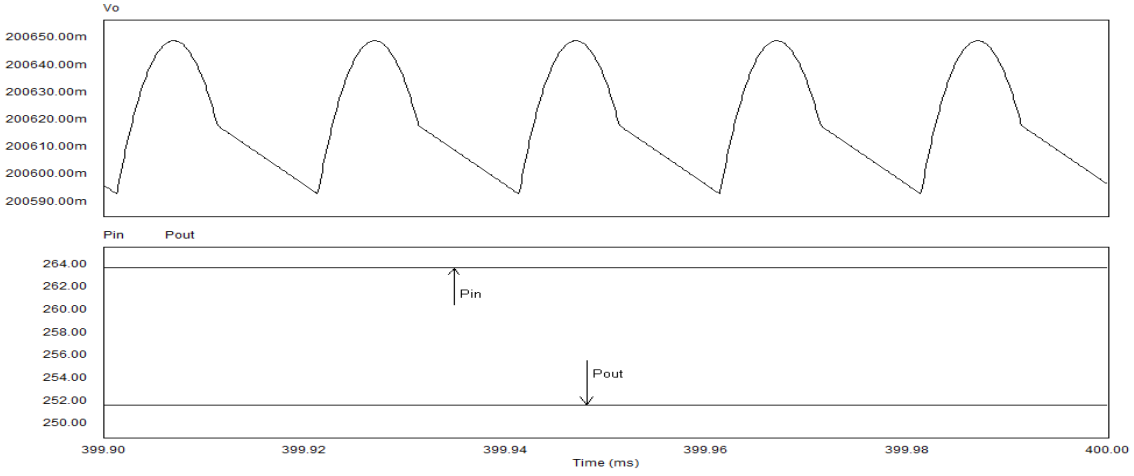

Fig. 5.22 Simulation Results of Forward Converter with Novel Triple Phase-shift Control (L_{01}=L_{02}=0, *Pout*=250W)

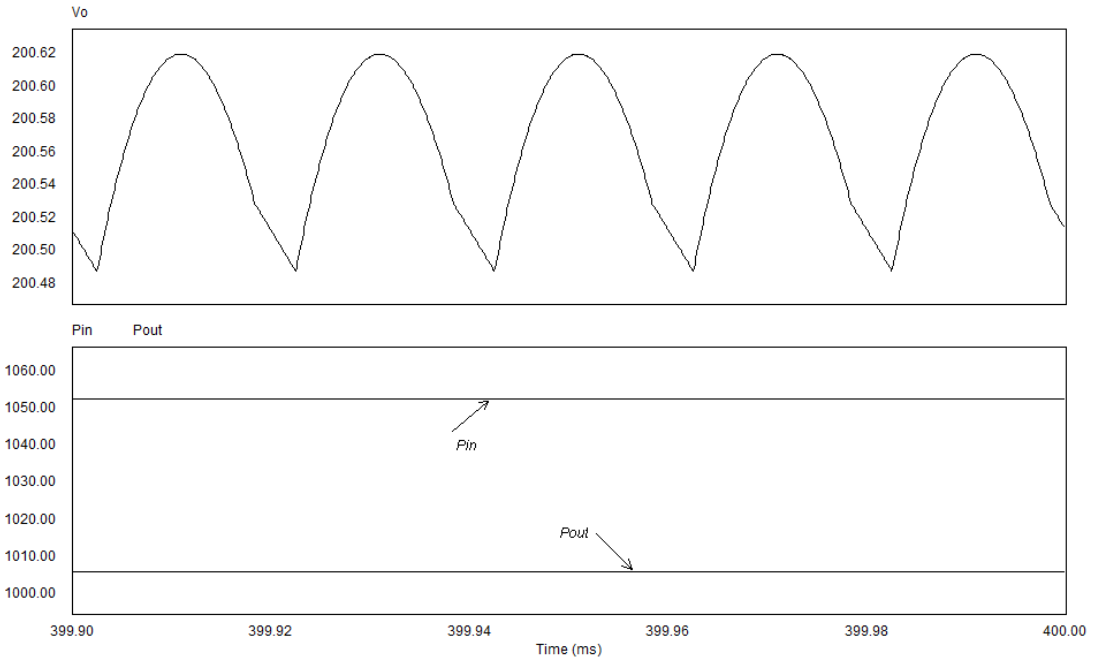

Fig. 5.23 Simulation Results of Forward Converter with Dual Phase-shift Control (L_{01}=L_{02}=0, *Pout*=1kW)

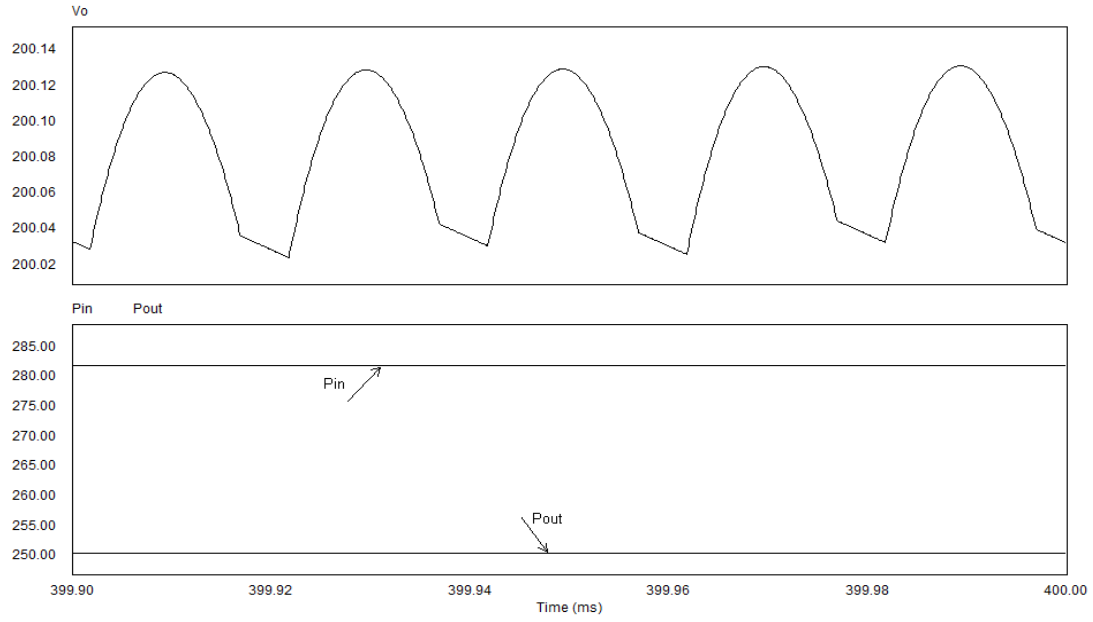

Fig. 5.24 Simulation Results of Forward Converter with Dual Phase-shift Control (L_{01}=L_{02}=0, *Pout*=250W)

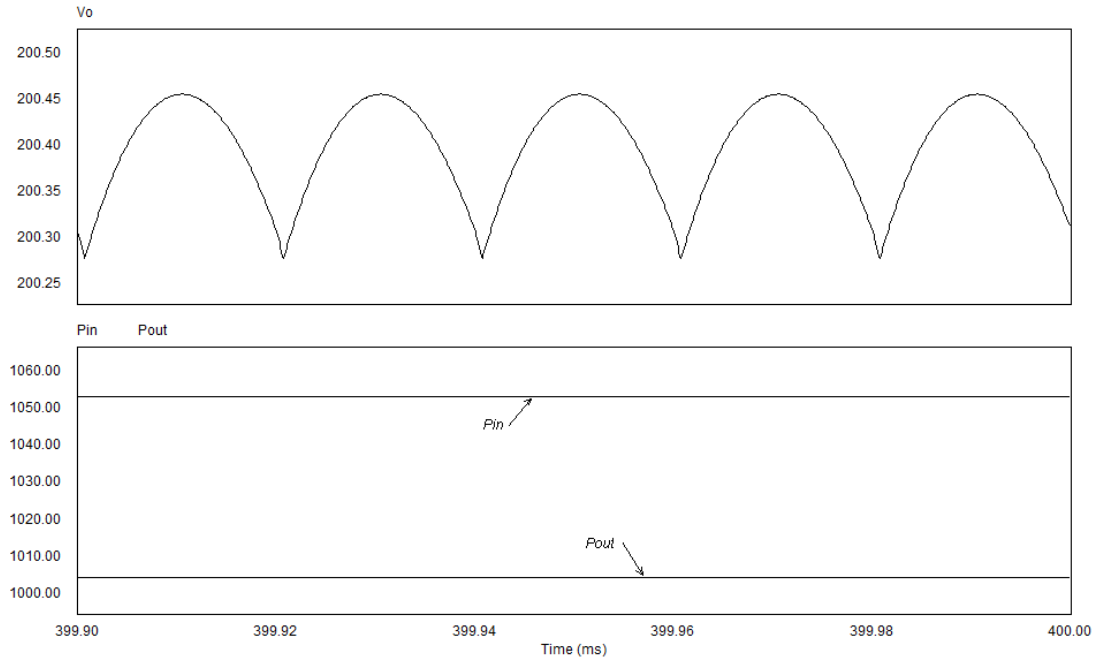

Fig. 5.25 Simulation Results of Forward Converter with Single Phase-shift Control (L_{01}=L_{02}=0, *Pout*=1kW)

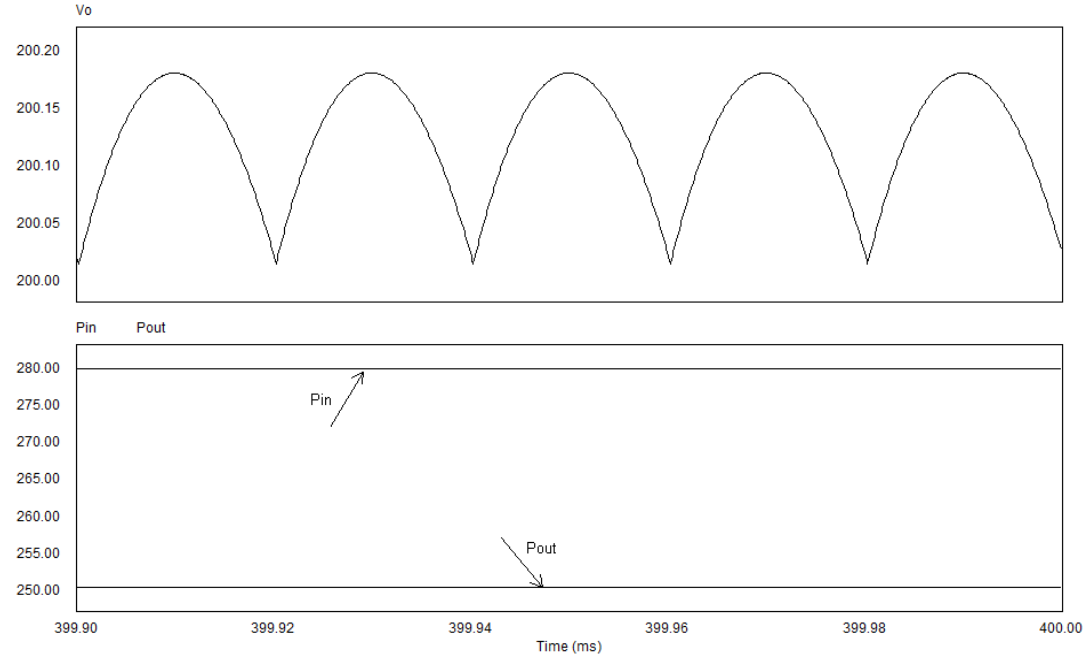

Fig. 5.26 Simulation Results of Forward Converter with Single Phase-shift Control (L_{01}=L_{02}=0, *Pout*=250W)

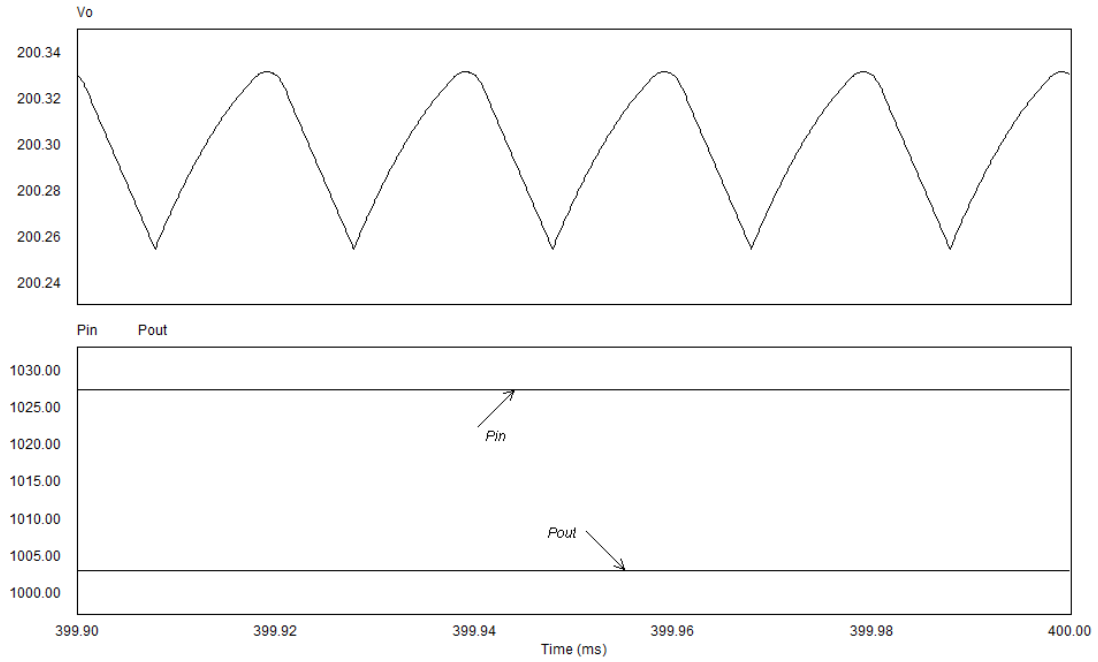

Fig. 5.27 Simulation Results of Forward Converter with Novel Triple Phase-shift Control (L_{01}=7.3uH, L_{02}=6.9uH, *Pout*=1kW)

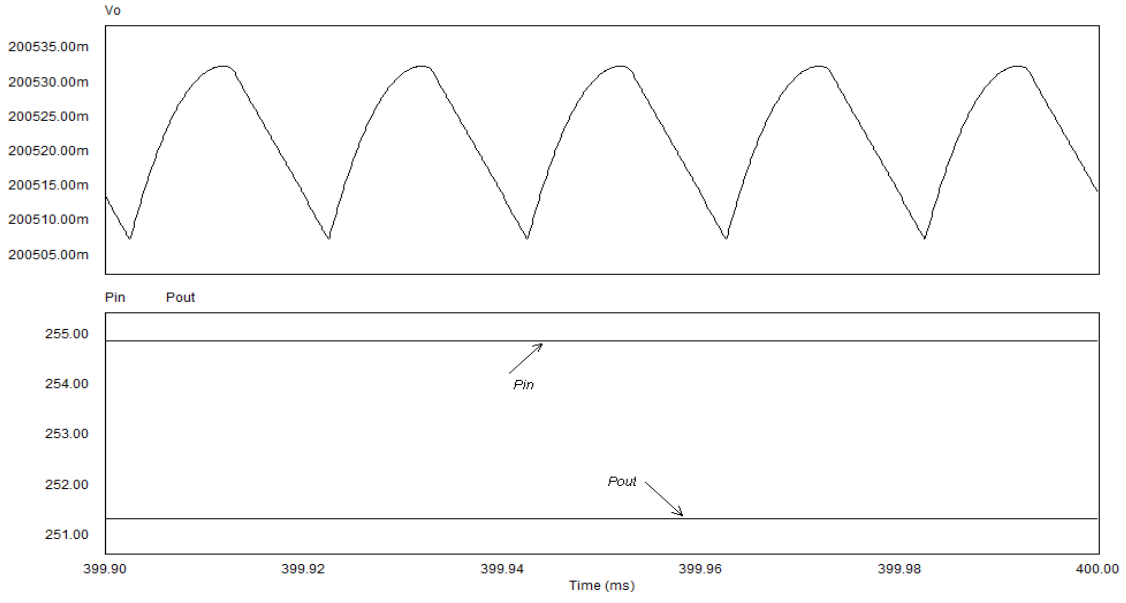

Fig. 5.28 Simulation Results of Forward Converter with Novel Triple Phase-shift Control (L_{01}=7.3uH, L_{02}=6.9uH, *Pout*=250W)

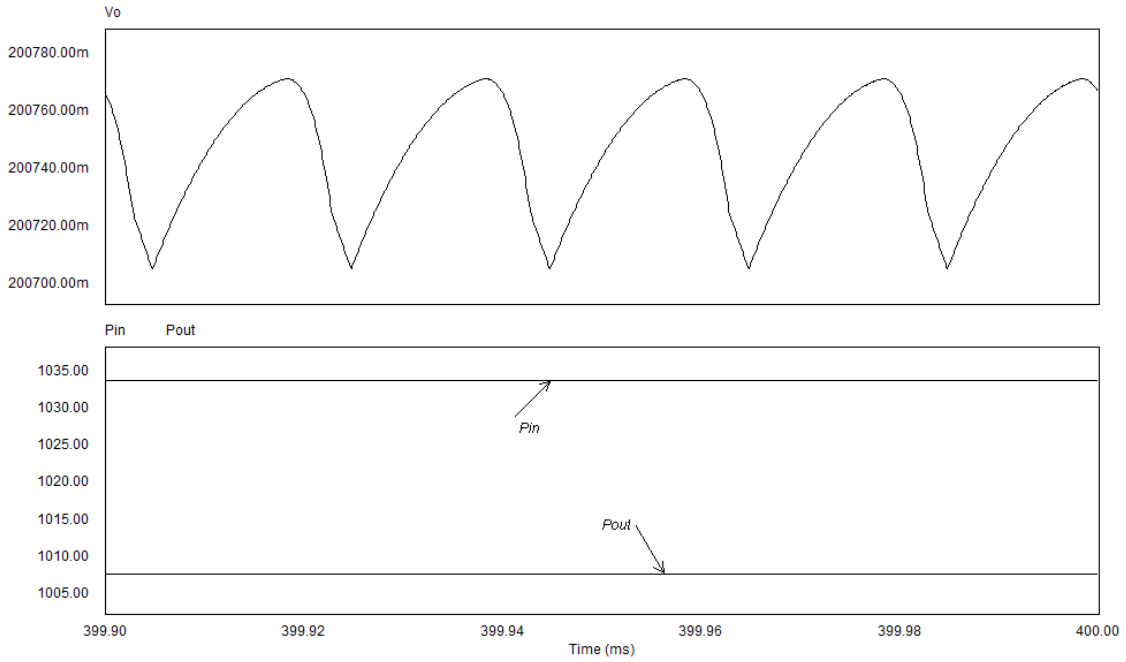

Fig. 5.29 Simulation Results of Forward Converter with Dual Phase-shift Control (L_{01}=7.3uH, L_{02}=6.9uH, *Pout*=1kW)

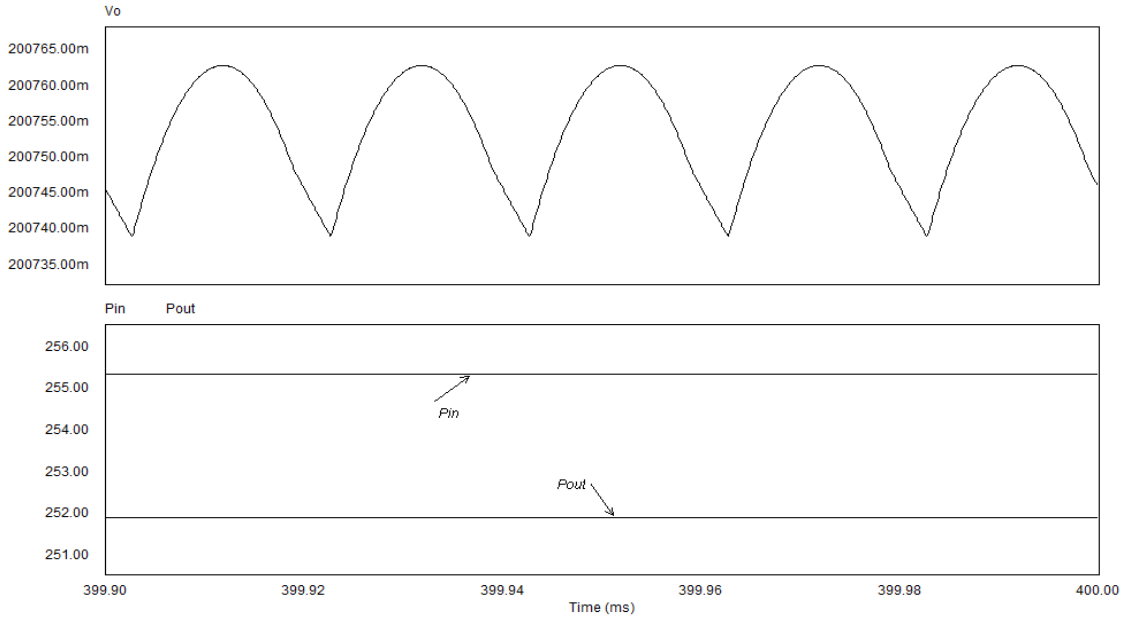

Fig. 5.30 Simulation Results of Forward Converter with Dual Phase-shift Control (L_{01}=7.3uH, L_{02}=6.9uH, *Pout*=250W)

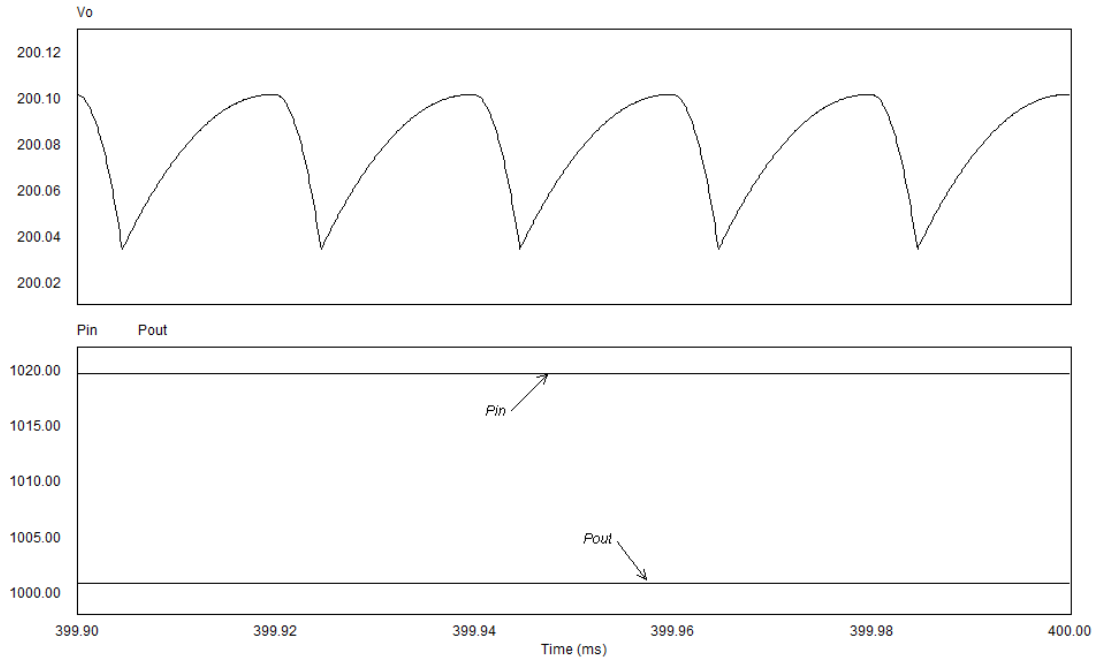

Fig. 5.31 Simulation Results of Forward Converter with Single Phase-shift Control (L_{01}=7.3uH, L_{02}=6.9uH, *Pout*=1kW)

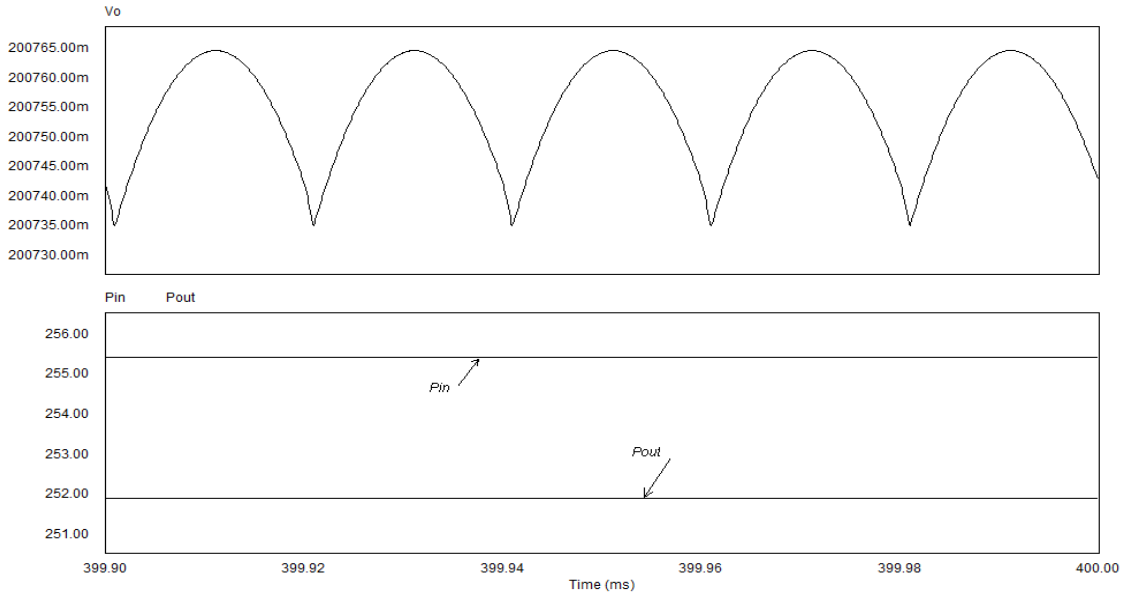

Fig. 5.32 Simulation Results of Forward Converter with Single Phase-shift Control (L_{01}=7.3uH, L_{02}=6.9uH, *Pout*=250W)

The following two tables give the efficiency comparison of the bidirectional dual full bridge converter with three different control methods when parameter and output power change.

Table 5.1 Forward Efficiency Comparison when Parameters and Output Power Change (L_{01}=L_{02}=0)

Output Power	Single Phase-shift Control	Dual Phase-shift Control	Novel Triple Phase-shift Control
1kW	95.4%	95.6%	96.7%
250W	89.4%	88.8%	95.4%

Table 5.2 Forward Efficiency Comparison when Parameters and Output Power Change (L_{01}=7.3uH, L_{02}=6.9uH)

Output Power	Single Phase-shift Control	Dual Phase-shift Control	Novel Triple Phase-shift Control
1kW	98.1%	97.5%	97.6%
250W	98.6%	98.6%	98.6%

Because the efficiency robustness of the bidirectional converter with three different control methods is compared with each other with the same power circuit in which all components parameters are totally the same, the convincing conclusion can be got directly with simulation results.

The bidirectional converter with single phase-shift plus PWM control is not simulated and compared with the bidirectional converter with novel triple phase-shift control. There are two control variables to adjust the efficiency and output voltage of the bidirectional converter with single phase-shift plus PWM control for parameters change and output power variation. Based on control theory, it can be derived that the efficiency robustness of the bidirectional converter with single phase-shift plus PWM control is inferior to that of the bidirectional converter with novel triple phase-shift control. It is unnecessary to compare a new method with all other different methods with simulation or experimental

results. If a new method can solve a problem effectively, e.g. efficiency robustness of the bidirectional converter, it is a meaningful method in engineering.

6: The Efficiency of the Bidirectional Converter over Wide Output Power Range

This bidirectional ZVS DC-DC converter with novel triple-phase-shift control is simulated with PSIM software for four different output powers. The corresponding efficiency is listed as following.

Table 5.3 Forward Output Power and Efficiency (L_{01}=7.3μH, L_{02}=6.9μH)

Pout (W)	1003.00	754.75	502.50	252.53
Efficiency	97.6%	97.6%	98.4%	98.5%

Table 5.4 Backward Output Power and Efficiency (L_{01}=7.3μH, L_{02}=6.9μH)

Pout (W)	1008.32	751.88	499.84	250.53
Efficiency	96.9%	97.3%	98.0%	98.4%

5.7 Main Contribution

The main contribution of this chapter is to analyze the bidirectional dual full bridge converter with novel triple phase-shift control qualitatively and quantitatively. The equivalent circuits and necessary equations of this bidirectional converter are built. The general expressions of voltage gain, average input power, average output power and efficiency are derived for this bidirectional dual full bridge converter with novel triple phase-shift control. This analysis will be very helpful to understand novel triple phase-shift control method thoroughly. There have been no relevant papers published until now.

5.8 Summary

This chapter analyzes the working theory of a bidirectional dual full bridge ZVS

DC-DC converter with novel triple phase-shift control method in detail. For one period, the nonlinear converter was separated into several linear stages. The equivalent circuits of each linear stage are determined and the corresponding necessary equations are found. The forward output voltage and input voltage gain, average active input power, average active output power and efficiency are solved theoretically. Relevant simulation demonstrations for this method are provided in this chapter. The simulation results demonstrate that this novel control method makes the efficiency and output voltage of this bidirectional converter more robust to parameters change and output power variation. Simulation results also show that the forward and backward efficiency of this bidirectional converter for four different output powers are very satisfactory. This suggests this novel triple-phase-shift control method can make the converter realize ZVS and work well in wide load scope.

Chapter 6 Maximum Output Power Analysis of Isolated Bidirectional Dual Full Bridge DC-DC Converter with Phase-shift Control Methods

[4]The working theory of isolated bidirectional dual full bridge DC-DC converter with novel triple phase-shift control is described in detail in chapter 5. Maximum output power of isolated bidirectional dual full bridge DC-DC converter with phase-shift control methods will be discussed in detail in this chapter. Additionally, an effective method to determine a suitable inductance value for a bidirectional converter will be introduced in this chapter, too.

6.1 Introduction

In recent years, the development of high power and wide power range isolated bidirectional DC-DC converters has become an important topic because of the requirements of electric automobiles, uninterruptible power supplies and aviation power systems [1], [6], [20], [33]. The objective of this project is to design a forward 1kW/200V and backward 250W/48V bidirectional converter. The dual active full bridge converter is symmetrical on both sides of the isolation transformer. It is suitable to be used as the power circuit to transfer energy back and forth, especially for high power case [11]. Therefore, it is chosen as the power circuit for this project. There is one series inductor--- L_{01} in Fig. 6.1. This inductor is mainly used to transfer energy between the

[4] A version of this chapter has been accepted for publication. K. Wu, W.G. Dunford and C.W. de Silva, "Maximum Output Power Analysis of Isolated Bidirectional Dual Full Bridge DC-DC Converter with Phase-shift Control Methods," accepted by *Asian Power Electronics Journal* in 2012.

voltage sources *Vs* and *Vo*, enlarge ZVS scope, eliminate the switching loss and ensure the converter have high efficiency over wide load scope.

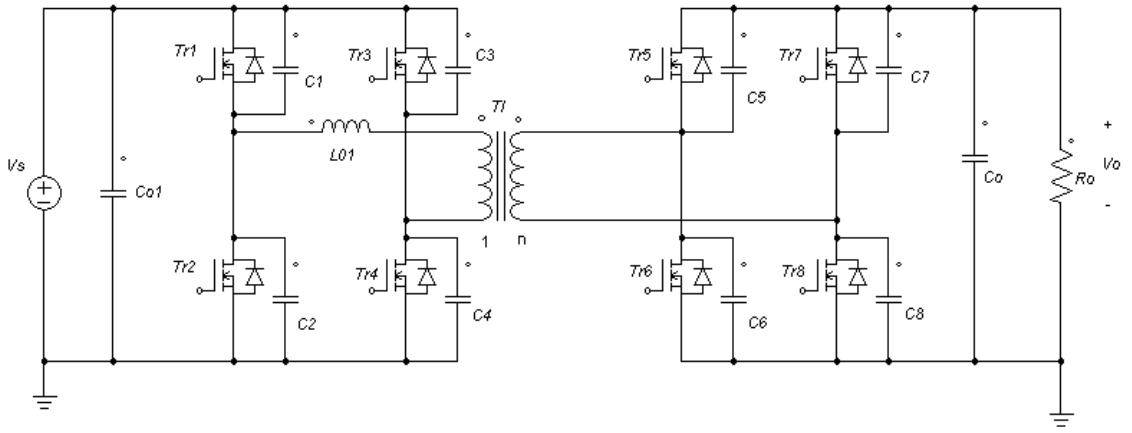

Fig. 6.1 Power Circuit of the Bidirectional Converter with Serial Inductor in the Primary Side of Transformer

There are several existing control methods for this power circuit, like single phase-shift control [1], dual phase-shift control [6] and phase-shift plus PWM control [12]. For phase-shift control method, the phase-shift will change for different output powers. It can be realized with a lead-lag compensator [15], [17]. The energy is controlled to transfer back and forth with the phase-shift controller. For practical applications, it is very important to make clear how to determine a suitable control method for this project and how to choose an appropriate inductance value so that the bidirectional converter can transfer the required power with high efficiency.

Because the bidirectional converter with phase-shift control is a very complicated nonlinear system affected by several factors, the mathematical method is not always correct to solve the maximum output power. Sometimes, contradictory results between the mathematical method and physical model may occur. This chapter will analyze these questions in detail. This analysis is very meaningful for the bidirectional converter design. The main problem will be described in detail in Section 6.2; objectives and rationale of this chapter will be described in Section 6.3; the maximum output power of a bidirectional converter with phase-shift control methods when a serial inductor is placed

on the primary side of the transformer will be analyzed and validated with corresponding simulation results in Section 6.4; the maximum output power of a bidirectional converter with phase-shift control methods when a serial inductor is placed on the secondary side of the transformer will be analyzed and validated with corresponding simulation results in Section 6.5; the method about how to choose the suitable inductance to make the bidirectional converter realize ZVS and transfer energy with high efficiency in the desired large load scope is proposed in Section 6.6; the main contribution of this chapter will be described in Section 6.7 and the main contents of this chapter is summarized in Section 6.8.

6.2 Problem Description

1、*Statement of the Problem*

The problem is to clarify the actual maximum output power of the bidirectional converter by only changing the phase-shifts with a given inductance and to discuss whether the maximum output power can be used as an effective standard to evaluate different control methods for a project. In order to solve these problems theoretically, the mathematical method and the simulation method are used to analyze the maximum output power of the bidirectional dual full bridge converter with single phase-shift control, dual phase-shift control and triple phase-shift control. Contradictory conclusions were obtained with these two methods for the same bidirectional converter. It is important to know how to determine a suitable control method for a project with an effective standard so that it can satisfy the specifications very well.

Furthermore, it is very important to know how to choose a suitable inductance value for the bidirectional converter so that it can realize zero voltage switching (ZVS) and transfer energy with high efficiency in the desired load scope. It is important to note that the minimum inductance should be used for the bidirectional converter.

Although this problem is very difficult and complex, it can be validated by simulation

results and practical application analysis. In practical application, the bidirectional converter can only be used to transfer rated power or less. Over-load is not permitted since this will damage the product. For a given rated power, the method to determine the required minimum inductance value will be much more meaningful than the method which can only provide maximum inductance value.

2: Components in the Bidirectional Power Circuits

L_{01}, L_{02} ---- Two series inductors

C_1=C_2=C_3=C_4=C_5=C_6=C_7=C_8 --- Eight snubber capacitors

Co, Co1 ---Two large filter capacitors

Ro --- Forward load resistor

The parameters of the main transformer are as follows:

Lp---Primary leakage inductance

Ls--- Secondary leakage inductance

Turns ratio: 1: n

The parameters of the eight power MOSFETs are as follows:

R_1, R_2, R_3, R_4, R_5, R_6, R_7, R_8 ---- On resistance

D_1, D_2, D_3, D_4, D_5, D_6, D_7, D_8 --- Anti-parallel diodes with power MOSFETs.

3: Variables Used in the Chapter

iap, ias ---Power circuit primary current and secondary current of the transformer

V_{g1}, V_{g2}, V_{g3}, V_{g4}, V_{g5}, V_{g6}, V_{g7}, V_{g8} ---Control signals for corresponding power switches.

Vs ---Input voltage

Vo ---Output voltage

V_{ds1}---Voltage across power switch Tr1

ω---Switching angular frequency of the bidirectional power converter

Pout----Average output power of the bidirectional converter

Pin----Average input power of the bidirectional converter

δ----Phase-shift angle (radian)

D1, D2, D3 —Phase-shift duty ratio

6.3 Objectives and Rationale

The objective of this chapter is to analyze and compare the maximum output power of bidirectional dual full bridge converter with single phase-shift control, dual phase-shift control and novel triple phase-shift control and to discuss whether the maximum output power should be used as a standard to evaluate different control methods or not. Additionally, an effective method will be introduced to determine a suitable inductance for the bidirectional converter.

Different control methods should be evaluated according to effective standards. It is very important to make clear whether these standards are meaningful or not. If a standard is not correct, a wrong conclusion will be got if it is used to evaluate different control methods. At present, maximum output power is used to evaluate different phase-shift control methods for a given bidirectional power circuit. This is not a meaningful standard because it is meaningless to compare over-load application capability.

After a suitable bidirectional power circuit and control method are determined for a project, it is important to know how to choose a suitable inductance for a bidirectional converter to transfer rated output power with high efficiency. The last part of this chapter describes how to select a suitable inductance for a bidirectional converter such that high efficiency can be achieved.

6.4 Maximum Output Power with a Serial Inductor in Primary Power Circuit

1、The Mathematical Phase-shift Limits and Maximum Output Power with Single Phase-shift Control Method

Because the single phase-shift control is simple and convenient, it is widely used for the bidirectional converter. The power transfer formula of the bidirectional dual full

bridge converter with single phase-shift control is as following [1]:

$$Po = \frac{Vs*Vo}{\omega*L} * \left(\delta - \frac{\delta^2}{\pi}\right) \quad (6\text{-}1)$$

Where ω ($=2*\pi*f$) is the switching angular frequency of the full bridge converter and L is the sum of transformer leakage inductance and that of the serial inductor L_{01} [1]. According to the above formula, it can be found that the phase-shift δ is equal to zero when the output power is equal to zero. By taking the derivative of Eq. 6-1, it can be found that the converter (inductor) can transfer maximum power at $\delta=\pi/2$ when the values of *L*, *Vs*, *Vo* and *f* are fixed. The maximum power is equal to:

$$Pomax = \frac{\pi*Vs*Vo}{4*\omega*L} \quad (6\text{-}2)$$

For this project, *Vs* =48V, *Vo* =200V, $L=L_{01}+Lp+Ls$ =6.9uH+0.6uH+1uH=8.5uH, *f*=25kHz. With these specified values, the maximum output power is equal to: *Pomax* =5.64kW

2、Simulation Studies and Discussion of the Maximum Output Power with Single Phase-shift Control

The simulation waveforms for the bidirectional converter with single phase-shift control for different output powers are presented here.

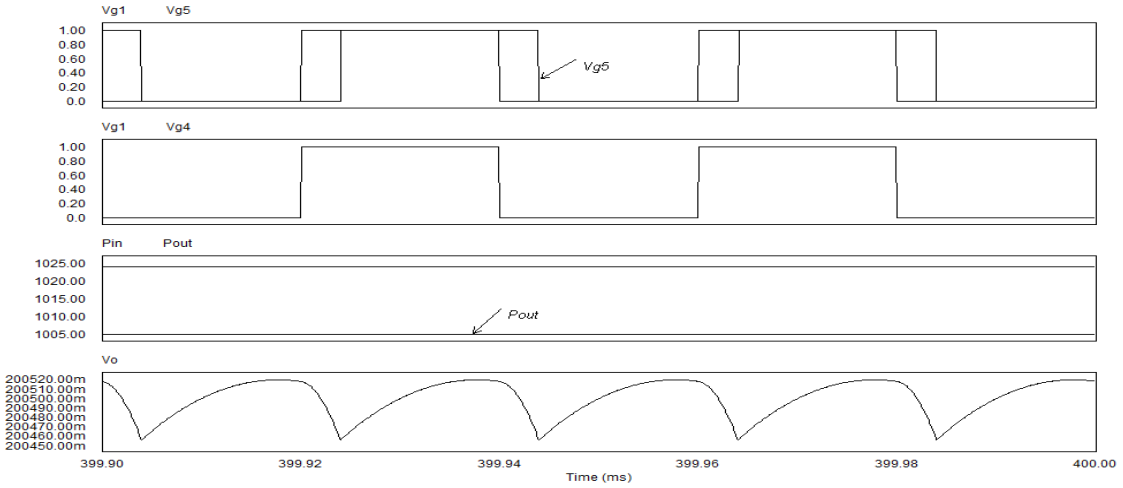

Fig. 6.2 Simulation Results of Forward Bidirectional Converter with Single Phase-shift Control for *Po*=1kW

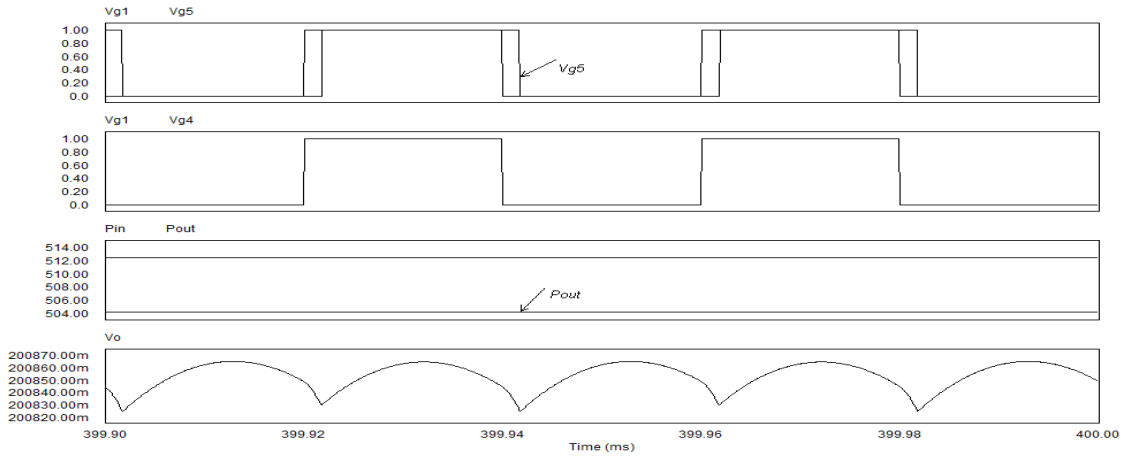

Fig. 6.3 Simulation Wave Forms of Forward Bidirectional Converter with Single Phase-shift Control for *Po*=500W

Compare Fig. 6.2 and Fig. 6.3, it can be found that this bidirectional converter with single phase-shift control can transfer rated output power (1kW) or less by changing the phase-shift value. According to the mathematical maximum output power formula (2), this converter can transfer maximum output power equal to 5.64kW by changing the phase-shift to $\pi/2$ when the values of L, Vs, Vo and f are fixed. In practice, the bidirectional converter cannot transfer this calculated maximum power no matter how the phase-shift is changed. This result can be seen clearly from the following simulation results for Po = 2kW.

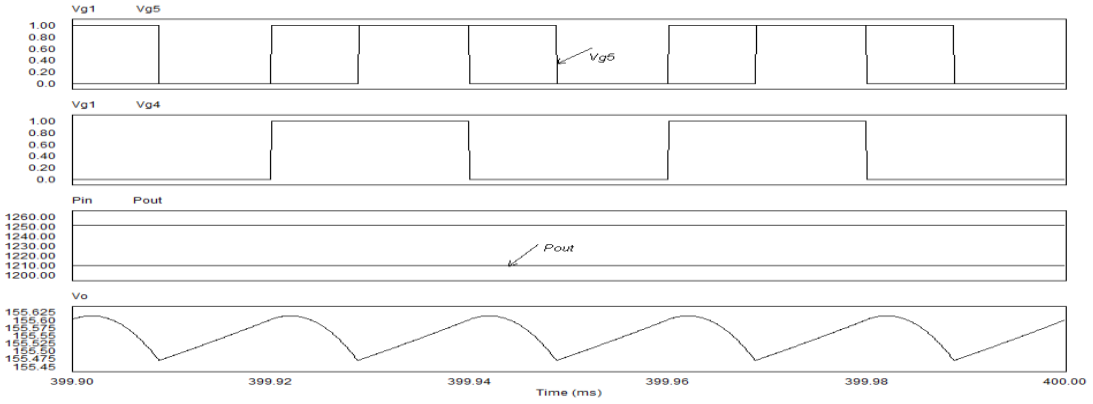

Fig. 6.4 Simulation Wave Forms of Forward Bidirectional Converter with Single Phase-shift Control for *Po*=2kW

It can be found that this converter cannot transfer output power (2kW) by only applying a single phase-shift change. The output voltage will be always lower than rated value (200V) no matter how the phase-shift value is regulated and the actual output power is approximately equal to 1.2kW. Obviously, it will be impossible to transfer 5.64kW to the output by only changing the phase-shift.

3：Simulation Studies and Discussion of the Maximum Output Power with Dual Phase-shift Control

The simulated results of the bidirectional power circuit with dual phase-shift control are presented here.

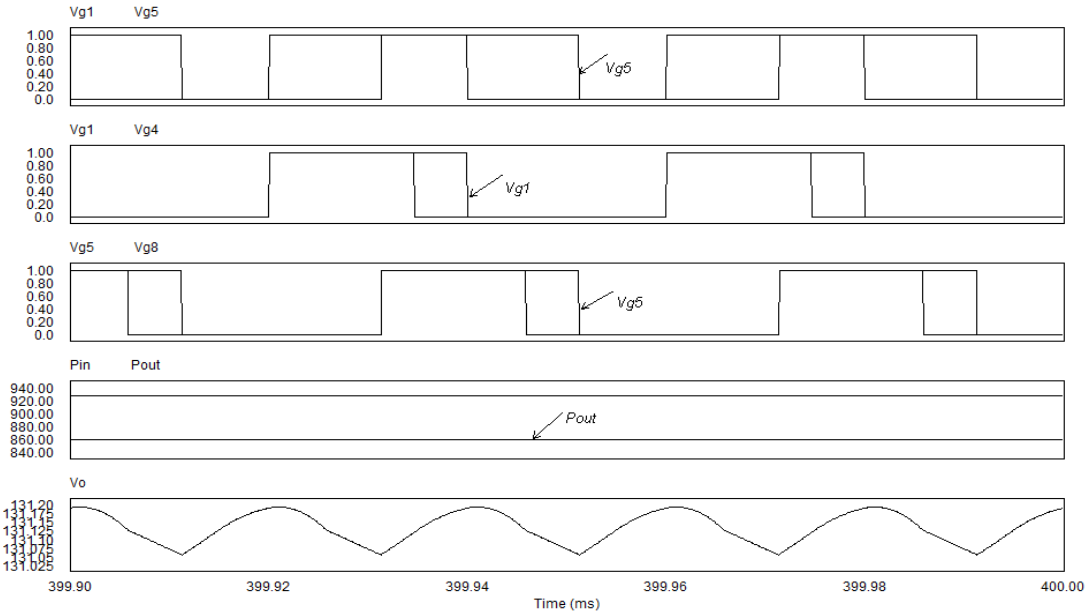

Fig. 6.5 Simulation Wave Forms of Forward Bidirectional Converter with Dual Phase-shift Control for *Po*=2kW

It can be found this converter cannot transfer output power (2kW) by dual phase-shift control. The output voltage will be always lower than the rated value (200V) and the actual output power is approximately equal to 860W. It can be found the actual output power for this power circuit with dual phase-shift control is less than that with single phase-shift control method. Obviously, it cannot transfer mathematical maximum output

power.

Clearly, these are contradictory to the conclusion given by the mathematical method. The mathematical maximum output power is meaningless since the converter will be overloaded. This is not permitted for practical applications since the product will be damaged.

4：Simulation Studies and Discussion of the Maximum Output Power with Triple Phase-shift Control

The simulated results of the bidirectional power circuit with triple phase-shift control are presented here.

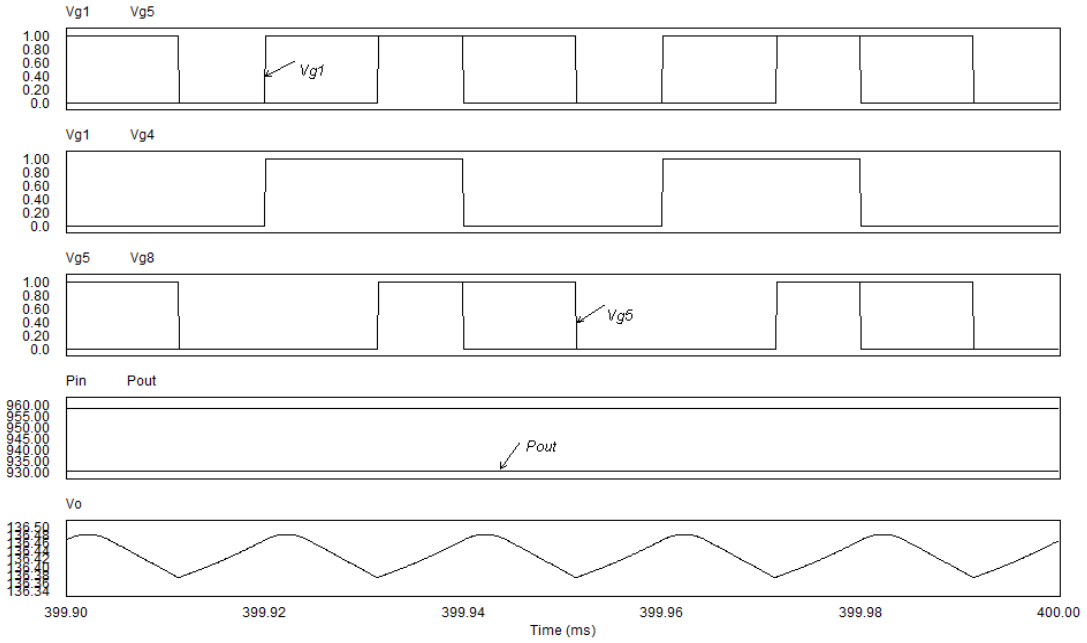

Fig. 6.6 Simulation Wave Forms of Forward Bidirectional Converter with Triple Phase-shift Control for *Po*=2kW

It can be found that this converter cannot transfer output power (2kW) with triple phase-shift control method. The output voltage will be always lower than the rated value (200V) and the actual output power is approximately equal to 930W. It can be found the actual output power for this power circuit with triple phase-shift control is less than that with single phase-shift control method. Clearly, it cannot transfer the mathematical maximum output power.

It can be found this converter cannot transfer output power (2kW) by phase-shift change only. The output voltage reduces and the output power remains approximately at 1kW. It will be impossible to transfer 5.64kW output power by only changing the phase-shift.

6.5 Maximum Output Power with a Serial Inductor in Secondary Power Circuit

1: The Mathematical Maximum Output Power with Dual Phase-shift Control Method

There are two control variables in dual phase-shift control the first phase-shift ratio *D1* between the primary control signal and corresponding secondary control signal, the second phase-shift ratio *D2* between diagonal control signals. This control method will make the energy transfer more flexible and more efficient than single phase-shift control. Please see the definition of phase-shift ratios *D1, D2* and period *Ts* in Fig. 6.8. It is a suitable control method to be used with the bidirectional dual full bridge converter. The power circuit for this project is shown in Fig. 6.7. The power transfer formula of the bidirectional dual full bridge converter with dual phase-shift control is as follows [6]:

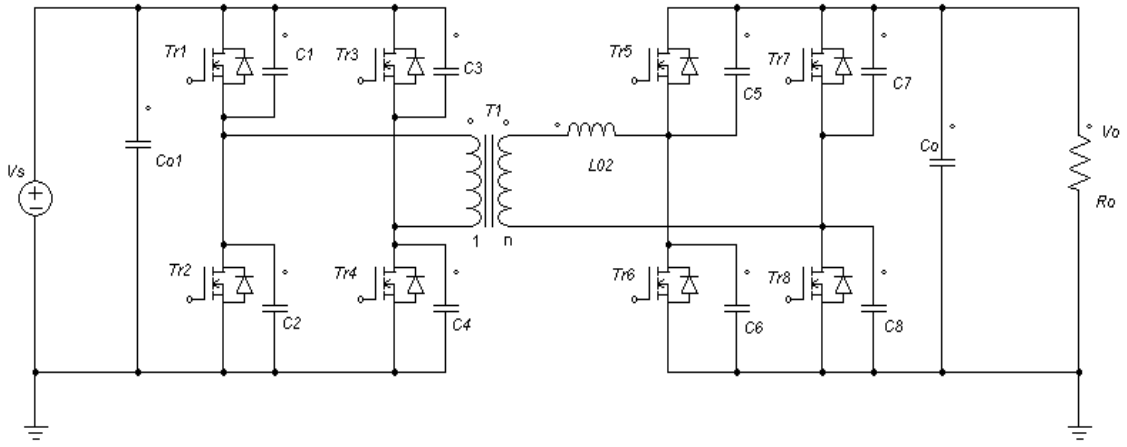

Fig. 6.7 Power Circuit of the Bidirectional Converter with Serial Inductor in the Secondary Side of Transformer

When $D1 \leq 1/2$, the expression of the output power is:

$$P_o = \frac{n*Vs*Vo}{2*fs*L} * \begin{cases} D2*(2-2*D1-D2) & 0 \le D2 \le D1 \\ D2*(1-D1-D2)+D1-D1^2 & D1 \le D2 \le 1\text{-}D1 \\ (1-D1)*(1-D2) & 1\text{-}D1 \le D2 \le 1 \end{cases} \quad (6\text{-}4)$$

When $D1>1/2$, the expression of the output power is:

$$P_o = \frac{n*Vs*Vo}{2*fs*L} * \begin{cases} D2*(2-2*D1-D2) & 0 \le D2 \le 1\text{-}D1 \\ (1-D1)^2 & 1\text{-}D1 \le D2 \le D1 \\ (1-D1)*(1-D2) & D1 \le D2 \le 1 \end{cases} \quad (6\text{-}5)$$

The global maximum output power is at ($D1$=1/3, $D2$=1/3) via the partial derivatives of output power expressions (6-4) and (6-5). The mathematical maximum output power is 4/3 times of that with single phase-shift control method. When the values of L, Vs, Vo and f are fixed, the maximum output power of the bidirectional converter with dual phase-shift control is equal to:

$$Pomax = \frac{\pi*Vs*Vo}{3*\omega*L} \quad (6\text{-}6)$$

This is because the general output power formula is the same for the case where the serial inductor is placed on the primary side of the transformer, and for the case where the serial inductor is placed on the secondary side of the transformer [1]. For this project, L_{02}=L_{01}=6.9uH, while the other parameters are the same as those in Fig.6.1; the mathematical maximum output power of this bidirectional converter with single phase-shift control is equal to 5.64kW. Therefore, the mathematical maximum output power of this bidirectional converter with dual phase-shift control is equal to 7.52kW. This is the theoretical maximum output power attained by changing these two phase-shifts values when other parameters are fixed.

2: *Simulation Studies and Discussion of Maximum Output Power with Dual Phase-shift Control*

In order to verify whether the results obtained by mathematical method is correct or not, the simulation results of the bidirectional converter with dual phase-shift control for different output powers are listed as follows:

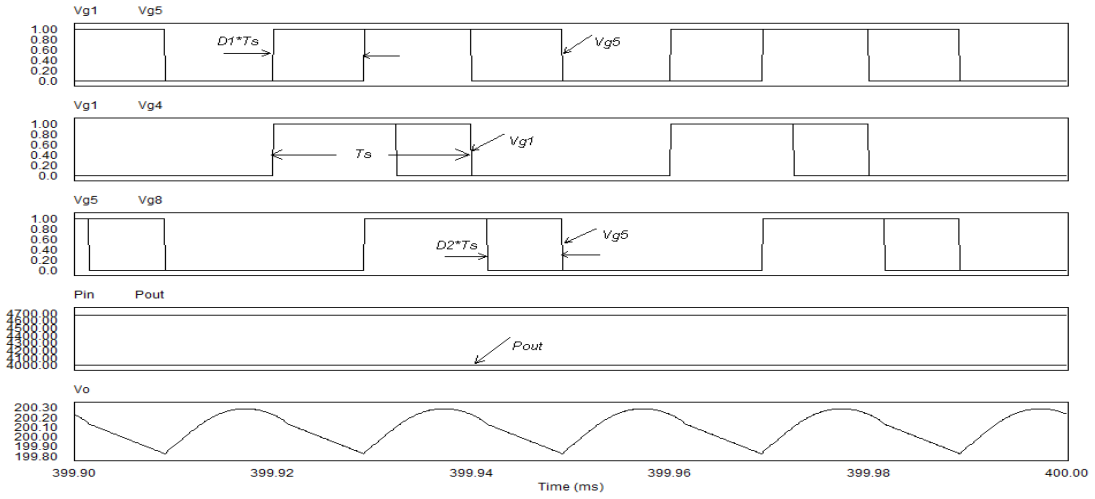

Fig. 6.8 Simulation Wave Forms of Forward Bidirectional Converter with Dual Phase-shift Control for *Po*=4kW

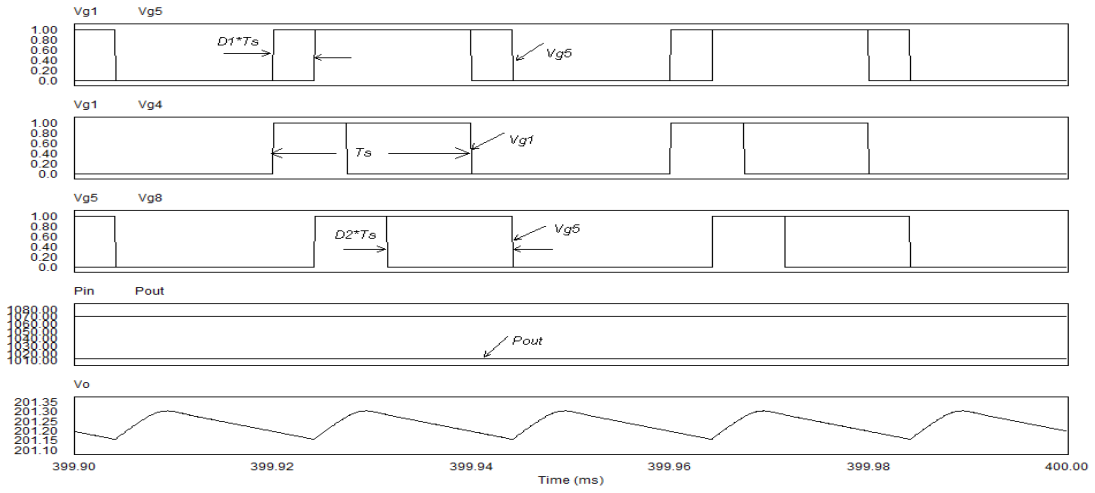

Fig. 6.9 Simulation Wave Forms of Forward Bidirectional Converter with Dual Phase-shift Control for *Po*=1kW

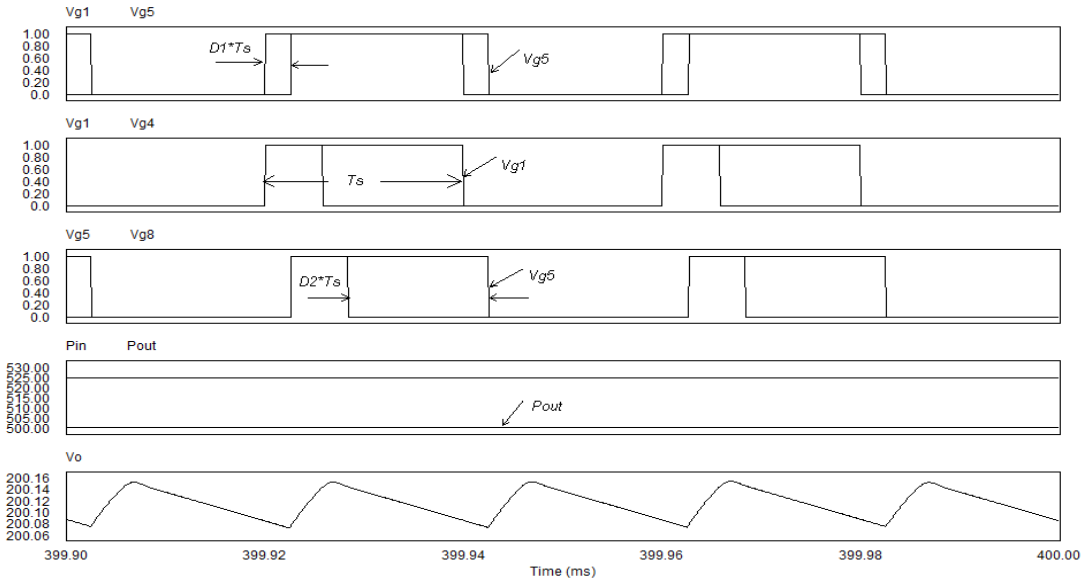

Fig. 6.10 Simulation Wave Forms of Forward Bidirectional Converter with Dual Phase-shift Control for *Po*=500W

By comparing the simulation results listed above, it can be found clearly the phase-shift ratio *D1* will increase as the output power increases, while the phase-shift ratio *D2* will decrease. In Fig.6.8, it was determined that the efficiency is equal to 85.6% when the output power is equal to 4kW. In Fig.6.9, it was determined that the efficiency is equal to 93.7% when the output power is equal to 1kW. Therefore, when the output power is only regulated by phase-shifts, the efficiency will reduce as the output power increases.

Besides this, it can be found that the mathematical conclusion about the maximum output power of the bidirectional converter with dual phase-shift control is incorrect. Although dual phase-shifts ratios *D1* and *D2* can vary in the large range, the bidirectional converter cannot transfer the maximum output power by only regulating the dual phase-shifts when other parameters are fixed for a specified rated output power bidirectional converter. This can be validated by the following simulation results which expect to transfer 5kW or 6kW output power by changing the dual phase-shifts with this bidirectional converter rated for 1kW output power.

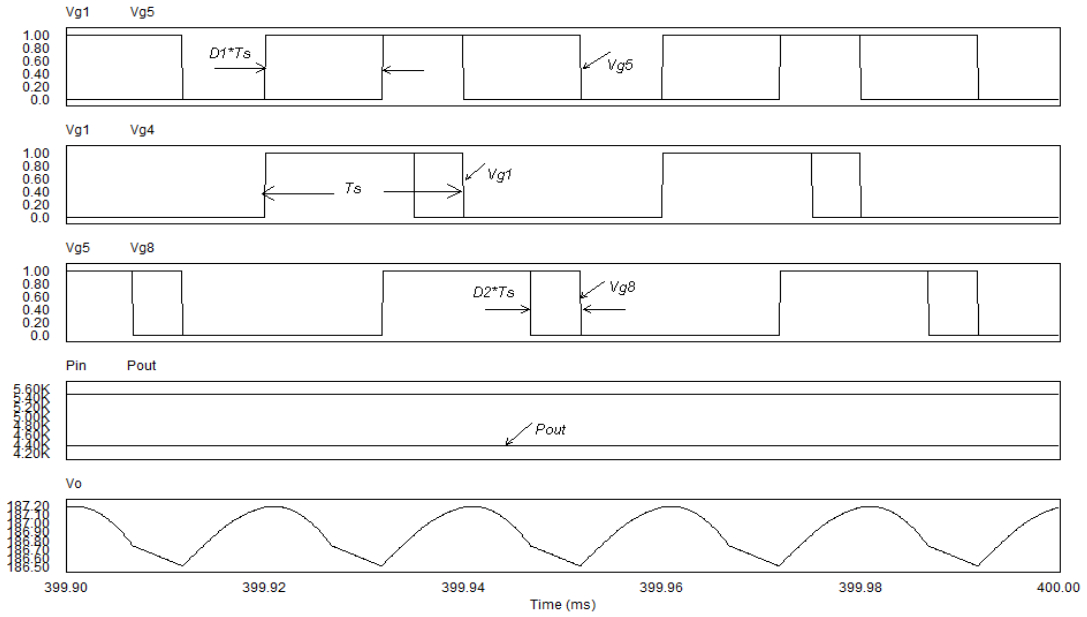

Fig. 6.11 Simulation Wave Forms of Forward Bidirectional Converter with Dual Phase-shift Control for *Po*=5kW

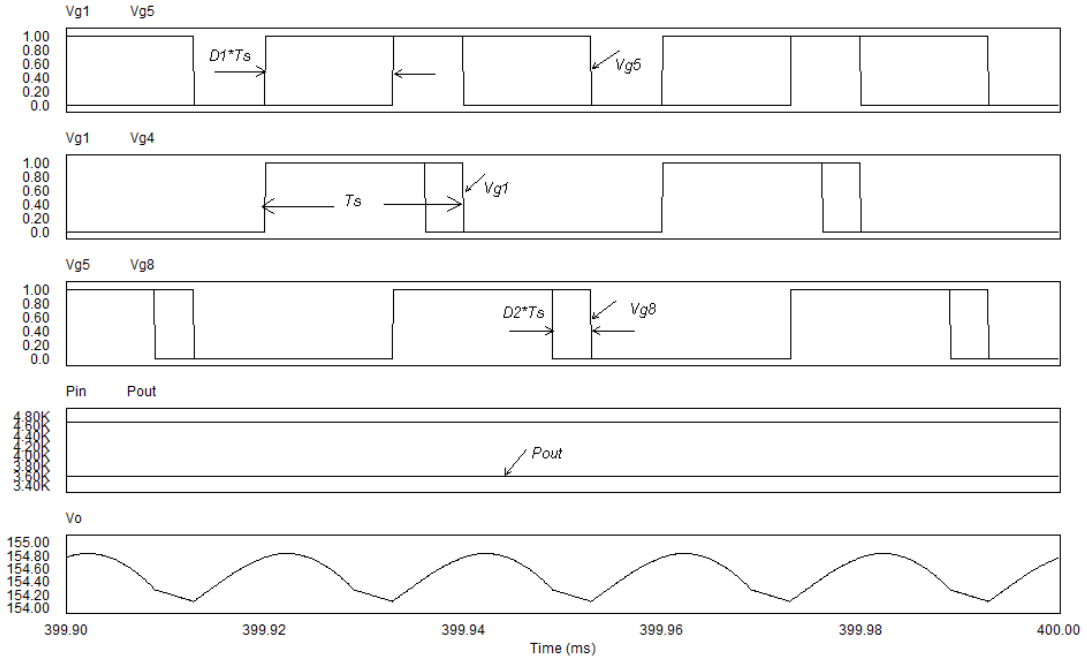

Fig. 6.12 Simulation Wave Forms of Forward Bidirectional Converter with Dual Phase-shift Control for *Po*=6kW

These simulation results suggest this bidirectional converter cannot transfer 5kW or

6kW output power by only changing dual phase-shifts. For the expected 5kW output power case, the bidirectional converter cannot transfer output power higher than 4.4kW no matter how the dual phase-shifts are regulated. The efficiency for this case is only equal to 81.3%. For the expected 6kW output power case, the bidirectional converter cannot transfer output power higher than 3.64kW no matter how the dual phase-shifts are regulated. The efficiency for this case is only equal to 82.4%. These results prove that the mathematical conclusion about the maximum output power is incorrect.

3: Simulation Studies and Discussion of the Maximum Output Power with Single Phase-shift Control

The simulation results for the bidirectional power circuit with single phase-shift control are presented here.

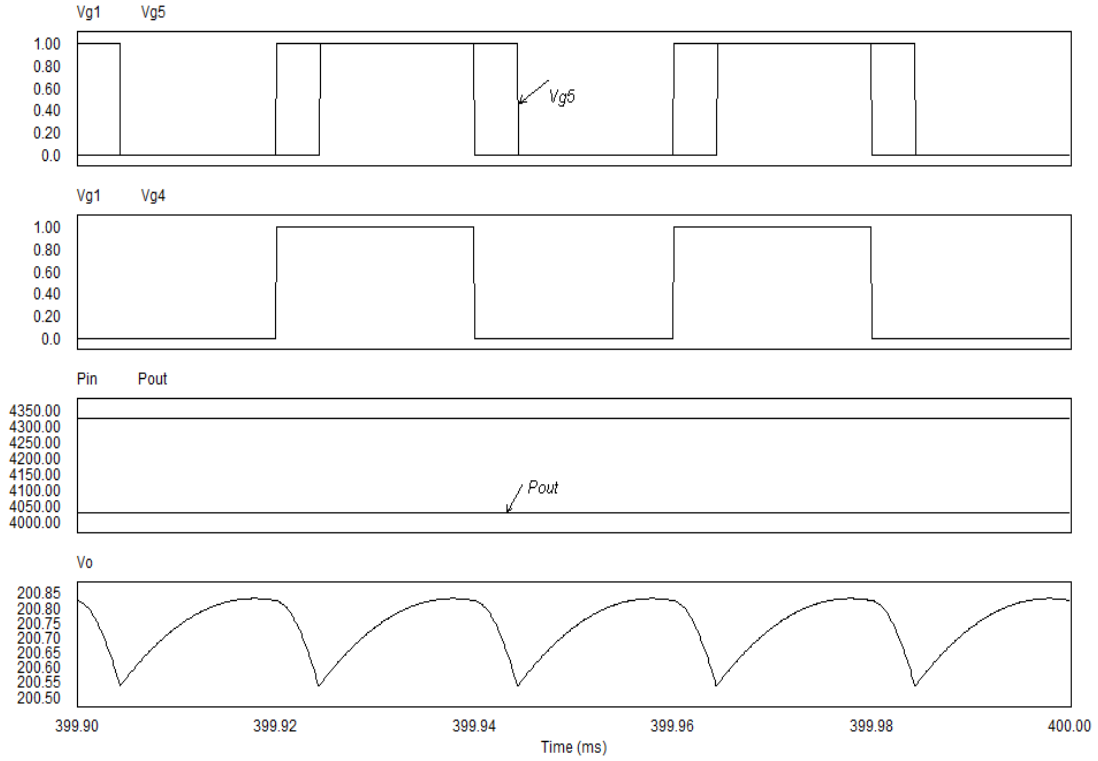

Fig. 6.13 Simulation Wave Forms of Forward Bidirectional Converter with Single Phase-shift Control for *Po*=4kW

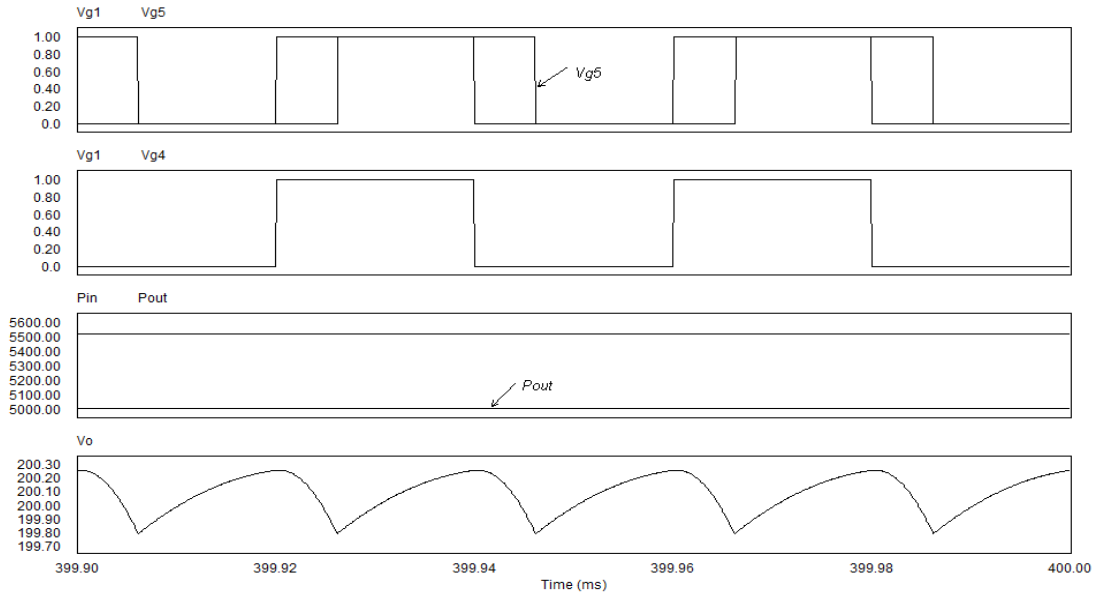

Fig. 6.14 Simulation Wave Forms of Forward Bidirectional Converter with Single Phase-shift Control for *Po*=5kW

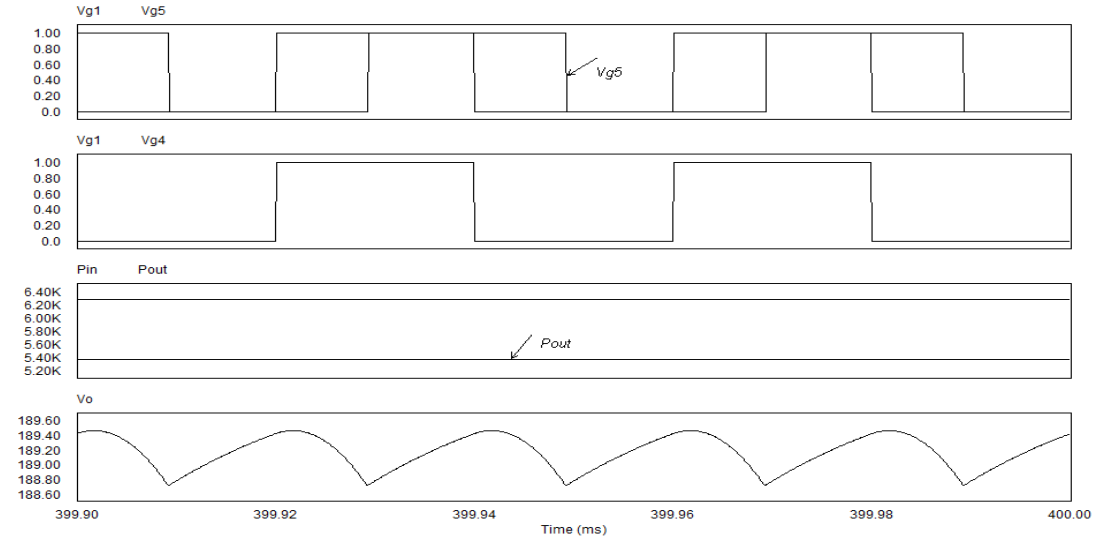

Fig. 6.15 Simulation Wave Forms of Forward Bidirectional Converter with Single Phase-shift Control for *Po*=6kW

In Fig.6.13, it can be found that the efficiency is equal to 93.2% when the output power of this bidirectional power circuit with single phase-shift control is equal to 4kW. In Fig.6.14, it can be found that the efficiency is equal to 90.6% when the output power

of this bidirectional power circuit with single phase-shift control is equal to 5kW. In Fig.6.15, it can be found that the efficiency is equal to 86.9% when the output power of this bidirectional power circuit with single phase-shift control is equal to 5.4kW. Obviously, it is higher than the actual output power of 4.3kW for the same power circuit with dual phase-shift control. However, it still cannot transfer the calculated 5.64kW maximum output power no matter how the phase-shift value is regulated. This suggests that the previous mathematical conclusion that the maximum output power with dual phase-shift control is equal to 4/3 times of the maximum output power with single phase-shift control is incorrect.

This also suggests that the mathematical conclusion of maximum output power with single phase-shift control is not correct. The actual output power when the serial inductor is placed on the primary side of the transformer is different from that when the same serial inductor is placed on the secondary side of the transformer which violates the theory seen after Eq. 6.1.

4: Simulation Studies and Discussion of the Maximum Output Power with Triple Phase-shift Control

The simulation results of this power circuit with triple phase-shift control are as follows.

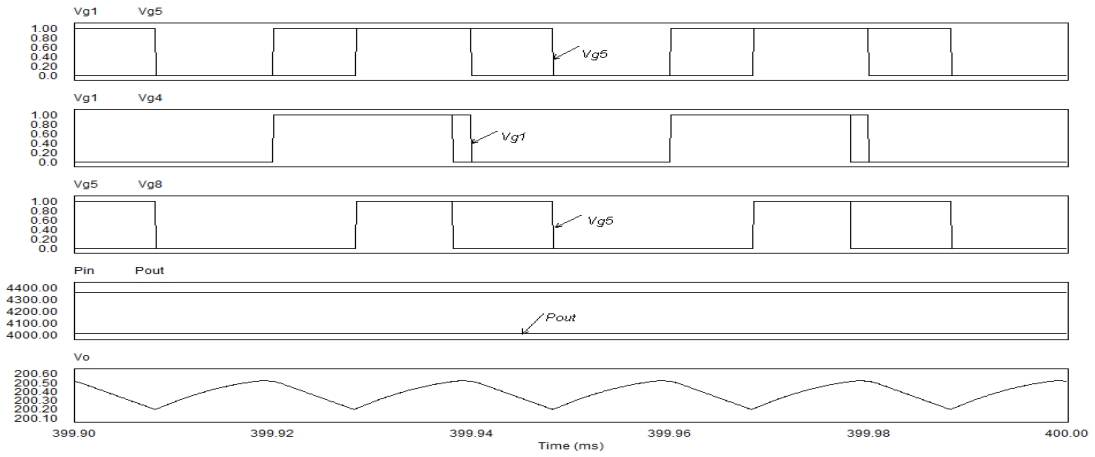

Fig. 6.16 Simulation Wave Forms of Forward Bidirectional Converter with Triple Phase-shift Control for *Po*=4kW

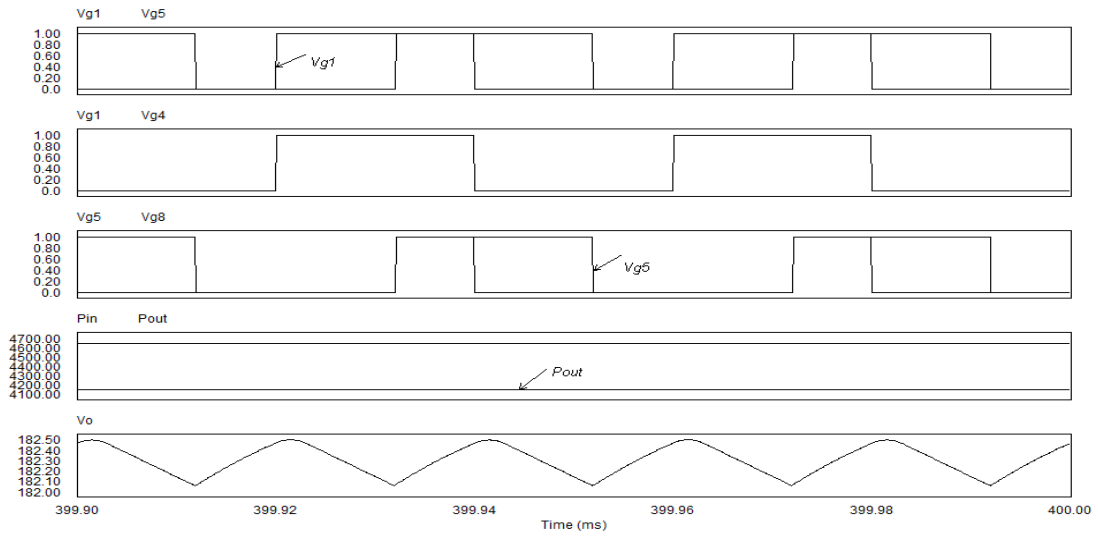

Fig. 6.17 Simulation Wave Forms of Forward Bidirectional Converter with Triple Phase-shift Control for *Po*=5kW

These simulation results suggest this bidirectional converter can transfer 4kW output power with the efficiency of 92.1%, but it cannot transfer 5kW output power by only changing triple phase-shifts. For the expected 5kW output power situation, the bidirectional converter cannot transfer output power higher than 4.1kW no matter how the triple phase-shifts are regulated. The efficiency for this case is equal to 89.4%.

From the maximum output power comparison of these three control methods with the same power circuit, it can be found the actual maximum output power of the bidirectional converter with single phase-shift control is higher than that of the other two methods. It seems that this is an advantage of single phase-shift control method. However, this advantage of single phase-shift control method is meaningless because maximum output power implies over-load operation for a rated output power product.

Therefore, it can be concluded that maximum output power should not be a standard to evaluate different control methods of a bidirectional converter because maximum output power will cause over-load operation. Over-load operation is not permitted in practical applications because it will damage the product. A meaningful standard to

compare different control methods should be whether it can make the bidirectional converter transfer rated output power or less with high efficiency and high output voltage stability under parameters change.

6.6 Method to Determine Inductance for Bidirectional Converter

It is important to choose a suitable inductance value for the bidirectional converter so that the converter can transfer the rated output power or less with high efficiency and high output voltage stability. Generally, the losses of the power converter include conduction loss and switching loss [29], [35]. For high switching frequency converters, switching loss is a very important factor to influence efficiency [40], [42], [44]. In order to eliminate switching loss, zero-voltage switching (ZVS) or zero-current-switching (ZCS) technology is used in the power circuit [39], [43], [45]. Based on the ZVS dual full bridge power circuit, an effective method about how to choose a suitable inductance value for the bidirectional converter is introduced in this section.

1: The Determination of Required Inductance with Mathematical Method

According to general output power formula (6-1) of the bidirectional converter with single phase-shift control [1], the general formula to solve the total inductance required for the bidirectional converter is as follows:

$$L = \frac{Vs*Vo}{\omega*Po} * \left(\delta - \frac{\delta^2}{\pi}\right) \quad (6\text{-}7)$$

Clearly, only the maximum inductance value at $\delta=\pi/2$ can be determined via derivative of formula (6-7) when parameters *Vs*, *Vo*, *Po* and *f* are fixed for the bidirectional converter. The maximum inductance formula is as follows:

$$Lmax = \frac{\pi*Vs*Vo}{4*\omega*Po} \quad (6\text{-}8)$$

For this project, *Vs* =48V, *Vo* =200V, *Po*=1kW, *f*=25kHz. From Eq.6.8, the maximum inductance is therefore equal to: *Lmax1* =48uH for *Po*=1kW. Clearly, this inductance value is too high to be used for the bidirectional converter. It is much higher than the inductance value that was used (*L*=8.5uH) in this bidirectional converter with single

phase-shift control. Therefore, a better method should be explored to determine a suitable inductance for the bidirectional converter design.

2: *An Effective Method to Determine the Suitable Inductance for the Bidirectional Converter*

It is well known that the minimum inductance should be used to complete the power transfer if it can satisfy the requirements. This will reduce the size of the power converter. The main point is that the total inductance must be able to make the converter realize ZVS operation even when output power is at its allowed minimum value. Only in this way, can the bidirectional converter transfer energy with high efficiency over wide output power range. Otherwise, the power converter cannot realize ZVS in low output power and efficiency will be greatly reduced.

Practically, this problem can be solved in this way. At first, simulate the bidirectional converter with a control method and only the leakage inductance of the isolation transformer with minimum output power to verify whether this converter can realize ZVS or not. If it cannot realize ZVS with only the transformer leakage inductance, a small serial inductance is required. The next step would be to include a small serial inductance in the power circuit and simulate the bidirectional converter to check whether the bidirectional converter can realize ZVS or not under the same possible minimum output power. If this bidirectional converter still cannot realize ZVS with this small serial inductor, increase the serial inductance value gradually and simulate the bidirectional converter again. Repeat this again and again until a minimum or sub-minimum serial inductance value is found to make the bidirectional converter realize ZVS under possible minimum output power.

The principle to decide the totally required minimum inductance is to ensure the bidirectional converter to realize ZVS under possible minimum output power [16], [41]. This is because ZVS is realized by charging and discharging snubber capacitors with the energy stored in the inductors. With the decrease of the output power, the current in

power circuit will be reduced and the energy stored in the inductor will be reduced as well. If the inductance is too small, it cannot provide enough energy for the bidirectional converter to realize ZVS over wide load scope. This can be validated by the following simulation results of the bidirectional converter with single phase-shift control.

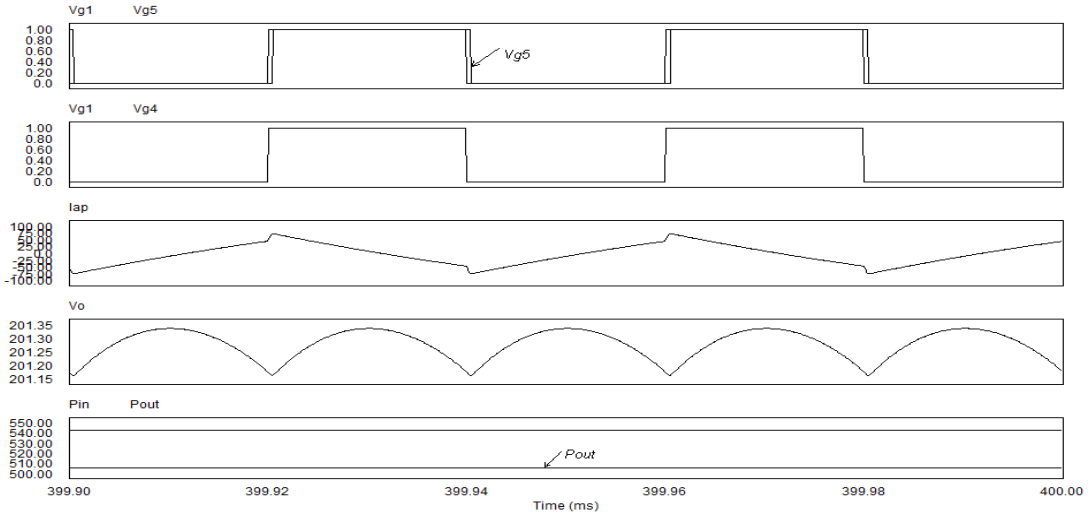

Fig. 6.18 Simulation Wave Forms of Forward Bidirectional Converter with Single Phase-shift Control for L_{01}=0.003uH/ *Po*=500W

In Fig. 6.18, it can be found that the primary current *Iap*>0 at the rising edge of control signal V_{g1}, therefore, the bidirectional converter cannot realize ZVS when L_{01}=0.003uH and *Po*=500W. In order to realize ZVS, the serial inductance L_{01} should be increased.

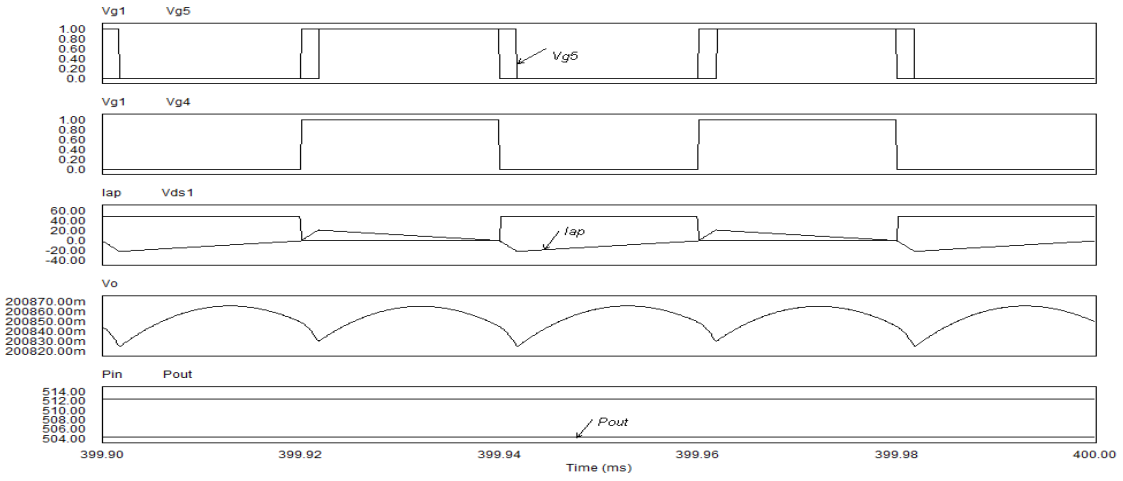

Fig. 6.19 Simulation Wave Forms of Forward Bidirectional Converter with Single Phase-shift Control for L_{01}=6.9uH/*Po*=500W

In Fig. 6.19, it can be found that the primary current *Iap*<0 at the rising edge of control signal V_{g1}. This suggests this bidirectional converter can realize ZVS at the present inductance value. The switching loss is eliminated and efficiency is improved.

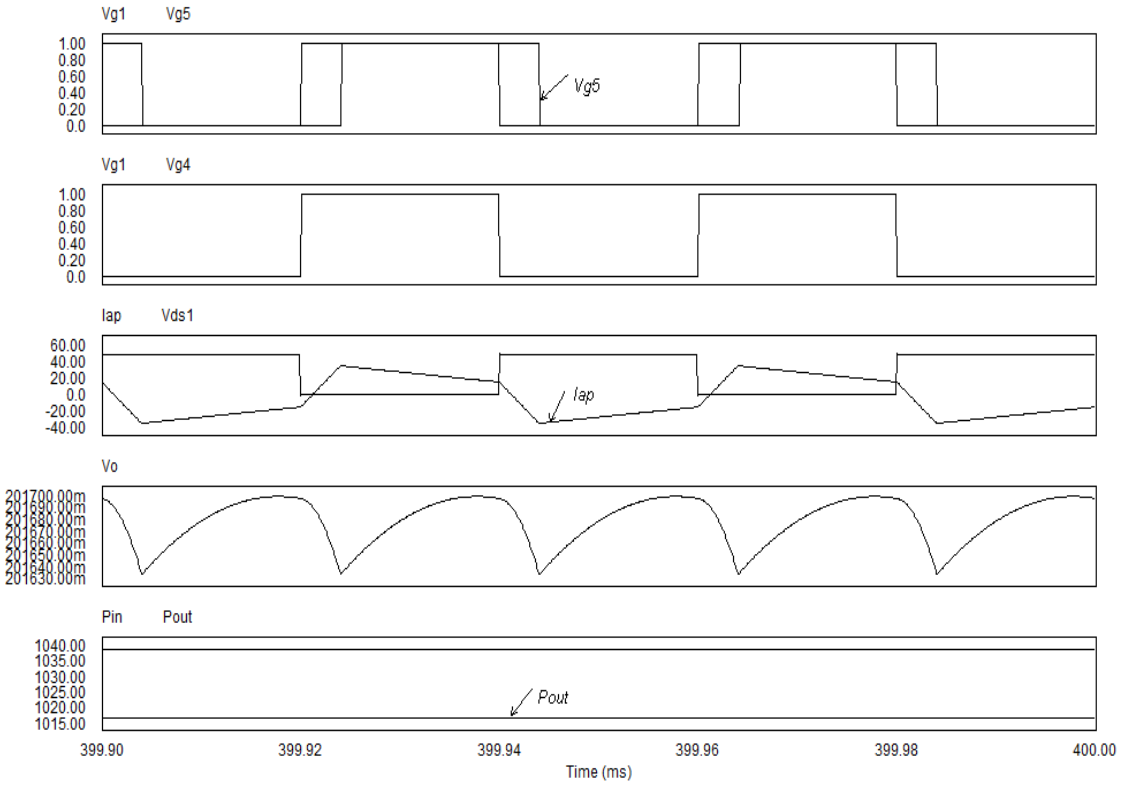

Fig. 6.20 Simulation Wave Forms of Forward Bidirectional Converter with Single Phase-shift Control for L_{01}=6.9uH/*Po*=1kW

In Fig.6.20, it can be found that the primary current *Iap*<0 at the rising edge of control signal V_{g1}. This suggests this bidirectional converter can realize ZVS very well and thus, the switching loss is eliminated and the efficiency is improved. This suggests the converter can realize ZVS better with the same inductance at higher output powers if the converter can realize ZVS with this inductance at a lower output power. Therefore, the minimum inductance for the bidirectional converter is that which can make the power converter realize ZVS when the output power is at its minimum operating point. This minimum inductance will make the bidirectional converter realize ZVS in the desired load range and transfer energy with high efficiency in this load scope. The suitable

inductance for the bidirectional converter with triple phase-shift control can be determined using a similar method.

6.7 Main Contribution

The main contribution of this chapter is to correct a wrong standard used to evaluate different control methods of bidirectional converters. This is a very important result and should be considered when trying to determine the optimal control method for a bidirectional converter. Otherwise, a wrong conclusion may be drawn for the control methods comparison. A suitable project topology cannot be obtained for the bidirectional converter design. The latter part of this chapter introduces an effective method to determine a suitable inductance for the bidirectional converter. By including this inductance, zero voltage switching can be achieved and the conversion efficiency is greatly increased. There are no relevant papers published in the world until now.

6.8 Summary

This chapter analyzes the maximum output power of a bidirectional dual full bridge DC-DC converter with single phase-shift control, dual phase-shift control and triple phase-shift control methods in detail. The maximum output power is solved with mathematical methods. However, contradictory conclusions were obtained for the same bidirectional converter with two circuit configurations and different control methods. This strange phenomenon is discussed in detail in this chapter. It can be found that the mathematical conclusion is meaningless because the converter would have to be overloaded for it to be true. It is shown that even if the elements' rated parameters are permitted, the bidirectional converter cannot transfer this maximum output power only by changing the phase-shifts. Therefore, it was concluded that the maximum output power should not be used as a standard to evaluate different control methods for a project. It is very important to make clear this point for the design of a bidirectional converter.

The last section of this chapter proposed an effective method about how to choose a suitable inductance for the bidirectional converter to make it realize ZVS and thus be able to transfer energy with high efficiency in large load scope.

Chapter 7 Conclusion and Future Work

7.1 Conclusion

In this thesis, the development of a bidirectional dual full bridge DC-DC converter with novel triple phase-shift control has been considered. A number of issues regarding the development of isolated bidirectional DC-DC converters have been investigated. This section will summarize the chapters and the major conclusions of the thesis.

In chapter 2, an isolated bidirectional dual full bridge DC-DC converter topology was presented as the main circuit after theoretical analysis and comparison of several commonly used bidirectional converters. After careful investigation of several control methods, the novel triple phase-shift control method was chosen to implement the control circuit for the bidirectional DC-DC converter project. Meanwhile, a theoretical calculation of the important component values of this bidirectional DC-DC converter was presented.

In chapter 3, a theoretical stability analysis method to determine the stability of this isolated bidirectional dual full bridge DC-DC converter with triple phase-shift control was presented in detail. A new Lyapunov function method was used to establish the stability of the bidirectional converter for arbitrary parameter changes. This new method can be used to determine the stability of other power converters as well.

In chapter 4, a new eigenvalue method was presented to determine the stability of the bidirectional converter under input voltage changes only. It is appropriate because it is very difficult to maintain the input voltage constant in practical applications. This method can be used when the system is so complex that it is difficult to find a suitable Lyapunov function for it.

In chapter 5, the working theory of the isolated bidirectional dual full bridge DC-DC converter with novel triple phase-shift control was analyzed in detail. The novel triple phase-shift control method was described; and the block diagram of the novel controller

was listed. Then, the equivalent circuits and the necessary equations in every stage were developed. The general expressions of Vo/Vs, average input power, average output power and efficiency were derived step by step.

In chapter 6, the maximum output power of the isolated bidirectional dual full bridge DC-DC converter with single phase-shift control, dual phase-shift control and triple phase-shift control methods was analyzed in detail. The conclusion about maximum output power derived with the current mathematical method was contradictory to that derived with power electronics simulation results. This problem was discussed in detail in this chapter. Then, an effective method to determine a suitable inductance value for the bidirectional converter design was described.

7.2 Significant Contributions

There are four significant contributions in this thesis related to the analysis and design of bidirectional DC-DC converters.

The first contribution is to develop and perform the stability analysis of a bidirectional dual full bridge converter for arbitrary parameter changes using the Lyapunov function method. By separating the power converter into several stages or sub-stages in one period, determining the stability of the bidirectional converter in every stage by using the Lyapunov function method and analyzing the stability at the interface of two neighboring stages, the stability of the bidirectional converter in one period can be determined. If suitable Lyapunov functions can be found for every stage or sub-stage, this new method can also be applied to theoretically determine the stability of other power converters with other control methods. A difficult problem that has existed in power electronics area for many years has been solved.

The second contribution is the development and execution of stability analysis of a bidirectional dual full bridge converter under input voltage changes only using the eigenvalue method. If a power converter is too complex for determining a suitable

Lyapunov function for one stage or sub-stage, the stability of the power converter can be analyzed theoretically with this second method. It can be used for other power converters with different control methods as well.

The third contribution of the thesis is to develop a novel triple phase-shift control method for the bidirectional dual full bridge converter. This novel control method will make the bidirectional converter transfer energy at high efficiency over a wide load range. Its efficiency is robust (insensitive) to parameter changes.

The fourth contribution is to correct a wrong standard often used to evaluate different control methods for bidirectional converters. This will make it possible to choose a suitable control method for a bidirectional converter to transfer rated power at high efficiency. Additionally, an effective method to determine a suitable inductance value for the bidirectional converter has been proposed.

7.3 Possible Future Work

In order to commercially realize the proposed isolated bidirectional dual full bridge DC-DC converter with novel triple phase-shift control, the next step would be to fabricate a prototype to verify its performance. The controller can be realized with the analog controller as described in this thesis or with another DSP controller that may be designed according to the basic method introduced in the thesis. If a DSP controller is used for the bidirectional converter, TMS320F2812 chip can be used to realize a digital controller. If satisfactory experimental results are obtained by adjusting some component values, a PCB control circuit including the basic DSP chip and relevant components can be built to reduce the layout problem and improve the reliability of the product.

References

[1] Shigenori Inoue and Hirofumi Akagi, "A Bidirectional DC-DC Converter for an Energy Storage System with Galvanic Isolation" *IEEE Transactions on Power Electronics, Vol.22, No.6, November 2007.*

[2] Zhe Zhang, Ole C. Thomsen, Michael A.E. Anderson, Jacob D. Schmidt and Henning R. Nielsen, "Analysis and Design of Bi-directional DC-DC Converter in Extended Run Time DC UPS System Based on Fuel Cell and Supercapacitor" *978-1-422-2812-0/09, IEEE 2009*

[3] Gang Chen, Dehong Xu and Yim-Shu Lee, "A Novel Fully Zero-Voltage-Switching Phase-Shift Bidirectional DC-DC Converter" *0-7803-6618-2/01, IEEE 2001*

[4] Huafeng Xiao, Liang Guo and Shaojun Xie, "A New ZVS Bidirectional DC-DC Converter With Phase-shift Plus PWM Control Scheme" *1-4244-0714-1/07, IEEE 2007*

[5] Chuanhong Zhao, Dehong Xu, Haifeng Fan,"A PWM plus Phase-Shift Control Bidirectional DC-DC Converter" *0-7803-7768-0/03, IEEE 2003*

[6] Hua Bai and Chris Mi, "Eliminate Reactive Power and Increase System Efficiency of Isolated Bidirectional Dual-Active-Bridge DC-DC Converters Using Novel Dual-Phase-Control" *IEEE Transactions on Power Electronics, Vol. 23, No. 6, November 2008*

[7] Panos J. Antsaklis, Anthony N. Michel, *A Linear Systems Primer*, Birkhäuser, Boston, 2007.

[8] Gui-Jia Su, Lixin Tang, "A Bidirectional, Triple-Voltage DC-DC Converter for Hybrid and Fuel Cell Vehicle Power Systems" *1-4244-0714-1/07, IEEE 2007*

[9] Leon M. Tolbert, William A. Peterson, Cliff P. White, Timothy J. Theiss, Matthew B. Scudiere, "A Bi-Directional DC-DC Converter with Minimum Energy Storage Elements" *0-7803-7420-7/02, IEEE 2002*

[10] N. Rajarajeswari and K. Thanushkodi, "A Bi-Directional DC-DC Converter with Adaptive Fuzzy Logic Controller" *ICGST-ACSE Journal, ISSN 1687-4811, Volume 8, Issue II, December 2008*

[11] L. Zhu, "A Novel Soft-commuting Isolated Boost Full Bridge ZVS-PWM DC-DC Converter for Bi-directional High Power Applications," *IEEE Trans. Power Electronics, vol. 21, no.2, pp.422-429, Mar. 2006*

[12] D.H. Xu, C.H. Zhao and H. F. Fan, "A PWM plus phase-shift control bi-directional DC-DC Converter." *IEEE Trans. Power Electronics. Vol. 19, no. 3, pp. 666-675, May 2004*

[13] Wu Kuiyuan, "A New Method to Realize ZVS-PWM in Full Load Range (A)," *Proceedings of IEEE VPPC 2006, UK*

[14] Wu Kuiyuan, "A New Method to Realize ZVS-PWM in Full Load Range (B)," *Proceedings of IEEE VPPC 2006, UK*

[15] Graham C. Goodwin, Stefan F. Graebe, Mario E. Salgado, *Control System Design*, Prentice Hall of India, 2006

[16] Kuiyuan Wu and William G. Dunford, "An Unusual Full Bridge Converter to Realize ZVS in Large Load Scope," *Asian Power Electronics Journal*, Vol. 2, No. 1, pp. 66-71, Apr. 2008

[17] C.W. de Silva, *Modeling and Control of Engineering Systems*, Boca Raton, FL: CRC Press/Taylor&Francis, 2009.

[18] Kuiyuan Wu, *Design and Implementation of A Boost Active Power Factor Corrector*, M.A.Sc. Thesis, Department of Electrical and Computer Engineering, University of British Columbia, Vancouver, Canada, 2008

[19] Aiguo Xu, Shaojun Xie, "A Multipulse-Structure-Based Bidirectional PWM Converter for High-Power Applications," *IEEE Transactions on Power Electronics*, vol.24, no.5, pp. 1233-1242, May 2009

[20] H.J. Chiu and L.W. Lin, "A bidirectional DC-DC converter for fuel cell electric vehicle driving systems," *IEEE Trans.on Power Electronics*, vol. 21, no. 4, pp. 950-958, July 2006.

[21] G.G. Oggier, G.O. Garcia, A.R. Oliva, "Switching Control Strategy to Minimize Dual Active

Bridge Converter Losses," *IEEE Transactions on Power Electronics*, vol.24, no.7, pp. 1826-1838, July 2009

[22] Y.V. Hote, D.R. Choudhury, J.R.P. Gupta, "Robust Stability Analysis of the PWM Push-Pull DC-DC Converter," *IEEE Transactions on Power Electronics,* vol.24, no.10, pp. 2353-2356, Oct. 2009.

[23] V. Valdivia, A. Barrado, A. Laazaro, P. Zumel, C. Raga, C. Fernandez, "Simple Modeling and Identification Procedures for "Black-Box" Behavioral Modeling of Power Converters Based on Transient Response Analysis," *IEEE Transactions on Power Electronics*, vol.24, no.12, pp. 2776-2790, Dec. 2009.

[24] F. Krismer, J.W. Kolar, "Accurate Small-Signal Model for the Digital Control of an Automotive Bidirectional Dual Active Bridge," *IEEE Transactions on Power Electronics,* vol.24, no.12, pp. 2756-2768, Dec. 2009

[25] L. Huber, B.T. Irving, M.M. Jovanoic, "Review and Stability Analysis of PLL-Based Interleaving Control of DCM/CCM Boundary Boost PFC Converters," *IEEE Transactions on Power Electronics,* vol.24, no.8, pp. 1992-1999, Aug. 2009.

[26] S. Karagol, M. Bikdash, "Generation of Equivalent-Circuit Models From Simulation Data of a Thermal System," *IEEE Transactions on Power Electronics*, vol.25, no.4, pp. 820-828, April 2010.

[27] Wu Chen, Xinbo Ruan, Hong Yan, C.K. Tse, "DC/DC Conversion Systems Consisting of Multiple Converter Modules: Stability, Control, and Experimental Verifications," *IEEE Transactions on Power Electronics,* vol.24, no.6, pp. 1463-1474, June 2009.

[28] J. Morroni, R. Zane, D. Maksimovic, "An Online Stability Margin Monitor for Digitally Controlled Switched-Mode Power Supplies," *IEEE Transactions on Power Electronics,* vol.24, no.11, pp. 2639-2648, Nov. 2009.

[29] Robert W. Erickson, Dragan Maksimovic, *Fundamentals of Power Electronics (Second Edition)*, Springer Science +Business Media, Inc. 2001

[30] Y. Hu, J. Tatler and Z. Chen, "A bidirectional dc/dc power electronic converter for an energy

storage device in an autonomous power system," in *Proceedings of. Power Electron. Motion Cont. Conf. (IPMEC)*, 2004, vol. 1. Pp. 171-176.

[31] Z. Ye, P. Jain, and P. Sen, "Circulating current minimization in high frequency AC power distribution architectures with multiple inverter modules operated in parallel," *IEEE Trans. Ind. Electron.* , vol. 54, no. 5, pp. 2673-2687, Oct. 2007

[32] K. Lo, Y. Lin, T. Hsieh, "Phase-Shifted Full-Bridge Series-Resonant DC-DC Converters for Wide Load Variations," *IEEE Trans. on Industrial Electronics*, pp. 1, 2011.

[33] Jianming Hu, Yuanrui Chen, Zijuan Yang, "Study and Simulation of One Bidirectional DC-DC Converter in Hybrid Electric Vehicle." in *Proceedings of Third International Conference on Power Electronics Systems and Applications*, 2009

[34] R.S. Yang, L.K. Chang, H.C. Chen, "An Isolated Full-Bridge DC-DC Converter with 1MHz Bidirectional Communication Channel," *IEEE Trans. on Industrial Electronics*, pp. 1, 2011.

[35] S. Inoue and H. Akagi, "Loss Analysis of a bidirectional isolated dc/dc converter," in *Proc. Int. Power Electron. Conf. (IPEC)*, 2005

[36] R. J. Wai, C.Y. Lin, J. J. Liaw, Y. R. Chang, "Newly-Designed ZVS Multi-Input Converter," *IEEE Trans. on Industrial Electronics*, pp. 1, 2011

[37] H. Ribeiro, B. Borges, "New Optimized Full-Bridge, Single Stage AC/DC Converters," *IEEE Trans. on Industrial Electronics*, pp. 1, 2011

[38] B. R. Lin, J. Y. Dong, J. J. Chen, "Analysis and Implementation of a ZVS/ZCS DC-DC Switching Converter with Voltage Step-Up," *IEEE Trans. on Industrial Electronics*, pp.1, 2011

[39] Huai Wang, Qian Sun, H.S.H. Chung, S. Tapuchi, A. Ioinovici, "A ZCS Current-Fed Full-Bridge PWM Converter With Self-Adaptable Soft-Switching Snubber Energy," *IEEE Transactions on Power Electronics*, vol.24, no.8, pp.1977-1991, Aug. 2009

[40] Tin-Jong Tai, Ke-Horng Chen, "Switching Loss Calculation (SLC) and Positive/Negative Slope Compensation Dynamic Droop Scaling (PNC-DDS) Technique for Hig- Efficiency Multi-Input-Single-Output (MISO) Systems," *IEEE Transactions on Power Electronics*,

vol.24, no.5, pp.1386-1398, May 2009

[41] J.A. Carr, B. Rowden, J.C. Balda, "A Three-Level Full-Bridge Zero-Voltage Zero-Current Switching Converter With a Simplified Switching Scheme," *IEEE Transactions on Power Electronics*, vol.24, no.2, pp.329-338, Feb. 2009

[42] Yali Xiong, Shan Sun, Hongwei Jia, P. Shea, Z.J. Shen, "New Physical Insights on Power MOSFET Switching Losses," *IEEE Transactions on Power Electronics*, vol.24, no.2, pp.525-531, Feb. 2009

[43] P. Das, B. Laan, S.A. Mousavi, G. Moschopoulos, "A Nonisolated Bidirectional ZVS-PWM Active Clamped DC-DC Converter," *IEEE Transactions on Power Electronics*, vol.24, no.2, pp.553-558, Feb. 2009

[44] R. Vargas, U. Ammann, J. Rodriguez, "Predictive Approach to Increase Efficiency and Reduce Switching Losses on Matrix Converters," *IEEE Transactions on Power Electronics*, vol.24, no.4, pp.894-902, April 2009

[45] E. Adib, H. Farzanehfard, "Zero-Voltage Transition Current-Fed Full-Bridge PWM Converter," *IEEE Transactions on Power Electronics*, vol.24, no.4, pp.1041-1047, April 2009

[46] S. K. Mazumder and K. Acharya, "Multiple Lyapunov Function Based Reaching Condition Analyses of Switching Power Converters," in *Proc. of IEEE Power Electron. Specialists Conference*, June 2006, pp. 2232-2239

[47] S. K. Mazumder and K. Acharya, "Multiple Lyapunov Function Based Reaching Condition for Orbital Existence of Switching Power Converters," *IEEE Transactions on Power Electronics*, vol.23, no.3, pp.1449-1471, May 2008

Appendix A Simulation Circuit of Forward Bidirectional Dual Full Bridge DC-DC Converter with Novel Triple Phase-shift Control

In order to be convenient to check this simulation circuit, it is appended as following:

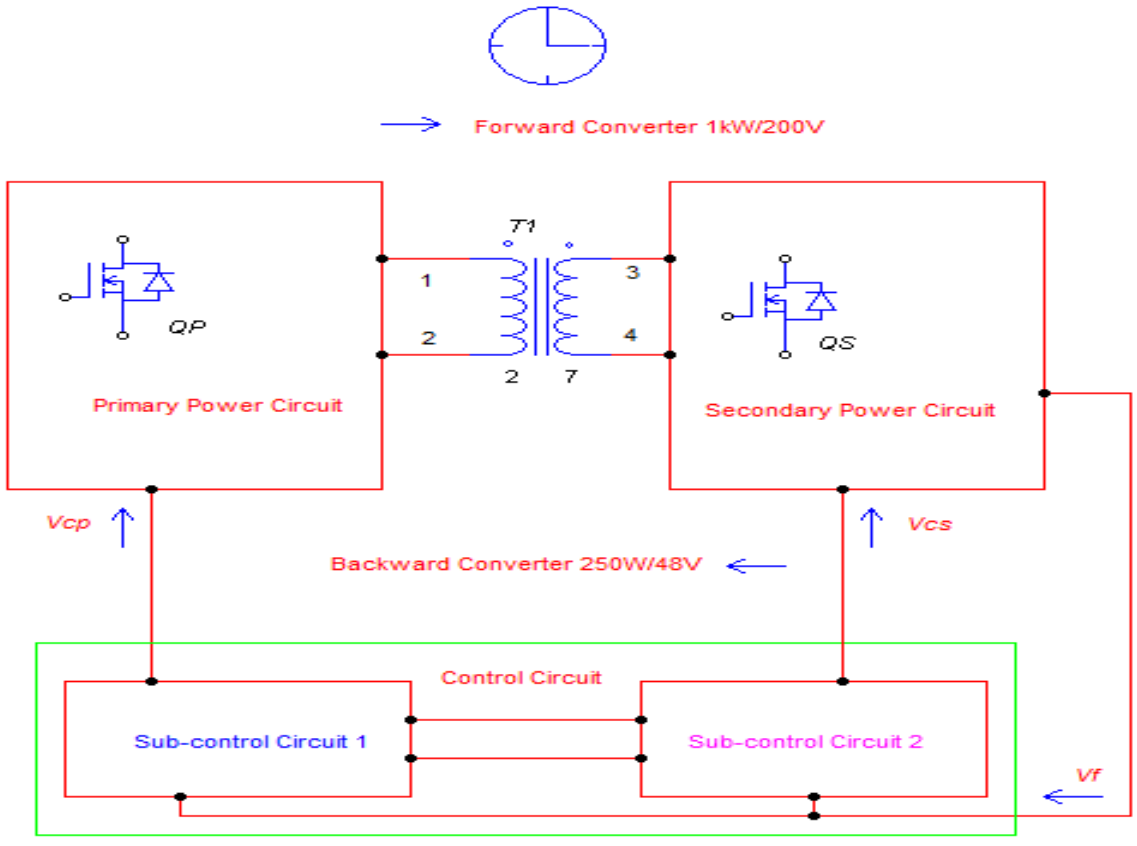

Fig. A.1 Block Simulation Circuit of Forward Bidirectional Dual Full Bridge DC-DC Converter with Novel Triple Phase-shift Control

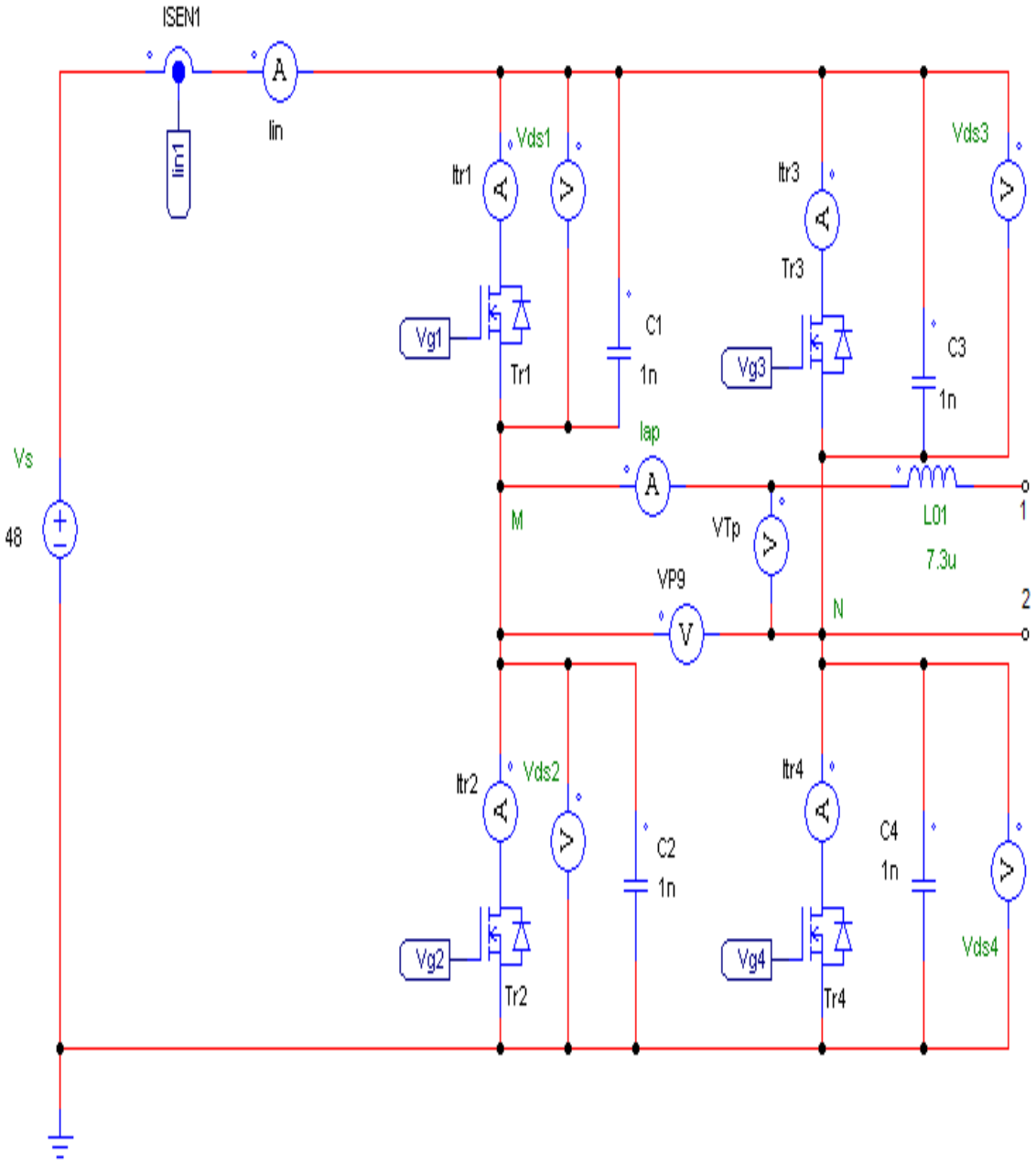

Fig. A.2 Simulation Primary Power Circuit of Forward Bidirectional Dual Full Bridge DC-DC Converter with Novel Triple Phase-shift Control

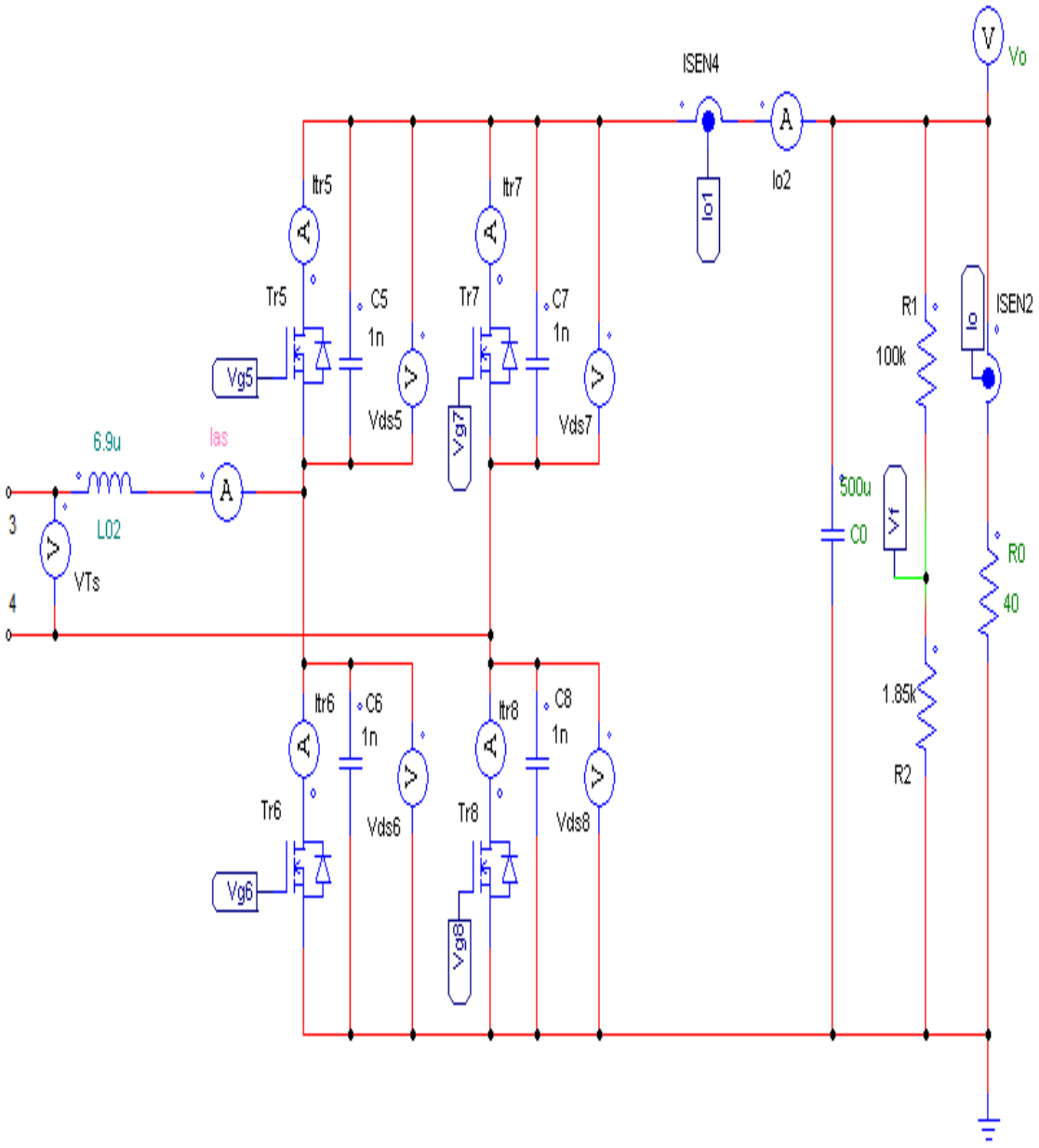

Fig. A.3 Simulation Secondary Power Circuit of Forward Bidirectional Dual Full Bridge DC-DC Converter with Novel Triple Phase-shift Control

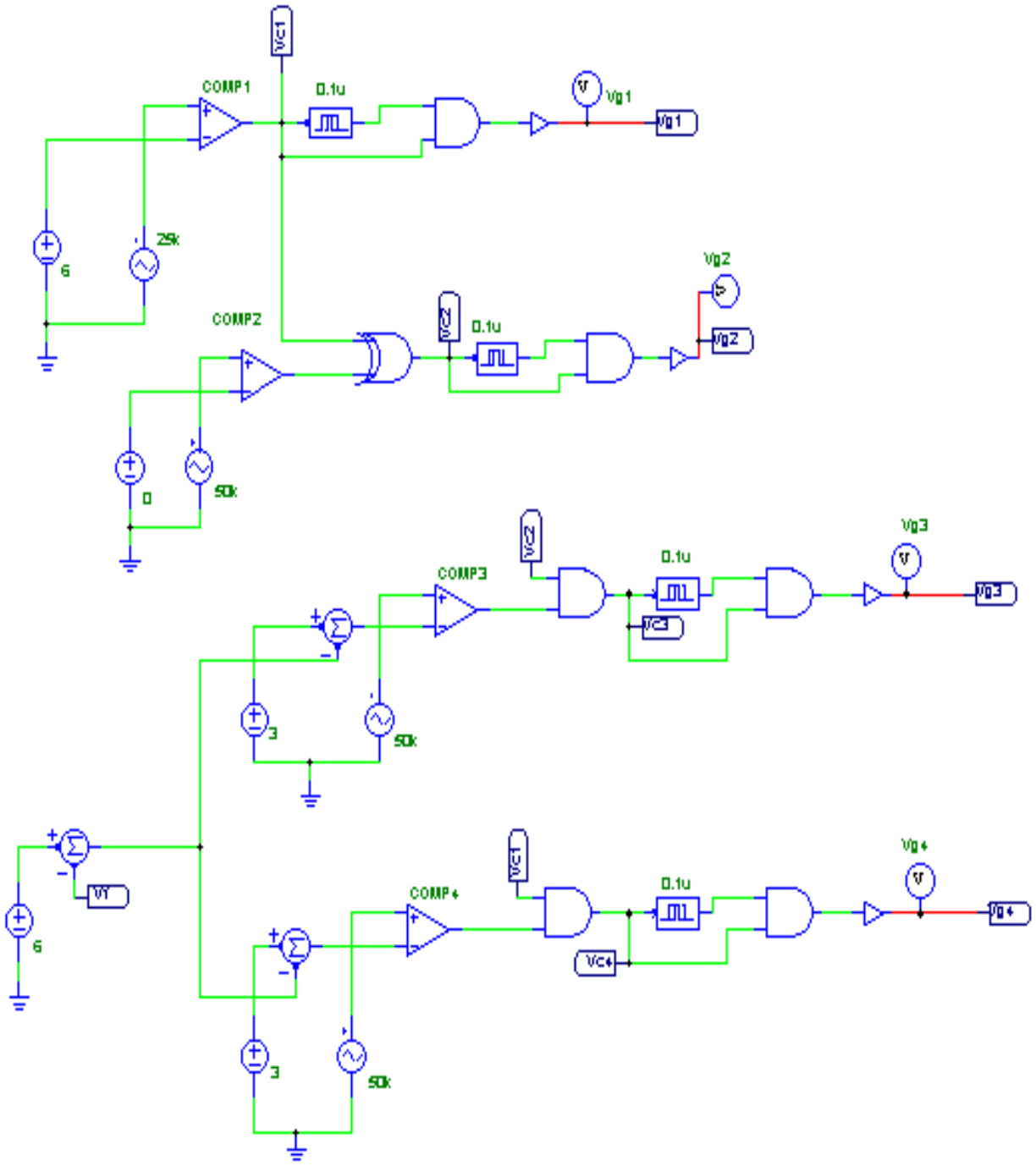

Fig. A.4 Simulation Sub-control Circuit 1 of Forward Bidirectional Dual Full Bridge DC-DC Converter with Novel Triple Phase-shift Control

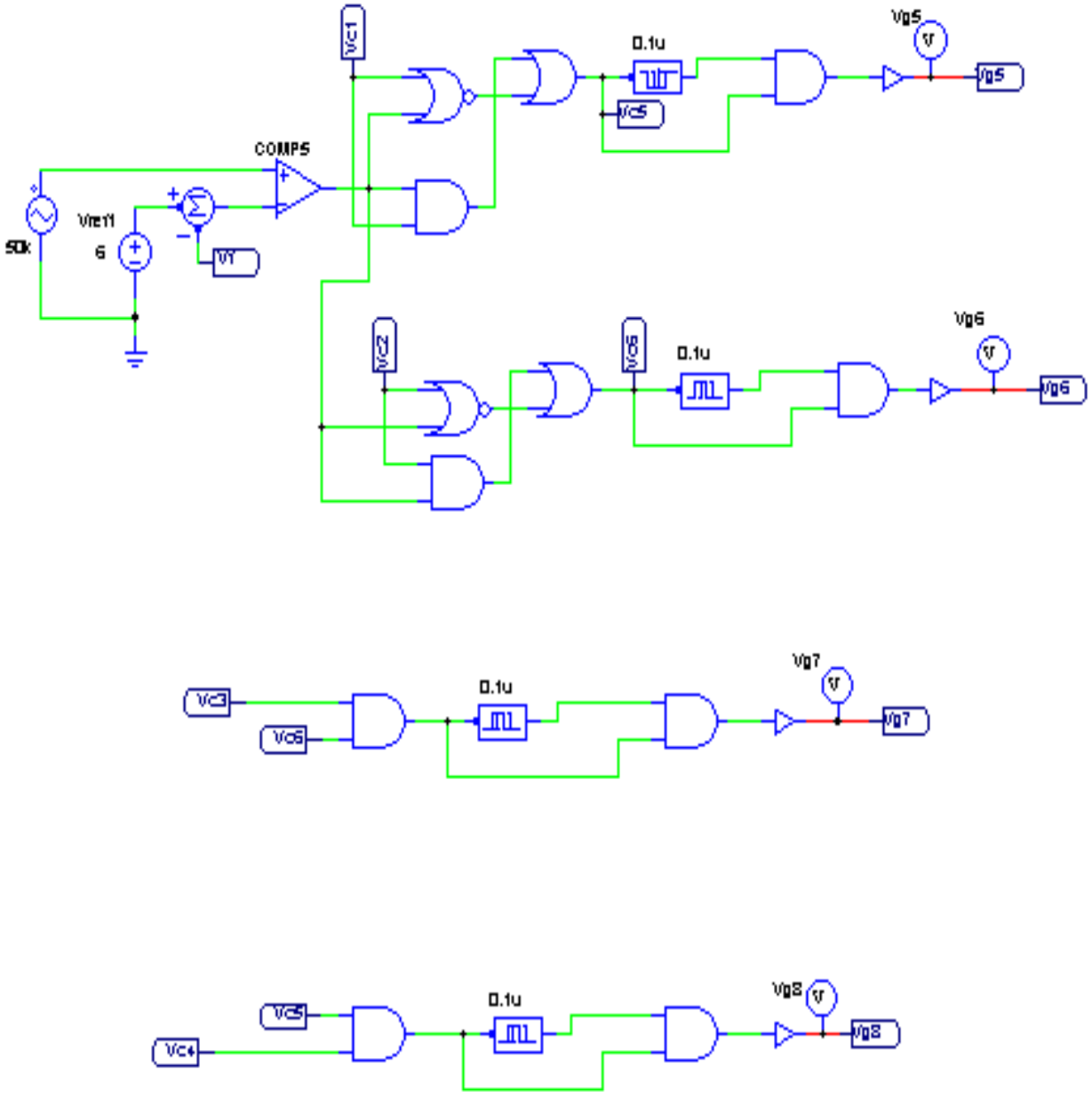

Fig. A.5 Simulation Sub-control Circuit 2 of Forward Bidirectional Dual Full Bridge DC-DC Converter with Novel Triple Phase-shift Control

The parameters of this bidirectional converter are as follows:

Two serial inductors:

L_{01}=7.3μH; L_{02}=6.9μH;

Eight snubbber capacitors paralleled with power switches:

C_1=C_2=C_3=C_4=C_5=C_6=C_7=C_8=1nF;

Output-filter capacitance:

Co=Co1=500μF;

Forward load resistance: Ro=40Ω;

The parameters of the main transformer are as following:

Primary leakage inductance: Lp=0.6μH;

Secondary leakage inductance: Ls=1μH;

Primary winding resistance: Rp=7mΩ;

Secondary winding resistance: Rs=10mΩ;

Turns ratio: n=7/2

The parameters of the 8 power switches are as following:

Tr1~Tr4: On resistance: 5mΩ; Diode Voltage drop: 1V

Tr5~Tr8: On resistance: 23mΩ; Diode Voltage drop: 0.6V

The dead time is equal to 0.1 micro-second.

Appendix B Simulation Circuit of Forward Bidirectional Dual Full Bridge DC-DC Converter with Dual Phase-shift Control

In order to be convenient to check this simulation circuit, it is attached in the following.

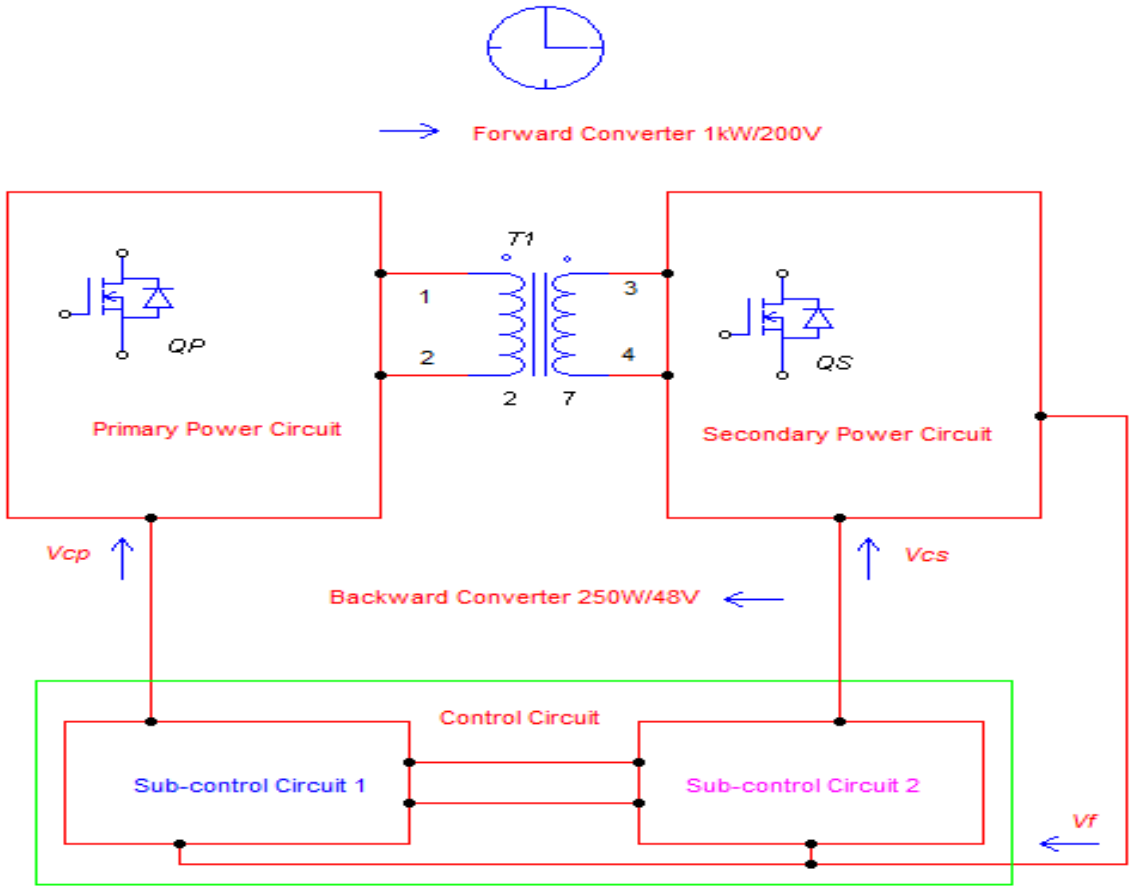

Fig. B.1 Block Simulation Circuit of Forward Bidirectional Dual Full Bridge DC-DC Converter with Dual Phase-shift Control

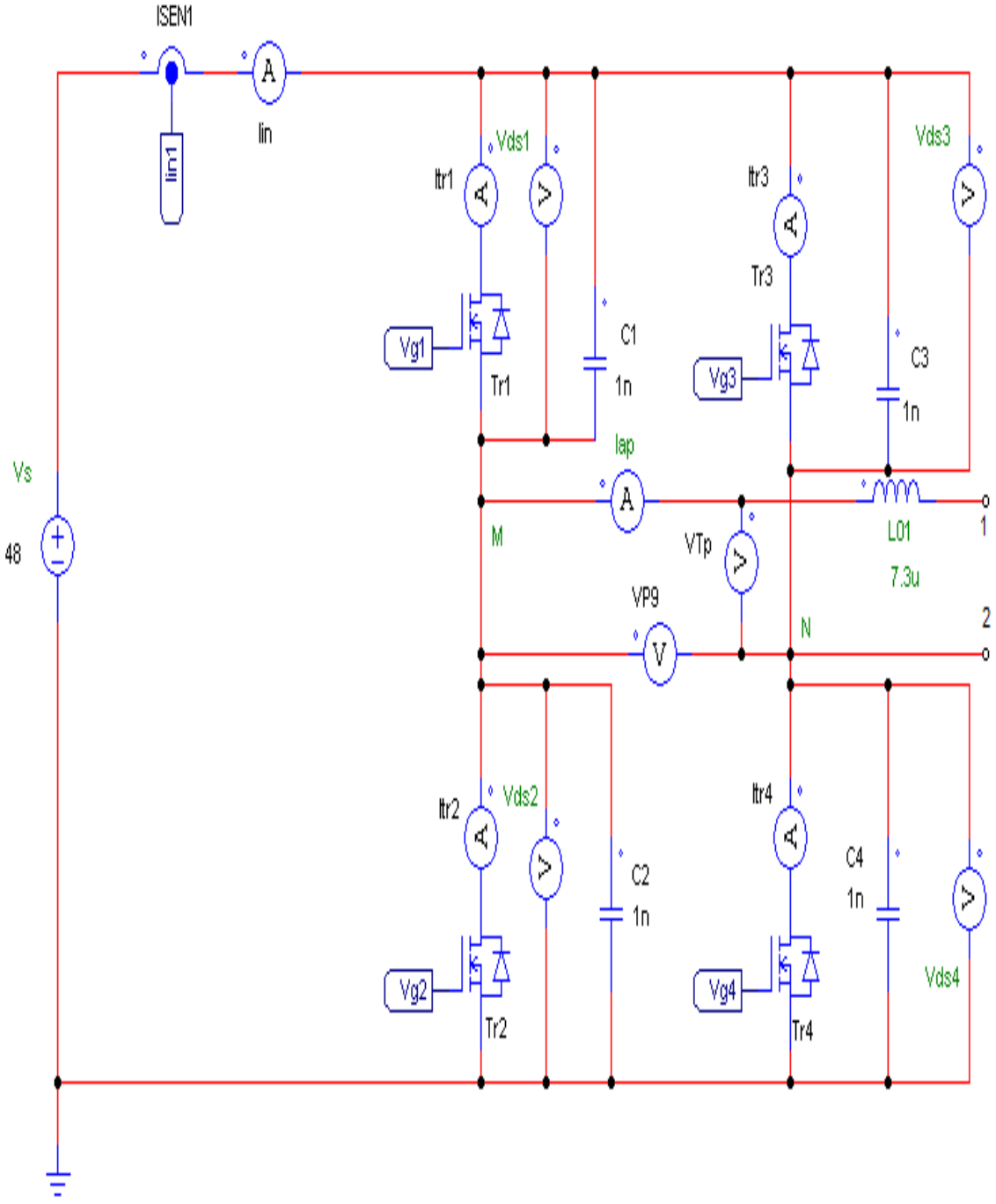

Fig. B.2 Simulation Primary Power Circuit of Forward Bidirectional Dual Full Bridge DC-DC Converter with Dual Phase-shift Control

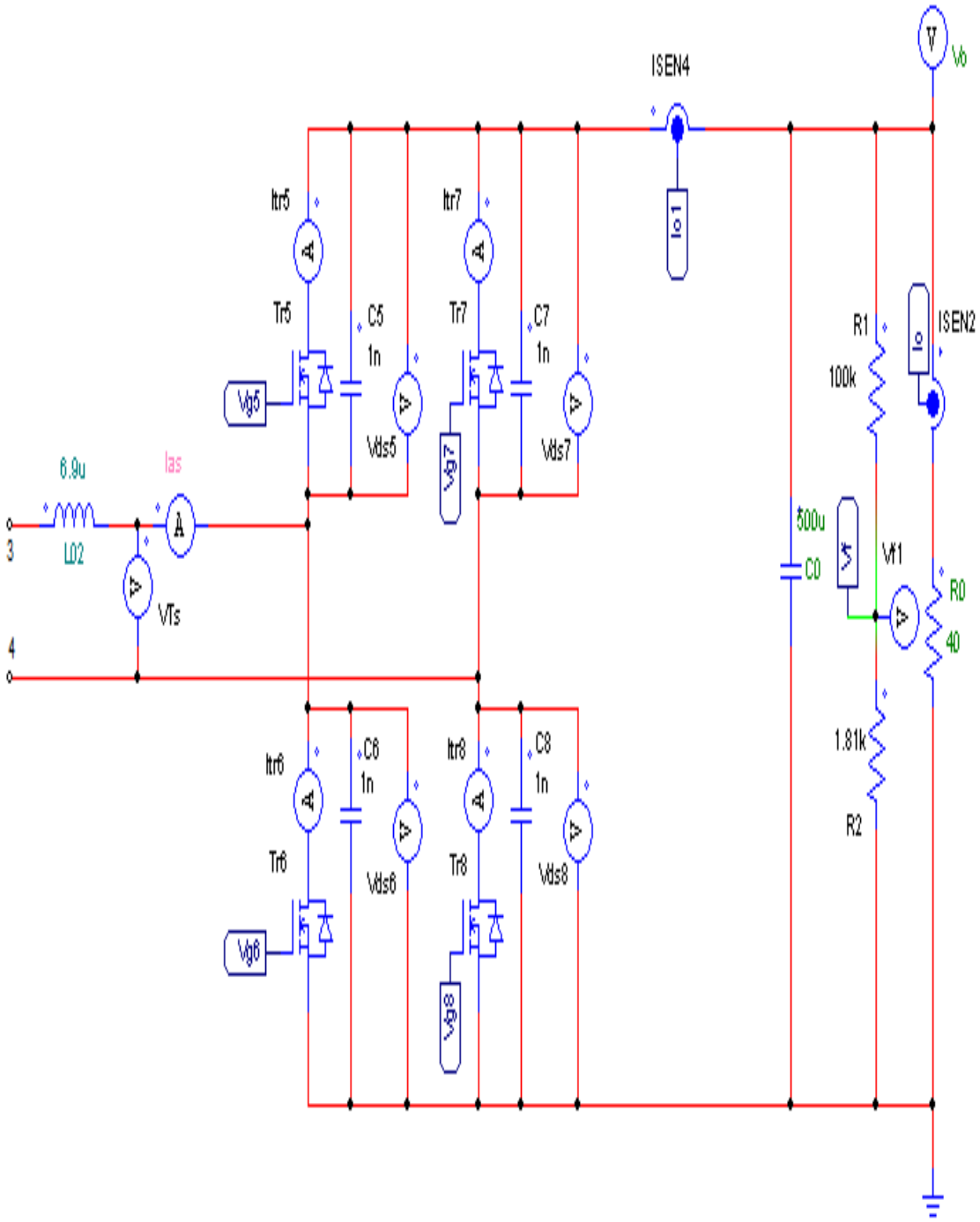

Fig. B.3 Simulation Secondary Power Circuit of Forward Bidirectional Dual Full Bridge DC-DC Converter with Dual Phase-shift Control

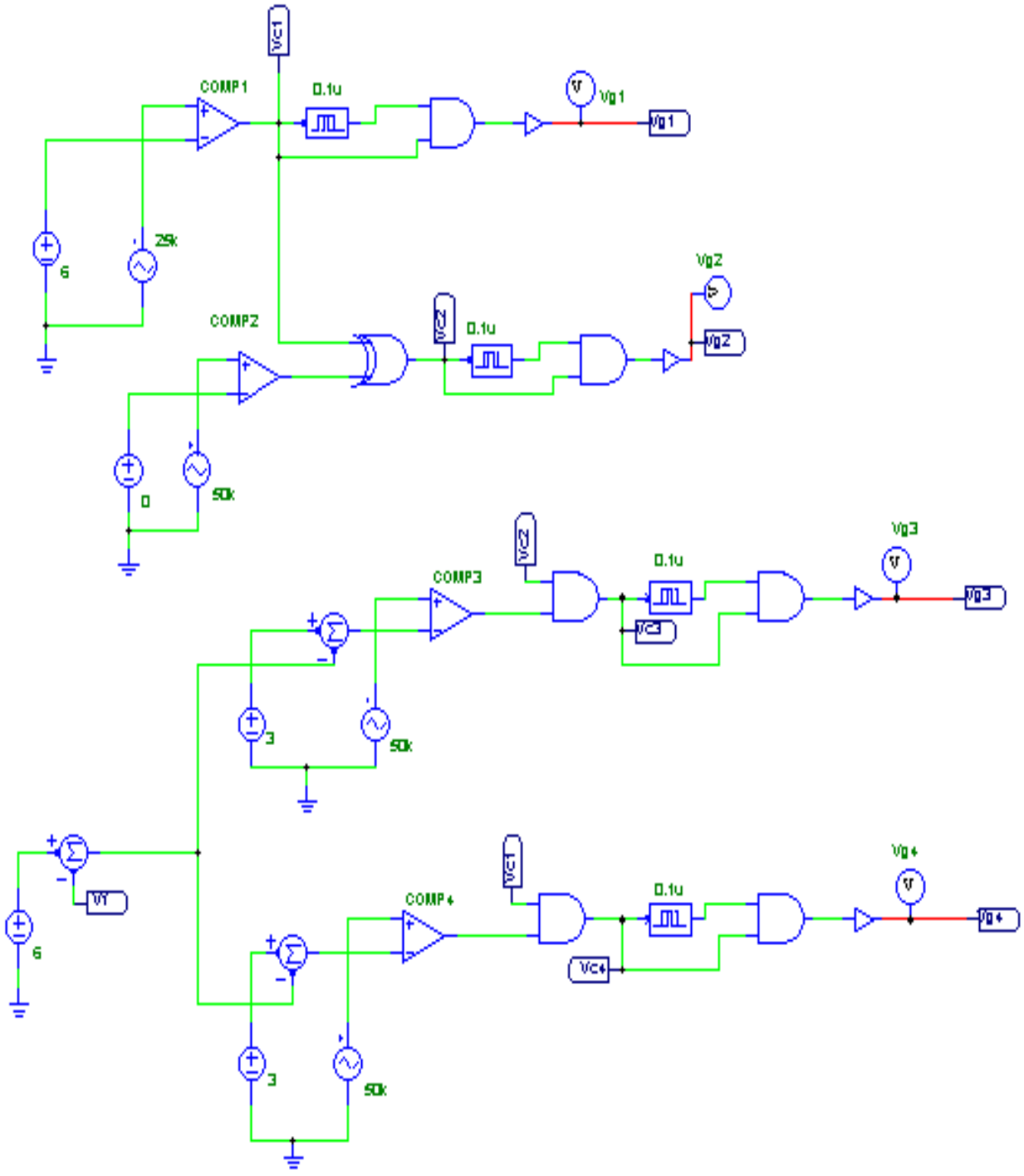

Fig. B.4 Simulation Sub-control Circuit 1 of Forward Bidirectional Dual Full Bridge DC-DC Converter with Dual Phase-shift Control

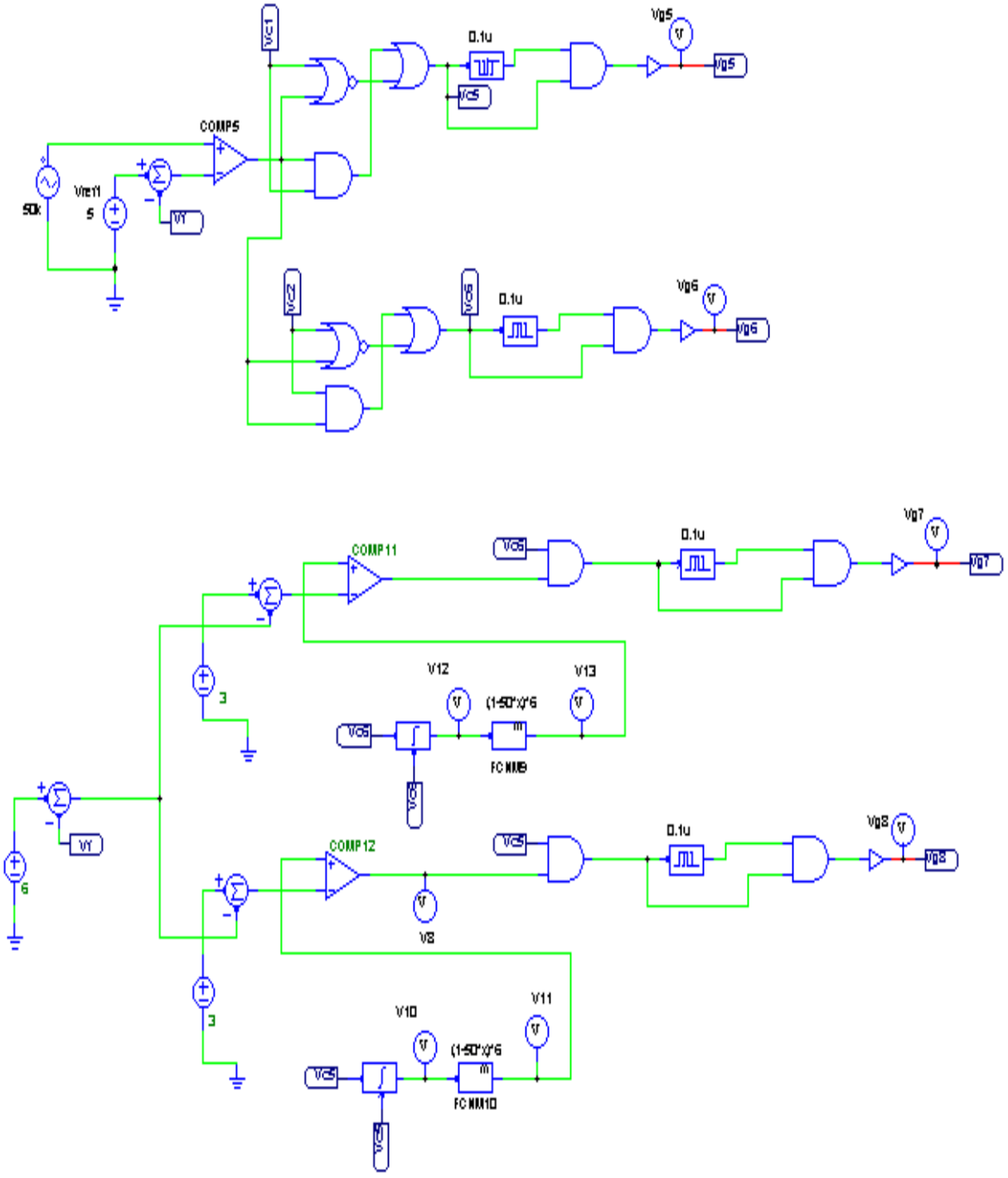

Fig. B.5 Simulation Sub-control Circuit 2 of Forward Bidirectional Dual Full Bridge DC-DC Converter with Dual Phase-shift Control

The parameters of this bidirectional converter are as follows:

Two serial inductors:

L_{01}=7.3μH; L_{02}=6.9μH;

Eight snubbber capacitors paralleled with power switches:

C_1=C_2=C_3=C_4=C_5=C_6=C_7=C_8=1nF;

Output-filter capacitance:

Co=Co1=500μF;

Forward load resistance: Ro=40Ω;

The parameters of the main transformer are as following:

Primary leakage inductance: Lp=0.6μH;

Secondary leakage inductance: Ls=1μH;

Primary winding resistance: Rp=7mΩ;

Secondary winding resistance: Rs=10mΩ;

Turns ratio: n=7/2

The parameters of the 8 power switches are as following:

Tr1~Tr4: On resistance: 5mΩ; Diode Voltage drop: 1V

Tr5~Tr8: On resistance: 23mΩ; Diode Voltage drop: 0.6V

The dead time is equal to 0.1 micro-second.

Appendix C Simulation Circuit of Forward Bidirectional Dual Full Bridge DC-DC Converter with Single Phase-shift Control

In order to be convenient to check this simulation circuit, it is attached as follows:

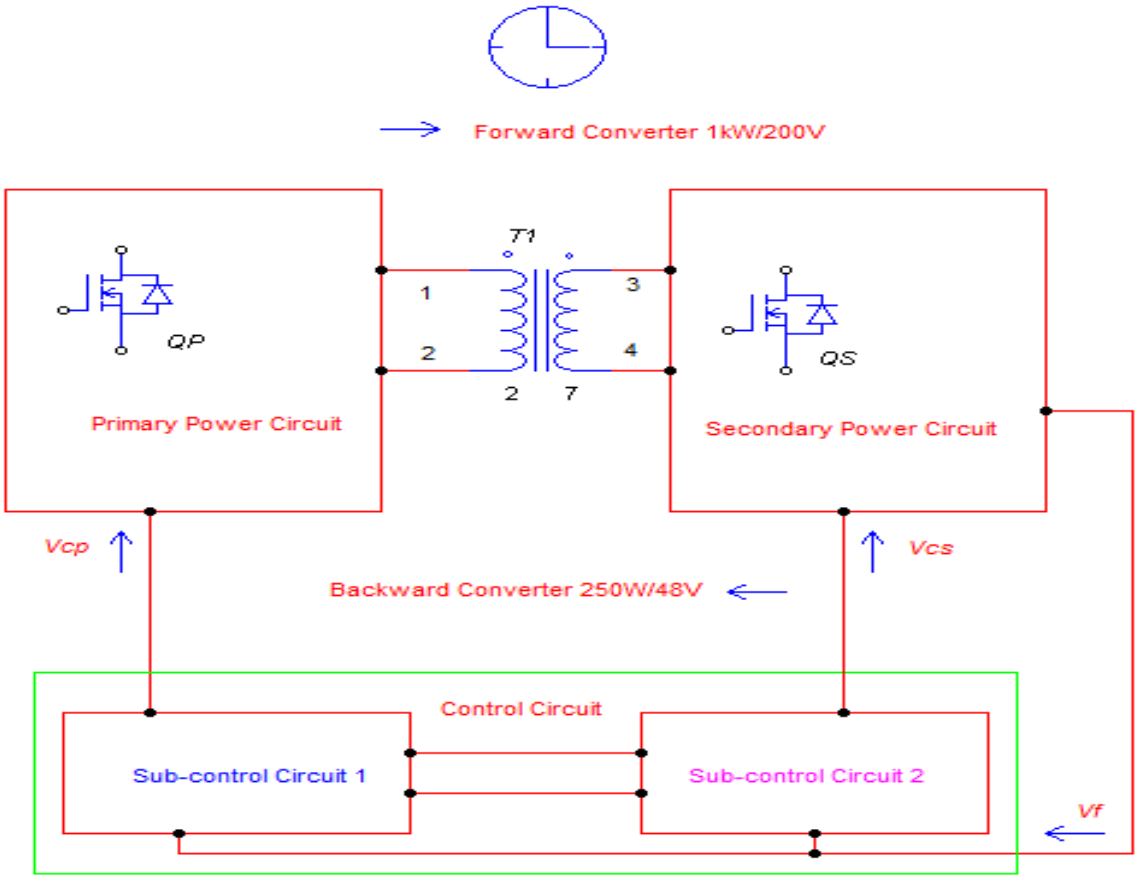

Fig. C.1 Block Simulation Circuit of Forward Bidirectional Dual Full Bridge DC-DC Converter with Single Phase-shift Control

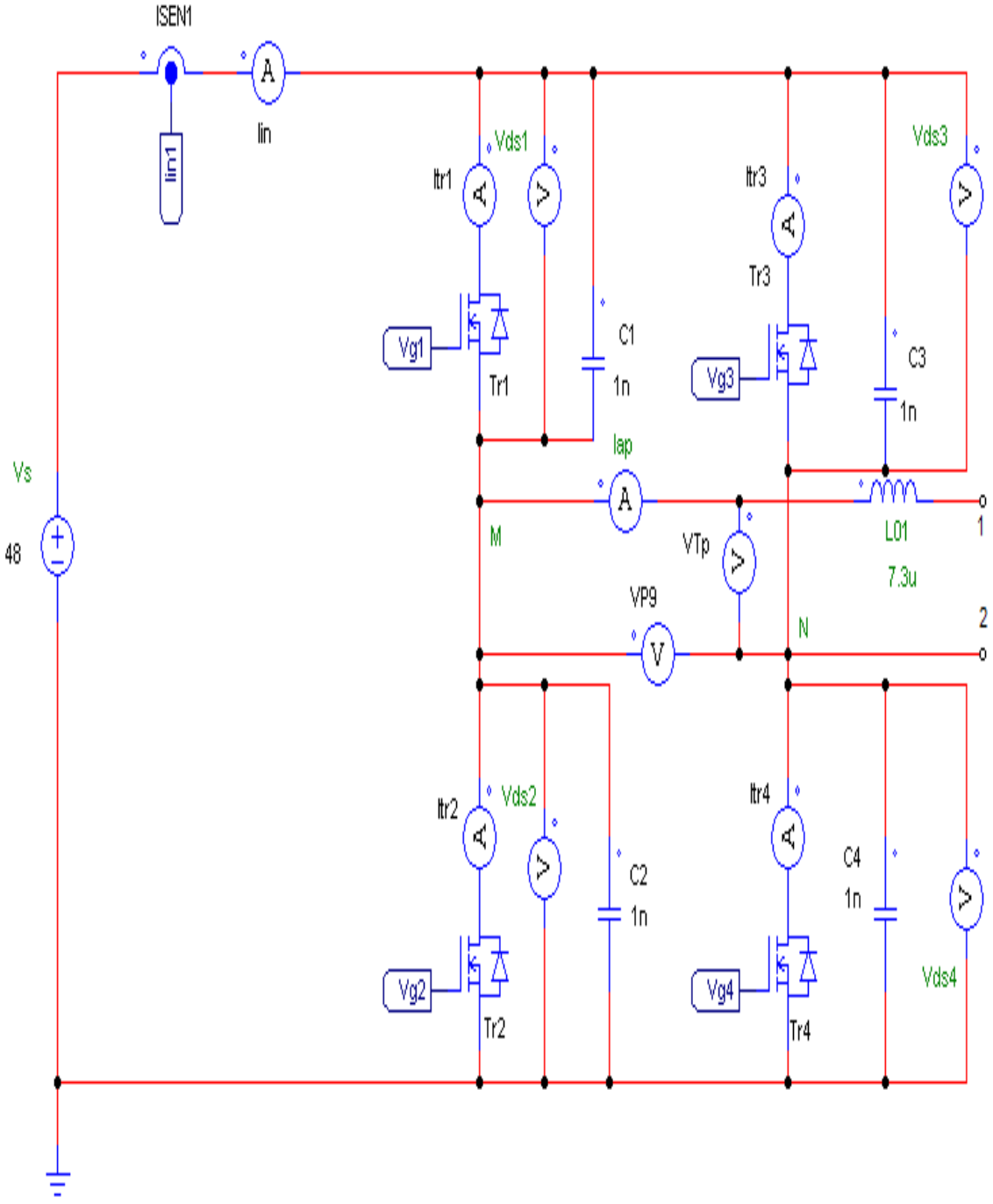

Fig. C.2 Simulation Primary Power Circuit of Forward Bidirectional Dual Full Bridge DC-DC Converter with Single Phase-shift Control

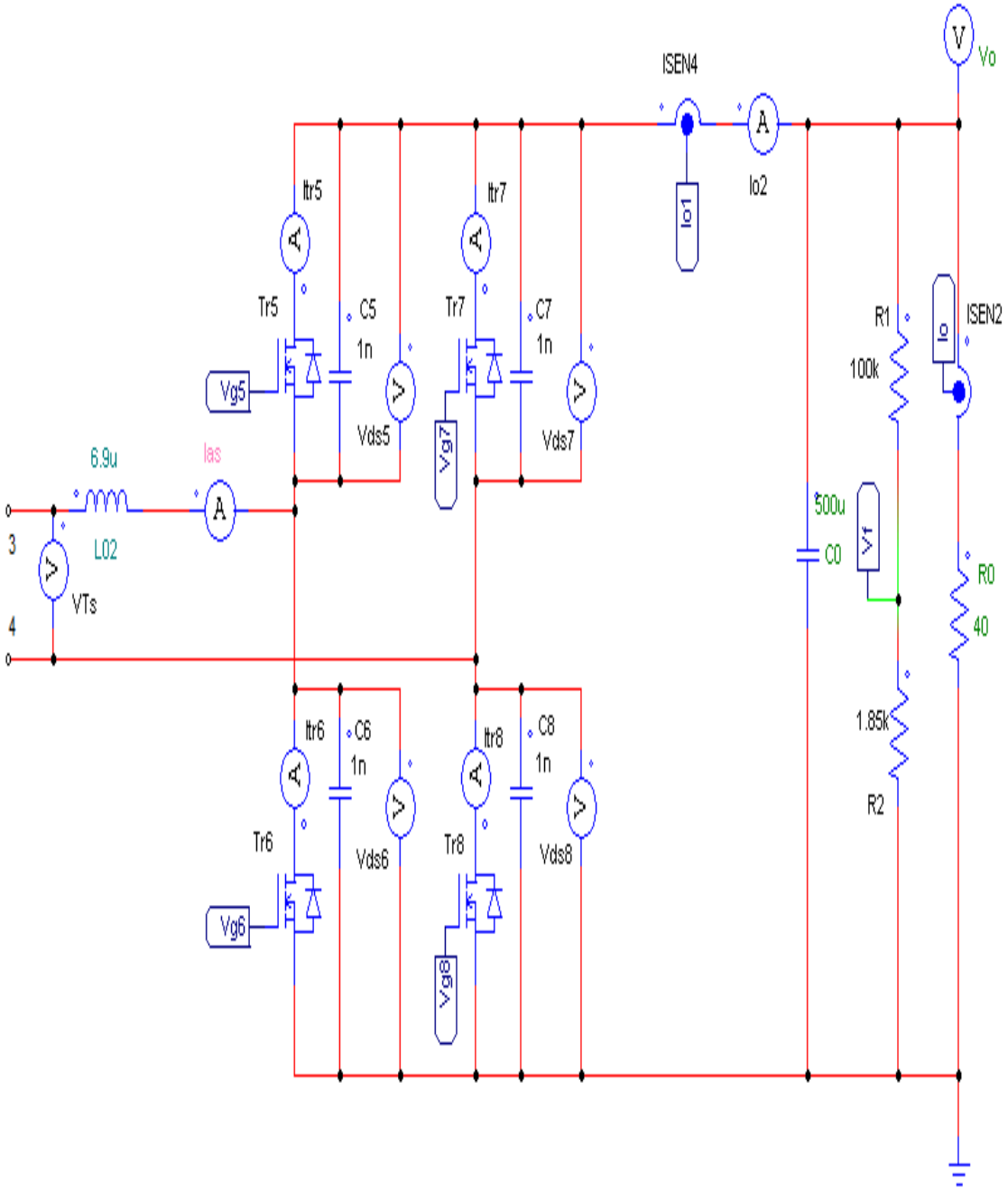

Fig. C.3 Simulation Secondary Power Circuit of Forward Bidirectional Dual Full Bridge DC-DC Converter with Single Phase-shift Control

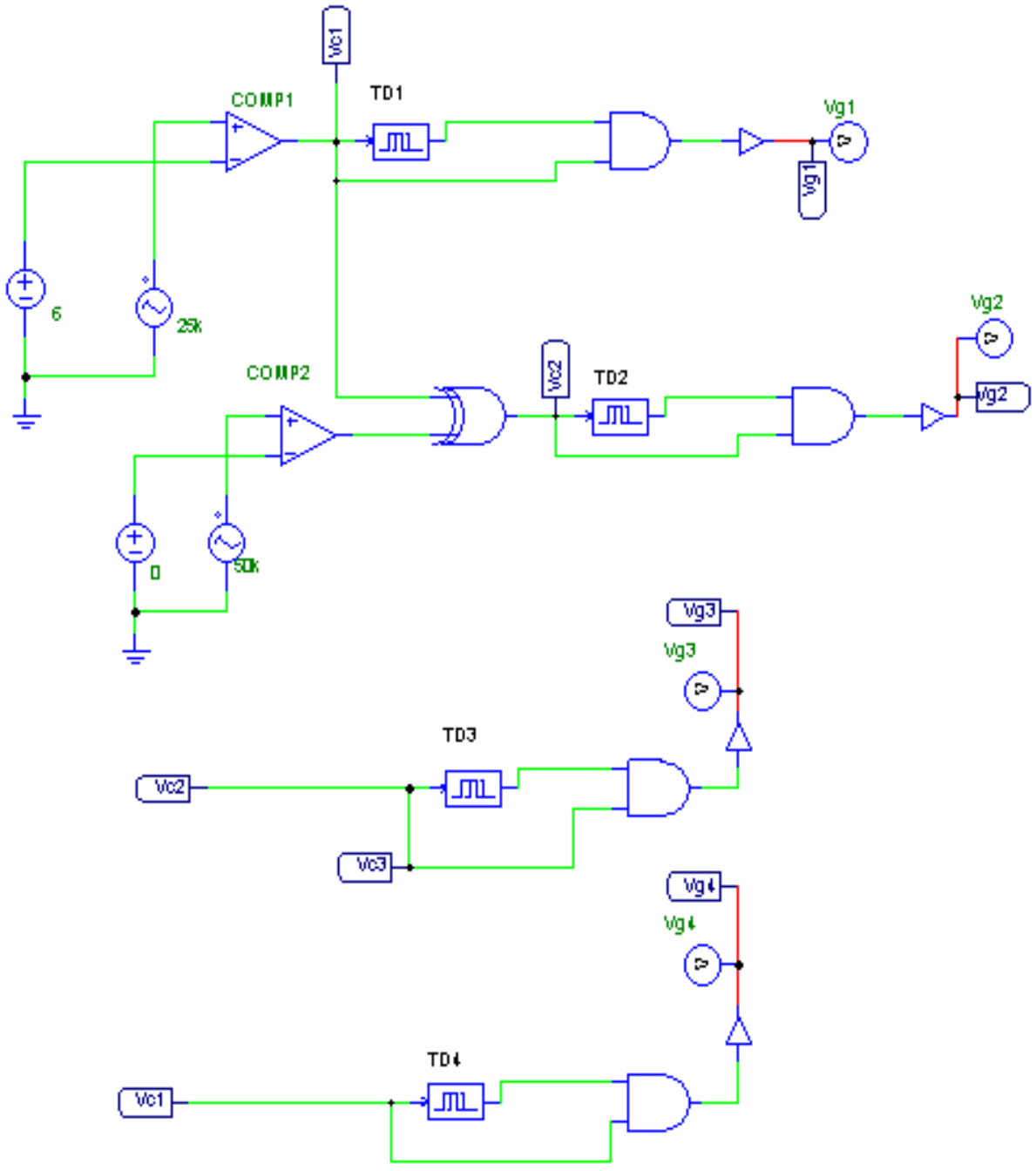

Fig. C.4 Simulation Sub-control Circuit 1 of Forward Bidirectional Dual Full Bridge DC-DC Converter with Single Phase-shift Control

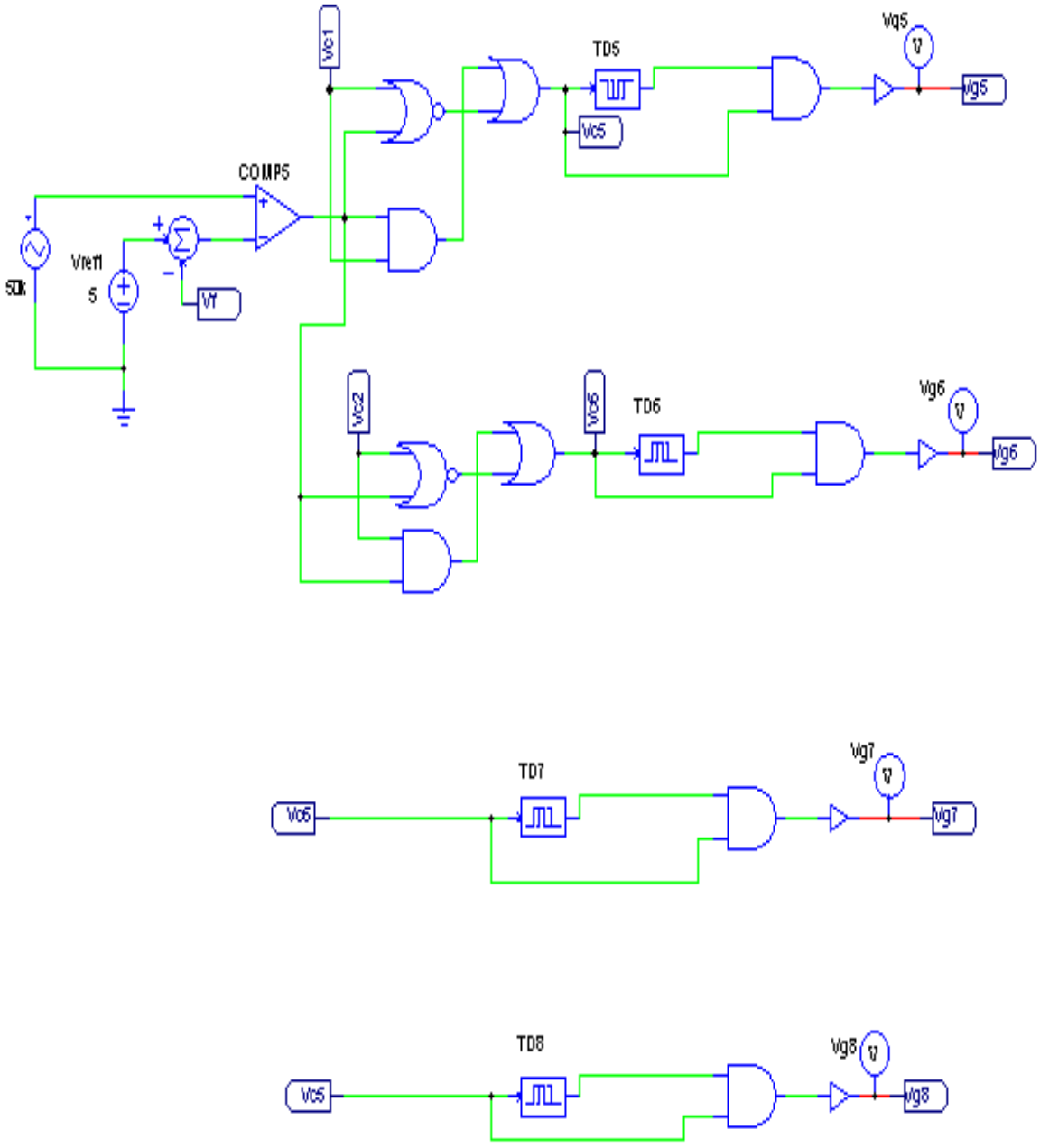

Fig. C.5 Simulation Sub-control Circuit 2 of Forward Bidirectional Dual Full Bridge DC-DC Converter with Single Phase-shift Control

The parameters of this bidirectional converter are as follows:

Two serial inductors:

L_{01}=7.3μH; L_{02}=6.9μH;

Eight snubbber capacitors paralleled with power switches:

C_1=C_2=C_3=C_4=C_5=C_6=C_7=C_8=1nF;

Output-filter capacitance:

Co=Co1=500μF;

Forward load resistance: Ro=40Ω;

The parameters of the main transformer are as following:

Primary leakage inductance: Lp=0.6μH;

Secondary leakage inductance: Ls=1μH;

Primary winding resistance: Rp=7mΩ;

Secondary winding resistance: Rs=10mΩ;

Turns ratio: n=7/2

The parameters of the 8 power switches are as following:

Tr1~Tr4: On resistance: 5mΩ; Diode Voltage drop: 1V

Tr5~Tr8: On resistance: 23mΩ; Diode Voltage drop: 0.6V

The dead time is equal to 0.1 micro-second.

Appendix D Simulation Circuit of Forward Bidirectional Full-half Bridge DC-DC Converter with Dual Phase-shift Control

In order to be convenient to check this simulation circuit, it is attached as follows:

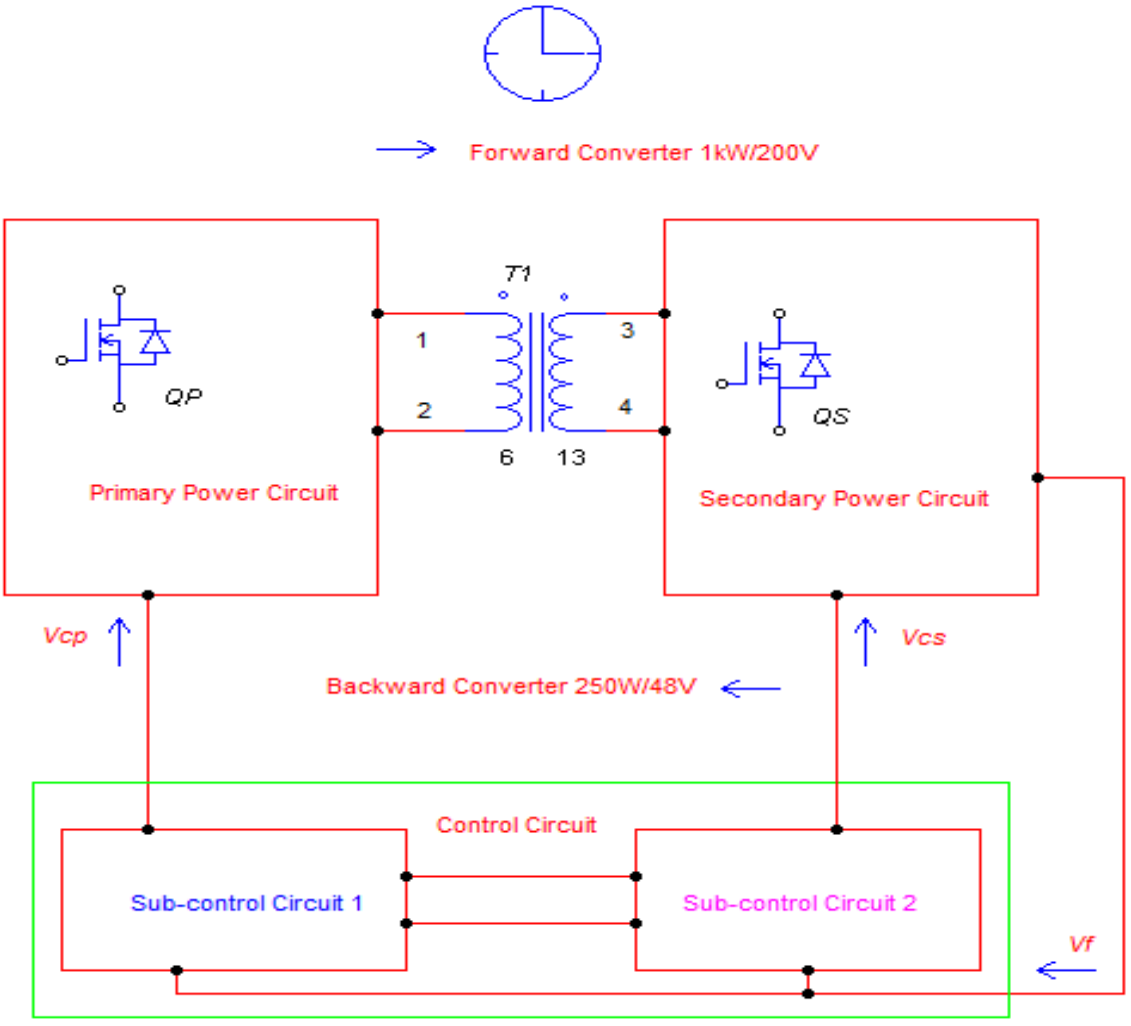

Fig. D.1 Block Simulation Circuit of Forward Bidirectional Full-half Bridge DC-DC Converter with Dual Phase-shift Control

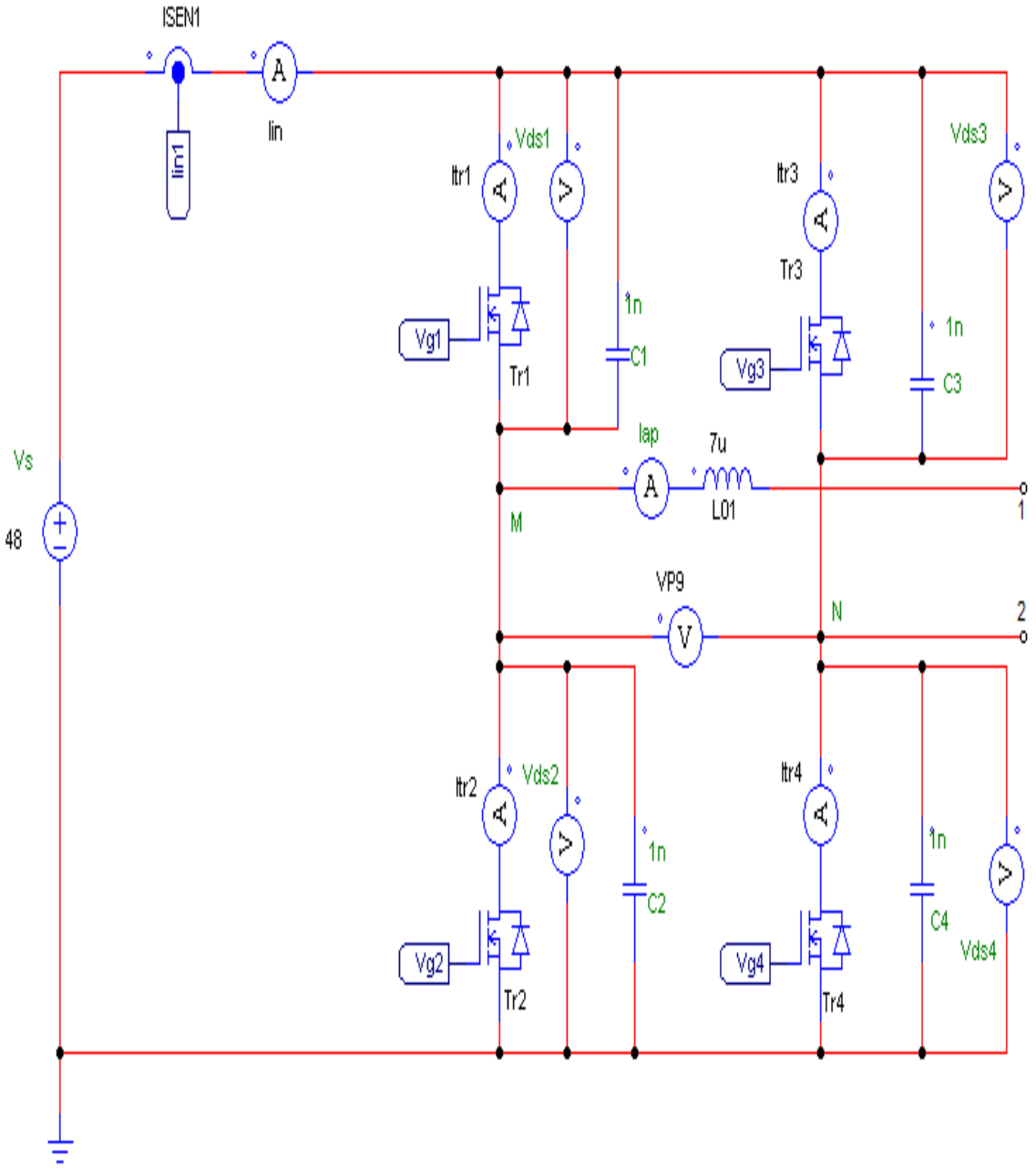

Fig. D.2 Simulation Primary Power Circuit of Forward Bidirectional Full-half Bridge DC-DC Converter with Dual Phase-shift Control

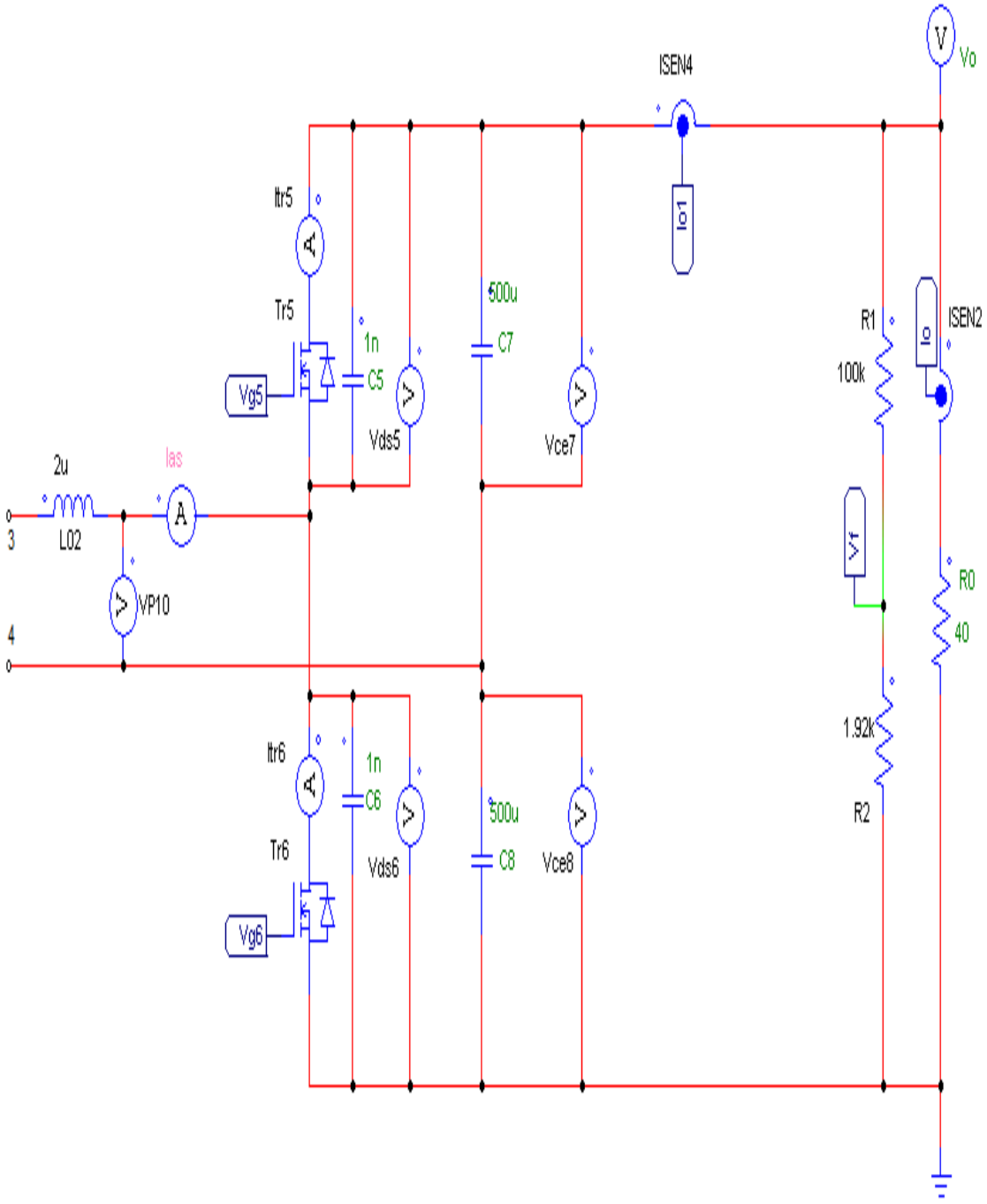

Fig. D.3 Simulation Secondary Power Circuit of Forward Bidirectional Full-half Bridge DC-DC Converter with Dual Phase-shift Control

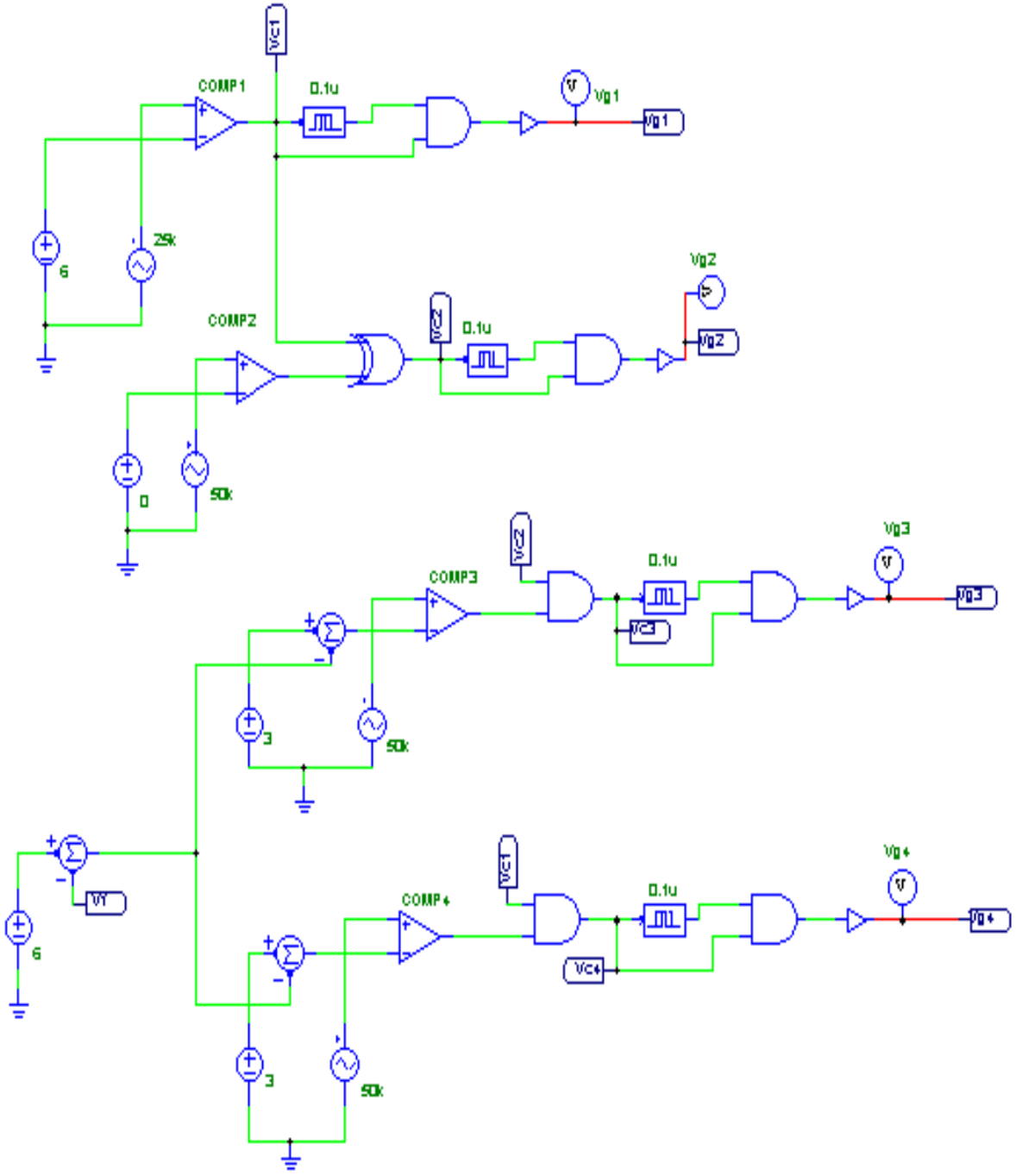

Fig. D.4 Simulation Sub-control Circuit 1 of Forward Bidirectional Full-half Bridge DC-DC Converter with Dual Phase-shift Control

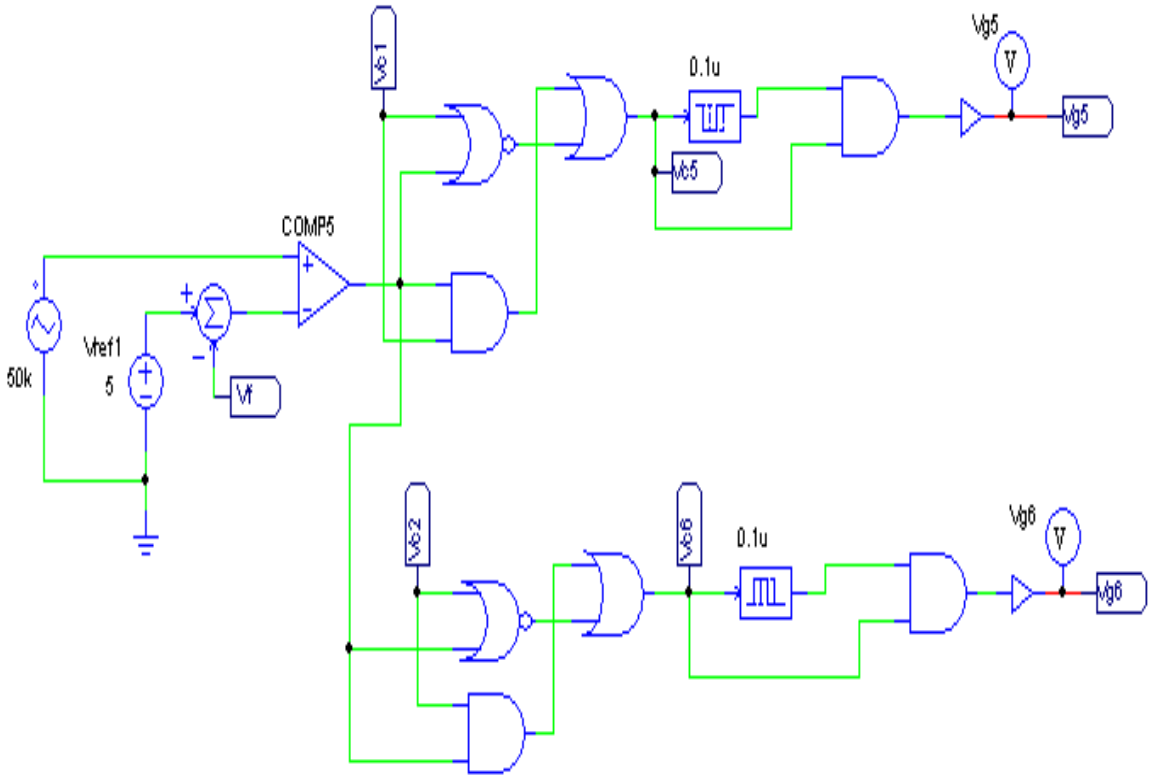

Fig. D.5 Simulation Sub-control Circuit 2 of Forward Bidirectional Full-half Bridge DC-DC Converter with Dual Phase-shift Control

The parameters of this bidirectional converter are as follows:

Two serial inductors:

L_{01}=7μH; L_{02}=2μH;

Six snubbber capacitors paralleled with power switches:

C_1=C_2=C_3=C_4=C_5=C_6=1nF;

Output-filter capacitance:

C_7=C_8=Co1=500μF;

Forward load resistance: Ro=40Ω;

The parameters of the main transformer are as following:

Primary leakage inductance: Lp=0.5μH;

Secondary leakage inductance: Ls=0.5μH;

Primary winding resistance: Rp=7mΩ;

Secondary winding resistance: Rs=10mΩ;

Turns ratio: n=13/6

The parameters of the 6 power switches are as following:

Tr1~Tr4: On resistance: 5mΩ; Diode Voltage drop: 1V

Tr5~Tr6: On resistance: 23mΩ; Diode Voltage drop: 0.6V

The dead time is equal to 0.1 micro-second.

Appendix E Simulation Circuit of Forward Bidirectional Voltage Clamped DC-DC Converter with Single Phase-shift Control

In order to be convenient to check this simulation circuit, it is attached as follows:

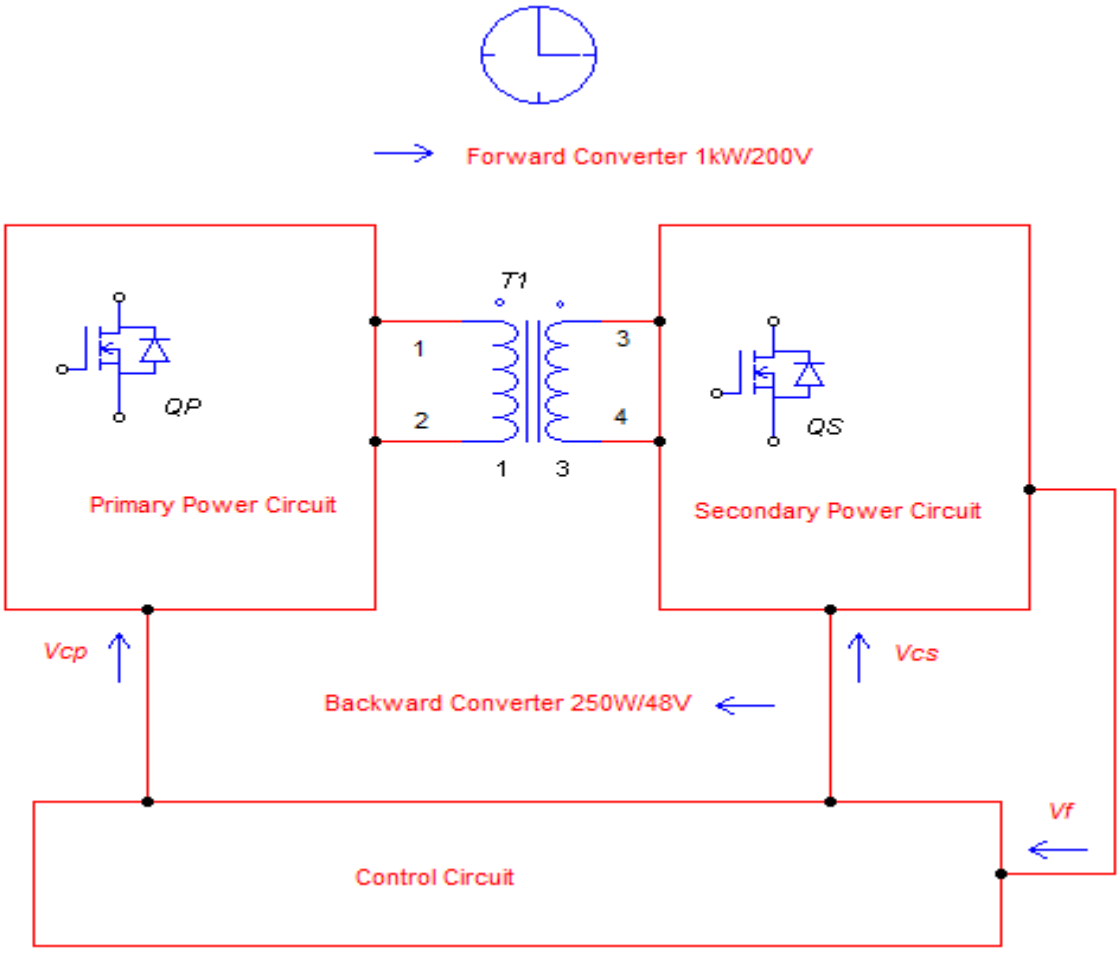

Fig. E.1 Block Simulation Circuit of Forward Bidirectional Voltage Clamped DC-DC Converter with Single Phase-shift Control

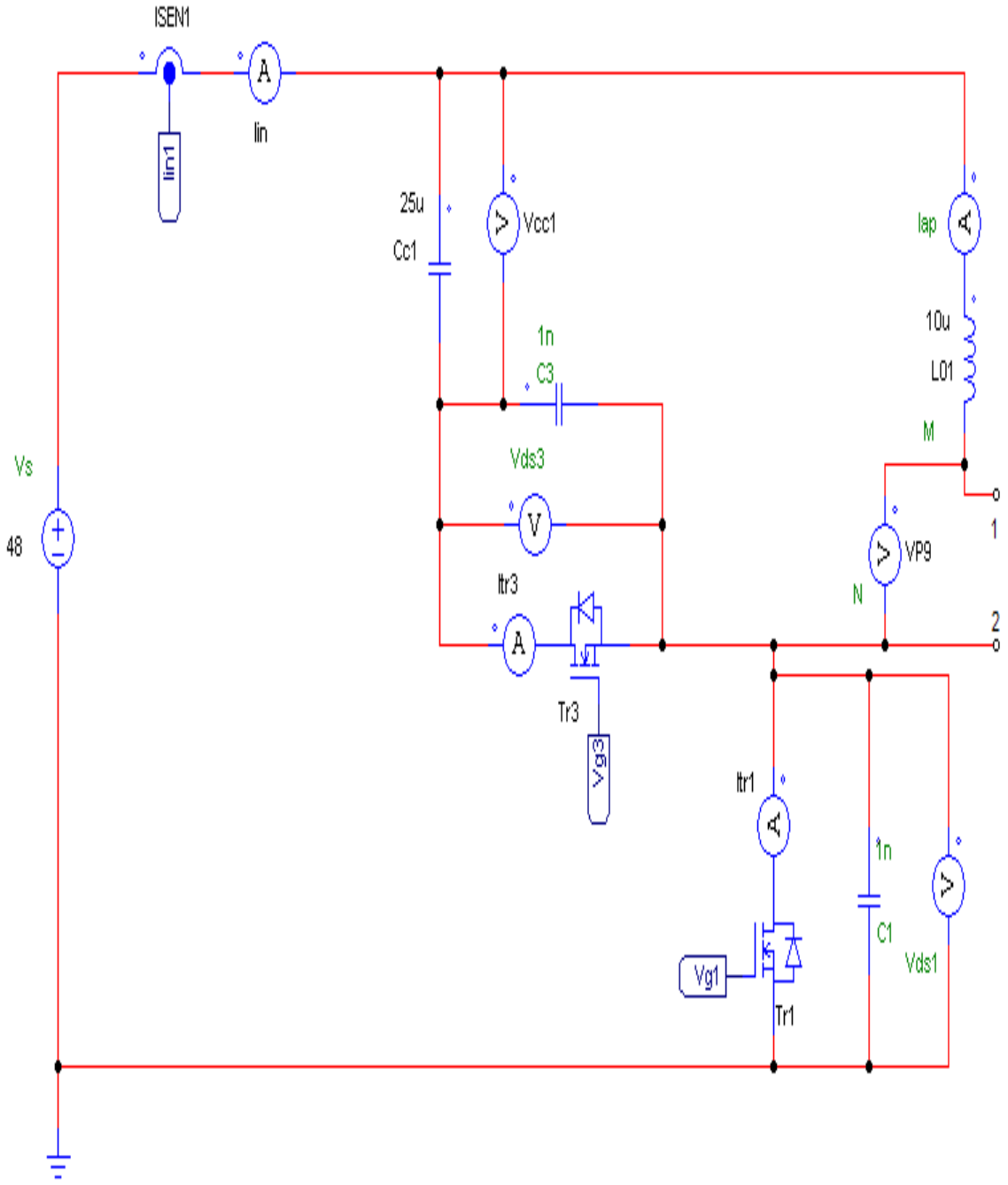

Fig. E.2 Simulation Primary Power Circuit of Forward Bidirectional Voltage Clamped DC-DC Converter with Novel Triple Phase-shift Control

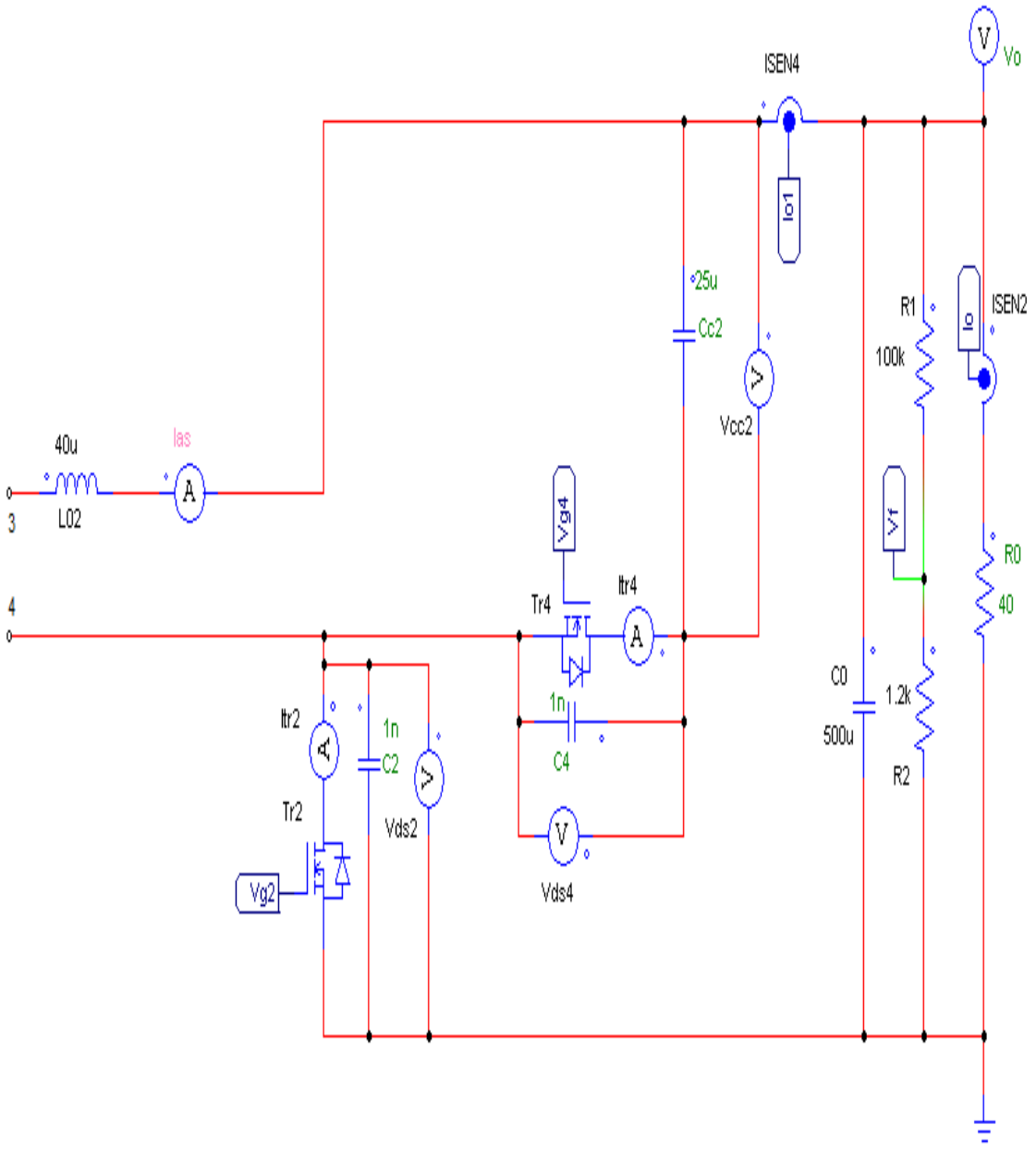

Fig. E.3 Simulation Secondary Power Circuit of Forward Bidirectional Voltage Clamped DC-DC Converter with Novel Triple Phase-shift Control

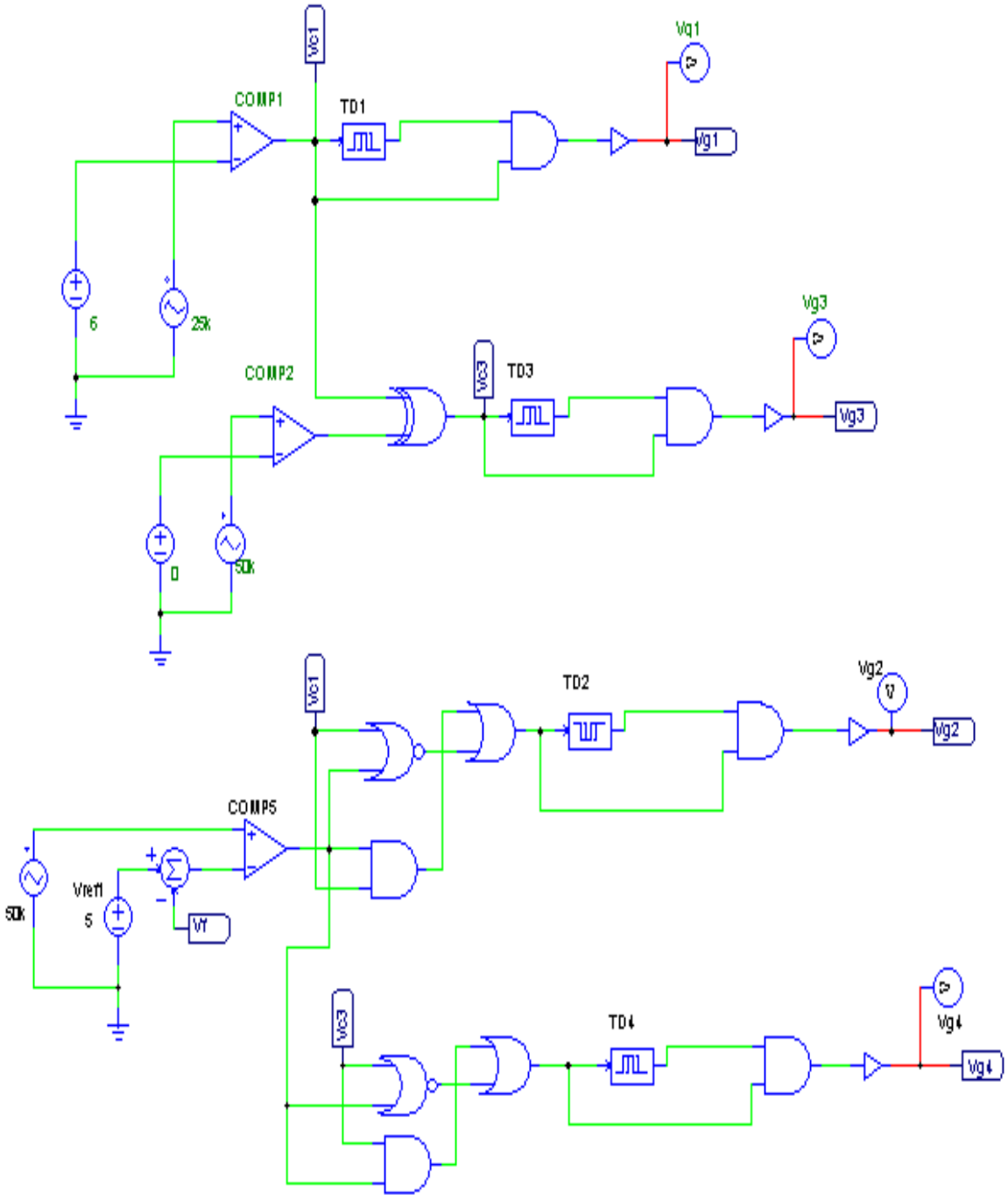

Fig. E.4 Simulation Control Circuit of Forward Bidirectional Voltage Clamped DC-DC Converter with Novel Triple Phase-shift Control

The parameters of this bidirectional converter are as follows:

Two serial inductors:

L_{01}=10μH*;* L_{02}=40μH;

Four snubbber capacitors paralleled with power switches:

C_1=C_2=C_3=C_4=1nF;

Output-filter capacitance:

Co=Co1=500μF;

Two voltage clamp capactiors:

C_{c1}=C_{c2}=25uF

Forward load resistance: Ro=40Ω;

The parameters of the main transformer are as following:

Primary leakage inductance: Lp=0.5μH;

Secondary leakage inductance: Ls=0.5μH;

Primary winding resistance: Rp=7mΩ;

Secondary winding resistance: Rs=10mΩ;

Turns ratio: n=3/1

The parameters of the 4 power switches are as following:

Tr1, Tr3: On resistance: 5mΩ; Diode Voltage drop: 1V

Tr2, Tr4: On resistance: 23mΩ; Diode Voltage drop: 0.6V

The dead time is equal to 0.1 micro-second.